Evolution of central complex development: cellular and genetic mechanisms

Dissertation

for the award of the degree

"Doctor rerum naturalium"

of the Georg-August-Universität Göttingen

within the doctoral program *Genes and Development*

of the Georg-August University School of Science (GAUSS)

submitted by

Max Stephen Farnworth

from Hanau, Germany

Göttingen, 2019

Thesis Advisory Committee

Prof. Dr. Gregor Bucher (advisor)
(University of Göttingen; Department of Evolutionary Developmental Genetics)

Prof. Dr. Halyna Shcherbata
(Hannover Medical School; Institute for Cell Biochemistry)

Prof. Dr. André Fiala
(University of Göttingen; Department of Molecular Neurobiology of Behavior)

Members of the Examination Board

First reviewer: **Prof. Dr. Gregor Bucher**
(University of Göttingen; Department of Evolutionary Developmental Genetics)

Second reviewer: **Prof. Dr. Halyna Shcherbata**
(Hannover Medical School; Institute for Cell Biochemistry)

Further Members of the Examination Board

Prof. Dr. André Fiala
(University of Göttingen; Department of Molecular Neurobiology of Behavior)

Prof. Dr. Christoph Bleidorn
(University of Göttingen, Department of Animal Evolution and Biodiversity)

PD Dr. Roland Dosch
(University Medical Center Göttingen, Department of Developmental Biochemistry)

Prof. Dr. Ralf Heinrich
(University of Göttingen, Department of Cellular Neurobiology)

Date of Oral Examination: September 30th, 2019

DECLARATION

I hereby declare that the doctoral thesis entitled
"*Evolution of central complex development: cellular and genetic mechanisms*"
has been written independently and with no other sources and aids than quoted.

_____ Göttingen, July 11th, 2019

For my family

Acknowledgements

First of all, I want to thank Prof. Gregor Bucher for the opportunity of a doctoral thesis as well as his optimism and patience. During a period of life with a lot of changes, you have helped and supported me with a good mixture of kindness and firm guidance.

I greatly acknowledge scientific help and support by my thesis committee members, Profs. Halyna Shcherbata and André Fiala.

I thank Elisa Buchberger for suffering through her role as my coffee partner and for her kind honesty and calming presence. I am so glad we became friends, as GIF-infused as possible.

I want to thank Dr. Nico Posnien for being a role model in how to balance all the different aspects of the scientific with the private life. But even more, we have ideas together, that we bravely (or naively?) put into practice.

I want to thank Kolja N. Eckermann for teaching me all the basics of Molecular Biology I should have known before I entered the lab and, together with Dr. Peter Kitzmann, for showing me the way of delicious coffee making.

I thank Dr. Peter Kitzmann for being such a good lab colleague with mad sport skills, integrity and the ability, together with Kolja, to come up with nicknames that stick, annoyingly, even four years after their invention.

I want to acknowledge all the help I received from Elke Küster, Claudia Hinners and Dipl.-Ing. Beate Preitz. Particularly Elke has set up so many single crosses of flies and beetles for me, with incredible patience for my lack of planning – thank you!

I want to thank Dr. Marita Buescher for helpful scientific input and for entertaining me through odd and surprisingly funny stories of her life, including a lot of cat stories...

I acknowledge the tremendous help by Dr. Felix S.C. Quade for all things 3D reconstruction.

I want to thank Luisa Mathilde Welp, Marvin Seifert, Lara Markus and Ehecatl A. Ruiz Alvarez for their experimental help.

I acknowledge tremendous last-minute help by Ann-Kathrin Müller in correcting this work.

Of course, all lab members of both departments deserve a big thank you. From all of you I have profited, in some shape or form! Particularly though Birgit Rossi, Merle Eggers, Bettina Hucke, Angelika Löffers, Helma Gries, Dhaval Patel, Prof. Ernst A. Wimmer, Prof. Sigrid Hoyer-Fender, Dr. Gerd Vorbrüggen, Dr. Ufuk Günesdogan, Hassan M. M. Ahmed, Dr. Bernhard G. M. Schmid (so many nice chats!), Dr. Stefan Dippel, Julia Kurlovich, Mila Ilic, Dr. Micael Reis, Martin Milner (see you next Tuesday!), Dr. Vera Terblanche, Magdalena Schacht (all the food!), Felix Kaufholz, Dr. Salim Ansari, Dr. Salim M. Hakeemi, Dominik Mühlen, Dr. Daniela Grossmann, Dr. Jürgen Dönitz and Dr. Bicheng He.

Financial support from the Göttingen Graduate Center for Neurosciences, Biophysics, and Molecular Biosciences (GGNB) is greatly appreciated.

I want to take the opportunity to acknowledge people not involved in this work: First of all, thanks for the advice, help and guidance, particularly by Prof. Martin Plath – who let me discover this 'brain evolution' topic of mine, Prof. Robert A. Barton – from whom I learned how to critically read and discuss topics, but also Dr. Roland Dosch, Dr. Stephen H. Montgomery and Prof. Julia Fischer for guidance on critical thinking, topical support and reflection.

I further want to acknowledge financial support during my Master's Studies by the German National Academic Foundation. Through Prof. Sarah Köster's mentorship, inspired courses by Profs. Peter Kappeler and Daniel Haun, and support by Prof. Katja Liebal, I was able to stay motivated pursuing an academic career.

I want to thank my friend Martin Meschkat. We cannot stop testing each other's statements, positions, and reflecting on each other's emotional stupidity and personal fallacies. I learn a lot from and with you. Oh, and you and my Billyard pal Dr. David Brockelt proof-read this thesis – thank you, and, I am so sorry!

So many more friends would be needed to be listed here with special mention, but the two pages are nearly full, so in short: Christian, Katha, Seb, Hannes, Daniel, Lena, Mo, Luisa and Johanna – thank you so much!

Last and most importantly, my family: My father, Peter, is the reason why I studied biology, why I have a 'scientist's' mind (or at least pretend to have) and I am incredibly thankful for your support throughout.

My mother, Wilma, is my role model for all the life skills I continue to fail at. I couldn't be prouder to be your son.

My brother, Christopher: it is a luxury to have someone who you know will always have your back, no matter what.

I am thankful to my brother Mark, for trying to teach me to believe in myself and to be more relaxed. I do not know what he would say to me having completed a doctoral thesis, but I hope he would have been proud.

My daughter Lilith has changed my life for the better. Her existence has not only changed my daily life, but how I think and how I exist. I am a much better person because of her.

My girlfriend, friend, life-partner and wife Tina: I still cannot believe that we not only share a life and family together, but that you believe in me. Without your support, I wouldn't have been able to do this work.

TABLE OF CONTENT

Abbreviations

µ	micro
bp	basepairs
CBL	lower division of the central body
CBU	upper division of the central body
CM	centro-medial lineages
CPU2	columnar neuron of the PB and CBU 2
CRISPR/Cas	Clustered Regularly Interspaced Short Palindromic Repeats/CRISPR-associated
DAL	dorso-anterior lateral lineages
dlrCBU	dorso-lateral root of the CBU
DM1-4	dorso-medial neuroblasts 1-4
DP	dorso-posterior lineages
EB	ellipsoid body
EGFP	enhanced green fluorescent protein
FB	fan-shaped body
fs	Fascicle switching
g	gram
GABA	γ-aminobutyric acid
GAL4	galactose-responsive transcription factor
GEKU	**G**öttingen, **E**rlangen, **K**ansas State University, **U**nited States Department of Agriculture
GOI	gene of interest
HDR	homology-directed repair
kb	kilobases
l	litre
lv	larval
LAL	lateral accessory lobes
lvCB	larval central body
m	milli
M	molar mass
MARCM	Mosaic analysis with a repressible cell marker
MEF	medial equatorial fascicle
mrCBU	medial root of the CBU
NHEJ	non-homologous end joining
NO	noduli
P2A	porcine teschovirus-1 peptide
PAM	protospacer-adjacent motif
PB	protocerebral bridge
PFN	protocerebral bridge–fan-shaped body–noduli neurons
pr	primordial
retinal homeobox	*rx* (gene), Rx (protein)
RNAi	RNA interference

1. Summary

Brains are conserved between insect species, as they consist of a set of anatomically similar areas, or neuropils. Simultaneously, these neuropils differ in size, shape, position and developmental timing between insect species, thus reflecting evolutionary adaptations to specific sensory cues and behavioural repertoires. Although divergences in a common framework are intriguing, the developmental mechanisms underlying the evolution of insect brains are hardly understood. One phenomenon in the evolution of development is heterochrony, i.e. a shift in relative developmental timing of morphological structures between species. The central complex, a neuropil in the insect brain that enables spatial orientation, appears at different developmental stages in different species. In this work, I compare central complex development between the fruit fly *Drosophila melanogaster* and the red flour beetle *Tribolium castaneum*. In *Drosophila*, the central complex is functionally an adult structure as it only appears during late larval and pupal stages. In *Tribolium*, however, parts of the central complex are already present at the end of embryogenesis. Here, I show work that establishes, uses and expands a new method to mark and compare homologous neurons throughout development in different species.

The main work is presented in manuscript 1, where I used a novel method of marking and comparing developing, homologous cell groups of the central complex of *Drosophila* and *Tribolium*. For this, I generated and characterized transgenic lines specific for the conserved transcription factor *retinal homeobox* (*rx*). I then determined which Rx-positive cell groups in the adult brain of *Drosophila* and *Tribolium* are homologous. These were then followed throughout development. We were able to identify a complex pattern of heterochronic events between *Drosophila* and *Tribolium* central complex development. Most importantly, we found that *Tribolium* precociously acquires a functional central complex neuropil that has distinct anatomical characteristics and thus represents an immature form of the central body.

Manuscript 2 describes two ways to construct transgenic lines, like the ones used in manuscript 1, through CRISPR/Cas mediated genome editing. One relies on homology-directed repair of a bicistronic construct, and results in an exact monitoring of a gene of choice, while the other is mediated by non-homologous end-joining to generate a gene-specific enhancer trap.

Manuscript 3 describes methods on how to dissect and stain *Tribolium castaneum* brains of different developmental periods. It describes how to perform *in situ* hybridisation and immunohistochemistry in adult and larval brains.

Generating tools such as genetic neural lineage marking (manuscript 1, 2) and establishing protocols that can be used in alternative model organisms (manuscripts 2 and 3) can facilitate more detailed understandings of the genetic and developmental underpinnings of brain evolution.

2. Introduction

2.1. The diversity of brain evolution

The brain is the organ in animals that integrates a multitude of information to coordinate behavioural output. It is the primary structure that governs the processing of sensory input and internal states to direct behavioural output and in consequence the interaction with the environment. Hence, a brain is essential to an animal's survival by controlling the behavioural repertoire and together with other factors defining a species' habitat and niche construction. As it is such an important entity in each individual, its evolution is a crucial question in every species' evolutionary history.

Brain evolution has been approached from multiple angles (Figure 1). Any listing of approaches and publications likely fails to be complete, but the selection provided here still highlights the diversity of facets of the evolution of brains and nervous systems (Figure 1).

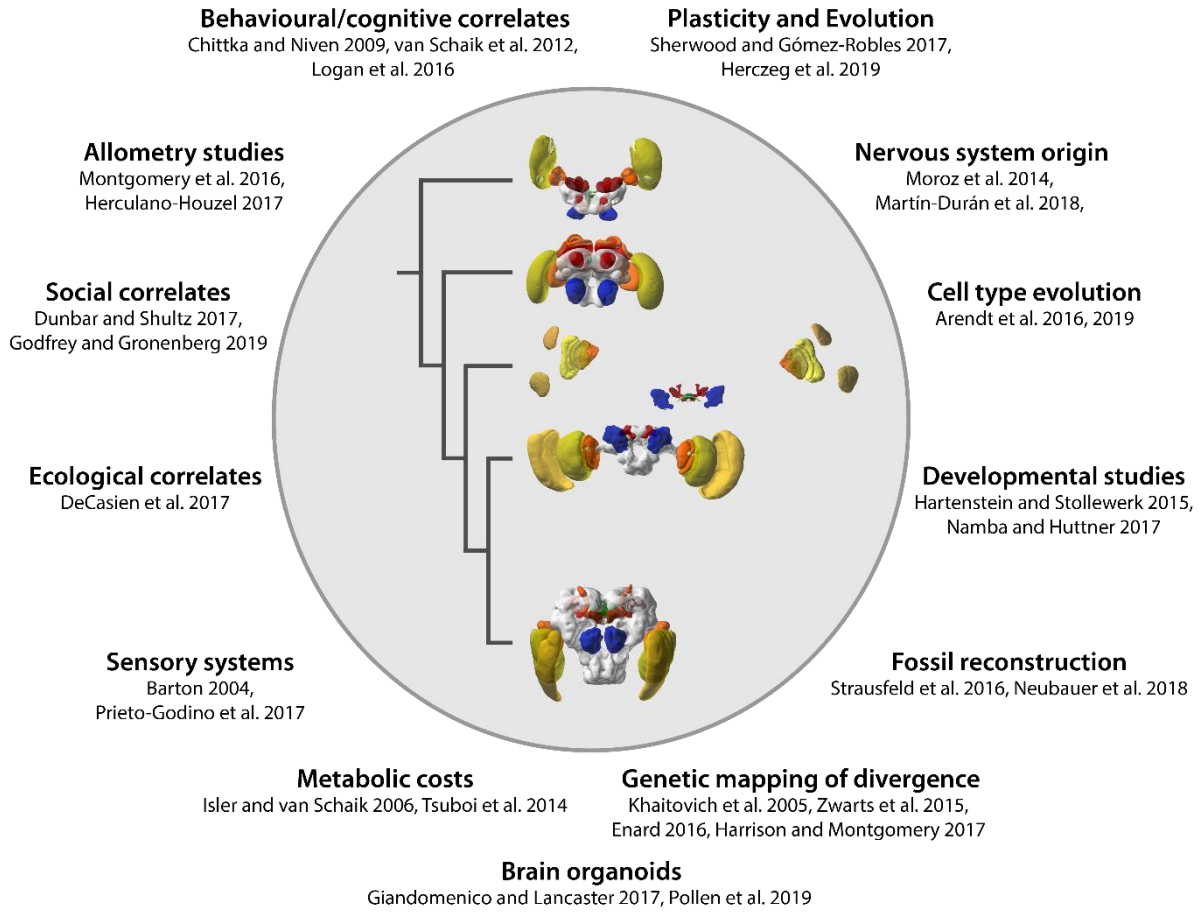

Figure 1: The evolution of brains is studied using various overlapping approaches. Different approaches are represented by exemplary publications and are arranged in non-specific order around a simplified insect phylogeny (based on Misof et al., 2014) with 3D reconstructed brains of representative species (www.insectbraindb.org), displaying anatomical differences in brains. For details see Figure 2.

The most common approach, often involving studies of allometry, is the comparison of species' whole brains or gross subareas that can be easily distinguished anatomically (Chittka and Niven, 2009; Gonzalez-Voyer et al., 2009; Montgomery et al., 2016; Striedter, 2005; Tsuboi et al., 2018). Such comparisons are not necessarily limited to extant species as insights into the origin of brains of specific clades were gained through endocast volume reconstruction (Neubauer et al., 2018) and fossil reconstruction in arthropods (Strausfeld et al., 2016) as well.

Information about sensory systems (Barton, 2004; Prieto-Godino et al., 2017), life history (Isler and van Schaik, 2012; Powell et al., 2017), ecological (DeCasien et al., 2017; Schulz-Mirbach et al., 2016), social (Dunbar and Shultz, 2017; Godfrey and Gronenberg, 2019) and behavioural/cognitive factors (Chittka and Niven, 2009; Logan et al., 2018; Stöckl et al., 2016; van Schaik et al., 2012) as well metabolic correlates (Isler and van Schaik, 2006; Tsuboi et al., 2014) have been included in such analyses to generate and test specific evolutionary hypotheses. For example, two not mutually exclusive hypotheses are the visual brain (Barton, 2004, 1998) and social brain hypothesis. (Dunbar, 1998; Dunbar and Shultz, 2007). The visual brain hypothesis emphasizes that increased visual specialisation including binocularity has caused the evolution of large brains in primates, while the social brain hypothesis posits that social factors such as group size have been the main drivers in this animal group.

An alternative correlate to brain area size for all these factors is cell number (Herculano-Houzel, 2017). For instance, Herculano-Houzel (2012) shows that the human brain is not especially large but scaled up in comparison to other mammals, as the number of neurons fit into allometric predictions.

As data of whole brain and brain area sizes is now available for many, particularly mammalian, species, phylogenetic comparative analyses can be performed to account for the underlying phylogenetic history (DeCasien et al., 2017; Miller et al., 2019; Nunn and Barton, 2001; Powell et al., 2017). For example, Miller et al. (2019) have revealed that an evolutionary shift in the relationship of brain and body size has occurred when hominids split from other primates. Analogous analyses using phylogenetic comparative methods on a large scale are still missing in arthropods (see 4. Discussion), although suitable volumetric data sets are available (see e.g. www.insectbraindb.org).

Underlying brain area size differences are genetic and developmental differences that have contributed to evolutionary transitions (Enard, 2016; Florio et al., 2015; Harrison and Montgomery, 2017; Hartenstein and Stollewerk, 2015; Khaitovich et al., 2005; Namba and Huttner, 2017; Stollewerk, 2016; Zwarts et al., 2015). For example, Zwarts et al. (2015) have

revealed over hundred genes that underlie natural variation in the morphology of an area in the insect brain.

In addition, the origin of nervous systems has been intensely studied (Arendt et al., 2015; Edgecombe et al., 2015; Hartenstein and Stollewerk, 2015; Martín-Durán et al., 2018; Moroz et al., 2014), including the evolution of cell types (Arendt et al., 2019, 2016). For example, such investigations include whether nervous systems have evolved once in an early common ancestor sharing homology or several times independently (Arendt et al., 2016; Martín-Durán et al., 2017; Moroz et al., 2014).

In summary, various approaches, methods and starting points exist to study the evolution of brains.

2.2. Insect brains are suitable subjects for evolutionary research

Many studies on brain evolution were performed on vertebrates, particularly primates, despite relatively low species number and important ethical concerns regarding invasive lab work (brain organoids elegantly circumvent ethical concerns; see Giandomenico and Lancaster, 2017; Pollen et al., 2019). An alternative are fish, because they show huge diversity in brain anatomy (Kotrschal et al., 1998). Through particularly pronounced adult neurogenesis in fish (Zupanc, 2001), studies on plastic versus evolutionary modification were made (Eifert et al., 2015; Herczeg et al., 2019; Sherwood and Gómez-Robles, 2017). The most species-rich group of animals, however, are arthropods (in particular, holometabolous insects, Stork, 2018; Stork et al., 2015). If diversity and experimental accessibility are used as primary reasoning for selecting model systems to study brain evolution, insects, particularly holometabolans, are most suited (see Figure 2 for exemplary diversity).

Studies dedicated to insect brains and their evolution have the potential to reveal genetic and cellular factors underlying brain evolution, because insects have brains with a relatively low number of cells, but still exhibiting behavioural complexity and diversity among species. Further, insects are experimentally very accessible, for instance for whole-mount immunohistochemistry and transgenic approaches. Specifically, their short developmental times and relatively small size make insects particularly easy to keep in the lab and hence, multigenerational research required for mapping or transgenesis as well as molecular work are facilitated by their small size. Their small brain sizes make them especially tractable for evolutionary research as they allow whole mount preparations and highly detailed anatomical descriptions with relative ease (el Jundi et al., 2018; el Jundi and Heinze, 2016; Stöckl et al., 2016), that go beyond the level of detail of most vertebrate anatomical descriptions (Striedter, 2005). Such studies performed so far show that all

insect (and arthropod; see Strausfeld, 2012) brains consist of the same set of brain areas, or neuropils (some color-coded in Figure 2, Strausfeld, 2009; Strausfeld et al., 2009). However, size, shape and position vary substantially (Figure 2, (Farris, 2013; Keesey et al., 2019; Montgomery and Merrill, 2016; Stöckl et al., 2016; Strausfeld, 2009, 2005; Strausfeld et al., 2009). Hence, they are conserved and divergent at the same time.

Finding factors underlying their immense diversity in behaviour, locomotion and habitat occupation (Whitfield et al., 2013) has the potential to reveal general principles of brain evolution. Studies of brain evolution in different clades can inform each other by the testing of general hypotheses, for example (such as mosaic brain evolution in Muscedere et al., 2014, or the social brain hypothesis in Lihoreau et al., 2012). Moreover, homologous structures were revealed by comparing vertebrate and insect brains which give insights into the evolution of bilaterians in general (Farris, 2008; Strausfeld and Hirth, 2013a; Wolff and Strausfeld, 2016).

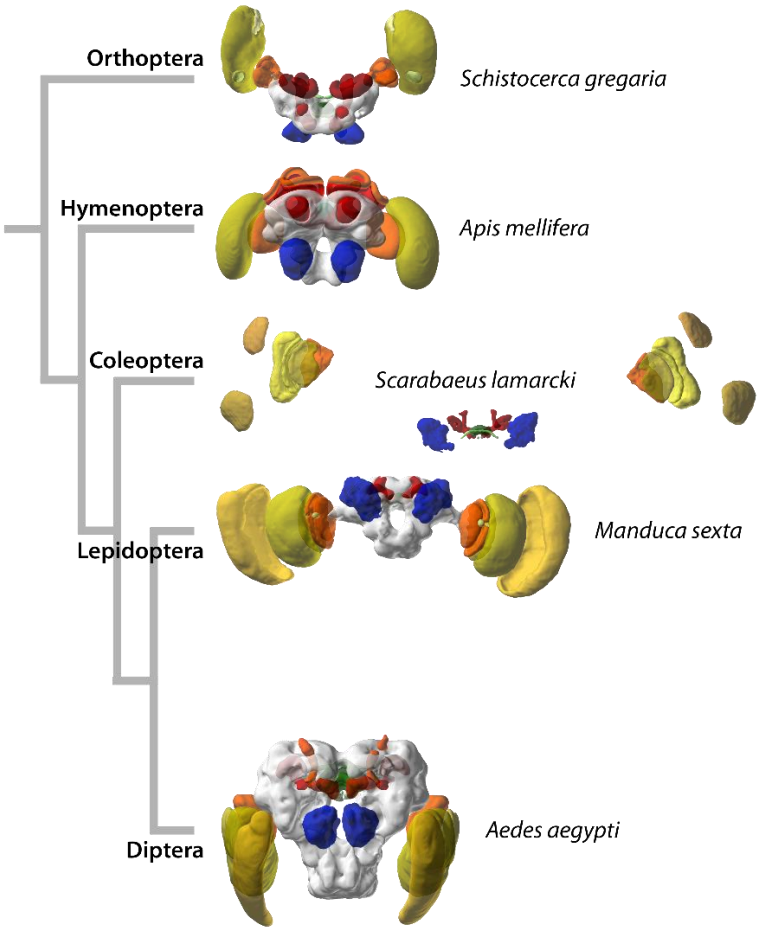

Figure 2: Diversity of insect brains in a common anatomical framework. 3D reconstructed brains (not to scale) of representative species of five orders in Insecta illustrate diversity in size, shape and position of neuropils that are common to all insects. Four neuropils are shown, besides unidentified neuropils (grey): These are central complex (green), mushroom bodies (red), antennal lobes (blue), optic lobes (yellow, orange). An example for the diversity displayed are mushroom bodies of *Apis mellifera* being large and having multiple calyces compared to the Dipteran

Aedes aegypti. Note also that the cerebrum of the Coleopteran *Scarabaeus lamarcki* is connected to distantly positioned optic lobes via optic stalks (not shown, see Immonen et al. 2017 for detail). All pictures were taken from www.insectbraindb.org. Source data is from Kurylas et al. 2008 (*Schistocerca gregaria*), Brandt et al. 2005 (*Apis mellifera*), Immonen et al. 2017 (*Scarabaeus lamarcki*), el Jundi et al. 2009 (*Manduca sexta*) and courtesy of Prof. L. Vosshall (*Aedes aegypti*). The strongly simplified phylogeny is based on Misof et al. (2014).

In summary, insect brains are well-suited for evolutionary research, with their diversity and ease of handling enabling approaches which are more difficult to perform in most vertebrate clades.

2.3. Comparing development of brains between insect species

Differences between brains of different insect species need to arise during development (see, however, adult neurogenesis in insects, Simões and Rhiner, 2017). Studying insect brain development on the level of anatomy (Farris and Sinakevitch, 2003), cell behaviour like proliferation (Boyan and Reichert, 2011) and sequencing data (Konstantinides et al., 2018) should reveal insights into how differences between brains arise.

The number of species available for detailed developmental studies is growing in the evo-devo field (Bolker, 2014; Jenner and Wills, 2007; Raff, 2000; Sommer, 2009), particularly through the increased possibility of genome and transcriptome sequencing (e.g. Martín-Durán et al., 2017), transgenesis (e.g. Berghammer et al., 1999) and genome editing in several species (Chen et al., 2016; Gilles and Averof, 2014).

The importance of developmental research for brain evolution combined with the availability of suitable tools in several species would theoretically allow for extensive studies. However, this potential is rarely used such that studies on brain development and evolution are scarce. While common developmental mechanisms such as asymmetric division of neuroblasts, neural lineage formation and development (Boyan and Williams, 2011; Boyan and Reichert, 2011; Ito and Awasaki, 2008; Reichert and Boyan, 1997; Stollewerk, 2016), as well as fascicle switching (Boyan et al., 2015) have been identified independently in several species, a direct comparison, i.e. of homologous cells throughout development, has been lacking. Hence, there have been homologous comparisons of adult brains between species on the one hand (e.g. through the shared expression of conserved neurotransmitters such as GABA, Homberg et al., 2018), and on the other hand detailed developmental studies in few model species, i.e. *Schistocerca gregaria* and *Drosophila melanogaster*. However, no studies at present have been conducted that compare the development of homologous cells between species.

This might be because of two reasons, i.e. the identification of homologous cells and the comparison of developmental periods in different species. First, a comparison of developmental

processes needs to rely on shared ancestry of investigated entities, i.e. cells or organs, such that detected differences reflect differences specific for each compared species lineage. Determining homologous cells, however, is far from trivial (see 4. Discussion, Arendt, 2005; Farries, 2013; Katz, 2007; Strausfeld and Hirth, 2013b; Striedter, 2002). Several arguments to assess homology have been used – especially shared gene expression (Arendt, 2005) and shared morphology (Wolff and Strausfeld, 2015) – and a comparison likely needs to incorporate several to claim deep homology (Strausfeld and Hirth, 2013a; but see Farries, 2013). Hence, homologous comparisons are quite difficult and require several preceding steps.

Second, species can differ strongly regarding absolute developmental time, the portion they remain in developmental stages (i.e. embryo, larva and pupa), and the timing of characteristic morphological events (Strobl and Stelzer, 2016). A comparison of developmental events in the brain needs to be based on a unified time metric to correct for differences in timing and morphology of the whole animal. For this, relative developmental time might be a first good measure, thus accounting for different metabolic rates that might underlie differences in absolute developmental time. However, without morphological criteria as addition, comparisons might be less meaningful (Smith, 2001). For example, a major developmental period like dorsal closure happens in *Tribolium* and *Drosophila* at different relative time windows (Strobl and Stelzer, 2016). Hence, the percentage at embryogenesis might be the same, but morphologically they might be different.

To conclude, while comparative developmental research is important to understand the evolution of insect brains, it is rarely done, as homologous structures and a comparative metric for development are difficult to identify. In this work, a suitable framework of comparison was employed and methods shown to facilitate comparative development on a cellular level.

2.4. The use of genetic neural lineages and alternative marking strategies

Insect neural stem cells produce all their progeny in a stereotypical fashion. Their cell bodies stay closely associated and their projections build one or a few common projections (e.g. Omoto et al., 2017). Such 'units' (Ito and Awasaki, 2008) have been identified as conserved in embryos of different insect species (Urbach and Technau, 2003a), and a specific set was compared during development between phylogenetically distant species as the desert locust and fruit fly (Boyan et al., 2017; Boyan and Williams, 2011; Boyan and Reichert, 2011). Hence, the conserved mechanism of neural lineage development makes insect brains suitable for comparative development (see manuscript 1, Boyan and Reichert, 2011; Hartenstein, 2019; Hartenstein et al., 2008; Ito and Awasaki, 2008; Spindler and Hartenstein, 2010; Urbach and Technau, 2003a). Moreover, neural

lineages as units are easier to define (e.g. by location; Lovick et al., 2013; Wong et al., 2013) than distributed cell bodies and projections. The conserved character of these units (Boyan et al., 2017; Boyan and Williams, 2011; Hartenstein, 2019; Urbach and Technau, 2003a) increase the likelihood of comparing homologous cells.

Three prerequisites need to be fulfilled to compare such neural lineages between species (Koniszewski et al., 2016). First, marking of complete development from neuroblast to adult structure needs to be possible. Second, a method needs to be technically transferrable to other species to be widely applicable. Third, it needs to be based on structures that are likely homologous.

The marking of a neural lineage (i.e. a neuroblast and all its offspring) from embryo to adult has remained challenging even in *Drosophila melanogaster*. Several methods have been used, i.e. DiI labelling (Bossing and Technau, 1994), MARCM (mosaic analysis with a repressible cell marker, Lee and Luo, 2001), gene-specific GAL4 lines (Jenett et al., 2012; Pfeiffer et al., 2010, 2008), and anatomical descriptions (Boyan and Williams, 2011, 1997). However, all these techniques come with restrictions. DiI labelling comprises the application of a lipophilic dye early in embryonic development that gets incorporated in a neuroblast and all its offspring in a non-invasive fashion, applicable in several arthropod species (Bossing and Technau, 1994; Kraft and Urbach, 2014; Scholtz and Gerberding, 2002). DiI labelling is, however, lost over time so that the method is limited to a small time-window. MARCM relies on a detailed crossing scheme to generate stochastically but permanently labelled offspring (Lee and Luo, 2001; Viktorin, 2014). Great insights have been generated with this method (Ito et al., 2013; Yang et al., 2013; Yu et al., 2013). However, the stochastic basis means that even in *Drosophila* the same cells are not always marked. Also, it is only established in *Drosophila* as several genetic tools are required to facilitate such a method. Along with the lack of marking of complete development, this method is not suited for comparative development. Gene-specific GAL4 lines contain small fragments of regulatory regions of genes, with the purpose of marking a few cells per line (Jenett et al., 2012; Pfeiffer et al., 2010, 2008). Such transgenic lines can be used to identify certain neuroblasts based on previous knowledge, and most parts of development can be monitored (Riebli et al., 2013). However, constructing such lines in several species involves establishing several techniques first, without the guarantee of suitable comparative labelling (similar limitations are valid for the 'flybow' technique; Hadjieconomou et al., 2011), because enhancers, particularly, can diverge substantially between species (Buffry et al., 2016; Khoueiry et al., 2017; Maeso et al., 2013). Anatomical descriptions can allow identification from neuroblast to adult structure and can be performed with relative ease in other species (Boyan and Williams, 2011, 1997). A morphological

criterion on its own, however, is not sufficient to claim homology (Arendt, 2005; Strausfeld and Hirth, 2013a).

Hence, the methods illustrated here do not satisfy the criteria described above, i.e. continuous marking, technical universality and marking of homologous cells, that would allow comparative developmental research based on homologous cells. Therefore, our lab has proposed an alternative method (Koniszewski et al., 2016) which I have used for the first time in manuscript 1: In this framework, the level of comparison is not the neural lineage but the so-called 'genetic neural lineage'. It is defined to comprise all cells that express the same transcription factor. While this is not sufficient to claim homology on its own it is very likely that genetic neural lineages contain or are even built predominantly by homologous cells. The concept exploits the conservation of a set of transcription factors expressed in a mostly restricted way in the anterior developing brain in most bilaterians (Arendt, 2008; Arendt et al., 2004; Davis et al., 2003; Denes et al., 2007; Eggert et al., 1998; Janssen, 2017; Kitzmann et al., 2017; Lichtneckert and Reichert, 2008; Lowe et al., 2003; Mathers et al., 1997; Mazza et al., 2010; Posnien et al., 2011; Steinmetz et al., 2010; Urbach and Technau, 2008). This conserved pattern suggests that molecularly homologous regions exist throughout bilaterians that give rise to structurally homologous brain structures and cell types. Hence, monitoring expression of such a gene likely marks cells that share ancestry. Moreover, several such genes are expressed from embryo to adult (Gold and Brand, 2014; Kraft et al., 2016; Kumar et al., 2009), thus fulfilling the criterion of continuous marking throughout development.

The common expression in bilaterian animals makes this basis also technically universal because customised antibodies can be produced for each species (see manuscript 1 for an example) and standard immunohistochemistry (see manuscript 3 for details). However, transcription factor expression is limited to nuclei and projections of marked cells would not be visualized. To allow such visualisation, gene-specific transgenic lines need to be designed that contain a fluorescent protein under the shared transcriptional control of such a conserved transcription factor (He et al., 2019; manuscript 1 and 2). Through the universally applicable system of CRISPR/Cas, any animal suitable for microinjection and rearing from eggs can be genomically edited (Gilles and Averof, 2014).

While the marking and comparison of neural lineages remains technically difficult, the concept of genetic neural lineages promises to reveal homologous cells that can be traced from embryo to the adult in several species.

2.5. Using CRIPSR/Cas to generate transgenic lines in alternative model organisms

Genetic neural lineages need to be labelled by transgenic lines that reflect the expression of one conserved transcription factor (Koniszewski et al., 2016). Generation of such transgenic lines has been done mainly through two strategies in two species, *Drosophila melanogaster* and *Tribolium castaneum*, i.e. enhancer traps and constructs containing gene regulatory regions (Hayashi et al., 2002; He et al., 2019; Jenett et al., 2012; Trauner et al., 2009). Enhancer traps in insects are (so far) based on random insertion via transposase activity (Johnston, 2002; Manseau et al., 1997; Trauner et al., 2009). Constructs that contain parts of the regulatory region of the gene of choice (Jenett et al., 2012; Pfeiffer et al., 2010, 2008) often show unspecific labelling as result of not containing all enhancers and random insertion into the genome (see manuscript 2 for details). While both strategies are suitable for a suite of choices, the development of CRIPSR/Cas as the main method to modify the genome offers an elegant way to produce more reliable results, and, in our case to construct gene-specific labelling of cells, thus avoiding stochasticity and most positional effects of previous methods.

CRISPR (Clustered Regularly Interspaced Short Palindromic Repeats)/Cas (CRISPR-associated) genome editing is based on the inert bacterial system for adaptive immunity (Jinek et al., 2012; for more details see manuscript 2 and Doudna and Charpentier, 2014; Hsu et al., 2014). A modification and simplification of this approach has allowed to exploit this system to modify nearly any genomic region in a specific manner (Gratz et al., 2014, 2013; Hsu et al., 2014; Port et al., 2014). Hence, also an expression marker such as EGFP can be edited into the region of a gene of interest, such as a conserved transcription factor (He et al., 2019; manuscript 1 and 2).

CRISPR/Cas has been used widely in insect organisms, where microinjection and multigeneration rearing is possible (Gilles and Averof, 2014). Because comparable transgenic lines can be generated in many species, this promises contributions to evo-devo research. Genetic neural lineages, as they have been used here in *Drosophila* and *Tribolium* (see manuscript 1), can at least in theory be generated in a similar way in several species where CRISPR/Cas is already established (e.g. *Gryllus*; Watanabe et al., 2017).

2.6. A beetle – fly comparison

Drosophila melanogaster is a gold standard when it comes to the number of tools developed (Çelik and Wernet, 2017; Hales et al., 2015). Second with regards to genetic amenability is the red flour beetle *Tribolium castaneum* (Pai, 2019; manuscript 1 and 2 for details). CRISPR is established (Gilles et al., 2015) and has been employed successfully for brain development topics (He et al.,

2019). Hence, a comparison of brain development in these two species is a suitable starting point, conducted in manuscript 1.

2.7. My doctoral work contained in three manuscripts and their contributions

This work presented in three manuscripts may possibly contribute to the field of brain evo-devo through a fly-beetle comparison and in turn to brain evolution in general as follows (for authors, contributions and status of the manuscript see introductory page before each manuscript):

The main experimental work is presented in manuscript 1 '*Sequence heterochrony between Drosophila and Tribolium causes emergence of a precocious larval form of the central complex*', in final preparations for submission to BioRxiv and eLife. Here, I employ the novel idea of genetic neural lineages (Koniszewski et al., 2016). We generated the respective tools and showed for the first time that this approach works. Specifically, we describe the heterochrony of one brain area, the central complex, between *Drosophila melanogaster* and *Tribolium castaneum*. Unexpectedly, two levels of heterochrony were revealed, i.e. shifts in embryonic and pupal development and changes in sequence of developmental events. We show that the larval central complex of *Tribolium* is distinct and precocious in its cellular architecture compared to the adult. These results have implications for central complex development and evolution. The approach of genetic neural lineages has implications for brain evolution and development in general.

Manuscript 2 '*The red flour beetle as model for comparative neural development: Genome editing to mark neural cells in Tribolium brain development*' and 3 '*Immunohistochemistry and fluorescent whole mount RNA in situ hybridization in larval and adult brains of Tribolium*' are methodological works and are in press for the book 'Brain Development: Methods and Protocols, 2nd version'.

Manuscript 2 describes two methods to mark genetic neural lineages using CRISPR/Cas in *Tribolium*. One approach is based on a bicistronic construct, of which the construction is labour-intensive, but results in exact labelling of the expression of a gene of choice (an example in *Drosophila* is presented in manuscript 1). The other approach is to construct an enhancer trap specific for the gene of choice, of which the construction is faster, albeit less exact in labelling (He et al., 2019). These methods have implications for the evo-devo field, as we describe ways to use the benefits of CRISPR in a model organism second to *Drosophila*, i.e. *Tribolium*. Such methods can be transferred to other insects (Gilles and Averof, 2014) and can generate new insights into the evolution and development of insects.

Manuscript 3, to which I contributed as co-author, describes how to use immunohistochemistry and *in situ* hybridisation in larval and adult brains of *Tribolium castaneum*. Such methods can be used in other labs as part of brain development and evolutionary research, and thus contribute to insect brain evo-devo as well.

I am co-author on two additional publications not included here (He et al., 2019; Koniszewski et al., 2016). Koniszewski et al. (2016) present tools for neurobiological research in *Tribolium castaneum* and propose the strategy of genetic neural lineages, which I verified through manuscript 1 and 2. He et al. (2019) explore the functional role of the conserved transcription factor *foxQ2* in brain and central complex development of *Tribolium*.

3. Results

Each manuscript starts with a description of the main aim in context of the whole thesis, the list of authors, my contributions and the manuscript status.

Manuscript 1: Sequence heterochrony between *Drosophila* and *Tribolium* causes emergence of a precocious larval form of the central complex

Pages 14-88

Manuscript 2: The red flour beetle as model for comparative neural development: Genome editing to mark neural cells in *Tribolium* brain development

Pages 89-119

Manuscript 3: Immunohistochemistry and fluorescent whole mount RNA *in situ* hybridization in larval and adult brains of *Tribolium*

Pages 120-144

3.1. Manuscript 1: Sequence heterochrony between *Drosophila* and *Tribolium* causes emergence of a precocious larval form of the central complex

This manuscript is the main part of primary data generated and illustrates that the approach of using genetic neural lineages, that the Bucher lab has developed previously, is functional and generates new insight. It is also a starting point of further similar analyses to generate additional comparative and highly useful analyses. In detail, the manuscript illustrates for the first time the usefulness of genetic neural lineages in brain evo-devo research, it characterises the heterochronic shift in central complex development between *Tribolium* and *Drosophila* and reveals a distinct larval form of the central body.

Authors

Max S. Farnworth, Kolja N. Eckermann, Gregor Bucher*

* = corresponding author

Status

in preparation for BioRxiv and eLife

My contributions

- Conceptualisation of the project and iteration of original idea[1]
- Conceptualisation of new established techniques used[2]
- Performed experiments[3]
- Data analysis and interpretation and figure generation[4]
- Writing of the manuscript[5]

[1] = together with GB, original idea by GB

[2] = experimental design of bicistronic line with KNE

[3] = together with LM (see Acknowledgements) who performed experiments for Supplementary Figures 3.1-1 and 3.1-3

[4] = aided by GB

[5] = together with GB

Title:

Sequence heterochrony between *Drosophila* and *Tribolium* causes emergence of a precocious larval form of the central complex

Authors:

Max S. Farnworth[1,3], Kolja N. Eckermann[2,3], Gregor Bucher[1,*]

[1] Department of Evolutionary Developmental Genetics, Johann-Friedrich-Blumenbach Institute, GZMB, University of Göttingen, Göttingen, Germany, [2] Department of Developmental Biology, Johann-Friedrich-Blumenbach Institute, GZMB, University of Göttingen, Göttingen, Germany, [3] Göttingen Graduate Center for Molecular Biosciences, Neurosciences and Biophysics (GGNB), Göttingen, Germany

[*] Corresponding author: Gregor Bucher gbucher1@uni-goettingen.de

Key words: Brain evolution, evo-devo, central complex, columnar neurons, DM1-4, *Tribolium*, *Drosophila*, heterochrony

3.1.1. ABSTRACT

The central complex is a brain area found in nearly all arthropod species. It facilitates a multitude of functions, most involving spatial orientation, and is remarkably similar in adults of different species of insects. Interestingly, while being conserved in adults, its appearance during development diverges between species. In the hemimetabolous desert locust all neuropils are present in an adult-like form directly after embryogenesis. In holometabolous insects, development is starkly modified such that, in the fruit fly *Drosophila melanogaster*, the central complex is an adult structure, as it is prefigured during embryonic and larval stages but only becomes functional in pupal stages. In the red flour beetle *Tribolium castaneum* some parts of the central complex are present already at the end of embryogenesis while others appear postembryonically. Such differences in developmental timing between species are coined heterochrony. A comprehensive understanding of this central complex heterochrony based on the comparison of homologous cells and throughout all developmental periods has been missing. However, a detailed comparison could identify the underlying cellular mechanisms and any modifications of conserved developmental programs.

Here we mark and compare the development of central complex columnar neurons of the DM1-4 lineage group in *Drosophila* and *Tribolium* from late embryogenesis to adulthood, using *genetic neural lineages*. For this, we generated antibodies and transgenic lines marking cells that express the conserved transcription factor *retinal homeobox* (*rx*). This comparative genetic approach revealed that heterochrony between *Drosophila* and *Tribolium* consists of multiple dimensions on a cellular level. We observed shifts in embryonic and pupal central complex development. Moreover, we saw a modification in the order of developmental events – or sequence heterochrony – that causes early emergence of an anatomically distinct larval central body and protocerebral bridge. This immature larval central body is functional, contains a small array of decussated fibres, and is morphologically distinct from any adult neuropil. Hence, in contrast to current understanding, this neuropil does not represent an adult-like upper division of the central body. Beyond the specific question of central complex heterochrony, we demonstrate a comparison of genetically and anatomically homologous cell groups using the approach of genetic neural lineages. We expect that our data and approach will be starting point for studies on the specific behavioural function of the larval central body of *Tribolium* to understand divergent patterns of central complex function, development and evolution. Moreover, with the rise of genetically tractable model organisms, our working approach of genetic neural lineages promises further comparisons of brain development on a cellular level, to further understand the developmental origins of brains and their evolution.

3.1.2. INTRODUCTION

3.1.2.1. Insect brain evolution – Diversity in a conserved architecture

Insect (and indeed arthropod) brains are conserved and at the same time highly divergent. Each species interacts with an environment that provides similar sets of stimuli. Hence, each species requires the same set of tools such as areas of neural processing (neuropils) directly connected to optic and olfactory sensory organs (i.e. optic and antennal lobes), a centre for learning and memory, the mushroom bodies, and a centre to integrate sensory information and control behavioural output, the central complex (Strausfeld, 2012, 2009). In contrast, how each species has developed their niche and adapted to specific environmental needs with specific behaviour and anatomy is reflected in differences in brain anatomy (Keesey et al., 2019; Montgomery and Merrill, 2016; Stöckl et al., 2016; Strausfeld, 2012). For example, insects such as aquatic beetles, who do not detect volatile odors, lack antennal lobes and have modified mushroom bodies (Strausfeld et al., 2009).

The diversity of brain structures is even larger when considering metamorphosis, particularly in the case of complete metamorphosis (holometaboly). Through the presence of a larval form in each holometabolous species, two life stages of each individual insect interact with the environment (Truman and Riddiford, 1999). Therefore, natural selection can cause modifications on behaviour, sensory detection and brain anatomy in each stage. A *Drosophila* larval brain, for example, differs strongly from the adult stage, because morphology and behavioural repertoire differ so much (Hartenstein et al., 2008; Ito and Awasaki, 2008; Maddrell, 2018). Moreover, in a number of insects, particularly hymenopterans, individuals of the same species have distinct brain anatomies, reflecting their tasks in the society (Gordon et al., 2019; Mysore et al., 2009; Zube and Rössler, 2008).

In summary, brains of different insect species consist of the same areas but differ in their size and shape of neuropils. Even within species, different life stages of individual and individuals of different castes can have different brain morphologies. How and why deviations from a common architecture in insect brains arise is one of the most interesting questions in insect evolution (Strausfeld, 2012).

Nearly all these differences need to be achieved during an individual's development (but see Simões and Rhiner, 2017 on adult neurogenesis). Examining developmental processes, comparing them between species and identifying commonalities and differences is therefore required to gain insight into how the selected anatomical differences are constructed (Konstantinides et al., 2018).

When comparing several insect species, the development of one set of insect brain neuropils, the central complex, is particularly intriguing: The appearance of central complex neuropils diverges between species (Koniszewski et al., 2016; Panov, 1959; Pfeiffer and Homberg, 2014). In hemimetabolous insects, such as the desert locust, all neuropils of the central complex are present after embryogenesis. In holometabolous species, development is either partially or completely shifted to pupal stages. Alterations when a central complex neuropil appears reflects the evolutionary phenomenon of heterochrony.

3.1.2.2. Heterochrony is a mechanism in the evolution of development with a largely unknown cellular basis

Heterochrony is an evolutionary phenomenon that connects development, i.e. ontogeny, with phylogeny (Gould, 1977; Raff and Wray, 1989; Smith, 2002). Specifically, it describes evolutionary shifts in relative developmental time through which differences in structure and function of organs can arise (Gould, 1977; Smith, 2001). For example, humans, compared to other great apes, retain juvenile features such as hairlessness into adulthood (Gould, 1977). Heterochronic differences can be apparent during development itself, as is the case for the central complex (Koniszewski et al., 2016; see Keyte and Smith, 2014 for limb development in marsupials, Nii et al., 2019 for termite caste development), or differences can translate into differences in the adult so that they are apparent there (neoteny in humans; Gould, 1977). Heterochrony is well-studied on a morphological level (Gould, 1977; Luque et al., 2019; Nii et al., 2019). However, in most studies on heterochrony the genetic or cellular bases are unknown (but see Keyte and Smith, 2014 for recent insights), particularly in the brain.

Hence, how cellular mechanisms of the brain such as cell proliferation and apoptosis, axogenesis, axon pruning, and functionalisation are modified to generate heterochrony remains elusive. Similarly, while basic differences in the appearance of neuropils of the central complex have been described (Koniszewski et al., 2016; Panov, 1959; Pfeiffer and Homberg, 2014), the cellular mechanisms involved are largely unknown.

3.1.2.3. Structure and function of the central complex

The central complex is a set of neuropils positioned in the middle of insect and arthropod brains (Loesel et al., 2002; Strausfeld, 2012; Thoen et al., 2017). It consists of four midline-spanning neuropils, i.e. the protocerebral bridge, the central body, comprised of upper and lower division (also referred to as fan-shaped and ellipsoid body, respectively), and paired noduli (Pfeiffer and Homberg, 2014). Except for the noduli, neuropils are vertically divided into columns

(or slices; Ito et al., 2014). The central body can further be divided into horizontally orientated layers. These subdivisions are indicators of its underlying neural connections and function (Honkanen et al., 2019; Pfeiffer and Homberg, 2014).

While the central complex consists of tracts and synaptic structures from several distinct cell types (Franconville et al., 2018; Wolff et al., 2015; Wolff and Rubin, 2018), two major types which explain its structure and function best are tangential and columnar neurons (el Jundi et al., 2018; Pfeiffer and Homberg, 2014). Tangential neurons have their cell bodies distant from the midline and project laterally into a given neuropil with large-field ramifications (el Jundi et al., 2018; Pfeiffer and Homberg, 2014). They connect other brain areas with the central complex. For example, the visual pathway from optic lobes to the ellipsoid body contains neurites of tangential neurons (Lovick et al., 2017). Columnar neurons, on the other hand, have their cell bodies near the protocerebral bridge (Andrade et al., 2019; el Jundi et al., 2018). Neurites connect the protocerebral bridge to other neuropils of the central complex, so that a high number of different types of columnar neurons can be classified. One example are PFN (protocerebral bridge – fan-shaped body – nodulus) neurons that connect three of the four neuropils with each other through small-field ramifications (Sullivan et al., 2019). An additional type of neurons, the CPU2 neurons (for nomenclature see Honkanen et al., 2019), then connects the central complex to the lateral complex, a set of neuropils that is further connected to other ganglia of the nervous system. From there neurites build a pathway into the thoracic ganglia to facilitate motor movement (Homberg, 1994).

Such small-field ramifications of columnar neurons divide neuropils of the central complex into 16 to 18 slices (Heinze and Homberg, 2008; Williams, 1975; Wolff et al., 2015). Together with a pattern of crossing fibres, comprising the anterior and posterior chiasma of the central complex, these divisions build the anatomical basis for central complex function (Honkanen et al., 2019).

The central complex has been linked to a multitude of functions from different domains of behavioural and sensory repertoires (see Honkanen et al., 2019; Pfeiffer and Homberg, 2014 for extensive reviews). However, the ancestral function of it is proposed to be navigational control (Heinze, 2017; Honkanen et al., 2019) where sensory information needs to be processed, compared to an internal state and output motor control constructed (e.g. Heinze and Homberg, 2007; Neuser et al., 2008; Strausfeld, 1999).

3.1.2.4. The central complex is developed by conserved cellular mechanisms

Comparative developmental research in insect brains is rare (Boyan et al., 2017; Farris and Sinakevitch, 2003). However, common cellular mechanisms, particularly well-studied for the central complex, have been identified that underlie development of brains in likely all insects. These are the development of clonally defined neural lineages (Boyan and Reichert, 2011; Ito and Awasaki, 2008; Stollewerk, 2016) and mechanisms of axogenesis (Boyan et al., 2015; Strausfeld, 2012).

Insect central brains are built up by about 100 neural stem cells (or neuroblasts) per hemisphere. Each neuroblast expresses a unique cocktail of transcription factors that is believed to cause production of a specific fate of the stem cell's offspring (Urbach and Technau, 2003b). Each of these 100 neuroblasts produces neural cells in a very stereotypical fashion (Izergina et al., 2009). Neuroblasts sit on the surface of the prospective brain cell body rind and produce progeny that are progressively more located into the middle of the brain (Hartenstein et al., 2008; Spindler and Hartenstein, 2010). Therefore, all offspring comprise a string of neural cells (Spindler and Hartenstein, 2010). Importantly, these neural cells stay in their position and produce common axonal projections that target similar functional areas of the brain (Williams and Boyan, 2008). Four of those 100 neuroblasts that are particularly well understood produce progeny that build up major parts of the central complex (Andrade et al., 2019; Boyan and Williams, 2011; Boyan and Reichert, 2011). These neuroblasts and their progeny carry synonymous names: DM1 (DPMm1, Z), DM2 (DPMpm1, Y), DM3 (DPMpm2, X), DM4 (CM4, W; Bello et al., 2008; Pereanu and Hartenstein, 2006; Williams and Boyan, 2008). DM1-4 produce nearly all columnar neurons of the central complex (Andrade et al., 2019). To achieve this high number of cells with only four neuroblasts, these neuroblasts have a specific mode of division. In contrast to other neuroblasts, they produce several intermediate progenitors that each produce ganglion mother cells that in turn divide into approximately 450 postmitotic cells per neuroblast (Bello et al., 2008; Boone and Doe, 2008; Boyan et al., 2010). Such neuroblasts, including DM1 - 4 (Boyan and Reichert, 2011; Izergina et al., 2009; Walsh and Doe, 2017), are referred to as type II neuroblasts.

A second conserved aspect of central complex development regards axogenesis of midline-positioned cells (Boyan et al., 2015, 2008). In all arthropods investigated, axons of cells likely belonging to homologs of the DM1-4 cluster, fasciculate in parallel commissures across the midline at the beginning of development. At 55 % of embryogenesis in *Schistocerca* and during early pupal phases in *Drosophila* (Boyan et al., 2017), axons particularly of DM1-3 defasciculate at stereotyped locations and re-fasciculate at more posterior points, i.e. they leave their axon bundle of origin to join another one. Because this pattern is repeated on both sides of the midline, the

result is a system of X-shaped, or decussating, tracts (Boyan et al., 2017). This pattern of axogenesis likely occurs in all arthropods, even independent of deviating mechanisms of neural stem cell development (Boyan et al., 2015).

These DM1-4 neural lineages have been compared and homologized between the prime model organisms for the central complex, *Schistocerca gregaria* and *Drosophila melanogaster* (Boyan et al., 2017; Boyan and Williams, 2011; Boyan and Reichert, 2011). Their development highlights the heterochronic shift between these species (Koniszewski et al., 2016; Pfeiffer and Homberg, 2014).

3.1.2.5. Central complex heterochrony – deviation from a common program?

The central complex of *Drosophila* is functionally an adult structure. While its structure is prefigured during embryonic and larval stages (Andrade et al., 2019; Riebli et al., 2013), it only acquires functionality during metamorphosis (Riebli et al., 2013; Young and Armstrong, 2010). Hence, larvae do not contain a functional central complex neuropil. In contrast, *Schistocerca*, an insect with incomplete metamorphosis (i.e. hemimetaboly), the central complex is functional and adult-like already after embryogenesis is completed (Boyan et al., 2017; Boyan and Liu, 2016).

An intermediate position is taken by a number of species (Panov, 1959), but best understood in the beetles *Tenebrio molitor* (Wegerhoff et al., 1996; Wegerhoff and Breidbach, 1992) and *Tribolium castaneum* (Koniszewski et al., 2016). Here, the upper division of the central body (CBU) was described to be present directly after embryogenesis, while lower division and noduli are still absent. The details of heterochronic appearance of central complex neuropils in such species are still not well described, however. This includes analysis of morphology and appearance of the protocerebral bridge, lower division of the central body and noduli, as well as pupal development. Further, most analyses so far were largely based on gross morphology of the neuropil but lacked cellular resolution.

While comparisons of central complex lineages have been made before (Boyan et al., 2017; Boyan and Reichert, 2011), a direct comparison of *homologous* neural cells over developmental time has been missing.

The wealth of knowledge on a) function, b) anatomy and c) the conserved cellular mechanisms behind the central complex and the lack of knowledge regarding cellular underpinnings of heterochrony offer the unique opportunity to investigate how modifications of common cellular mechanisms translate into heterochronic development. Such a comparative development needs to be based on the comparison of homologous cells.

3.1.2.6. A comparison of the development of insect brains using genetic neural lineages

How do we compare the development of insect brains, particularly the central complex? Through the conserved clonal architecture of the insect brain, comparison on the level of homologous neural lineages would promise to yield the most meaningful results (Boyan et al., 2017). Optimal requirements are a) marking development from neuroblast to adult structure (to monitor the complete developmental process) and b) marking of homologous cells (Koniszewski et al., 2016).

Both requirements can be fulfilled by using genetic neural lineages, an approach suggested by Koniszewski et al. (2016) and used for the first time in this study. Here, marking is based on the expression of a highly conserved transcription factor. A set of such transcription factors is almost exclusively expressed in anterior regions in embryos of evolutionary distant animals among the whole bilaterian clade (Arendt, 2008; Arendt et al., 2004; Davis et al., 2003; Denes et al., 2007; Eggert et al., 1998; Janssen, 2017; Kitzmann et al., 2017; Lichtneckert and Reichert, 2008; Lowe et al., 2003; Mathers et al., 1997; Mazza et al., 2010; Posnien et al., 2011; Steinmetz et al., 2010; Tosches and Arendt, 2013; Urbach and Technau, 2008). Because of this high degree of conservation between such divergent animals, we assume that expression patterns between different species of insects are especially conserved. Lastly, these transcription factors give identity to neuroblasts and resulting neural cells (Urbach and Technau, 2003b). Moreover, early development of the embryonic brain is likely conserved (Reichert, 2009; Urbach and Technau, 2003a). Taken together, marking all cells expressing such a conserved factor is likely to mark homologous cells from neuroblast to adult brain (Koniszewski et al., 2016). In order to mark such genetic neural lineages (i.e. cells marked by the same transcription factor), antibodies against transcriptions factors of choice need to be generated. To mark their projections, transgenic lines with a cytoplasmic fluorescent signal under control of a transcription factor need to be constructed (Koniszewski et al., 2016). The assumption is that by using genetic neural lineages we will mark homologous cells (Arendt, 2005; Reichert, 2009) from embryo to adult (Gold and Brand, 2014; Kraft et al., 2016; Kumar et al., 2009) such that development of these cells can be followed throughout large parts of development.

How homology of brain structures can be tested has been subject of long-standing debates (Arendt, 2005; Katz, 2007; Strausfeld and Hirth, 2016, and articles in the same issue). This includes that shared expression of a conserved transcription factor might not necessarily imply homology, as independent cooption of the same gene regulatory network is possible (Katz, 2007; Nielsen and Martinez, 2003). Therefore, to corroborate basic homology through conserved gene

expression, morphological criteria should be included (Koniszewski et al., 2016). For neurons in the brain, further criteria are cell body location and projection pattern. While the location of single cell bodies might be variable to some degree, through the clonal architecture of the insect brain we assume that if we compare groups of cell bodies instead of single cells, a conserved picture can be identified (such as in Boyan et al., 2017). Projection pattern is the third criterion. The central complex is a highly conserved neuropil, and its function is determined by conserved projection patterns (Boyan et al., 2017, 2015; Heinze and Homberg, 2008). Hence, a substantial deviation from a conserved pattern seems unlikely. Taken together, these three criteria allow us to formulate robust hypotheses of likely homology.

Neural lineages are challenging to mark from neuroblast to adult, even with a toolbox as large as in *Drosophila*. Hence, alternatives employed are mostly MARCM lineage marking or morphological identification using specific GAL4 lines (Larsen et al., 2009; Riebli et al., 2013). Although these tools yield exceptional results, they are not easily transferrable to other species. Alternatively, homology has been based previously on the expression of certain neuromodulators (Katz, 2007; Katz and Harris-Warrick, 1999). However, neuromodulators in insect brains are expressed late (Boyan and Liu, 2016; Herbert et al., 2010; Pfeiffer and Homberg, 2014) and their expression would not mark earlier developmental stages.

Therefore, as previously suggested (Koniszewski et al., 2016), we will display data identifying genetic neural lineages in genetic and morphological homologous cell groups in the two species *Tribolium* and *Drosophila*.

3.1.2.7. Using *Tribolium* and *Drosophila* as model systems for a comparison based on a common toolkit

This strategy can be only achieved in particularly genetically amenable species. While *Drosophila* is the gold standard with reference to the plethora of tools available (Çelik and Wernet, 2017; Hales et al., 2015), *Tribolium castaneum*, the red flour beetle, has been developed as an alternative genetic insect model species in recent years (Pai, 2019). A well-annotated genome Richards et al., 2008), systemic RNAi (Bucher et al., 2002), piggyBac transposition (Berghammer et al., 1999; Trauner et al., 2009), UAS-GAL4 system (Schinko et al., 2010), in-vivo imaging (Sarrazin et al., 2012; Strobl and Stelzer, 2014) and CRISPR (Gilles et al., 2015) are all established.

Similar tools are therefore available in both species to mark the same genetic neural lineages.

3.1.2.8. Retinal homeobox as a marker of genetic neural lineages

A set of conserved transcription factors has been previously identified (e.g. (Posnien et al., 2011). Of those, the paired-like homeobox protein *retinal homeobox* (*rx*, *Drosophila*: CG10052; *Tribolium*: TC009911) is particularly useful to identify homologous lineages contributing to the central complex. It is expressed in the anterior median region in all bilaterian embryos investigated (Arendt, 2008; Arendt et al., 2004; Davis et al., 2003; Eggert et al., 1998; Janssen, 2017; Mathers et al., 1997; Mazza et al., 2010; Posnien et al., 2011). Moreover, loss-of-function phenotypes include a modification of the central complex in both *Drosophila* and *Tribolium* (Davis et al., 2003; Koniszewski, 2011), making it likely that *rx* is expressed in central complex contributing cells. Interestingly, lethality of loss-of-function animals corresponds to the heterochrony observed as *Tribolium* individuals die as L1 larvae, which already show a functional central complex neuropil while *Drosophila* specimens die as pharate adults where the central complex becomes functional for the first time. Therefore, *rx* is a suitable gene to mark genetic neural lineages by generating specific antibodies and transgenic lines.

3.1.2.9. Homologous Rx genetic neural lineages mark the developing central complex and illustrate the complex nature of the heterochronic shift

In this work we developed tools for comparative Rx labelling and used these to follow columnar neurons contributing to the central complex throughout development. Using this approach, we determined several heterochronic shifts in certain steps of central complex development. Unexpectedly, we also found a deviation from the order of conserved events. Against previous assumptions, we propose that the *Tribolium* larval central body is distinct to the adult form in its anatomical characteristics and the developmental events that cause its appearance. Hence, from our data we conclude that the larval central body is a precociously developed form, present before any larval growth period, but being functional already. Data provided will contribute to the question how conserved cellular mechanisms of central complex development are and offer a new approach of marking neural lineages to identify homologous neurons across species (Boyan and Reichert, 2011). Moreover, our investigations open up the larval central complex of *Tribolium castaneum* as a target of future scrutinized examination to further the understanding of central complex development and evolution.

3.1.3. RESULTS

3.1.3.1. Tools that mark Rx genetic neural lineages in two species

In order to identify homologous genetic neural lineages, we first needed to mark Rx expressing cells and their projections in both *Drosophila melanogaster* and *Tribolium castaneum*. To that end, we developed and characterised suitable tools. First, we generated and validated an antibody for *Tribolium* Rx (Tc-Rx) (Supplementary Figure 3.1–1) and used a previously published antibody targeting *Drosophila* Rx (Dm-Rx) (Davis et al., 2003). Next, we identified an enhancer trap in the *Tc-rx* locus from the GEKU enhancer trap screen (Trauner et al., 2009) and confirmed coexpression of EGFP with Tc-Rx (Supplementary Figure 3.1–1). The enhancer trap marked only a 5-10 % subset of Tc-Rx-positive cells but all EGFP-positive cells – except the eye marker – were Tc-Rx positive as well (Supplementary Figure 3.1–2). As appropriate imaging lines were missing in *Drosophila* (see 3.1.5 Material and Methods), we generated an imaging line using CRISPR/Cas9 mediated homology-directed repair. We replaced the endogenous stop codon with a P2A peptide followed by an EGFP coding sequence. Hence, a bicistronic mRNA had been transcribed and subsequently translated into separate Dm-Rx and EGFP proteins (Supplementary Figure 3.1–3). These tools allowed us to identify Rx expressing cells and their projections in order to reveal a specific group of homologous lineages.

3.1.3.2. Rx is expressed in conserved domains in adult brain and embryo

We first wanted to identify conserved and potentially homologous domains of Rx expression in the brain of *Drosophila* and *Tribolium* in general, and particularly those associated with the central complex. For this, we performed antibody stainings against Rx in the adult brain (Figure 3.1–1A, B) and embryo (Figure 3.1–1C, D). Note that axes of the brain relative to body axes are not conserved in insects. Hence, our comparison between species was based on the neuraxis. Essentially, '*Drosophila* posterior' becomes neuraxis-dorsal while '*Drosophila* anterior' equals neuraxis-ventral (Figure 3.1–1, Supplementary Figure 3.1–4 for orientation of brains and definitions of neuraxes in both species).

Antibody staining revealed a conserved pattern of Rx-positive neural cells in both species at both time points. We identified four Rx-positive domains at similar regions in both species' adult brains (Figure 3.1–1A, B). In the n-ventral fraction of the brain (Figure 3.1–1 A^{i} and B^{i}), there was an n-anterior-lateral domain (I). Another domain was positioned n-anterior-medially to the antennal lobe (II). In the n-dorsal fraction (Figure 3.1–1 A^{ii} and B^{ii}), there was a domain lateral to the protocerebral bridge (III) and a fourth near the midline adjacent to the protocerebral bridge

(IV). The large degree of similarity of the location of Rx-positive neural cell groups suggested that these domains could be homologous between the species.

In embryos of both species, Rx was expressed in the labrum (white arrowheads in Figure 3.1–1 C, D) as well as the anterior-lateral part of the neuroectoderm and the prospective brain (white arrows in Figure 3.1–1 C, D). Note that while *Tribolium* embryos were prepared such that the prospective brain hemispheres lied flat, the *Drosophila* head remained in its original position. Brain lobes were folded and thus nearer to each other than in *Tribolium* (bend and zipper model, Posnien et al., 2010). Considering these morphological differences, the expression patterns were very similar.

In summary, Rx antibody staining revealed domains of expression in the embryo and adult brain that were conserved between both species at both the start and endpoint of development.

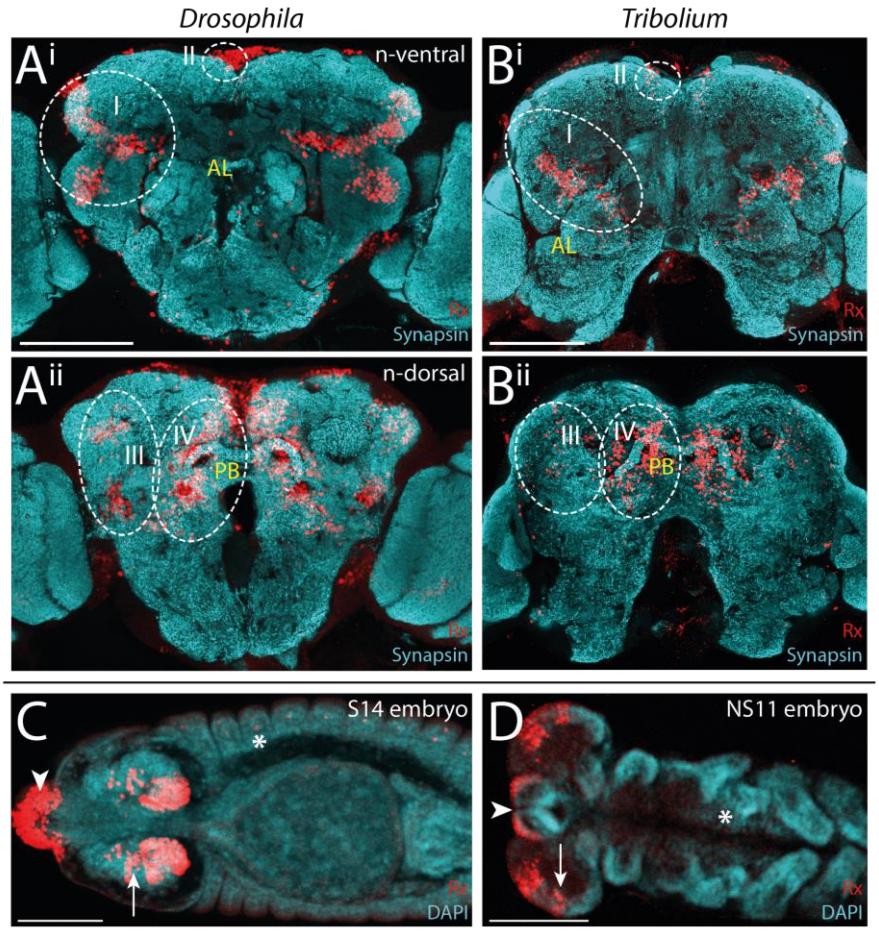

Figure 3.1–1: Rx expression is conserved in *Drosophila* and *Tribolium* adult brains (A, B) and embryos (C, D). A, B: Immunostainings against Rx and synapsin in both species revealed four large domains of Rx expression (I-IV, dotted white lines). These were characterized by their shape and position relative to the rest of the brain, revealed by synapsin-positive areas. Two domains were found on the n-ventral side (i) and two on the n-dorsal side (ii). For a more detailed description and tentative links of these transcription factor expression domains to known neural lineages, see Supplementary Figure 3.1–5 and Supplementary Table 3.1–1. **C, D:** In the *Drosophila* (S14) and

Tribolium embryo (NS11), two main conserved domains of Rx expression were detected. There was strong expression in the labrum (arrowhead), in the neuroectoderm and prospective larval brain (arrow). In addition, single cells were marked in the peripheral nervous system and ventral nerve cord (asterisk; for *Tribolium* see Supplementary Figure 3.1–1). Abbreviations: AL antennal lobes, PB protocerebral bridge, CB central body, n neuraxis-referring, S stage (Campos-Ortega and Hartenstein, 1985), NS neurogenesis stage (Biffar and Stollewerk, 2014). Scale bars represent 100 μm.

3.1.3.3. Identification of Rx-positive neural cell clusters and a group of homologous lineages

We then sought to identify homologous cell clusters contained in the four Rx domains. For this, we mapped cell body locations and projection patterns to previously described neural lineages of the *Drosophila* brain (Supplementary Figure 3.1–5, Supplementary Table 3.1–1; Lovick et al., 2013; Wong et al., 2013). Neural lineages constitute developmental and functional units of the brain (e.g. Omoto et al., 2017) and are suitable identifiers for further characterisation and identification of homology (Boyan et al., 2017). The assignment was based on location of Rx-positive cell clusters– relative to each other and to synapsin-marked neuropils – and their projection patterns visualized by EGFP from our transgenic lines. Thus, three criteria were used to then identify cell clusters homologous between *Drosophila* and *Tribolium*: Rx expression, cell body location and projection pattern.

We identified Rx-positive cell clusters in eleven previously characterised neural lineages (Lovick et al., 2013; Wong et al., 2013; Supplementary Figure 3.1–5, Supplementary Table 3.1–1). All of them were present in both species' brains, hence no species-unique lineages were identifiable. Of these eleven lineages, four in *Drosophila* and seven in *Tribolium* were only partially or not at all marked by pronounced projections (Supplementary Table 3.1–1). The identification of these seven in *Tribolium* was based mainly on knowledge of *Drosophila* neuronal lineages and is therefore tentative (see 3.1.9.3 Supplementary Results for details on assignments).

We thus propose that Rx expression can be linked to eleven neural lineages in the adult *Drosophila* brain and tentatively also to the *Tribolium* brain. Lineages had similar cell body positions, and – where visible – projection patterns. The lineages DM1-4 (Supplementary Figure 3.1–5, Supplementary Table 3.1–1) were particularly well marked in both species with prominent projections into all neuropils of the central complex. Hence, they were subjected to a detailed analysis of cell body location and patterns of projections, to in turn corroborate their homology between *Drosophila* and *Tribolium*.

3.1.3.4. Rx transgenic lines mark homologous groups of columnar neurons belonging to lineages DM1-4

To test the provisional homology of Rx-positive DM1-4 cell clusters established before and to offer a basis for a subsequent comparison throughout development, we made detailed scans and 3D reconstructions. With these, we were able to confirm a similar cell body location (Figure 3.1–2 A, B, G^{i}, H^{i}, see 3.1.9.3 Supplementary Results for a detailed description of their sub-groups) and similar projection pattern (Figure 3.1–2 C-F, G^{ii}, H^{ii}) of Rx-positive cell clusters belonging to the DM1-4 lineages. In both species Rx-positive DM1-4 cell clusters projected from stereotypical cell body positions around the protocerebral bridge into distinct fibre bundles and into the central body and noduli. In detail (see Figure 3.1–2 A, B, G, H), DM4 cell bodies lay around the lateral tip of the protocerebral bridge and their axons projected n-ventrally through the medial equatorial fascicle (MEF) (Note that partially overlapping with the DM4 cell group were cell clusters belonging to lineages DM5/6, with only faintly visible projections, however; Supplementary Figure 3.1–5, Supplementary Table 3.1–1; 3.1.9.3 Supplementary Results). Cell bodies of DM2/3 were near each other at the more n-antero-lateral point of the protocerebral bridge. Their axons both projected in distinct tracts through the dorsal root of the CBU (dlrCBU, also dlrFB; Riebli et al., 2013). Cell bodies of the DM1 lineage lay next to the midline and particularly in *Drosophila* more n-antero-laterally to the protocerebral bridge. They projected through the medial root of the CBU (mrCBU, also mrFB, Riebli et al., 2013). Note that the fibre bundles MEF, dlrCBU and mrCBU have not been annotated previously in the *Tribolium* brain. We based our annotations on the characterisation of DM1-4 lineage group projections, as well as the typical anatomical position of fibre bundles (see Dreyer et al., 2010 for previously annotated regions and neuropils in the *Tribolium* brain). In both species, fascicles of these cell clusters projected into the CBU sequentially from n-dorsal to n-ventral (first DM1, then DM2, DM3 and most n-ventrally, DM4; see Figure 3.1–2 G^{ii} and H^{ii}) and made up the posterior plexus of the CBU (CBUppl, FBppl in Andrade et al., 2019).

The DM1-4 lineage group make up the columnar neurons of the central complex almost exclusively (Andrade et al., 2019; Boyan and Williams, 2011) and have been homologized previously between *Schistocerca gregaria* and *Drosophila melanogaster* (Boyan et al., 2017). Indeed, all cell clusters connected the protocerebral bridge, where each cell cluster had parts of their dendrites, to the other parts of the central complex, in particular the CBU and noduli (Figure 3.1–2 C, D) and to lesser extent the CBL (Figure 3.1–2 E, F). Note that the *Drosophila* bicistronic line marked all Rx-positive cell bodies resulting in thicker tracts, while the *Tribolium* enhancer trap

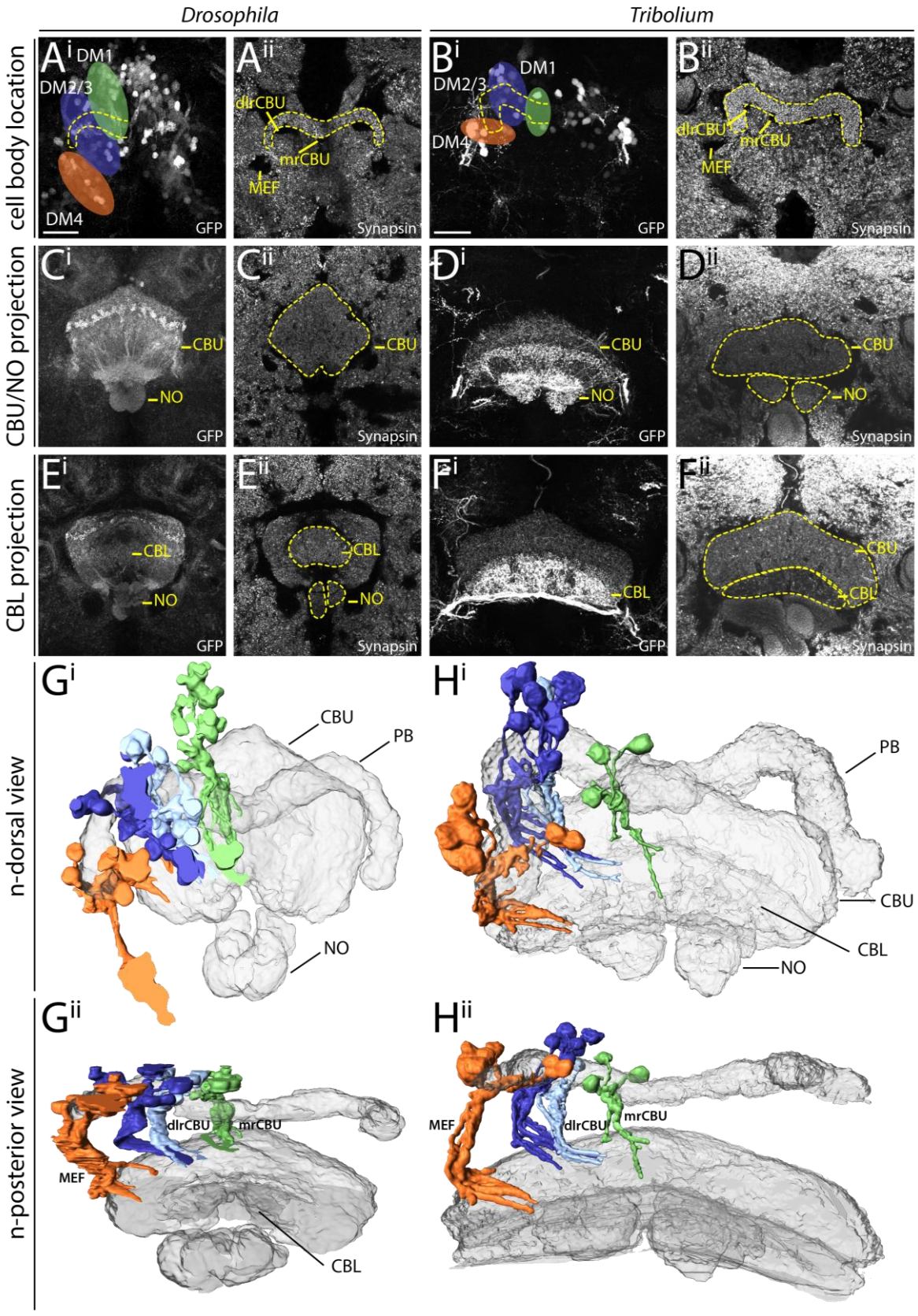

Figure 3.1–2: Homologous Rx cell clusters contribute to the central complex columnar neurons of lineages DM1-4. A to F depict parts of stacks on which the 3D reconstructions in G and H are based. Homology of cell clusters (and simultaneous identification of the respective lineages) was established using three criteria. First, cells needed to express Rx so that clusters qualified as genetic neural lineages. All cells depicted and reconstructed

expressed Rx. Second, these cell groups shared distinct cell body locations and third, they needed to share similar projection patterns. **A, B:** The stereotypical positioning of cell groups of lineages DM1-4 around the protocerebral bridge (marked by yellow dotted line in A^i and B^i) are shown for *Drosophila* (A) and *Tribolium* (B). **C, D:** The resulting pattern of GFP expressing neurites of these cell groups is depicted for the CBU and NO fraction. **E, F:** Much less signal was found in the CBL fraction. Note that the *Tribolium* DM4 group had a very high GFP expression level, so that those projections were particularly visible in the CBL (see Supplementary Figure 3.1–2 for transgenic line information). Respective central complex neuropils are outlined with yellow dotted lines and identified by yellow descriptors. **G, H:** 3D reconstructions of a synapsin background stain in grey-transparent and of those homologous cell clusters where we could clearly identify connections between neurites and cell bodies. G depicts an n-dorsal view as this is the same plane as shown in A-F, and H depicts an n-posterior view, and thus the similarity in projection into the central complex. In both species each cell cluster belonging to a certain lineage had a stereotypical position. DM1 (green) projected from a medial position at the protocerebral bridge through the mrCBU; DM2/3 (blue shades) shared a fibre tract coming from the n-antero-lateral tip of the protocerebral bridge through the dlrCBU. DM4 (orange) projected from the n-postero-lateral tip of the protocerebral bridge through the MEF into the central complex. Due to the large number of marked cells, the projections could not be followed further. GFP channels (i) are maximum intensity projections, while synapsin channels (ii) are SMEs (Shihavuddin et al., 2017). Abbreviations: DM dorso-medial lineage, CBU upper division of the central body, dlrCBU dorsal root of the CBU (in other publications, dlrFB, see Andrade et al., 2019), mrCBU medial root of the CBU (in other publications, mrFB, see Andrade et al., 2019), MEF medial equatorial fascicle, NO noduli, CBL lower division of the central body. Scale bars represent 25 μm and apply to all panels of each species.

marked only a subset of the Rx expressing DM1-4 cells. The projections were, thus, fewer and marked tracts thinner. During development, though, the number of Rx/GFP-positive DM1-4 cell clusters increased in *Tribolium* (see Figure 3.1–5 and 7 in particular), resulting in thicker projections. Notably, the *Tribolium* DM4 Rx expressing group showed a very high GFP expression, so that the projections into the CBU, noduli and CBL as well as the connections to the LAL (lateral accessory lobes) appeared much stronger than in *Drosophila* (Figure 3.1–2 B/D/F^i). Rather than reflecting a different projection pattern, it was likely a particularity of the *Tribolium* enhancer trap. Note also that single tracts could hardly be assigned when inside the neuropils.

Classification of Rx expressing cell clusters in the *Drosophila* brain was aided additionally by performing Rx immunostainings in the R45F08-GAL4 line (Supplementary Figure 3.1–6), a pointed GAL4 enhancer construct that marks secondary neurons of the DM1-3 and 6 lineages (Riebli et al., 2013). This analysis revealed that approximately 90 % of R45F08-GAL4 marked cells also express Rx. Further, we crossed the Rx-GFP bicistronic line to the R45F08-GAL4 line to score overlap in projections. Indeed, R45F08 projections seemed to be a subset of Rx-GFP projections.

In summary, 3D reconstructions revealed that transgenic lines of both species mark Rx expressing cell clusters that share a similar cell body location and show similar stereotypical projection patterns. They connect the different neuropils of the central complex with each other

and are thus classified as columnar neurons and hence part of the DM1-4 lineage group. We conclude that these Rx expressing cell clusters are homologous between both species and therefore suitable to compare heterochronic central complex development.

3.1.3.5. Comparison of developmental time between *Drosophila* and *Tribolium*

For the cross-species comparison of central complex development, we examined how long *Drosophila* and *Tribolium* occupied the phases of embryogenesis, larval stage and metamorphosis. *Drosophila* completes its development at 25°C in nine days (24 hours in embryogenesis, 75 hours in larval and 100 hours in pupal development, in our transgenic line) while *Tribolium* takes approximately 27 days at 32°C (72 hours in embryogenesis, 432 hours/18 days as larva and approximately 140 hours/six days in pupation, in our transgenic line), hence three times as long as *Drosophila*. The relative portion each animal stays in larval development and pupation are divergent as well. While larval development in *Tribolium* takes 65 % of total developmental time, for *Drosophila* it takes 40 %. As a result, *Tribolium* pupation is shorter, spanning approximately 21 % of development time while *Drosophila* pupation occupies 50 %.

3.1.3.6. DM1-4 lineages produce divergent central complex structures in the freshly hatched L1 larva of *Drosophila* and *Tribolium*

We revealed that Rx-positive cell clusters belonging to DM1-4 lineages build up a very similar projection of the adult central complex, with similar cell body location and typical projection. We then asked how this conserved picture was reflected in the larval hatchling and how it related to the central complex heterochrony, i.e. the early appearance of a central body in *Tribolium* and the absence of functional central complex neuropils in *Drosophila* larvae (Andrade et al., 2019; Koniszewski et al., 2016). For this, we examined the DM1-4 group and their projections in the first instar larval brain.

For this we dissected L1 larvae, less than one hour old, and stained brains in similar fashion as adult brains (see 3.1.5 Material and Methods). The position of brains and scans differed between species (Figure 3.1–3 A-D), and thus also the position of DM1-4 cell clusters (Figure 3.1–3 E/F^{i}). The *Drosophila* brain was scanned from dorsal and respective n-anterior surface to ventral/n-posterior, while *Tribolium* was scanned from n-dorsal to n-ventral. In *Drosophila* L1 larvae, spatial arrangement of cell bodies and projections of the DM1-4 group differed from the adult (Figure 3.1–3 E^{i}) and no functional neuropil was present (Figure 3.1–3 E^{ii}), which could

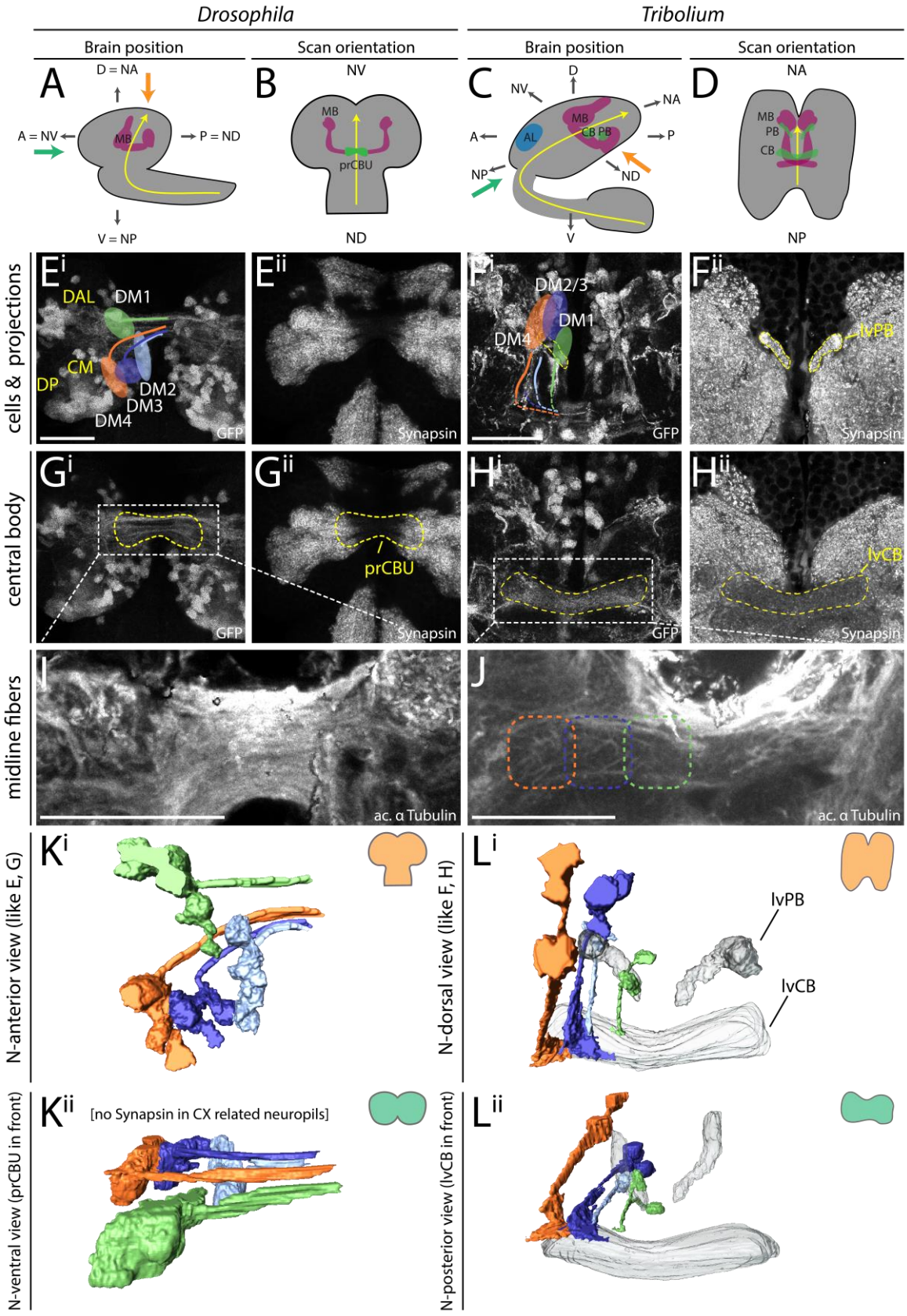

Figure 3.1–3: Rx cell clusters of the DM1-4 lineages in L1 brains of *Drosophila* and *Tribolium* show a different pattern of projection and innervate a differently developed central complex. A, C: The *Drosophila* (A, B, E, G, I, K) and *Tribolium* (C, D, F, H, J, L) L1 brain is positioned differently in the respective head, as displayed by a sketch of a lateral view. Indicated are body and neuraxes, with additional indication of the larval MB (magenta),

AL (blue), CB and PB (green) and the neuraxis position (yellow arrow). A thick orange arrow indicates the direction of the performed scan starting from n-anterior in *Drosophila* and n-dorsal in *Tribolium* displayed in panels E,G,I,K[i] and F,H,J,Li, respectively. A thick green arrow indicates the orientation in I/J[ii] which is displayed such that in both cases the central complex structure is in front. **B, D:** The resulting scan orientation is depicted with a rough sketch of the outlines of the respective L1 brains. **E-L:** Analysis of Rx cell clusters of the DM1-4 lineage group and underlying structures revealed species differences in cell cluster position and projection as well as neuropil architecture. In *Tribolium*, arrangement and projection were similar to the adult, while in *Drosophila* it differed strongly. Synapsin staining revealed absence of any central complex neuropils in *Drosophila* and presence of larval central body and protocerebal bridge in *Tribolium*, while acetylated α-Tubulin staining revealed a stack of parallel fibers in *Drosophila* and an already decussated structure in *Tribolium*. **E-H:** Projections (SME, Shihavuddin et al., 2017) of a L1 brain stained against GFP (i) and synapsin (ii) were depicted to show position of cells and tracts belonging to the homologized DM1-4 lineages (E, F) as well as their projection into the prospective central body (G, H). In F[i/ii], dotted lines indicate synapsin-positive central complex neuropils in *Tribolium* (dotted lines in F[i] indicates interpreted projection) and in G[i/ii] approximate position of the primordium in *Drosophila*. In addition, in E[i] the approximate position of other lineage groups of the *Drosophila* brain are shown, i.e. dorso-antero-lateral (DAL), dorso-posterior (DP) and centro-medial (CM) lineages (yellow). **I, J:** Anti-acetylated-α-Tubulin immunostaining (N=2 for *Drosophila* stainings) revealed globally a differing architecture of the central body region in both species, mirroring the data revealed by anti-GFP and anti-synapsin stainings. While the *Drosophila* midline-spanning fibers build up a thick stack of fascicles, containing the future central body, in *Tribolium* the functional central body contains already decussated fibers (note, however, the differing degrees of such pattern in comparison to decussated fibers during metamorphosis, Fig. 8). **K, L:** Cells indicated in E and F and their projections were 3D-reconstructed to depict the spatial relationship between the lineages and highlight the differences between the species. Since the brains were scanned from different positions, the resulting positioning of the 3D reconstructed surface was different. Upper panels (i) are the same orientation as in the projections in E-H, while the lower panels (ii) are oriented such that the prCBU and lvCBU are in front (see green arrow in A and C). Synapsin-positive neuropils are depicted in grey transparent in L. Abbreviations: n neuraxis-referring, D dorsal, A anterior, V ventral, P posterior, MB mushroom bodies, prCBU primordium of the CBU (in other publications prFB, Andrade et al., 2019), CBU upper division of the central body, PB protocerebral bridge, AL antennal lobes, DM dorso-medial lineage group, lv larval. Scale bars represent 25 μm.

have aided the localization of respective cell clusters. Further, many other lineages were marked as well, such as the dorso-antero-lateral (DAL), dorsoposterior (DP) and centromedial (CM) lineages (Figure 3.1–3E[i]). This made the assignment of cell clusters to DM1-4 lineages more difficult. We therefore used recent lineage classifications based on EM data as guide (Andrade et al., 2019), with emphasis on their anatomical position to each other and how they are situated in the brain (Figure 3.1–3E/K[i]) and were thus able to identify cell clusters belonging to the DM1-4 lineage group. In specific, lineages DM2 and 3 lay more dorsal than DM1 and 4, with DM1 being anterior and DM4 most posterior (Figure 3.1–3E/K, in accordance with Andrade et al., 2019). Note that DM1 cells lay n-ventral/anterior (up in panels E and G) to the midline projections, while DM2-4 cells lay n-dorsal/posterior (below). DM2 and 3 were situated more medially while DM4 lay slightly more lateral with the other lineages belonging to the CM cluster.

In *Tribolium*, we observed an arrangement of cell clusters similar to the adult, close to a larval protocerebral bridge (Figure 3.1–3F). We could therefore assign cell clusters to the DM1-4

lineages. Specifically, DM4 was the most lateral and most n-dorsal, DM2/3 were n-ventro-medial to the DM4 group, and most n-ventro medial lay DM1 (Figure 3.1–3F/K[i]).

The projections these cell groups produced were very different in the two species (Figure 3.1–3 G/H). In *Tribolium*, the columnar neurons crossed through a functional, albeit unfused, larval protocerebral bridge (lvPB, see Figure 3.1–3 F) and formed a common projection across the midline that consisted of fascicles n-dorsally, and slightly more n-ventrally formed a synapsin expressing functional neuropil, the larval central body (lvCB, see Figure 3.1–3 H). Note that we were not able to detect any synapsin-negative fibre bundles that would be reminiscent of the mrCBU, dlrCBU and MEF through which the DM1-4 lineages project in the adult. In contrast to *Tribolium*, DM1-4 groups in *Drosophila* formed a common projection that crossed the midline forming later the primordium of the CBU (prCBU, or prFB, see Andrade et al., 2019, Figure 3.1–3 G), constituting a bundle of fascicles. This structure was not functional judged by the absence of any presynaptic sites (see absence of synapsin staining in Figure 3.1–3 E/G[ii]). Likewise, we did not detect a synapsin-positive structure, which could represent a larval PB (synapsin marked lvPB and lvCB are marked in grey in Figure 3.1–3 L; due to their absence in *Drosophila* there was no grey neuropil marked). Moreover, a staining against the global axonal marker acetylated α-Tubulin revealed that all midline-spanning structures in *Drosophila* resemble a stack of parallel fibres, confirming what we detected with an anti-GFP staining (Figure 3.1–3 I). The same staining in *Tribolium* revealed a pattern of crossing, decussated fibres in the larval central body, corroborating the necessity of decussation for a functional neuropil ((Figure 3.1–3 J). Importantly, these decussations were not detectable in the anti-GFP staining, in contrast to pupal decussation patterns (Figure 3.1–8), highlighting that larval decussation possibly resembles a lower degree of crossing.

A comparative analysis of Rx-positive cell clusters belonging to the DM1-4 lineage thus revealed that these cells make up a previously described primordium for the CBU in *Drosophila*, but in *Tribolium* make up a functional larval central body with small decussations, and project through a functional larval protocerebral bridge. Hence, while adult structures of the central complex are highly similar, structures in the L1 brain are different.

3.1.3.7. Comparative late embryonic development reveals a delay in *Tribolium* to build up midline-crossing structures

We next asked when the differences in the larval central complex emerge during embryonic development in Rx-positive DM1-4 cell clusters.

For this, we defined three main events as most relevant for subsequent central complex development, i.e. a first axon projection emerging from marked cell groups, first midline-crossing projection and first emergence of a projection that is comparable to the larval projection pattern. We then screened embryos for the first occurrence of said events in Rx/GFP double-positive cells. Note that a staging of late embryonic development after 48 hours (Biffar and Stollewerk, 2014) is missing so far in *Tribolium*, so that we speak of 'at least' NS15 in F^{ii} and use the relative developmental time of 81 % preferentially. In both species we saw first axons forming at similar points in relative embryonic development (Figure 3.1–4 A, B, *Drosophila* 37 %, *Tribolium* 39 %). The appearance of a first midline-crossing projection appeared earlier in *Drosophila* than in *Tribolium* (Figure 3.1–4 C, D, *Drosophila* 43 %, *Tribolium* 58 %). Also, a first larval-like projection, based on which Rx/GFP-positive cell clusters could again be assigned to DM1-4 lineages, appeared earlier in *Drosophila* (Figure 3.1–4 E/F, *Drosophila* 51 %, *Tribolium* 81 %). Assigning Rx-positive cell clusters to the DM1-4 lineage group before late embryonic stages such as 51 % (S15) was not unambiguously possible in neither species. We tentatively indicated the location of DM1 in Figure 3.1–4C. Also, we indicated the location of a medial cell, which could belong to the DM1 group in Figure 3.1–4B^{i} and D^{i}.

We conclude that while both species start with axonal projections at a similar relative point in time, they diverge from each other at crucial events of central body development. Specifically, midline-crossing events and further development to a larval-like structure are delayed in *Tribolium* embryonic development compared to *Drosophila*.

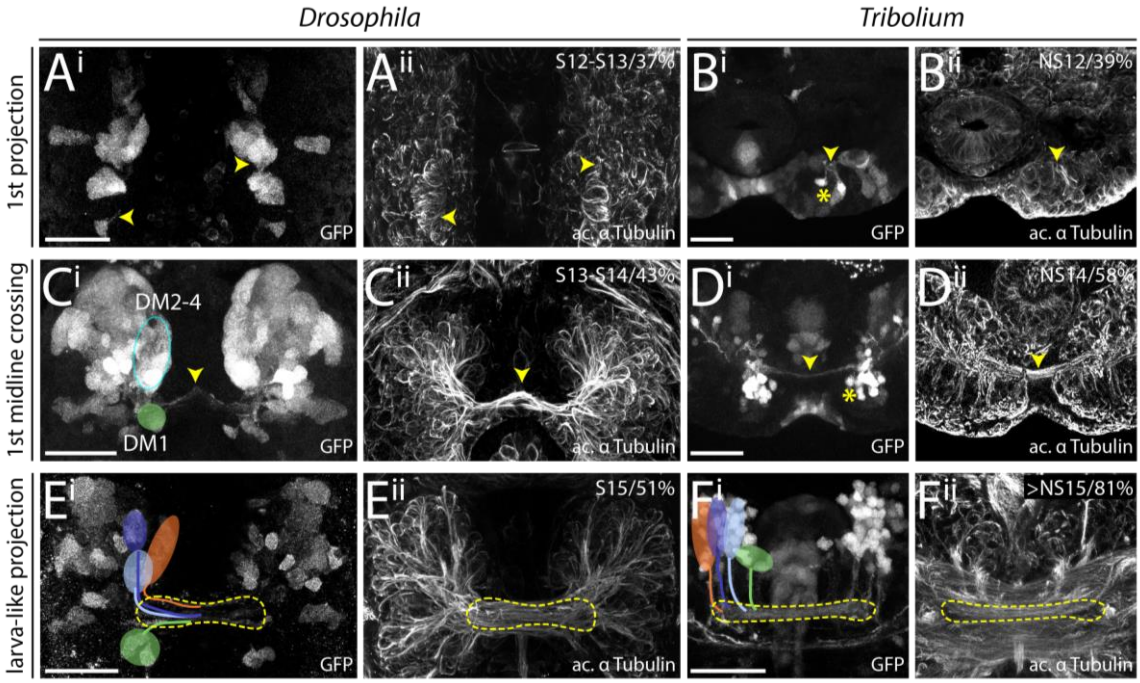

Figure 3.1–4: Comparison of late embryonic development of Rx cell clusters that contribute to midline-crossing groups reveals a partial delay of projection development in *Tribolium* embryos. A, B: Development of first axons happened at similar time frames in *Drosophila* and *Tribolium*. **C-D:** First midline-crossing fibers appeared earlier in *Drosophila* than in *Tribolium*. **E-F:** A development of a larva-like projection was delayed in *Tribolium*. Where possible, we assigned cell clusters to DM1-4 lineages (colour-coded as previously). Shown are projections (SME in D^{ii}, E^{i}) of stainings against GFP (^{i}) and acetylated α-Tubulin (^{ii}). Stages and the percentage of embryogenesis completed are shown in the upper right corner of acetylated α-Tubulin (^{ii}) panels. Stages in *Drosophila* correspond to Campos-Ortega and Hartenstein (1985) and in *Tribolium* to Biffar and Stollewerk (2014). Yellow arrowheads indicate first axons in A and B, verified by acetylated α-Tubulin staining, and show midline-crossing tracts that belong to Rx expressing cell groups in C and D. Asterisks in B^{i} and D^{i} likely indicate the same group of cells present at both stages. In C^{i} the likely position of lineages DM1 (green) and DM2-4 (blue oval form) are indicated. In E and F, identified Rx cell clusters belonging to DM1-4 lineages are indicated (green, light blue, dark blue and orange) as well as the formed tracts into the embryonic anlagen of the central body (yellow dashed line). Posterior is up, except for in panel F. Scale bars represent 25 μm and apply to panels i and ii.

3.1.3.8. During the larval period, central complex structures grow but do not change basic morphology

We asked next how the structures of the central complex built during embryogenesis (Figures 3 and 4) change during the larval period.

We examined the position of cell clusters and their projections at 50 % (Figure 3.1–5 A-D) and at the end of the larval period (Figure 3.1–5 E-H). In both species, we observed growth of central complex structures. In *Drosophila*, the primordium of the CBU increased in thickness, particularly from 50 % to the end of larval development (compare Figure 3.1–5C^{i} to G^{i}). The prCBU remained devoid of synapsin-positive staining (Figure 3.1–5 C^{ii}, G^{ii}). The position of cell body groups changed, however. From L1 (Figure 3.1–3 E^{i}) into 50 % of larval development (Figure 3.1–5 A^{i}), cell groups belonging to the DM2 and 3 lineages got shifted n-ventrally, taking

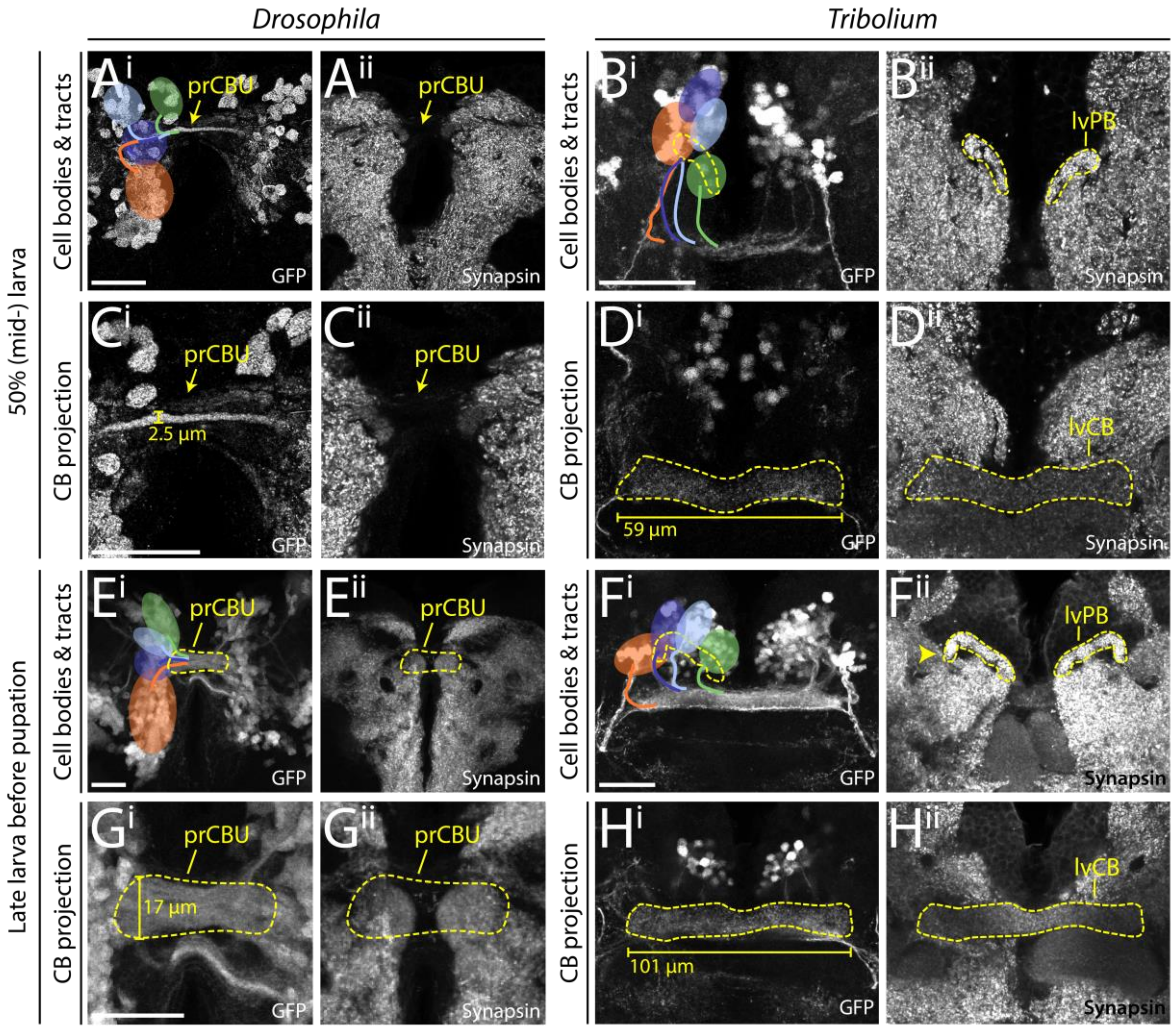

Figure 3.1–5: Comparison of development of DM1-4 Rx cell clusters shows substantial growth of the prCBU and larval central complex neuropils, alongside an increase of DM1-4 offspring. During larval stages the identified cell clusters and their projections retained their position, but proliferated so that larger cell clusters and thicker and larger projections were built. Depicted are projections (SMEs in A, B^{ii}, C, D, F^{ii}, H^{ii}, Shihavuddin et al., 2017) of immunostainings against GFP (^{i}) and synapsin (^{ii}) at mid-larval stages (**A-D**, 50 % of larval developmental time) as well as late larval stages before pupation (**E-H**). *Tribolium* mid-larval stage is represented by N = 2 individuals. Approximate position of cells and their tracts belonging to each lineage of the DM1-4 cluster are marked in respective colors (DM1 green, DM2 light blue, DM3 dark blue, DM4 orange). In addition, neuropils of the *Tribolium* larval central complex are contoured by yellow dotted lines (B, D, F, H). The primordial CBU (prCBU, previously prFB, see e.g. Andrade et al., 2019) of the *Drosophila* larval brain is contoured at the late larval stage (E, G), and its position is marked by a yellow arrow at 50 % larval development (A, C). Bars in C, D, G and H indicate the size increase of midline structures. In *Drosophila*, the prCBU increased in width from 2.5 to 17µm from 50 to 95 % of larval development. In L1, the prCBU is non-distinguishable from other midline-crossing structures using the Rx-GFP line. The *Tribolium* central body of the L1 brain displayed in Figure 3.1–3 was 51.6 µm long, the mid-larval lvCB was 58.7 µm and the late larval lvCB was 100.9 µm long. For *Drosophila* n-ventral and for *Tribolium* n-anterior is up (see Figure 3.1–3 for details). Abbreviations: prCBU primordium of the upper division of the central body, lvPB larval protocerebral bridge, lvCB larval central body. Scale bars represent 25 µm and apply to panels i and ii and in case of *Tribolium* to D and H respectively.

a position in between DM1 and DM4. DM2 shifted the most, so that it was situated lateral to DM1 at 50 %. The positions changed again from 50 % to the end of larval development (~ 95 %) (Figure 3.1–5 E^{i}) where cell clusters became arranged in one line along the neuraxis, DM1 most n-ventral, DM4 most n-dorsal.

In *Tribolium*, the projection grew in length and thickness (Figure 3.1–5 D^{i}, and 5 H^{i}) as did synapsin-positive central complex neuropils (Figure 3.1–3 F/H^{ii}, 5 B/D^{ii}, and 5 F/H^{ii}). In addition, the position and shape of the protocerebral bridge changed. Specifically, while in L1 and 50 % larval brains the protocerebral bridge was more oriented along the n-anterior/posterior axis, in late larval brains, it was shifted more into a perpendicular position. In addition, a lateral bend formed (arrowhead in Figure 3.1–5 F^{ii}). The modification of shape during the larval period corresponded with changes observed in the DM1-4 cell clusters. From L1 to 50 %, the positions remained highly similar (Figure 3.1–3 F^{i}, 5 B^{i}, and 5 H^{i}). From 50 % to the end of the larval period, DM4 got positioned at the lateral bend of the protocerebral bridge most laterally while DM1 became located most medially. In both species' larval brains, we qualitatively observed an increase in number of cells contributing to central complex projections (e.g. compare right hemispheres in Figure 3.1–5 A^{i} to E^{i} and B^{i} to F^{i}).

We conclude that the larval period of central complex development is mainly characterised by an increase in cell number and growth of the innervated central complex structures. Apart from a minor shift of cell bodies, the established structure of the L1 brain is mostly maintained during the larval period. Importantly, the *Drosophila* central complex precursor structures remain synapsin-negative while in *Tribolium* both the lvCB and lvPB are synapsin-positive.

3.1.3.9. The *Drosophila* central complex acquires functionality at later stages of pupal development compared to *Tribolium*

Last, we examined Rx expressing DM1-4 cell clusters at different pupal stages to reveal how the underlying neuropils develop (Figure 3.1–6) and how the projections observed in the adult (Figure 3.1–2) are established during metamorphosis (Figure 3.1–7 and 8).

To that end, we first determined the duration of pupation in the used Rx-specific transgenic lines. Pupation in the *Tribolium* Rx-GFP line took approximately 140 h, while pupation in the *Drosophila* Rx-GFP line took approximately 100 h. A developmental progress of 5 % equals 7 h in *Tribolium*, and 5 h in *Drosophila*. We dissected brains of equal relative developmental times (e.g. 15 % equalled 15 h in *Drosophila* and 21 h in *Tribolium*). Specifically, we included 0 (prepupal stage), 5, 15, 20, 30 and 50 % (see 3.1.5 Material and Methods for details on staging).

To observe when central complex neuropils acquire their functionality, we performed anti-synapsin stainings (co-stained with Rx/GFP, see Figure 3.1–7 and 8).

In *Drosophila,* the protocerebral bridge appeared first at 5 % of pupal development, as thin paired protrusions with a wide gap between them (Figure 3.1–6C^{i}), developed further in thickness and grew medially until it fused between 30 and 50 % of the pupation process (Figure 3.1–6 I/K^{i}). A division into slices became most visible at 50 % (Figure 3.1–6 K^{i}). The upper division of the central body in *Drosophila* appeared first at 5 % of pupal development as a slightly bent bar with only low concentration of pre-synaptic sites (Figure 3.1–6 C^{ii}). Strength of synapsin staining increased considerably at the 15 % stage, coinciding with the emergence of layers and slices (or columns, (Ito et al., 2014), visible as horizontally and vertically oriented heterogeneous structures inside the CBU (arrows and bars, respectively, Figure 3.1–6 E^{ii}). This coincided with projections forming a columnar division (Figure 3.1–7 C^{ii}). Thickness increased from 30 % onwards resulting in the appearance of a fan-like structure typical for the *Drosophila* CBU (Figure 3.1–6 G/I/K^{ii}). The *Drosophila* CBL occurred first n-ventral to the CBU as a bent bar at 15 % pupation, coinciding with the appearance of noduli (Figure 3.1–6 E^{iii}). The CBL then continuously bent further until it formed a toroid form that is nearly closed at 50 % pupation (Figure 3.1–6 K^{ii}). At 30 and 50 % pupation the structure thickened as well. Noduli appeared as one small paired subunit at 15 % of pupation (Figure 3.1–6 E^{ii}), and only at 50 % an additional discernible subunit was added (Figure 3.1–6 K^{ii}. Note that adult noduli are comprised of three to six subunits (Wolff and Rubin, 2018), i.e. there is additional development after 50 % of pupation.

In *Tribolium*, the larval protocerebral bridge developed further by reducing the gap at the midline from late larval stages (Figure 3.1–6 B/D/F^{i}) and fusing between 5 and 20 % (Figure 3.1–6 D/F/H^{i}; note that we observed considerable heterogeneity in our dataset with respect to protocerebral bridge fusion). A division into slices indicating a columnar innervation by DM1-4 cell clusters was only faintly visible at any stage, including the adult (see Figure 3.1–2), in form of indentations in the bar-like structure as well as different staining strengths (exemplary indication

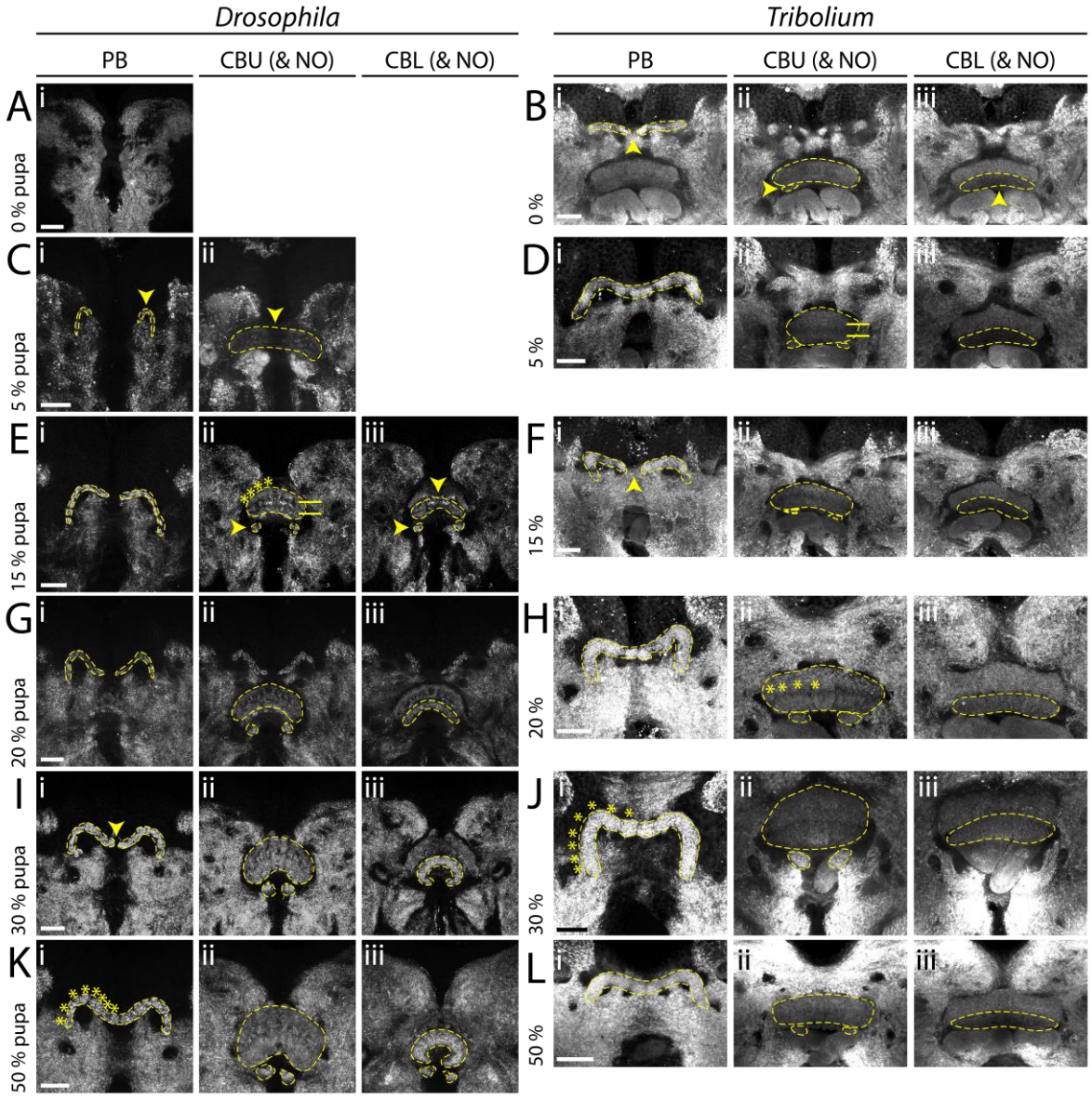

Figure 3.1–6: Pupal development of central complex neuropils of *Drosophila* (A, C, E, G, I, K) **is delayed approximately 10 % in comparison to *Tribolium*** (B, D, F, H, J, L). Displayed are substack projections of an anti-synapsin staining of the same brain used for tracing Rx-positive cell clusters (see Figures 3.1–7, 8) to highlight the development of the PB, CBU, CBL and NO. Neuropils are contoured by yellow dotted lines. Following events in the *Drosophila* pupal brain are particularly highlighted by yellow arrowheads: Appearance of a functional PB (C^{i}), CBU (C^{ii}), NO ($E^{ii/iii}$) and CBL (E^{iii}), as well as the last stage of an unfused PB (I^{i}). Following events in the *Tribolium* pupal brain are particularly highlighted by yellow arrowheads: The last stage of an unfused PB (B^{i}, F^{i}, note the variability in the timing of fusion), appearance of NO (B^{ii}) and CBL (B^{iii}). A division into distinct layers in the CBU are marked by horizontal bars. A division into slices in the PB and CBU is marked by asterisks. Abbreviations: CBU upper division of the central body, CBL lower division of the central body, PB protocerebral bridge, NO noduli. Scale bars represent 25 µm.

in Figure 3.1–6 J^{i}; differing degrees of columnar divisions of the central complex of insects has also been noticed by Strausfeld, 2012). The larval central body of *Tribolium* divided into an upper and lower division at the beginning of pupation (Figure 3.1–6 $B^{ii/iii}$). The CBU then increased in

size, and a distinct layering into at least two layers began at 5 % where the bar-like structure from the larval CB was modified (Figure 3.1–6 D[ii]), so that it got widened in the n-anterior/posterior axis. In addition, division into slices was visible from 20 % onwards (asterisks in Figure 3.1–6 H[ii]). Note that through slight deviations in positioning of the pupal brains, the CBU appears thicker in some stages than in others (compare 20 % with 30 % in Figure 3.1–6 H to J). This difference is, however, related to the angle of imaging, not a morphological feature. The CBL appeared right at the beginning of pupation, as a gap between the mushroom body medial lobes and the prospective CBU, with weak synapsin signal intensity (Figure 3.1–6 B[iii]). Increase in strength of synapsin staining was most notable from 15 to 20 % of pupation (Figure 3.1–6 F/H[iii]). The form remained bar-shaped and was positioned n-postero-ventrally to the CBU. Noduli appeared as longitudinal segments at the prepupal stage, n-posterior to the CBU and more n-dorsally than the CBL (Figure 3.1–6 B[ii]). They thickened considerably in the n-anterior/posterior axis at 20 % pupation (Figure 3.1–6 H[ii]). They built up into two subunits distinguishable by synapsin staining between 30 and 50 % (Figure 3.1–6 J/L[ii]) and developed further until eclosion into likely three subunits (data not shown).

We conclude that there is a delay in the appearance of the protocerebral bridge, central body and noduli in the *Drosophila* pupal brain in comparison to *Tribolium*. There seems to be a more complex pattern in the appearance of slices and layers in the CBU which together appear in *Drosophila* at 15 % while layers appear in *Tribolium* first, at 5 %, and slices most visibly at 20 %. Most notably, the *Tribolium* larval central body undergoes substantial remodelling into upper and lower division and the CBU develops further into a structure with different layers. This structure is therefore distinct from the larval central body neuropil (Figures 3.1–3 and 3.1–5).

3.1.3.10. Rx expressing DM1-4 cell clusters project into and build the central complex during metamorphosis similarly in both species

We next examined the pupal development of Rx DM1-4 cell clusters and their projections contributing to the central complex. Figures 3.1–7 and 3.1–8 display the same brains displayed in Figure 3.1–6. In *Drosophila* pupal brains, we observed a shift in cell cluster position along with the changes in brain shape. Specifically, the larval brain with paired spheres nearly touching each other is modified to the adult-like structure where the central complex lies between the two hemispheres. As a result, the larval array of DM1-4 cell clusters on a line along the n-anterior/posterior axis changed, recreating the shape of the protocerebral bridge (Figure 3.1–7 A-F[i]). DM1-3 moved to n-anterior on a curved line, oriented horizontally and DM4 n-posterior to DM2 and 3. The corresponding tracts underwent massive rearrangement. Most notably,

crossings were created by fascicle switching of the DM1-3 tracts (Boyan et al., 2017). This occurred first laterally at 5 % of pupal development (Figure 3.1–7B[ii]) coinciding with the occurrence of the CBU but became most notable at 15 % (Figure 3.1–7C[ii]). This resulted in a columnar organisation of the tracts themselves at 20 % (Figure 3.1–7D[ii]) and in the projection into the CBU at 15 and 20 % (Figure 3.1–7C/D[iii]). DM2-4 contributed most likely to the noduli (most notably visible at 20 and 30 %, Figure 3.1–7 D/E[ii]). Following single tracts, however, was not possible because several tracts project close to each other. Rx-marked projections into the central body and noduli reflected the overall neuropil shape (Figure 3.1–6). One exception is that we saw a lot of Rx-positive tracts at the prospective noduli, which were not yet synapsin-positive (see Figure 3.1–7 B[iii]). Also, we were not able to see a pronounced projection into the CBL, already present at 15 % pupation (Figure 3.1–6 E[iii]). Although later on, there was a visible projection into the CBL, it seemed to be relatively low in intensity, when compared to the projections and the neuropil at 50 % (Figure 3.1–6 K[iii], Figure 3.1–7 F[iv]).

In *Tribolium* pupal brains, the cell bodies of the Rx expressing DM1-4 clusters remained in similar spatial arrangement contrasting the finding in *Drosophila* (Figure 3.1–8 A-F[i]; note, however, slight deviations in positioning of the brain during imaging, at 30 %). Most notably from 0-15 %, DM1-3 cells formed tracts, which partially underwent fascicle switching, from the n-anterior region of the central body to n-posterior half of the prospective CBU, to the most n-posterior fraction, the prospective CBL, and n-dorsally, where fibres likely projected into the LAL and into regions in the superior protocerebrum (Figure 3.1–8 A-C[ii]). The resulting division into slices was most visible at 15 % in the CBU (Figure 3.1–8 C[iii]) and 30 % in the CBL by dense points of staining (Figure 3.1–8 E[iv]). Projections into the CBU and CBL were most prominent throughout, while projections into the noduli were of lower intensity (see Figure D-F[iii]). Note that, similar to the adult (Figure 3.1–2), there was a very strongly marked projection likely coming from the DM4 group in the central body that was connected to the lateral accessory lobes (e.g. Figure 3.1–8F[iv]).

We conclude that during metamorphosis, the projections belonging to DM1-4 Rx cell clusters recapitulate the development of the neuropils and their heterochronic differences (Figure 3.1–6). While development differs in detail, most steps occur in the same sequence of events in both species. Fascicle switching and building of decussated fibres is visible in both species, though delayed in *Drosophila*, alongside the resulting organisation in distinct slices. Importantly, while low-degree fascicle switching has already occurred during *Tribolium* embryogenesis, not detectable in Rx expressing cells (Figure 3.1–3), in the pupa it was prominently visible in Rx cells, indicating that there might be two differing degrees of fascicle switching per developmental period. Moreover, *Drosophila* DM1-4 projections into the CBL were visible after the neuropil was

distinguishable in synapsin stainings. The reverse happened in the noduli, where projections appeared before the neuropil.

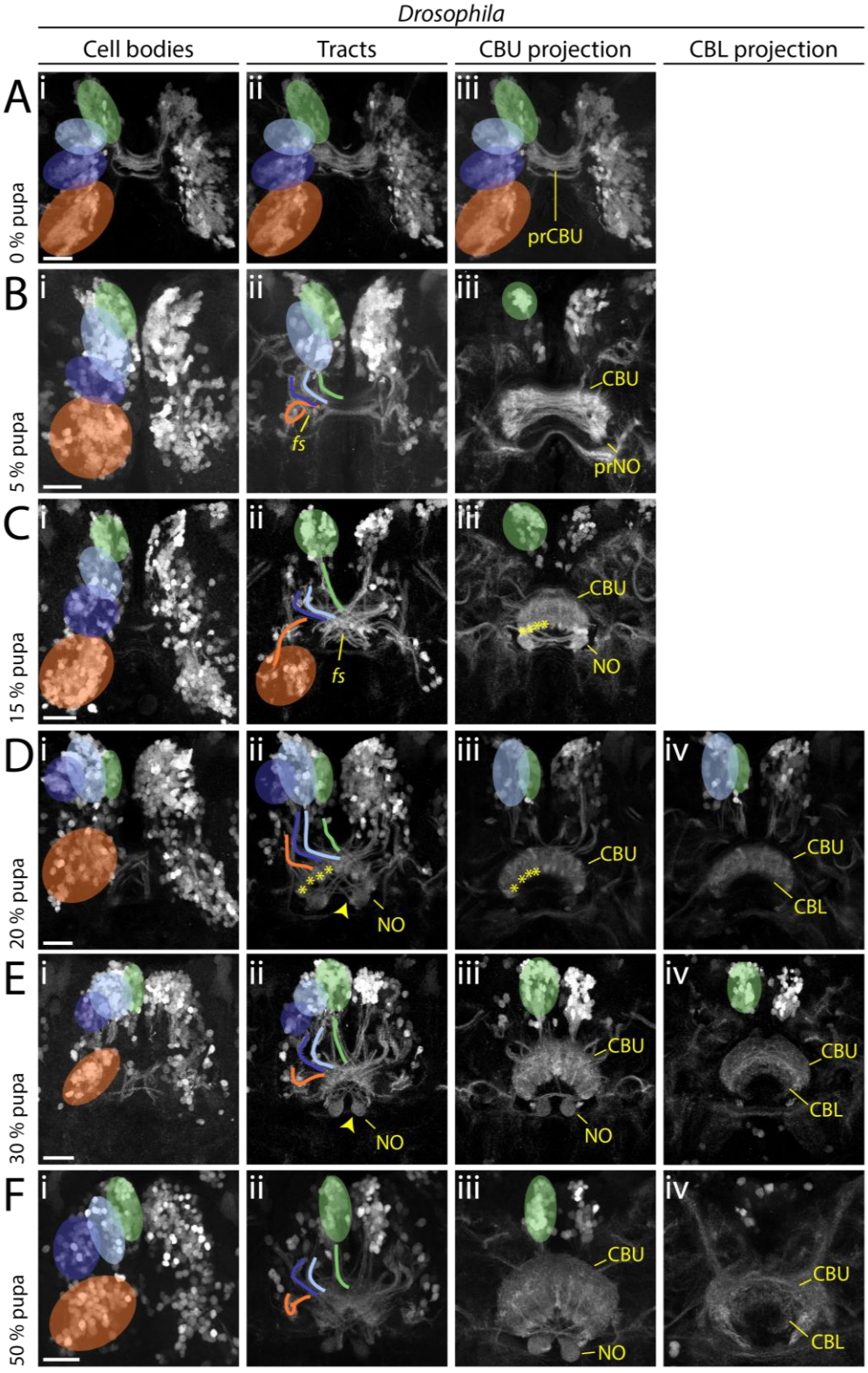

Figure 3.1–7: Pupal development of *Drosophila* Rx DM1-4 cell clusters illustrates fascicle switching events with resulting columnar fibre organisation and development of central complex neuropils. Displayed are

sub-projections of an anti-GFP staining of the same brain per time point (A 0 % pupa, B 5 % pupa, C 15 % pupa, D 20 % pupa, E 30 % pupa, F 50 % pupa), to display the development and positioning of cell clusters (i) belonging to the DM1-4 lineage and their tracts (ii) (DM1 green, DM2 light blue, DM3 dark blue, DM4 orange) and final projections into the developing central complex neuropils (CBU iii, CBL iv). In addition, following events are highlighted: Fascicle switching (*fs*) of DM1-3 was visible from 5 % onwards (B^{ii}, C^{ii}), with the formation of four columns of the CBU per hemisphere (asterisks in C^{iii} D^{ii}, D^{iii}). Connections to the developing NO appeared at 20 and 30 % of pupal development (yellow arrowheads, in D^{ii}, E^{ii}). Abbreviations: CBU upper division of the central body, CBL lower division of the central body, PB protocerebral bridge, NO noduli, prCBU primordium of the CBU (in other publications prFB, Andrade et al., 2019), prNO primordium of the NO, fs fascicle switching event. Scale bars represent 25 µm.

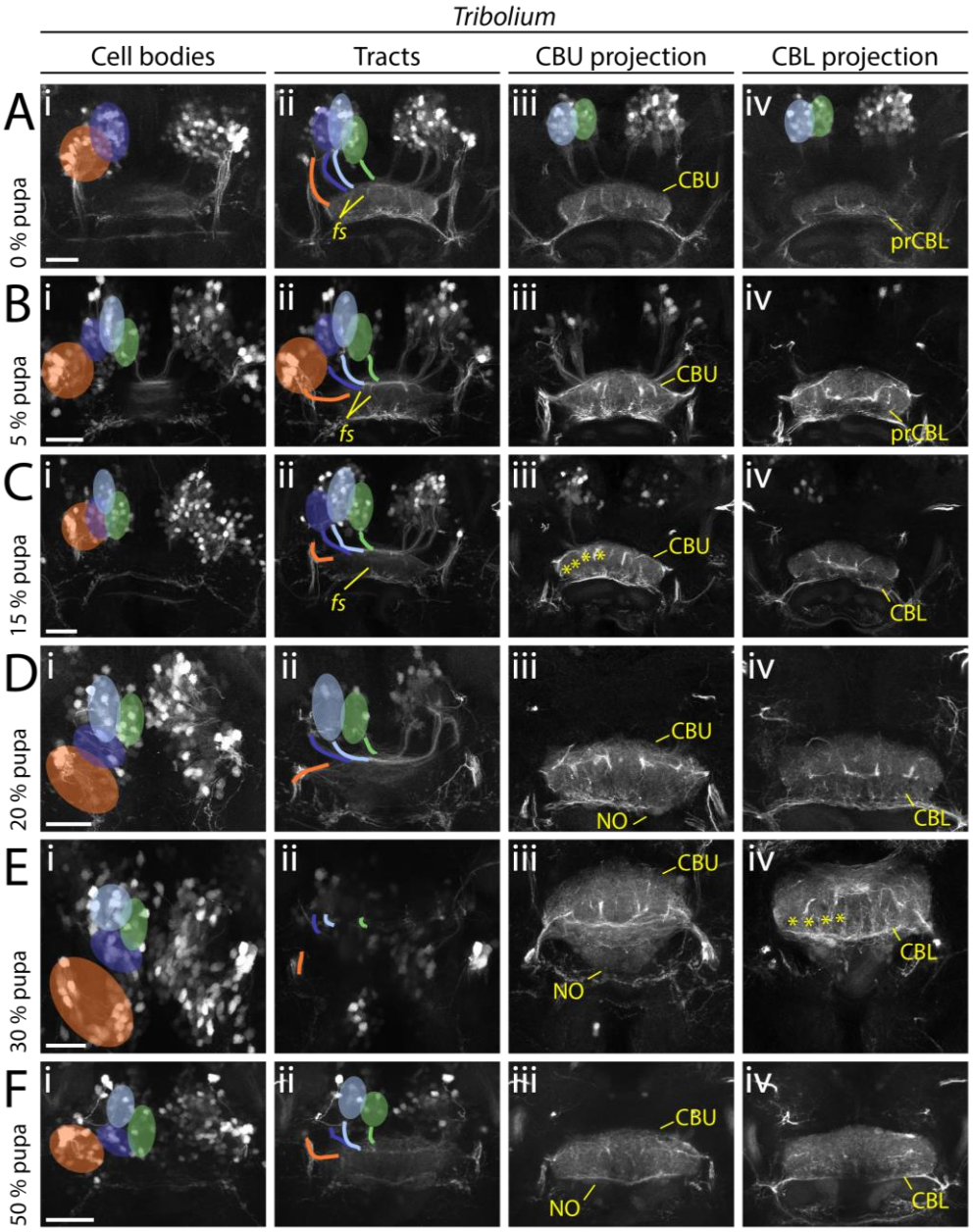

Figure 3.1–8: Pupal development of *Tribolium* Rx DM1-4 cell clusters illustrates fascicle switching events and columnar fibre organisation, and thus shows that the developing adult central body is distinct from the larval form. Displayed are sub-projections of an anti-GFP staining of the same brain per time point (A 0 % pupa, B 5 % pupa, C 15 % pupa, D 20 % pupa, E 30 % pupa, F 50 % pupa), to display the development and positioning

of cell clusters (i) belonging to the DM1-4 lineage and their tracts (ii) (DM1 green, DM2 light blue, DM3 dark blue, DM4 orange) and final projections into the developing central complex neuropils (CBU iii, CBL iv). In addition, following events are particularly highlighted: Fascicle switching (*fs*) of DM1-3 was visible from 0 % onwards (A^{ii}, B^{ii}, C^{ii}), with a resulting formation of four columns of the CBU and CBL per hemisphere (most clearly visible in C^{iii} and E^{iv}, marked by asterisks). Abbreviations: CBU upper division of the central body, CBL lower division of the central body, PB protocerebral bridge, NO noduli, prCBL primordium of the CBL, fs fascicle switching event. Scale bars represent 25 µm.

3.1.4. DISCUSSION

3.1.4.1. Shifted timing of conserved series of events and precocious acquisition of functionality underlie central complex heterochrony

In this work, we identified conserved Rx expressing cells belonging to the DM1-4 lineage group (Figure 3.1–1), identified them as homologous in both species (Figure 3.1–2) and followed their development from late embryogenesis into the adult (Figures 3.1–3 to 8). This allowed us to compare differences and similarities of homologous neurons during heterochronic development of the central complex.

In order to summarize differences in central complex development, we defined fourteen events, where *Tribolium* and *Drosophila* differ in absolute and relative timing as well as order (Figure 3.1–9). To illustrate these differences, we have plotted events of central complex development on an absolute and relative time scale (Figure 3.1–9). Note that *Drosophila* and *Tribolium* differ strongly in absolute time and in the relative portions of their ontogenetic stages (see x-axis in Figure 3.1–9A, see 3 Results). Also, some events appear to be simultaneous (e.g. events 9-11), which is more likely a result of a low resolution in time increments rather than a morphological trait (Fritsch et al., 2013; Nunn and Smith, 1998).

We identified two different types of changes in the sequence of the fourteen events of central complex development (Figure 3.1–9): First, some events change their position within the sequence. Second, some developmental events remain in sequence, but shift their developmental timing.

A crucial change in sequence position, and the most notable difference between *Drosophila* and *Tribolium* central complex development, regards the stage when synapsin staining indicates functionality of central complex neuropils (Figure 3.1–9). In *Tribolium*, functionality in the protocerebral bridge and central body is acquired at the end of embryogenesis (event 7 and 8), together with a low degree of fascicle switching (event 6). Importantly, this occurs before the growth period during larval development (events 4 and 5 in Figure 3.1–9). Hence, in *Tribolium* a central body is functional at a precocious stage before larval development where the central body still resembles a broad commissure with only a low degree of fascicle switching having occurred, lacking apparent columnar structure and thus, not resembling an adult counterpart neuropil. It has a specifically larval, i.e. immature, morphology. In *Drosophila*, in contrast, functionality is acquired during metamorphosis, in early pupal stages, *after* the larval growth period (Figure 3.1–6, 7, 9). Hence, the sequence is modified, from event sequence 4-5-6-7-8 in *Drosophila* to event sequence 4-6-7-8-5 in *Tribolium* (Figure 3.1–9).

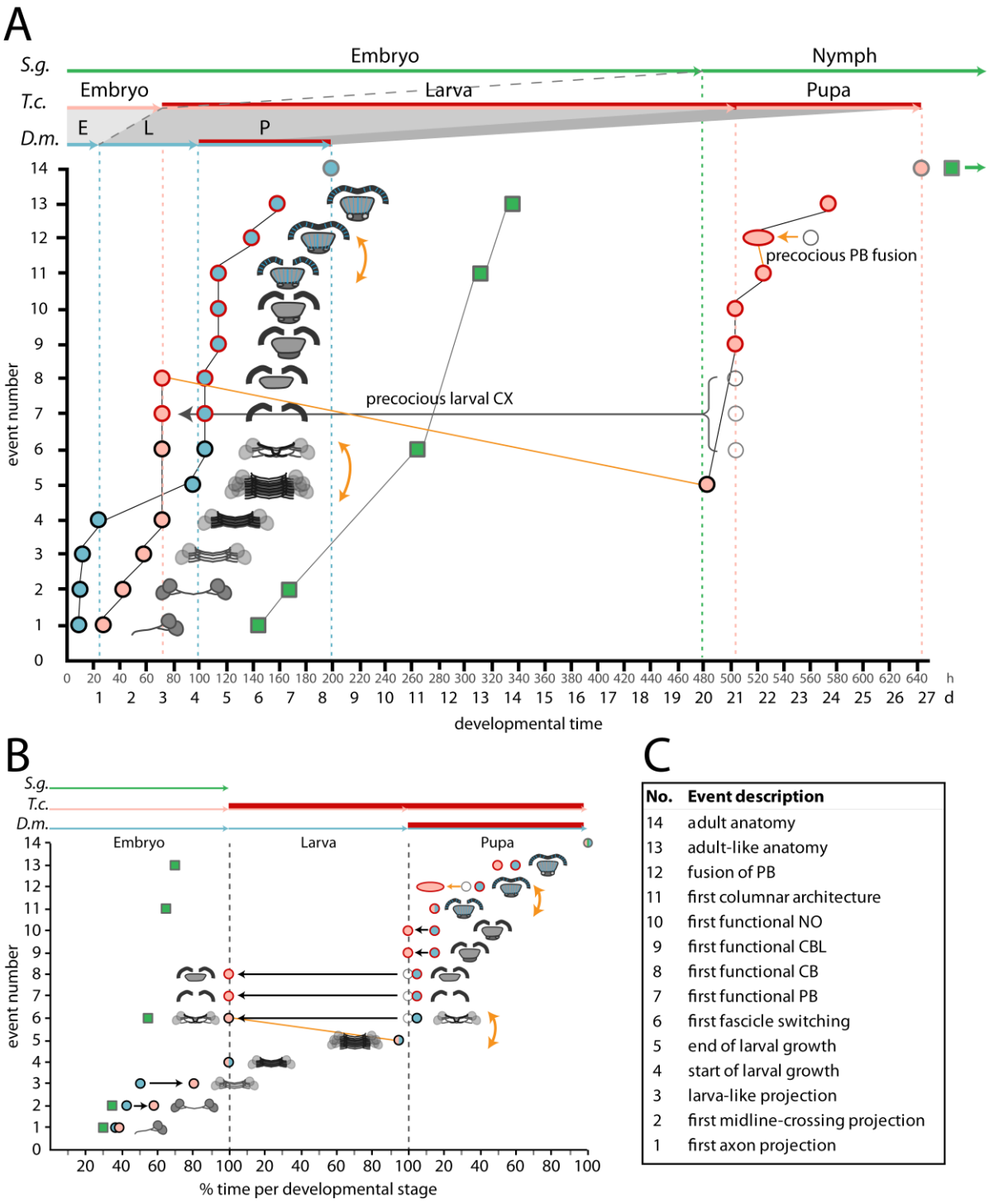

Figure 3.1–9: Summarizing scheme illustrating the changes of developmental events underlying central complex heterochrony. A depicts heterochronic differences on an absolute time scale and **B** on a relative time scale of fourteen events (**C**). These fourteen events are plotted on the y axis and displayed as small sketches next to the time points (circles). Time points and durations for *Drosophila* (*D.m.*) are displayed in blue, for *Tribolium* (*T.c.*) in pink and for *Schistocerca gregaria* (*S.g.*) in green (see below for details). Red contours in circles and red lines on the top x-axis indicates the presence of a functional central complex neuropil, i.e. synapsin-positivity. Sequence heterochronies are indicated by orange lines and arrows, while heterochronic shifts are indicated by black arrows. The progression from one event to the next is indicated by a thin line. This highlights the sequence heterochrony between the larval growth period and early acquisition of functionality including fascicle switching. Moreover, we observed sequence heterochrony with respect to the fusion of the protocerebral bridge, heterochronic shifts with respect to the larval

central complex (events 6-8), embryonic events 2-3 and pupal events 9 and 10. *Schistocerca* data – when available – was taken from Boyan et al. (2017, 2008) and Herbert et al. (2010). Developmental periods, i.e. embryo, larva and pupa are indicated by vertical dotted lines and horizontal arrows. Events were defined as (1) the first axonal projection of Rx-positive cells in the prospective central complex region, (2) the first projection of Rx-positive cells that spans over the midline, (3) a pattern of projections and cell body location that allows clear identification of DM1-4 lineage origin and is thus similar to the larval pattern, (4) the beginning of larval growth in the L1 larva, (5) the end of larval growth at the end of development of the last larval instar, correlated with an increase in size of central complex structures, (6) the first occurrence of fascicle switching, causing a decussated fibre pattern, (7) the first synapsin-positive structure identifiable as protocerebral bridge, (8) the first synapsin-positive structure identifiable as a central body, (9) the first synapsin-positive structure identifiable as a lower division of the central body, i.e. the first division into lower and upper central body part, (10) the first synapsin-positive structure identifiable as nodulus, (11) a first division into columns, either in a GFP or synapsin signal, (12) the fusion of the protocerebral bridge at the midline, (13) an anatomy that grossly resembles the adult pattern, particularly with respect to the DM1-4 cell bodies and tracts and, (14) central complex anatomy in the adult.

An additional change in sequence regards the fusion of the protocerebral bridge (event 12) and columnar organization of the central body (event 11). In *Tribolium*, the protocerebral bridge first fuses and then the central body develops slices, or columns (Ito et al., 2014), while in *Drosophila* columns become visible first while the fusion follows delayed (see events 11 and 12 in Figure 3.1–9). In summary, these data show that even within a sequence of stereotypical developmental events selected steps can change their position. Unexpectedly, these sequence changes cause formation of a functional, but precocious form of the *Tribolium* central body.

Differences in timing but not in event order are apparent as well. In the embryo, we observed a delay in development of midline-crossing projections of Rx cell clusters in *Tribolium* embryos in comparison to *Drosophila* (events 2 and 3, Figure 3.1–4, 3.1–9). These differences are pronounced in comparisons of relative developmental time (i.e. 58 and 81 % in *Tribolium* versus 43 % and 51 % in *Drosophila*). We have no *a priori* explanation for the delay in event 3 in *Tribolium* embryogenesis. Inclusion of available data from the hemimetabolous insect *Schistocerca* makes the picture even more intriguing, as here all events we defined are likely to happen during embryogenesis (Boyan et al., 2017, Figure 9).

Another delay in a conserved sequence of events is found during pupal development. *Drosophila* pupae have an approximate delay of 10 % in events 9 to 13 compared to *Tribolium* in relative developmental time (Figures 3.1–6 to 9). A possible explanation is a corresponding relative delay in eye development which in *Drosophila* starts with the appearance of an eye patch at 12-15 % of pupal development (Bainbridge and Bownes, 1981). An analogous development starts in *Tribolium* pupae already at approximately 5 % (this study, Ho, 1961 and Dippel, unpublished).

Our analysis of DM1-4 lineages in *Drosophila* fits to previous accounts of *Drosophila* central complex metamorphosis (Riebli et al., 2013; Young and Armstrong, 2010). Both works, however,

used DN-Cadherin as marker for fasciculating axons (Iwai et al., 1997), to indicate functionality and thus concluded that a fan-shaped body primordium and protocerebral bridge are present as early as the third larval instar (Andrade et al., 2019). We were not able to detect any synapsin-positive structures during that time, however. In this study we see presence of synapses as the primary sign of a functional neuropil. Moreover, we identified a CBL earlier than Riebli et al. (2013), Young and Armstrong (2010). A phenotype as underlying reason seems unlikely, since the other events and the total pupation time are comparable to wild type and are similar to these works. A misassignment is possible but notice that first identification in both works are when a toroid shape is already nearly closed. Neuromodulator stainings (e.g. Homberg et al., 2018) might come to aid to verify our assignment.

To summarize, we conclude that central complex heterochrony (reviewed in Koniszewski et al., 2016; Pfeiffer and Homberg, 2014) between *Tribolium* and *Drosophila* is not only the late acquisition of functionality in *Drosophila* (Young and Armstrong, 2010) and the larval presence of the central body in *Tribolium* (Koniszewski et al., 2016), but includes delays in *Tribolium* embryogenesis, simultaneous reshuffling of event order, and an acceleration of events during pupal stages when compared to *Drosophila*.

3.1.4.2. Absolute and relative developmental time as well as morphological events as metrics for comparative central complex development

We employ mostly relative developmental time as metric to compare central complex development in *Tribolium* and *Drosophila*. The inclusion of data on morphological events in the whole embryo (Strobl and Stelzer, 2016), however, changes our interpretation of heterochrony with differences being less pronounced: First axonal growth (event 1) occurs in the phase of germ band retraction in both species. Rx-positive midline-crossing projections (event 2) are built in both species at the end of germ band retraction, although there is a 15 % difference in developmental time. The final stage of central complex development included in our analysis shows a difference not only time-wise (51 versus 81 % of embryogenesis) but also with respect to overall embryonic development, because at 51 %, *Drosophila* is in dorsal closure phase, while *Tribolium* is already in the final muscle development phase at 81 % (Strobl and Stelzer, 2016).

We thus find that possible heterochronies (when measured along relative time) reflect overall embryonic development and are not organ specific. Although we still find specific central complex heterochrony in the delay of event 3 in *Tribolium*, the changes in shift interpretation by including descriptions of morphological events (Strobl and Stelzer, 2016) highlight that, if

possible, developmental comparisons should rely on time *and* morphological events (as proposed by Smith, 2001).

For pupation, we use absolute and relative time as a comparative developmental metric, with defined start and end points, i.e. restricted movement at the end of larval development and eclosion. Additional comparable morphological events (as suggested by Smith, 2001) would potentially modify our impression of heterochrony (like in the mapping of embryonic heterochrony above). However, mechanisms of *Tribolium* and *Drosophila* pupation show some pronounced differences, which make such a comparison challenging. For example, *Drosophila* retains its larval cuticle and forms it to a pupal case (Bainbridge and Bownes, 1981), while *Tribolium* hatches from the last larval cuticle at the start of pupation (for basic information on *Tribolium* pupae, Sokoloff, 1972). This means that determining and including a comparative morphological event metric might not be possible or feasible. A detailed comparative study on the morphological development of different organ systems in whole pupae of both species would be necessary to identify potentially conserved sets of events that can be homologized.

In our summarizing analysis, we used absolute as well as relative times (Figure 3.1–9). Absolute time has been described to be of limited use for evo-devo research (Jeffery et al., 2002a, 2002b). Substantial differences in absolute time can occur because of different developmental rates which are dependent on several factors such as temperature and nutrition. Hence, some studies have come to distinct conclusions looking at both metrics (Gomez et al., 2008; in Keyte and Smith, 2014). We see value to mention both metrics, with the usefulness depending on which aspect of development is chosen. While embryogenesis and the larval period differ so strongly, pupal development differs only by a factor of 1.4 (100 versus 140 hours in *Drosophila* and *Tribolium*, respectively): Hence, the conclusion of a small delay in *Drosophila* could have been drawn from both absolute and relative time (see Figure 3.1–9, e.g. events 9 and 10, 15 h/ % in *Drosophila* versus 7 h/5 % in *Tribolium*).

3.1.4.3. The larval central complex of *Tribolium* represents a distinct functional form to the adult structure

The most pronounced heterochronic shift in central complex development causes the early appearance of a partial larval central complex in the *Tribolium* L1 larva (Koniszewski et al., 2016). We describe here that the larval protocerebral bridge and central body are structurally different forms to their adult counterparts.

3.1.4.3.1. Morphological differences between larval and adult form

In the first instar larva, we observed a protocerebral bridge that is not yet fused at the midline, tilted at 30-45° angle, and a central body of a simple bar shape. The innervation of these structures by the marked lineages is such that we can see tracts from n-anterior to n-posterior, then jointly projecting into the central body and subsequent 'dotted' labelling, overlapping with the synapse-rich area of the central body. We found weakly decussated fibres in this larval central body, so that fascicle switching must have occurred (Boyan et al., 2008). However, columns were not visible in synapsin and α-Tubulin stainings or in cell projections. The pattern of innervation and neuropil structure is maintained and extended during larval stages, highlighting that the structure serves a function specific for the larval stage of *Tribolium*. During pupal stages this larval form gets strongly modified through pronounced fascicle switching, a subdivision into lower and upper division (but see section below), a distinct forming of layers stereotypical for every adult upper division of the central body (e.g. el Jundi et al., 2018), and a pronounced division into slices (or columns, but see Ito et al., 2014) with synapsin-negative spaces as well. The protocerebral bridge gets longer, fuses at the midline, and receives its handlebar shape on which the investigated lineage groups are positioned. These events during metamorphosis are similar to *Drosophila* central complex development.

3.1.4.3.2. Is the larval form a precocious upper or lower division of the central body?

The common conclusion is that the fan-shaped body/upper division of the central body develops first (Andrade et al., 2019; Koniszewski et al., 2016; Panov, 1959; Riebli et al., 2013; Wegerhoff and Breidbach, 1992; Young and Armstrong, 2010). Huetteroth et al. (2010) speak only of a larval central body, not specifying whether it is lower or upper division. Also, one of the earliest publications on this topic (Pereanu and Hartenstein, 2006) only refers to a primordium of the central complex. We did not find any evidence in the *Drosophila* literature verifying upper division identity, exclusion of lower division identity or data that shows a distinction of larval to adult structure. Panov (1959) made the conclusion of a larval CBU because of the presence of a small tract of commissural fibres below the CBU, i.e. a prospective CBL. A similar observation was done by Wegerhoff and Breidbach (1992). Koniszewski et al. (2016) and Homberg et al. (2018) have characterized neuromodulator profiles that aid this discussion. Koniszewski et al. (2016) characterized the neuromodulator profile of the larval and adult central body of *Tribolium* and have observed similarity between both, which lead the authors to conclude that the structure is most likely the upper division. Complementary to that, Homberg et al. (2018) have investigated GABA immunostainings – a characteristic neurotransmitter for the CBL - in a diving beetle larva

and observed that only low immunostaining is present in a subset of cells. They thus come to a similar conclusion as Koniszewski et al. (2016). Moreover, they conclude from the fact that diving beetle larvae have articulated legs, that a lower division might not be essential for coordinated leg movement. A GABA staining in the larval central body of *Tribolium* would be necessary to corroborate the findings, thus far.

Nevertheless, the adult and larval upper division are different units, as we have shown in this work, particularly through the reduced pattern of decussated fascicles and a lack of columns/slices and layers. This raises the question whether the structure can be defined as future upper division, or just as larval central body, distinct from any of the adult structures. We propose to speak of 'larval central body', avoiding any speculation.

3.1.4.3.3. Functional and evolutionary implications of the existence of a specific larval central body

The distinct morphological differences found in our study leads us to conclude that there are two forms of the central body and protocerebral bridge, one for each period of an animal's life of locomotion, feeding, predator evasion and other direct environmental interactions. Hence, two forms of a neural circuits may exist in the central body, which might lead to different behavioural outputs and on which modification through natural selection can occur separately.

A functional synapsin-positive central body in freshly hatched larvae has been reported only in *Tribolium castaneum* (this study, and Koniszewski et al., 2016). Previous publications show the presence of such a functional structure in another Coleopteran, *Tenebrio molitor*, using neuromodulator expression and classic stains such as Bodian and Golgi stain (Panov, 1959; Wegerhoff, 1999; Wegerhoff et al., 1996; Wegerhoff and Breidbach, 1992). A central body in later larval stages was reported for Lepidopterans (Huetteroth et al., 2010; Panov, 1959; S.H. Montgomery, personal communication) and Hymenopterans (Hähnlein and Bicker, 1997; Panov, 1959). Panov (1959) presents data from late larvae of a diverse range of species of other orders as well, leaving the impression that one cannot see a clear pattern of absence or presence of a larval central body in a specific order (note, however, that it might be worthwhile to confirm analyses with standard immunostainings and confocal microscopy).

However, a clear distinction to the adult structure and description of the anatomical differences has been lacking. We offer this necessary detail of central complex development and evolution in *Tribolium*. It is likely that a similar morphological distinction is possible in other species. For example, the shape of the larval central body of *Manduca sexta* (Huetteroth et al., 2010) and *Tenebrio molitor* (Wegerhoff et al., 1996; Wegerhoff and Breidbach, 1992) and the

Tribolium neuropil seem very similar in their simple bar shape. A similarity between the larval central complex of *Tenebrio molitor* and of the larval structure in the Branchiopod *Triops cancriformis* (Fritsch and Richter, 2010) has been noticed (Strausfeld, 2012). A uniform non-layered central body and a simplified protocerebral bridge in the *Tribolium* larval brain is indeed like the larval form of *Triops*, which possess a rudimentary protocerebral bridge and a non-columnar central body (Fritsch and Richter, 2010; Strausfeld, 2012) or indeed similar to a crayfish brain (e.g. Figure 4 in Homberg, 2008).

The novel information of two distinct degrees of fascicle switching in two developmental periods heightens the importance of this mechanism to generate a functional neuropil (Boyan et al., 2015). Which functions can be generated with a weakly decussated neuropil? Decussated fibres have been linked to the necessity of coordinating multi-joint legs (Strausfeld, 2012). Also, the degree of columnar divisions has been linked to differing degrees of motor repertoire (Strausfeld, 2012, see Figure 11.12). Whether the similarity in central complex structures between larvae of a Branchiopod and a *Tribolium* larva also reflects a similarity in motor repertoire can only be speculated. Hence, how do *Tribolium* larvae coordinate their multi-joint larval legs with a weakly decussated and possibly non-columnar central body? In order to answer questions of the specific function of the larval central complex, also in distinction from adult functions, behavioural assays would need to be performed, focusing on leg movement patterns and whether they are able to make turns in response to stimuli. For example, a split protocerebral bridge also occurs in species who perform simple bilateral movements (Strausfeld, 1999). Hence, how do *Tribolium* larvae move in contrast to adults?

Tribolium larvae have a range of requirements for larval central complex function likely distinct from the adult form, with the absence of wings, shorter multi-joint legs and no faceted eyes, only having stemmata (Ho, 1961). A correlation between the presence of walking legs and presence of central body and the well-studied function of the central complex in motor control, indicates a possible causal link (Strausfeld, 1999). Note, however, that the data by Panov (1959) tentatively illustrates that the presence of walking legs cannot be the only correlate of a larval central body, as larvae of *Pieris brassicae*, for example, have shortened multi-joint legs (Kim, 1959), but possibly no central body neuropil (Panov, 1959). Panov (1959) presents a correlation between larvae of species with poorly developed vision. Note still that evidence of blind adult arthropods having a columnar central complex (Böhm et al., 2012; Boyan et al., 2015; Strausfeld, 2012, 1998) make the picture more complex. For a clearer illustration of such correlations, presence of larval central bodies would need to be confirmed by comparative methods, in larvae of a range species from

which basic information regarding appendage and visual organ development as well as range of motion is known.

What are the possible underlying factors causing an early appearance of a functional neuropil in *Tribolium*? As a heterochronic shift in juvenile hormone secretion is one main possible factor in the evolution of metamorphosis (Truman and Riddiford, 1999), a similar role of juvenile hormone and candidate transcription factors (e.g. *Kr-h1*, Jindra, Truman and Riddiford, unpublished) in the early central complex appearance is plausible.

3.1.4.3.4. Are DM1-4 cells of the larval central body pontine neurons?

A question with regard to cell types and their distinct morphology is whether the neurons of DM1-4 at the end of embryogenesis are pontine neurons that connect different columns of the upper division of the central body with each other (Andrade et al., 2019). In *Drosophila* pontine neurons are born first as primary neurons – specifically, small undifferentiated neurons – that comprise the early primordial fan-shaped body (Andrade et al., 2019). Secondary neurons then fasciculate with these pontine neurons and comprise unicolumnar neurons that we mainly investigated in this study. Hence are all larval central body neurons belonging to DM1-4 pontine neurons? Can they on their own generate a functional neuropil? Alternatively, is there a deviation from *Drosophila* so that we observe not only pontine but other types of neurons built by DM1-4 lineages? A detailed analysis with similar methods as in Andrade et al. (2019) can contribute answers to these questions. These may be FIB-SEM (focused ion-beam scanning electron microscopy), in combination with an HRP-coupled GFP antibody so that a brown precipitate via DAB incubation can visualize projections of the approximately 50 x 15 x 13 μm (x, y, z) large larval central body of *Tribolium*. As alternative, expansion microscopy (Cahoon et al., 2017; Jiang et al., 2018) in combination with more limited marking of fewer cells might help with questions regarding distinct central complex cell types .

3.1.4.4. Central complex heterochrony is defined by a complex set of growth and sequence heterochronies

Heterochrony is a major evolutionary phenomenon connecting ontogeny and phylogeny (Gould, 1977; Raff and Wray, 1989; Smith, 2003, 2002, 2001) through 'phyletic alterations based upon changes in developmental timing of ancestral features' (Gould, 2000). Most often, a direct comparison to the ancestor is not possible (but see Fritsch et al., 2013), also in the case of central complex heterochrony, where only extant species have been compared (this study, Koniszewski et al., 2016; Panov, 1959).

Gould (1977) has characterized heterochrony in terms of differences in size and shape, while Alberch et al. (1979) added dimensions of growth and differentiation (both described in Smith, 2001 as growth heterochrony). De Beer et al. (1951) and Smith (2003, 2002, 2001) have added developmental sequence modifications as heterochrony, and coined it sequence heterochrony.

How do the changes described in this study fit these definitions? Differences in timing in embryonic and pupal development can be most easily described in terms of growth heterochrony, with delayed embryonic development in *Tribolium* and a delayed pupal development in *Drosophila* being a paedomorphosis (a juvenilized shape, e.g. Gould, 2000, see Figure 3.1–9). Although we define embryonic and pupal central complex development in events and not in growth parameters, the fact that the order of these events is conserved and only shifted is most easily understood in terms of growth heterochrony. Sequence heterochrony (Keyte and Smith, 2014; Smith, 2001) has happened in the appearance of a larval central complex in *Tribolium* before the larval growth period (Figure 3.1–9). The developmental sequence of the central complex has been modified such that a protocerebral bridge and a central body with specific larval morphology appear at the end of embryogenesis in *Tribolium*. This would equal a peramorphosis in morphological terms (Gould, 2000; Smith, 2001). However, with the correlation of a larval central complex and the presence of larval walking legs (Strausfeld, 1999; see section on the larval central complex) and the likeliness that the basic groundplan of all holometabolan larvae contains walking legs (Peters et al., 2014), we conclude that – in comparison to a hypothesized ancestor – *Drosophila* larval development of the central complex is a paedomorphic phenomenon.

An additional aspect of central complex heterochrony is that adult structures are highly similar in all investigated species (Figure 3.1–2, e.g. Honkanen et al., 2019). In some cases, adult structures differ, because of the heterochronic shifts during development (such as the prominent example of human neoteny, described in Gould, 1977, or also recently in Luque et al., 2019). Examples like central complex development include therian limb development (Keyte and Smith, 2014 and references therein) as well as differential development of termite castes (Nii et al., 2019). The phenomenon of a conserved adult structure after heterochronic development likely illustrates evolvability in development of involved structures. Development of limbs in marsupials and placental mammals (Keyte and Smith, 2014), wings in termites (Nii et al., 2019) and the central complex in *Drosophila* and *Tribolium* illustrate modifications in bauplan development with a similar conserved outcome.

Moreover, if we adapt the hypothesis that a pronymphal stage in *Schistocerca* equals all larval stages in *Drosophila* and *Tribolium* (Truman and Riddiford, 1999), the complete heterochronic shift would be less pronounced, but still present. While *Schistocerca* would still have a completely

functional central complex in a pronymphal stage (Boyan and Reichert, 2011), *Drosophila* would have a protocerebral bridge and upper division of the central body as structures comprised of fasciculated axons (DN-Cadherin-positive; Young and Armstrong, 2010). *Tribolium* would have a large nearly fused protocerebral bridge and a larval central body, both synapsin-positive (see Figure 3.1–5).

3.1.4.5. Inclusion of *Schistocerca* data indicates a conserved sequence of central complex development

To get a more complete picture of central complex heterochrony it is necessary to include analogous analyses in *Schistocerca gregaria* or other hemimetabolous species. Data available (Boyan et al., 2017, 2008; Herbert et al., 2010) possibly suggest that, with regard to the sequence of events, *Drosophila* is more similar to *Schistocerca* than *Tribolium*.

In *Schistocerca*, midline-crossing fibres build a complex set of parallel commissures (at 50 % embryogenesis, Boyan et al., 2008). Subsequently, fascicle switching starts at 55 % with columns developed at 80 % (Boyan et al., 2008). In parallel functionality is acquired, with evidence based on several neuromodulators (Herbert et al., 2010). This would be like the pattern of crossing fascicles and synapsin acquisition in *Drosophila* pupae. Hence, the phase that is achieved at 50 % embryogenesis in *Schistocerca* seems to be extended into pupal stages in *Drosophila*. Although functionality has not been shown with synapsin staining, thus far (G. Boyan, personal communication), data present indicates that there is no sequence heterochrony between *Drosophila* and *Schistocerca*, hence no precocious acquisition of functionality with a low degree of fascicle switching, like in *Tribolium*.

This finding could lead to a complete re-interpretation of heterochronic events. So far, it was believed that *Drosophila* was most derived in shifting central complex development completely to the adult while some species retained aspects of the central complex in the embryo (Koniszewski et al., 2016; Pfeiffer and Homberg, 2014). *Drosophila* might still show a derived mode, but only when comparing to a possibly more basal Holometabolan like *Tribolium*, where larvae have walking legs and outward mouthparts (Peters et al., 2014). In comparison to *Schistocerca*, it has possibly regained a more conserved sequence of central complex developmental events, and has only shifted the acquisition of functionality to metamorphosis. Hence, a possible scenario would be that through the evolution of a larval period came a distinctly larval central complex, visible in *Tribolium*, which was then secondarily lost in *Drosophila*, which consequently regained a more ancestral sequence of events.

3.1.4.6. Central complex development can be divided into developmental modules of associated and dissociated events

Modifications in sequence of processes such as central complex development may not have endless variations in the insect world (e.g. Conway Morris et al., 2015; Nijhout and Emlen, 1998 and articles in the same issue). It is more likely that certain constraints play a role in the development and evolution of the central complex, as is likely true in brains in general (Montgomery et al., 2016). We suspect that some events must be followed by others, thereby comprising developmental modules (as formulated by Raff and Raff, 2000; Raff, 1996; Smith, 2001, figure 7). These events are, therefore, associated due to specific underlying molecular and cellular mechanisms. In contrast, dissociation occurs to allow novel elements to be introduced by natural selection (Raff, 1996; Smith, 2001). Our data allow first insights into which events may be linked and which can be dissociated, i.e. how large the portion of developmental constraints is that restrict the variability of phenotypes for selection (Smith, 2002). The sequence of building midline structures by first forming axons, followed by first midline crossing fascicles with more additional fascicles crossing the midline subsequently (events 1-3) build a consecutive sequence in both species. These could therefore equal a developmental module, as single events are closely associated. In addition to associated events, we observe a dissociation of larval growth (events 4 and 5) from subsequent fascicle switching and acquisition of a functional (i.e. synapsin-positive) neuropil (events 6-8). Events 4-5 and 6-8 would be in themselves associated, but from each other dissociated. Dissociation then causes the precocious appearance of functional neuropils in *Tribolium*. Development of noduli and the lower division of the central body (events 9 and 10) seem to be another module, as they happen in both species in the same time frame. Fusion of the protocerebral bridge (12) and the acquisition of a visible columnar architecture (11) seem to be dissociated, as the order has been reversed in *Tribolium* compared to *Drosophila*.

We speculate, that event modules could have a common underlying genetic factor or cellular mechanism that drives or causes a cascade of subevents. The next module, dissociated from the first, would have a distinct mechanism from the first. An example of dissociated modules may be that the ablation of fan-shaped body pioneers does not influence the next developmental module, i.e. the developing unicolumnar neurons (Andrade et al., 2019).

The interpretation by Raff and Raff (2000), Raff (1996) and Smith (2001) of development consisting of associated modules and variability in the program being produced by dissociated events, is reminiscent of longstanding discussions regarding the evolution of mammalian brains (e.g. reviewed in Montgomery et al., 2016). Here, allometric scaling relationships of brain regions have been interpreted as the result of developmental constraints, with only basic developmental

programs being modified (concerted evolution, Finlay and Darlington, 1995) or functional constraints, where selection acts on functionally interconnected parts of the brain (mosaic evolution, Barton and Harvey, 2000). In the case of central complex development, we find indication for both original theories: While there are specific modules and events that seem unmodified in order – at least in the two species investigated – , but shifted in timing, there are other events that differ in their order between both species.

The pattern of associated and dissociated events as well their differences in order and time point in central complex development can be interpreted as morphological indicators of robustness as well as evolvability (Alberch, 1991; Losos, 2014; Payne and Wagner, 2019; Pigliucci, 2008; Wagner, 2008). Specifically, developmental modules would overlap with the concept of modularity, i.e. the measure of how much a system can be subdivided into independent parts, while the association of certain events would indicate a robustness to modifications. Our data give insight into the evolvability of the central complex: The end point of central complex development is similar and thus conserved in both species. The developmental programs govern the same set of robust modules. However, time shifts and reshuffling of event order demonstrate evolvability of a developmental program in reaching a conserved end point.

3.1.4.7. Use of genetic neural lineages facilitates insights into Brain evo-devo

Our finding that the larval central body is not just a precociously formed copy of the adult neuropil, but a distinct but functional larval form illustrates the importance of conducting developmental studies of homologous cells in different species as part of evolutionary research. Without developmental research, a comparison of *Tribolium* and *Drosophila* would have yielded a very similar result of conserved adult neuropils. Simultaneously the lack of a *Drosophila* central complex larval form (at least a functional, i.e. synapsin-positive one) and the presence of a *Tribolium* form illustrates the importance of conducting comparative research as part of developmental studies.

Our approach of using genetic neural lineages, in which homology can be established on a conserved genetic basis with the addition of morphological criteria, and cells can be followed throughout development, is particularly useful for detailed comparative investigations on a cellular level, that require to be based on homology. This includes the analysis of projection patterns, which are essential for neuropil function and thus most relevant for the evolution of the brain. The alternative approach of single cell sequencing (Konstantinides et al., 2018) is fascinating indeed and will hopefully complement study of cells in their native environment such as ours and offer new questions.

Our approach, however, has limits as well. The use of transcription factors as markers, requires the use and generation of suitable transgenic lines and is therefore work-intensive and restricted to organisms with sufficient genomic information and established genome editing tools.

However, with the simultaneous rise of tractable genetic models, particularly through the relative ease of the CRIPSR/Cas system (Gilles and Averof, 2014), we hope that our idea further offers an opportunity that can be used in a multitude of species. A direct possibility would be to include *Gryllus bimaculatus* (Watanabe et al., 2017) and perform identical transgenic line construction, Rx stainings and subsequent characterisation of the DM1-4 lineage cluster expressing Rx throughout development. *Gryllus* would be a suitable representative of a hemimetabolous species.

3.1.4.8. Conclusion & Outlook

To summarize, we were able to compare for the first time homologous genetic neural lineages from embryogenesis to adult, establishing the use of genetic neural lineages as a suitable method transferrable to most insect species and relevant for brain evo-devo. We illustrate two aspects of central complex development and evolution: First, we characterised central complex heterochrony in detail and highlighted that likely developmental modules, disentangled from each other, can be shifted and modified during central complex evolution. Second, *Tribolium* and likely other insects have two distinct functional forms of the central complex on which selection can act, with a specific non-columnar and weakly decussated architecture

Possible future topics have opened with this, to further the understanding of central complex development and evolution: The larval central body can be used to determine alternative ways to build a functioning central complex neuropil, with FIB-SEM, as complementary study to e.g. Andrade et al. (2019). Also, the behavioural consequences of a larva-specific central body are fascinating indeed. In addition, with emphasis on *rx* we observed that while *rx* is expressed in DM1-4 lineage offspring, it is likely not expressed in the respective type II neuroblasts (Bayraktar and Doe, 2013 for antibody screening; Posnien et al., 2011a, Figure 2). This is complementary to the expression in mushroom body neuroblasts where *rx* is expressed in neuroblasts and first postmitotic neurons (Kraft et al., 2016). Hence, like others, we were not able to bridge the gap between neuroectoderm neuroblast maps (Urbach and Technau, 2003b) and the type II DM1-4 lineages (Izergina et al., 2009; Walsh and Doe, 2017). A molecular examination of whether type II neuroblasts (Boyan and Reichert, 2011) are also present in *Tribolium* would help to understand central complex development in this species and overall.

3.1.5. MATERIAL AND METHODS

3.1.5.1. General considerations

We adhered to the nomenclature presented in Ito et al. (2014), except for our reference to the DM4 ipsilateral fascicle as tract. With this we stay in tradition of referring to the fascicle as W tract (Boyan et al., 2017). In addition, we referred to central body divisions as upper and lower division, instead of fan-shaped and ellipsoid, to facilitate cross-species comparison and avoid confusion regarding the form of these structures.

Animals were reared under each species' respective standard conditions (Brown et al., 2009; Roberts, 1998). Timed stages were determined at 32°C for *Tribolium castaneum* and 25°C for *Drosophila melanogaster*, which corresponds to the respective upper limit of rearing temperature.

Where possible, females were selected for stainings to minimize variability and exclude sex differences. Specifically, only female brains were used in all pupal stages (through pre-selection of *Drosophila* larvae, and direct analysis of *Tribolium* pupae), late larval stages in *Drosophila* and adult stages.

If not otherwise specified, depicted tissues are representatives of a dataset of at least N=3 brains that was checked for consistency of the respective labelling.

All stacks from which figures were created can be found under figshare (https://figshare.com/account/home#/projects/64799).

All *Drosophila* and *Tribolium* stocks, antibodies and dyes, as well as primers that we used in this study can be found in the Supplementary Tables 3.1–2-4.

3.1.5.2. Tc-Rx antibody generation and verification

To identify Rx-positive cell groups, protein detection through antibody staining is necessary. An antibody for the *Drosophila* Rx (Dm-Rx) protein was kindly gifted by Dr. Uwe Walldorf (Davis et al., 2003). Its specificity was verified by absence of staining in Dm-Rx null mutant brains and by a similar expression pattern as *Dm-rx* RNA (Davis et al., 2003; Eggert et al., 1998).

We tested cross-specificity of this antibody to the *Tribolium* Rx (Tc-Rx) protein. However, no staining was detected (data not shown). As the antigenic region of Dm-Rx used for antibody generation by Davis et al. (2003) is absent or highly diverged in the *Tribolium* Rx protein (like in a number of other species, see Supplementary Figure 3.1–1A), we used the Tc-Rx N-terminal region (amino acids 1-107), avoiding highly conserved homeobox and OAR domains (Supplementary Figure 3.1–1A) to generate a suitable antibody. This 321 bp long region was amplified (primers including linker sequences: *Tc-rx-N_fw* and *Tc-rx-N_rev*, Supplementary Table

3.1–2) from wildtype cDNA and cloned into a Golden Gate vector containing a 6x His-Tag and a sequence encoding for a SUMO polypeptide (KNE001, pET SUMO-GoldenGate) with a molar ratio of 1:5 of insert to vector (see 3.1.9.4 Supplementary Material and Methods for source, modifications and cloning information).

For subsequent protein expression and purification, we essentially followed Monecke et al. (2014). The vector was transformed into bacteria of the BL21-DE3 Rosetta strain. The peptide was expressed in TB (Terrific Broth) medium with the addition of 15 mM Glucose by 0.8 mM IPTG induction at an OD_{600} of 0.8 for four hours, harvested (5,000×g, 20 min, 4°C), resuspended in lysis buffer (50 mM Tris-HCl pH=7.5, 150 mM NaCl, 10 mM Imidazole) fractionated using a microfluidizer 110S (Microfluidics, MA, USA) and cell debris removed by centrifugation (30,000×g, 30 min, 4°C). The peptide was subsequently purified by immobilized metal ion affinity chromatography using an ÄKTAprime plus and Nickel-charged affinity columns (both GE Healthcare Lifesciences, Chicago, USA). Main steps included affinity chromatography with a linear gradient of elution buffer (50 mM Tris-HCl pH=7.5, 150 mM NaCl, 400 mM Imidazole), cleavage of the His_6-SUMO tag with SUMO protease (1:50 molar ratio protease to peptide) with simultaneous dialysis (50 mM Tris-HCl pH=7.5, 150 mM NaCl) over night at 4°C, a second affinity chromatography to remove the His_6-SUMO tag and finally a size exclusion chromatography with the Superdex 30 16/60 (GE Healthcare) and storage in 1X PBS. The purified protein fragment was used for polyclonal antibody generation and subsequent affinity purification of the antibody (Kaneka Eurogentec S.A., Belgium).

To exclude possible off-targets of the antibody and to validate whether the protein was correctly detected by the antibody (Uhlen et al., 2016), we performed a combination of *Tc-rx* in situ hybridisation (DIG-labelled full length probe, 0.4 µl in 30 µl hybridisation buffer) and Tc-Rx antibody staining in *Tribolium* embryos (as in Posnien et al., 2009, Buescher et al., in press; Supplementary Figure 3.1–1B, C). We found a high degree of overlap between the antibody staining and in situ hybridisation (Supplementary Figure 3.1–1B). No additional staining in the embryo was observed, so that off-targets seem unlikely. To confirm specificity for the endogenous protein, we performed parental RNAi against *Tc-rx* (1.5 µg/µl) following standard procedures (Posnien et al., 2009). We then performed antibody stainings, including a control staining against Engrailed (to exclude differences in staining intensity) in knockdown and wildtype animals (Supplementary Figure 3.1–1C). All steps from fixation to imaging were performed using a standardized protocol. Maximum intensity projections of 34 animals were grouped into three different Tc-Rx staining intensity groups. A blinded categorisation into wildtype and knockdown animals was performed and revealed that all knockdown animals belonged to middle or low

strength categories confirming a reduction of Tc-Rx. Hence, the new antibody against Tc-Rx is highly specific for the provided antigen (affinity purification) and the endogenous protein (Supplementary Figure 3.1–1B and C).

3.1.5.3. Generation of a *Drosophila* bicistronic Rx transgenic line

In order to generate a comprehensive picture of projections of all Dm-Rx-positive cells and to enable subsequent comparative development of Rx-positive cell groups, we generated a bicistronic line (Supplementary Figure 3.1–3, see also Farnworth et al., in press) using the CRISPR/Cas9 technique (e.g. Gratz et al., 2013). We also screened available transgenic lines, i.e. two VT-GAL4 lines (https://stockcenter.vdrc.at) that include small fragments of the Dm-Rx regulatory region and hence only covered very small portions of Dm-Rx expression (data not shown).

We built a bicistronic construct as part of the CRISPR repair template, consisting of the C-terminal part of the *Dm-rx* gene, the CDS encoding for EGFP and a P2A peptide (Kim et al., 2011; Szymczak-Workman et al., 2012), The 22 amino acid long peptide (Kim et al., 2011) is suggested to cause ribosomal skipping (Donnelly et al., 2001). This sequence, if placed between two genes or CDS enables the transcription of one long mRNA of *Dm-rx*-P2A-EGFP, but the translation of two separate proteins. The P2A and EGFP sequences were inserted by using a guide RNA with the target sequence near the *Dm-rx* STOP codon (guide A, Supplementary Figure 3.1–3). This should result in a common expression of Dm-Rx and EGFP in the same cells, without disturbing the function of either gene through e.g., a fusion product, but with EGFP being in the cytoplasm and Dm-Rx retaining its nuclear localisation.

We included the fluorescent eye marker 3XP3-DsRed (Berghammer et al., 1999) for the identification of positive transformants after transgenesis. Note that we avoided other eye or body markers, such as mini-white because of their size, to keep the likelihood of homology-directed repair as high as possible. In order to reduce the possible influence of the 3XP3 promotor on Dm-Rx or GFP we inserted the eye marker in the downstream intergenic region, by using a guide RNA targeting the intergenic region (guide B, Supplementary Figure 3.1–3). To facilitate homology-directed repair we included two flanking homology arms (Supplementary Figure 3.1–3; see 3.1.9.4 Supplementary Material and Methods for the vector map of MF01). As a result, our repair template consisted of seven fragments, which we assembled using a Gibson Assembly® kit (New England Biolabs, MA, USA), following the manufacturer's instructions:

1. Backbone: pJET 1.2/blunt (K1231, ThermoFisher Scientific, MA, USA), EcoRV linearized

2. left homology arm (F (Fragment) 1): 1 kb (kilobases) of the C-terminus of *Dm-rx* (CG10052) excluding STOP codon
3. P2A peptide (F2): insect codon-optimized sequence (see 3.1.9.4 Supplementary Material and Methods) from KNE020 (unpublished)
4. EGFP (F3): from plasmid gifted by the Wimmer department, University of Göttingen
5. 3' UTR and intergenic region (F4): is the region between guide A and B3 (see Supplementary Figure 3.1–3)
6. 3XP3-dsRED-SV40 (F5): eye marker, from plasmid gifted by the Wimmer department, University of Göttingen
7. Right homology arm (F6): 1 kb downstream of guide B3 cut site (three base pairs upstream of its PAM (protospacer adjacent motif))

The target for guide A would thus be between F1 and F2, and the target for guide B between F5 and F6.

In order to identify single nucleotide polymorphisms in the target strain, integrate the right sequences for F1, F4, F6 and to identify suitable target sites and guide RNAs, we isolated genomic DNA (as described in Farnworth et al., in press) from the Act5C-Cas9, Lig4[169] donor stock (Zhang et al., 2014), and PCR amplified and sequenced the *Dm-rx* C-terminal region, 3' UTR and intergenic region (primers *DmRx_CDS_3'UTR_fw, DmRx_CDS_3'UTR_rev, DmRx_3'UTR_int-region_fw, DmRx_3'UTR_int-region_rev*, Supplementary Table 3.1–2). These regions were used to locate target sites (see Supplementary Figure 3.1–3 A[iii]) via the CRISPR Optimal Target Finder (http://targetfinder.flycrispr.neuro.brown.edu/). No off targets were present for all targets selected. Annealed oligonucleotides were cloned into a U6:3-BbsI vector (based on pCFD3-dU6:3gRNA, Addgene #49410, Port et al. (2014), kindly provided by Hassan M.M. Ahmed (Wimmer department, University of Göttingen, unpublished)) via a GoldenGate reaction, following procedures in Farnworth et al. (in press) but using BbsI (New England Biolabs, MA, USA). Successful cloning was verified by sequencing the complete chimeric RNA scaffold (including trans-activating crRNA, Port et al., 2014). guideRNAs were quality controlled by using a T7 Endonuclease I assay (see Farnworth et al., in press for procedure). Injection procedures followed descriptions in Eckermann et al. (2018).

Based on the T7 Endonuclease I assay, we selected one guide for the guide A target site, and three with overlapping target sites for the target of guide B (B1-3) (Supplementary Figure 3.1–3 A[iii]).

Next, we designed a 1 kb long F1 (left homology arm) so that it ended before the STOP of *Dm-rx*, as Guide A caused a Cas9 cut only 8 bp downstream of the *Dm-rx* STOP. F4 was designed

from the 3'UTR start to the cut site of guide B3 (note that guide B1 and B2 were near B3), with modifications of all PAMs in primers P7 and P8. F6 was 1 kb long, starting at the cut site of guide B3.

All fragments for the Gibson Assembly® were amplified using the primers P1 to P12 (see 3.1.9.4 Supplementary Material and Methods), containing overlaps to the neighbouring fragment. F1, 4 and 6 were amplified from the previously isolated genomic DNA of Act5C-Cas9, Lig4[169]. We then used three assembly reactions (roman numerals in primers P1 to P12). The first assembled F1 to F3, the second F4 to F6, and the third assembled the products of the first two reactions.

The four plasmids containing guides and MF01 were precipitated (Eckermann et al., 2018; Farnworth et al., in press) to ensure DNA purity and increase viability of embryos after injection. We then made three injection mixes, each containing one of the guides B1 to B3 (250 ng/µl), guide A (250 ng/µl) and MF01 (400 ng/µl), diluted in 1x injection buffer (Eckermann et al., 2018). Subsequent injections followed descriptions in Eckermann et al. (2018).

We injected 1203 embryos of which 424 G_0 adults survived. We crossed them singly to three w^{1118} virgins of the opposite sex and received 224 F1 stocks. We then screened them under a fluorescence stereo microscope (Leica M205 FA, Leica, Wetzlar, Germany) for the presence of the 3XP3-DsRed eye marker. We detected 27 positive stocks. Note, however, that we observed heritable variability in strength and location of DsRed inside the *Drosophila* eye. We thus took four of the 27 positive stocks, with varying degree of eye marker strength and screened wandering third instar larval brains for any detectable differences in the presence of a GFP fluorescence signal resembling known Dm-Rx antibody staining (Davis et al., 2003). All four stocks did not vary in GFP expression and showed equal similarity to a Dm-Rx antibody staining. To verify this tendency, we performed immunostainings in offspring embryos of these four lines and detected GFP and Dm-Rx signal through a GFP antibody staining. Embryos of all four stocks showed near 100 % overlap to Dm-Rx and a cytoplasmic signal. Finally, to verify that insertion was performed as planned (Supplementary Figure 3.1–3 A[ii]), we isolated genomic DNA from one whole adult male of each of the four stocks using the Zymo Research *Quick*-DNA Miniprep Plus kit (Zimo Research, Irvine, CA, USA) following the manufacturer's Solid Tissues Protocol. We then amplified DNA fragments containing the whole region by nested PCR (primers *DmRx_trans-ver_fw, DmRx_trans-ver_rev, DmRx_trans-ver_nested_fw, DmRx_trans-ver_nested_rev*, Supplementary Table 3.1–2). We sequenced the regions surrounding the cut sites with primers *DmRx_trans_seq_Ct_fw* and *DmRx_trans_seq_iRe_rev (*Supplementary Table 3.1–2). All four stocks showed correct sequencing at guide A cut sites, but only the line used in this study showed

completely correct sequences, thus allowing us to perform suitable experiments and closer characterisation (Supplementary Figure 3.1–3 C-F).

To verify that EGFP is indeed localised in the cytoplasm, we performed immunostainings for Dm-Rx and GFP in embryos. With higher magnification we were able to see a substantial amount of GFP in the cytoplasm surrounding the nuclei marked by Dm-Rx (see Supplementary Figure 3.1–3 C) and DAPI (not shown). We also wanted to know whether expression from the transgenic Dm-Rx locus was qualitatively different from the endogenous expression as to ensure that we investigated Dm-Rx expression similar to a wildtype situation. For this we performed immunostainings against Dm-Rx in the adult *Drosophila* brain with identical settings and imaged them identically (see Supplementary Figure 3.1–3 D). We were not able to detect any absence of domains (see Supplementary Figure 3.1–3 D). Differences between the wildtype strain w^{1118} and our transgenic line were – if present – as large as differences between individual brains of the same genetic background.

We then tested whether the expression of Dm-Rx and EGFP in the same cells is maintained in the adult brain (Supplementary Figure 3.1–3 E and F). Indeed, by qualitative assessment we were able to see an approximately 100 % coexpression, with prominent projections marked as well (see Figure 3.1–2).

We thus concluded that the Rx-GFP bicistronic line was suited for our use.

3.1.5.4. Characterisation and validation *Tribolium* Rx-GFP enhancer trap

We identified a suitable *Tribolium* transgenic line in the GEKU base website (# E01101, http://www.geku-base.uni-goettingen.de/; Trauner et al., 2009). Insertion had been mapped to the upstream region of *Tc-rx* (Trauner et al., 2009; Supplementary Figure 3.1–2 A). To identify to which degree Tc-Rx expressing cells also express GFP we performed co-stainings in adult brains. We found that n-ventral Tc-Rx-positive cells were not marked by the line at all (see Supplementary Figure 3.1–5) while n-dorsal domains were only partially marked (see Supplementary Figure 3.1–5 B). However, by manually checking each GFP expressing cell, we found that all cells expressing GFP in the region surrounding the protocerebral bridge, also expressed Tc-Rx (Supplementary Figure 3.1–2 B, D). Hence, there were no cells that were marked false-positively. Interestingly, there were more GFP expressing cells showing overlap to Tc-Rx expression in all other stages of development (Supplementary Figure 3.1–2 E). To ensure that Tc-Rx was expressed similar to the wildtype situation, we performed identical immunostainings against Tc-Rx and imaging with identical settings in the transgenic line and wildtype v^{w} background (Lorenzen et al., 2002; Supplementary Figure 3.1–2 C). We found that differences

between conditions were no larger than the differences observed between individuals of the same condition. We thus concluded that the Rx-GFP enhancer trap was suitable for further experiments.

3.1.5.5. Generation of homozygous stocks of Rx-GFP transgenic lines

A homozygous stock of the *Tribolium* Rx-GFP enhancer trap was generated by genotyping adult wing tissue (as described in Strobl et al., 2017; Farnworth et al., in press), with primers *GEKU-Rx-GFP_wt_fw*, *GEKU-Rx-GFP_wt_rev*, *GEKU-Rx-GFP_trans_rev* (Supplementary Table 3.1–2).

A homozygous stock of the *Drosophila* Rx-GFP bicistronic line was generated by crossing the male offspring (G2) of the G1 cross to female virgins of a w^-; wg^{Gla-1}/CyO balancer (a kind gift by the Wimmer department, University of Göttingen). CyO positive animals (G3) were selected and crossed to each other, to create homozygous positive animals (G4) for the transformation marker (3XP3-dsRed-SV40).

Both transgenic lines were homozygous viable.

3.1.5.6. R45F08-GAL4 crosses

To reveal the overlap of secondary cells of the DM1-3 and 6 lineages marked by the R45F08-GAL4 line (Jenett et al., 2012; Riebli et al., 2013) with Dm-Rx expressing cells we performed two crosses and subsequent immunostainings (Supplementary Figure 3.1–6).

First, we crossed the R45F08-GAL4 line with a UAS-mcD8::GFP line and investigated offspring third instar larvae to visualize the characterized cells and subsequently stained with anti-GFP and anti-Rx antibodies (Supplementary Figure 3.1–6 A/B).

Second, to visualize an overlap of Dm-Rx expressing cells and R45F08 labelled cells, we first crossed the *Drosophila* Rx-GFP bicistronic line each separately with R45F08-GAL4 and UAS-mcD8::RFP. The respective offspring was then crossed to each other. We then dissected 15 brains of third instar larvae, stained them with anti-RFP and anti-GFP, screened for the presence of RFP and GFP label and imaged double-positive brains (Supplementary Figure 3.1–6 C).

3.1.5.7. Staging of *Tribolium* and *Drosophila* animals

Table 3.1–1 displays all stages and their description included in our study. Particularly pupal staging and the late larval stages were determined using time (which allowed us to calculate relative times of pupation) and morphology as criteria to confirm the timed staging.

Drosophila embryonic stages were determined using the staging of Campos-Ortega and Hartenstein (1985) and pupal stages using staging in Bainbridge and Bownes (1981) (Table 1 displays the most important pupal selection criteria). Eye colouring and morphology were not included in staging due to the w^{1118} background (see 3.1.9.4 Supplementary Material and Methods). Information on the length of embryonic development used in Figure 3.1–9 was derived from Campos-Ortega and Hartenstein (1985). Length of larval development and pupation was measured for our Rx-GFP bicistronic line specifically.

Tribolium embryonic stages were determined using the staging of Biffar and Stollewerk (2014) and for late embryonic stages using staging of Scholten and Klingler (unpublished). *Tribolium* pupal and late larval staging was aided by Ho (1961) and Dippel (unpublished). Information on length of embryonic development used in Figure 3.1–9 was derived from Biffar and Stollewerk (2014) and Scholten and Klingler (unpublished). Total developmental time was taken from Sokoloff (1974). Larval and pupal developmental length was measured for our Rx-GFP enhancer trap specifically.

Table 3.1–1: Stages and their definition included in this study.

Drosophila			***Tribolium***	
Stage	**Time (h)**	**Description**	**Time (h)**	**Description**
Embryos	variable	All staging follows Campos-Ortega and Hartenstein 1985	variable	Staging to 48 h: Biffar and Stollewerk 2014; >48 h: Scholten and Klingler (unpublished)
L1	≤ 1 after hatching	selection after removing any previously hatched larvae on apple agar plate	≤ 1 after hatching	selection by falling through 300 µm gaze sieve on which embryos were kept
50 % (mid-) larva	37.5	timing started after selection like for L1, end of L2 larval development	~ 216 (9 d)	timing started after selection like for L1, approximately L4 stage
95 % (late-) larva	70-75	up to event 2 (see Bainbridge and Bownes 1981), crawled to top, no movement	410-432 (17-18 d)	last larval stage, stemmata migration started, see Ho 1961
0 % pupa	0	up to event 8 (see Bainbridge and Bownes 1981), particularly shortened body, white puparium	0	stemmata migration ended (medial position near vertex), see Ho 1961
5 % pupa	5	up to event 14 (see Bainbridge and Bownes 1981), operculum ridge visible, abdominal gas bubble	7	2 rows of ommatidia, shiny cuticle, see Ho 1961, and Dippel (unpublished)
15 % pupa	15	up to event 25 (see Bainbridge and Bownes 1981), particularly anterior bubble, expelled armature	21	4 rows of ommatidia, mandible tip sclerotized, see Ho 1961, and Dippel (unpublished)
20 % pupa	20	up to event 26 (see Bainbridge and Bownes 1981), criteria of 15 % and prominent Malphigian tubules	28	4-6 rows of ommatidia, mandible tip sclerotized, see Ho 1961, and Dippel (unpublished)
30 % pupa	30	up to event 27 (see Bainbridge and Bownes 1981), criteria of 20 %, yellow body, eyes not included	42	6 rows of ommatidia, mandible tip sclerotized, see Ho 1961, and Dippel (unpublished)
50 % pupa	50	criteria of 30 %, otherwise only time	70	7 rows of ommatidia, see Ho 1961, and Dippel (unpublished)
adult	≤ 12 after eclosion	eclosed with signs of virgin females (light body coloring)	≤ 24 after eclosion	eclosed with light brown body coloring

3.1.5.8. Specimen fixation and immunohistochemistry

Methanol fixation of *Drosophila* embryos was performed following standard protocols (Rothwell and Sullivan, 2007). Fixation of *Tribolium* embryos was based on Schinko et al. (2009a) with following modifications: Fixation was performed with 2 ml of fixation buffer PEMS (0.1 M PIPES, 2 mM MgCl, 5 mM EGTA, pH = 6.9); we added 180 µl of 37 % formaldehyde (F 1635, Merck, Darmstadt, Germany) and fixed embryos between 25 and 32 min; devitellinisation was first conducted with a 0.9 µm canula, for older stages (> 40 h) we followed with a 0.8 µm canula.

Immunohistochemistry of embryos was based on procedures in Buescher et al. (in press), with the addition of preceding washes in a descending methanol series (75, 50 and 25 % Methanol with PBS-T 0.1 %), followed by two rinse steps and three 10 min washes.

For all stainings normal goat serum was used as blocking solution (NGS, G9023, Merck, Darmstadt Germany, see Table 3.1–2). Fixative for all other stages except for embryos was 4 % PFA (wt/vol, paraformaldehyde, (e.g. P6148, Merck, Darmstadt, Germany) in PBS, 130 mM NaCl, 7 mM Na_2HPO_4, 3 mM KH_2PO_4, Riemensperger et al., 2011). Washing buffer for all stages except embryos was phosphate buffer (PB, see Ostrovsky et al., 2013 for recipe). Brains were dissected using Dumont No. 5 forceps in ice-cold PB. All steps were performed in 180 µl volume in 9-well PYREX™ Spot Plates (ThermoFisher Scientific, MA, USA) on an orbital shaker. Protocols were adapted from Riemensperger et al. (2011) and Ostrovsky et al. (2013).

Table 2: Immunohistochemistry in stages (excluding embryos) of both species. There are two variations of adult stainings. Antibodies were used as in 3.1.9.4 Supplementary Material and Methods except for synapsin. PB phosphate buffer (Ostrovsky et al., 2013), T Triton-X-100 with % in PB, PFA paraformaldehyde, NGS normal goat serum.

Preparation steps	L1 larvae	Larvae	Pupae	Adults
Fixation	1 h on ice, in 4 % PFA	50 % larva: 1 h on ice, in 4 % PFA, other: 1.5 h on ice, in 4 % PFA	1.5 h on ice, in 4 % PFA	1.5-2 h on ice, in 4 % PFA
Post-fixation washes	1 rinse, 3 30 min washes in PB-T 0.1 %	50 % larva: 1 rinse, 3-4 30 min washes in PB-T 0.1 %, other: 1 rinse, 3-4 30 min washes in PB-T 0.3 %	1 rinse, 3-4 30 min washes in PB-T 0.2-0.3 %	I: 1 rinse, 3-4 30 min washes in PB-T 0.3 %, II: 1 rinse, 3-4 30 min washes in PB-T 0.5 %
Blocking	o/n at 4°C in 4 % NGS in PB-T 0.1 %	o/n at 4°C in 5 % NGS in PB-T 0.1 % (50% larva), or 0.3 % (other)	o/n at 4°C in 5 % NGS in PB-T 0.2-0.3 %	I: o/n at 4°C in 5 % NGS in PB-T 0.5 % II: 24 h at 4°C in 5 % NGS in PB-T 0.3 %
First antibody	4 h at RT in 2 % NGS in PB-T 0.1 %, Synapsin 1:30 (Dm), 1:20 (Tc)	4-6 h at RT in 2 % NGS in PB-T 0.1 % (50%), 0.3 % (other), Dm Synapsin 1:30, Tc 1:20-30	5 h at RT or 40-48 h at 4°C in 2 % NGS in PB-T 0.2-0.3 %, Synapsin 1:25 (Dm), 1:15 (Tc)	I: 6 h at RT in 2 % NGS in PB-T 0.5 %, II: 72 h at 4°C in 2 % NGS in PB-T 0.3 %, Synapsin 1:25 (Dm), 1:15 (Tc)
Post-1st antibody washes	1 rinse, 3 30 min washes in PB-T 0.1 %	1 rinse, 4 30 min washes in PB-T 0.1 % (50%), 0.3 % (other)	1 rinse, 4 40 min washes in PB-T 0.2-0.3 %	1 rinse, 4 50 min washes in PB-T 0.3/0.5 %
Secondary antibody	o/n at 4°C in 2 % NGS in PB-T 0.1 %	o/n at 4°C in 2 % NGS in PB-T 0.1 % (50%), 0.3 % (other)	o/n to 24 h at 4°C in 2 % NGS in PB-T 0.2-0.3 %	I: 24 h at 4°C in 2 % NGS in PB-T 0.5 % II: 48 h at 4°C in 2 % NGS in PB-T 0.3 %
Post-2nd antibody washes	1 rinse, 1 30 min wash including DAPI, 1 rinse, 3 30 min washes, all in PB-T 0.1 %	1 rinse, 1 30 min wash including DAPI, 1 rinse, 3 30 min washes, all in PB-T 0.1 % (50%), 0.3 % (other), 2 h wash in PB	1 rinse, 1 30 min wash including DAPI, 1 rinse, 3 30 min washes, all in PB-T 0.2-0.3 %, 2 h wash in PB	1 rinse, 1 30 min wash including DAPI, 1 rinse, 4 30 min washes, all in PB-T 0.3/0.5 %, 3 h wash in PB
Embedding medium	VectaShield H-1000 (Vector Laboratories)	RapiClear 1.47 (SUNjin Lab, Hsinchu City, Taiwan)	RapiClear 1.47 (SUNjin Lab, Hsinchu City, Taiwan)	RapiClear 1.47 (SUNjin Lab, Hsinchu City, Taiwan)

3.1.5.9. Image acquisition, and processing and 3D reconstruction

If not otherwise specified, imaging was performed at a Leica SP8 confocal microscope (Wetzlar, Germany). Objectives used were either a Leica apochromat 20x (NA = 0.75) or a 63x HC PL APO CS2 (NA = 1.30) glycerol-immersion objective. DAPI was excited by a Diode laser (405 nm), Alexafluor 488 (ThermoFisher Scientific, MA, USA) by an Argon laser (488 nm), Alexafluor 555 by a DPSS laser (561 nm) and Alexafluor 647 by a HeNe laser (633 nm). Detection was performed with Hybrid detectors and photomultipliers, at an 8-bit depth. Averaging was depending on which staining was performed, set on line or frame averaging of 4. Step size was set to system optimized values defined by the LASX software. Image size was set between 1,024 x 1,024 and 2,048 x 2,048 pixels. Images were processed, adjusted for brightness and contrast, cropped, merged and rotated using the Fiji software (Schindelin et al., 2012). Maximum

intensity projections and smooth manifold extractions (SMEs; Shihavuddin et al., 2017) to retain 3D spatial relationships were calculated using Fiji as well (Schindelin et al., 2012).

3D reconstructions were performed in Amira 5.4.1 (Visage Imaging, Fürth, Germany). We created Labelfield data with the same pixel and voxel size resolution as the original data set. We then used the Segmentation Editor to identify and create material for each tract and central complex neuropils by employing the Wand tool. Subsequent marking was modified for visual ease using the grow, fill holes and smooth functions of the Segmentation Editor. We then created 3D surfaces with the Surface Generator.

In some cases, projections were too thin to be recapitulated in the 3D surface. For this, where we logically inferred a connection of axons that was only faintly marked by the original file, we used the Brush tool.

We only reconstructed the axon connections to certain cell bodies where we were sure that they are directly connected. This excluded a few cell bodies from the analysis, particularly in the *Drosophila* adult brain.

3.1.6. ACKNOWLEDGEMENTS

We acknowledge the help of Lara Markus by providing embryonic and larval immunostainings, and of Felix Quade by supporting 3D reconstructions. We thank Prof. Uwe Walldorf for providing the Dm-Rx antibody, Dr. Nico Posnien for providing the *rx* full length probe used for in situ hybridisation and Prof. Christian Wegener for providing the anti-synapsin antibody. We thank Dr. Achim Dickmanns and the Department of Molecular Structural Biology in Göttingen for tremendous help regarding protein expression and purification. Further we want to acknowledge substantial help regarding brain anatomy and homologous cell group identification by Prof. Volker Hartenstein. We want to further thank Dr. Stephen H. Montgomery and Prof. Robert A. Barton for fruitful discussions surrounding the project. We are particularly grateful to the Departments of Evolutionary Developmental Genetics and Developmental Biology, and especially to Drs. Marita Buescher, Stefan Dippel and Nico Posnien, for experimental planning, sharing of unpublished data and discussions on the project. We acknowledge tremendous technical support by Elke Küster and Claudia Hinners. We want to thank Profs. Riddiford, Truman and Marek for providing unpublished information regarding metamorphosis. Lastly, MSF acknowledges financial support by the Göttingen Graduate Center for Molecular Biosciences, Neurosciences and Biophysics (GGNB).

3.1.7. AUTHOR CONTRIBUTIONS

GB conceived the original idea. GB, KNE and MSF designed experiments, KNE and MSF conducted experiments, MSF and GB analysed data, MSF and GB wrote the manuscript. All authors approved the final version of the manuscript.

3.1.8. COMPETING INTERESTS

The authors have no competing interests.

3.1.9. SUPPLEMENTARY INFORMATION

3.1.9.1. Supplementary Figures

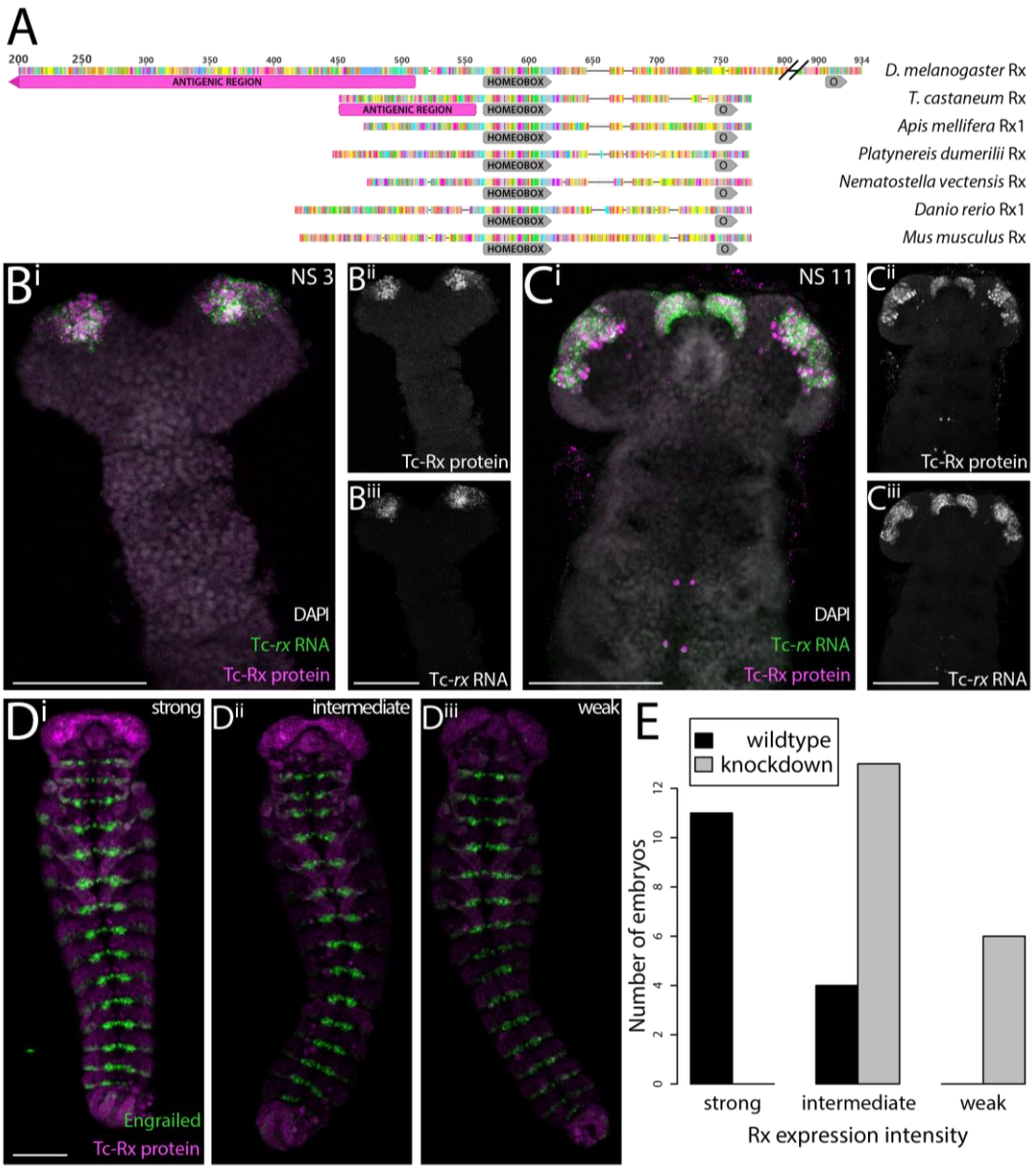

Supplementary Figure 3.1–1: Generation and validation of the Tc-Rx antibody. A. Alignment (Geneious 11.1.5, Geneious Alignment) of Rx proteins of *Drosophila* and *Tribolium* as well as representative species. The conserved homeobox and OAR (O) domains (grey) are present in all proteins. Antigenic regions for the Dm-Rx (Davis et al., 2003; Eggert et al., 1998) and the Tc-Rx antibody are displayed in magenta. The Dm-Rx protein was shortened for better display (amino acids 1 to 200 and most between 800 and 900 are not displayed). Notice that the *Drosophila melanogaster* (*D. melanogaster*) antigenic region appears to be absent in *Tribolium castaneum* (*T. castaneum*) and all other species. **B-C.** Tc-Rx protein and *Tc-rx* RNA expression in *Tribolium* embryos of neurogenesis stages 3 and 11 (Biffar and Stollewerk, 2014) were depicted (Zeiss LSM510, 40x immersion objective) as maximum intensity projections (DAPI for structure as average projection). Anterior is to the top. Animals were mounted dorsal up. The signal detected in the antibody staining against Tc-Rx protein (magenta) overlapped to a high degree with the signal detected in the in situ hybridization (green). Note that while the protein of Tc-Rx was located in the nucleus, *Tc-rx* RNA was also in the cytoplasm of the cell soma which resulted in a different cellular localisation. **D.** To validate the specificity of the Tc-Rx antibody, we performed a RNAi mediated *Tc-rx* knockdown. Indeed, Tc-Rx expression was

reduced in knockdown embryos. Depicted are three categories of Tc-Rx expression (i.e. Tc-Rx antibody staining intensity, magenta, as maximum intensity projections) after knockdown (strong, equalling wildtype, in D^{i}, intermediate in D^{ii}, weak in D^{iii}. To accommodate for differences in intensity of staining, a co-staining against Invected/Engrailed with the respective antibody was performed. **E.** 34 RNAi embryos were categorized into the three expression intensity groups in a blinded experiment. Wildtype animals showed a high level of expression and were mostly grouped in category 'strong' with some in category 'intermediate'. No knockdown animals were grouped into the 'strong' category, most in 'intermediate' and some in 'weak' (Fisher's exact test, $P<0.001$). Scale bars represent 100 µm.

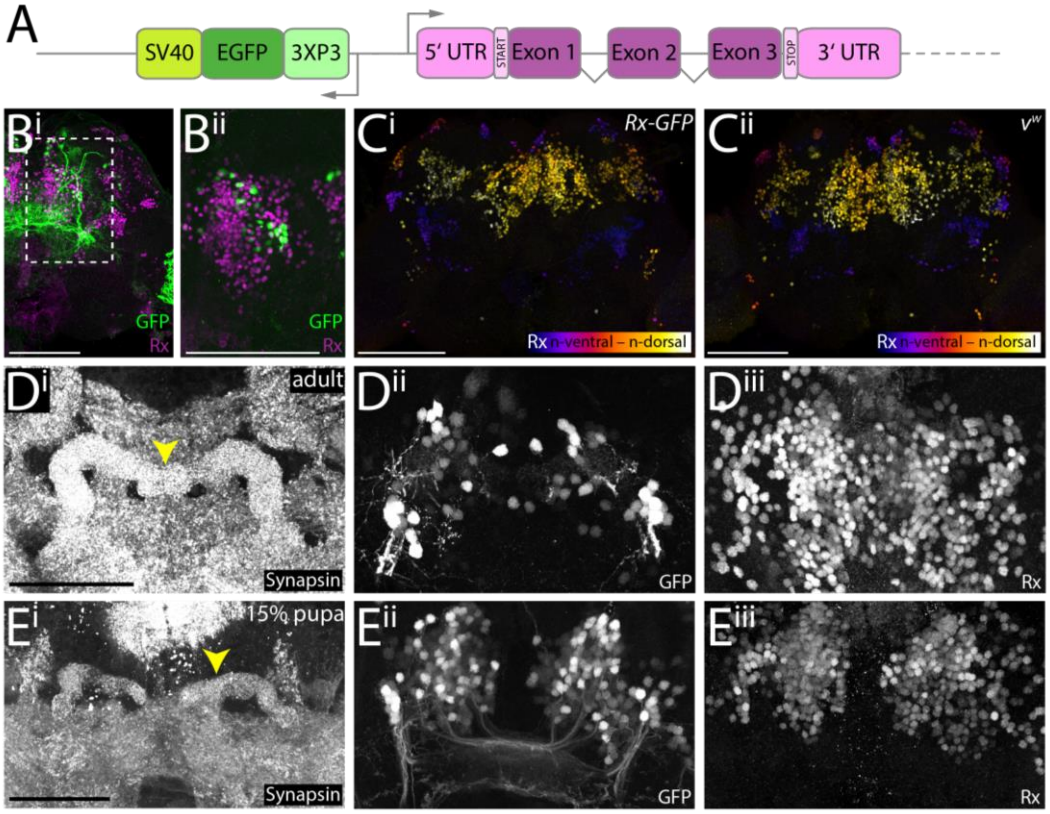

Supplementary Figure 3.1–2: Characterisation and validation of *Tribolium* Rx-GFP enhancer trap line. A. The *Tribolium Rx-GFP* enhancer trap was taken from the GEKU screen collection (Trauner et al., 2009) where enhancer traps were generated by *piggyBac*-mediated transposition. A 3XP3-EGFP-SV40 cassette randomly inserted upstream of the *Tc-rx* gene in opposite direction (insertion site mapped by Trauner et al., 2009). **B.** Maximum intensity projections of immunostainings against GFP and Tc-Rx in adult brains of the *Rx-GFP* enhancer trap line. The enhancer trap only marked a small subset (approximately 5-10 %) of Tc-Rx expressing cells in the adult. This also applies to the n-dorsal region (B^{ii}). However, all GFP expressing cells also expressed Tc-Rx. Coexpression was verified manually. **C.** The introduction of the enhancer trap cassette did not visually influence Tc-Rx expression, as domains were highly similar between transgenic Rx-GFP (B^{i}) and wildtype *vermillion-white* (v^{w}, B^{ii}) animals, as visualised by color-coded maximum intensity projections. Observed qualitative differences in Tc-Rx expression in the transgenic or wildtype condition (N=3 each) were approximately as large as the differences between the genetic backgrounds. **D.** A crop of a maximum intensity projection of cells surrounding the adult protocerebral bridge (yellow arrowhead, D^{i}) shows the coexpression of GFP (D^{ii}) and Tc-Rx (D^{iii}) in a subset of cells that were subsequently used in this study. **E.** An analogous analysis in young pupal brains of cells surrounding the protocerebral bridge (E^{i}) revealed more GFP expressing cells (E^{ii}) with overlap to Tc-Rx cells (E^{iii}) than in the adult (D). Scale bars in B and C represent 100 µm and in D and E 50 µm.

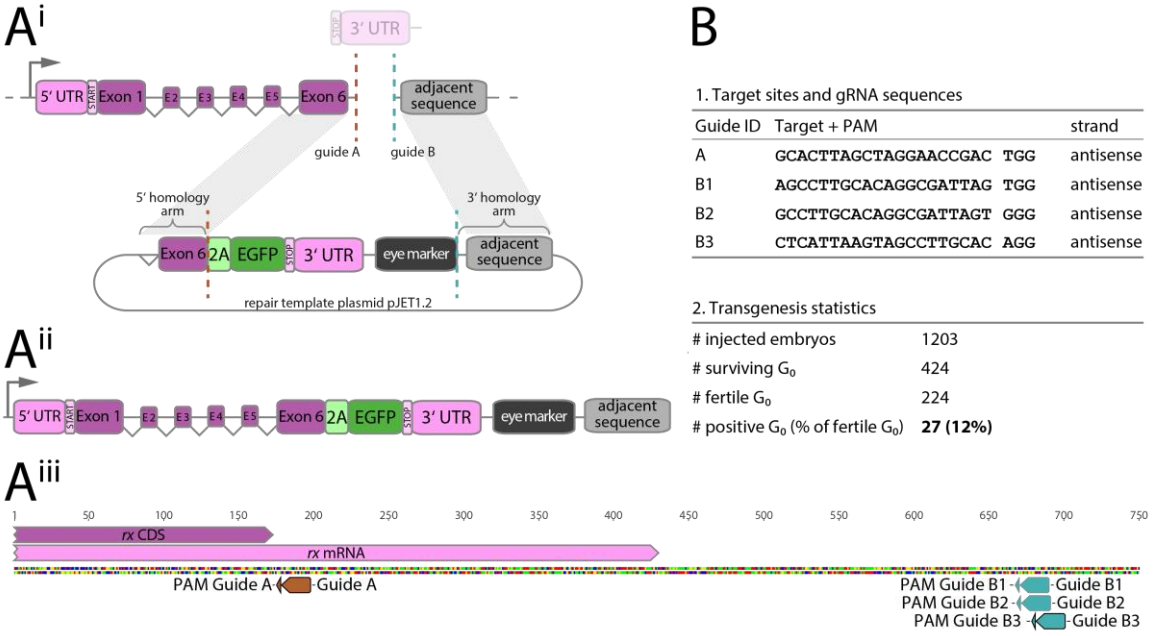

B

1. Target sites and gRNA sequences

Guide ID	Target + PAM	strand
A	GCACTTAGCTAGGAACCGAC TGG	antisense
B1	AGCCTTGCACAGGCGATTAG TGG	antisense
B2	GCCTTGCACAGGCGATTAGT GGG	antisense
B3	CTCATTAAGTAGCCTTGCAC AGG	antisense

2. Transgenesis statistics

# injected embryos	1203
# surviving G_0	424
# fertile G_0	224
# positive G_0 (% of fertile G_0)	**27 (12%)**

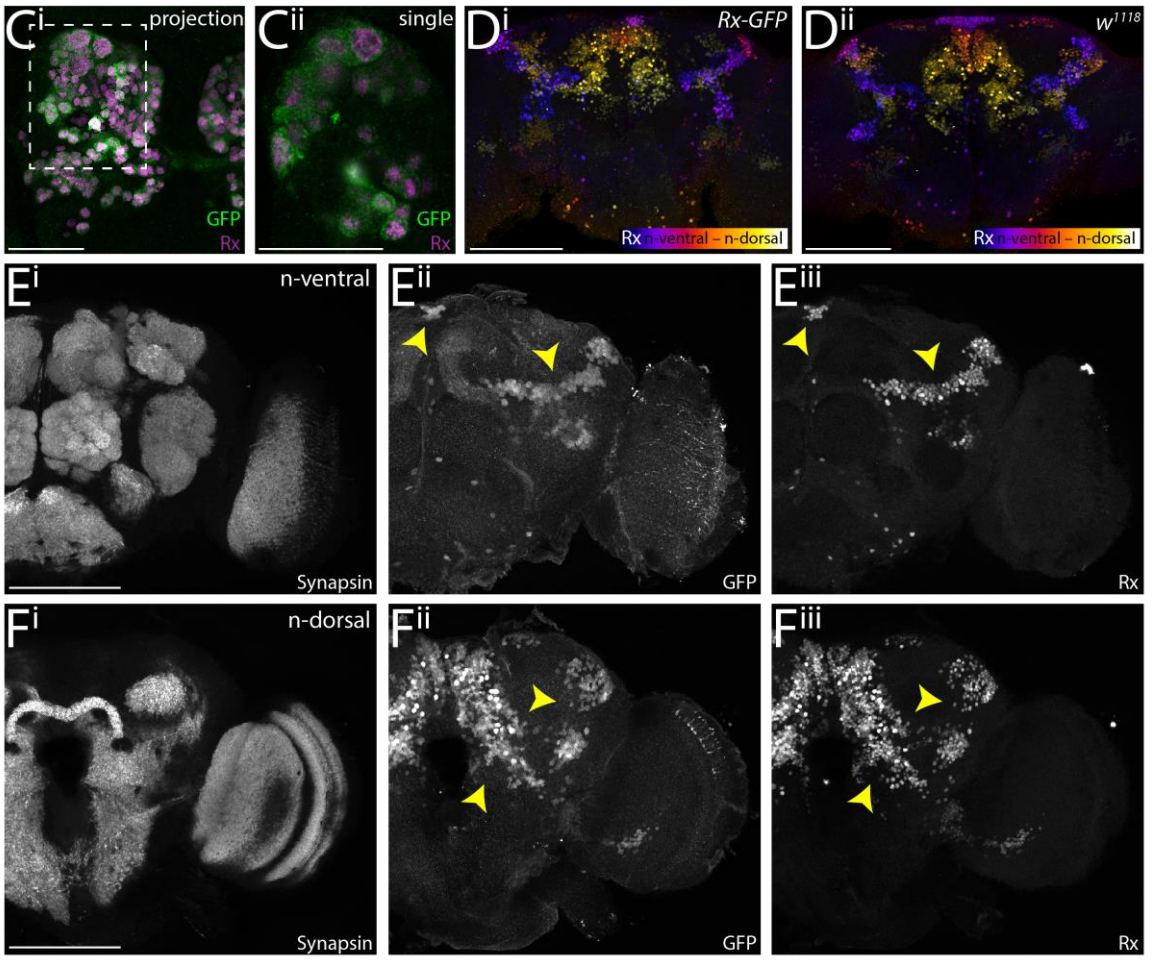

Supplementary Figure 3.1–3: Strategy, generation and validation of *Drosophila* bicistronic *Rx-GFP* transgenic line. A^{i}. Strategy of building an Rx-GFP bicistronic line (modified from Farnworth et al., in press). Two gRNAs next to the endogenous STOP codon (guide A, brown) and downstream of the *Dm-rx* 3'UTR (guide B, blue) were used. The repair template included a P2A peptide, EGFP, the endogenous region between guide A and B (*Dm-rx* 3'UTR and a fraction of intergenic region), and the 3xP3-DsRed-SV40 eye marker, as well as 1 kB homology arms flanking the insertion sites. **A^{ii}.** The resulting transgenic locus formed a common open reading frame of both *Dm-rx*

and *gfp* with a STOP after *gfp*. **A^{iii}.** Four gRNAs were used in different combinations to generate independent transgenic lines. The gRNAs inducing the transgenic line used in this study are marked in bold (guide A and B3). **B.** gRNA sequences and transgenesis statistics for the *Drosophila* Rx-GFP transgenic line. **C^{i}.** Immunostaining of anti-Dm-Rx (magenta) and anti-GFP (green) in the Rx-GFP transgenic line showed that all visible cells that expressed Dm-Rx also expressed GFP, shown in a smooth manifold extension (SME) projection (Shihavuddin et al., 2017) of a brain hemisphere of a S16 embryo. The region marked with a dotted line in C^{i} is shown in **C^{ii}** as a single slice. Here, the different cellular localisations are visible. Dm-Rx retained its nuclear localisation, while GFP located to the cytoplasm. Hence, the P2A peptide of the inserted construct was functional. **D.** The transgenic line had normal Dm-Rx expression, shown by anti-Dm-Rx immunostaining and depth color-coded maximum intensity projection in the Rx-GFP line (D^{i}) and the origin wildtype strain w^{1118} (D^{ii}). Observed qualitative differences in Dm-Rx expression in the transgenic or wildtype condition (N=3 each) were approximately as large as the differences between the genetic backgrounds. **E and F.** Dm-Rx and EGFP expression matched in adult brains (see yellow arrowheads for exemplary double-positive areas). Maximum intensity projections of synapsin immunostainings (E^{i}, F^{i}), GFP (E^{ii}, F^{ii}) and Dm-Rx (E^{iii}, F^{iii}) in an adult *Drosophila* brain. Anti-synapsin (E^{i}, F^{i}) marked brain position. E is n (neuraxis)-ventral and F is n-dorsal (Ito et al., 2014). Scale bars in D-F represent 100 µm and in C 25 µm.

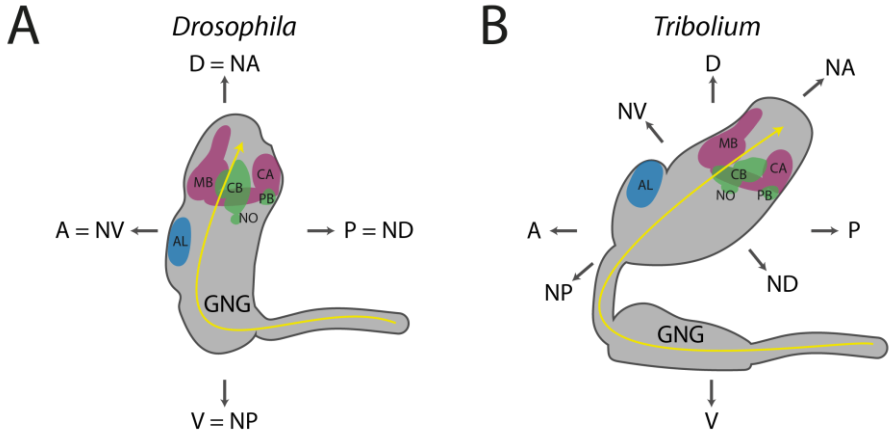

Supplementary Figure 3.1–4: Illustration of the body- and neuraxes in *Drosophila* and *Tribolium* brains, as seen from a lateral view. The *Drosophila* (**A**) and *Tribolium* (**B**) brains differ in their orientation within the head. While the *Drosophila* brain is oriented perpendicular to the ventral nerve cord, the *Tribolium* brain (or specifically the cerebral ganglia, excluding the GNG) is oriented more than 90° with respect to the ventral nerve cord and appears 'bent' towards posterior. This leads to discrepancies in the axis description of neuropils such as the AL being anterior in *Drosophila*, while it is more dorsal in *Tribolium*. Similarly, the PB is posterior in *Drosophila* but more ventral in *Tribolium*. To facilitate cross-species comparisons, Ito et al. (2014) have suggested to use the neuraxis nomenclature which we follow throughout, to make consistent axis statements. In this system, the AL are n-ventral (NV) and the PB n-dorsal in both species. Depicted is a simplified schematic of an adult *Drosophila* central brain (excluding the optic lobes) in lateral view including the approximate position of the fused GNG (A). Axis assignment follows Ito et al. 2014. The shape of the *Drosophila* brain and the three neuropils (CX, MB, AL) was generated from the adult brain at https://v2.virtualflybrain.org/, while the shape of the *Tribolium* cerebrum (central brain not fused to the GNG, see Ito et al., 2014) and neuropils (B) was generated from a volume-rendered Phalloidin stain (original data not shown). The approximate shape and position of the GNG was recreated from Dippel et al. (2016). Abbreviations: AL antennal lobes, PB protocerebral bridge, CB central body, NO noduli, MB mushroom body (excluding CA), CA calyx, n neuraxis-referring, D dorsal, A anterior, V ventral, P posterior, GNG gnathal ganglia.

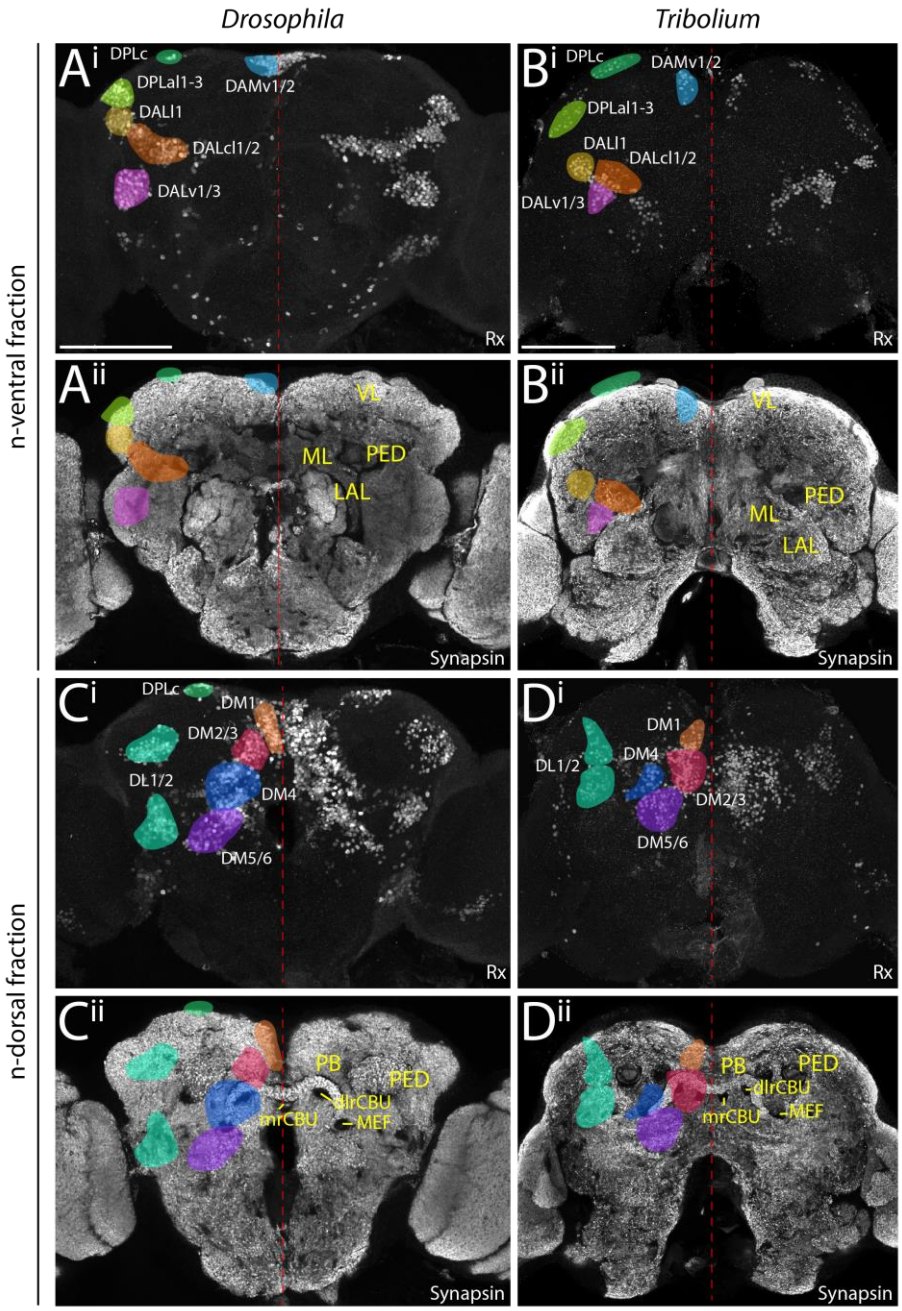

Supplementary Figure 3.1–5: Conserved expression of Rx protein in the adult brain of *Drosophila melanogaster* (A, C) and *Tribolium castaneum* (B, D) as well as lineages marked by Rx expression. We mapped the marked Rx-positive cells to previously described lineages of the *Drosophila* brain using locations relative to other brain structures and their projection pattern as criterion (Lovick et al., 2013; Wong et al., 2013; www.mcdb.ucla.edu/Research/Hartenstein/dbla/index.html and references therein). We tentatively named *Tribolium* cell clusters by using similar locations and projections as compared to the *Drosophila* atlas, used as guide. A list of all lineages with names and descriptions can be found in Supplementary Table 3.1–1. Hemispheres are separated by a red dotted line for orientation. Due to the cell body rind expression of Rx, domains and proposed lineages could be separated into two fractions, n-ventral and n-dorsal, corresponding to each half of the insects' brains (Ito et al., 2014). For each species, one image stack was used and separated into two fractions. Rx expression is displayed by a maximum intensity projection of a sub-stack of an anti-Rx immunostaining (i). Basic anatomical structure of the insects' brains is displayed by a SME projection (Shihavuddin et al., 2017) of synapsin immunostaining (ii). On this projection, in the left hemisphere the locations of the proposed lineages are shown colour-coded, while on the right hemispheres, basic anatomical structures are annotated that assist understanding

differences in domain position between the species (yellow). Abbreviations: VL vertical lobe, ML medial lobe, PED peduncle, LAL lateral accessory lobes, mrCBU medial root of the upper division of the central body, dlrFB dorso-lateral root of the CBU, PB protocerebral bridge, MEF medial equatorial fascicle. Scale bars represent 100 µm.

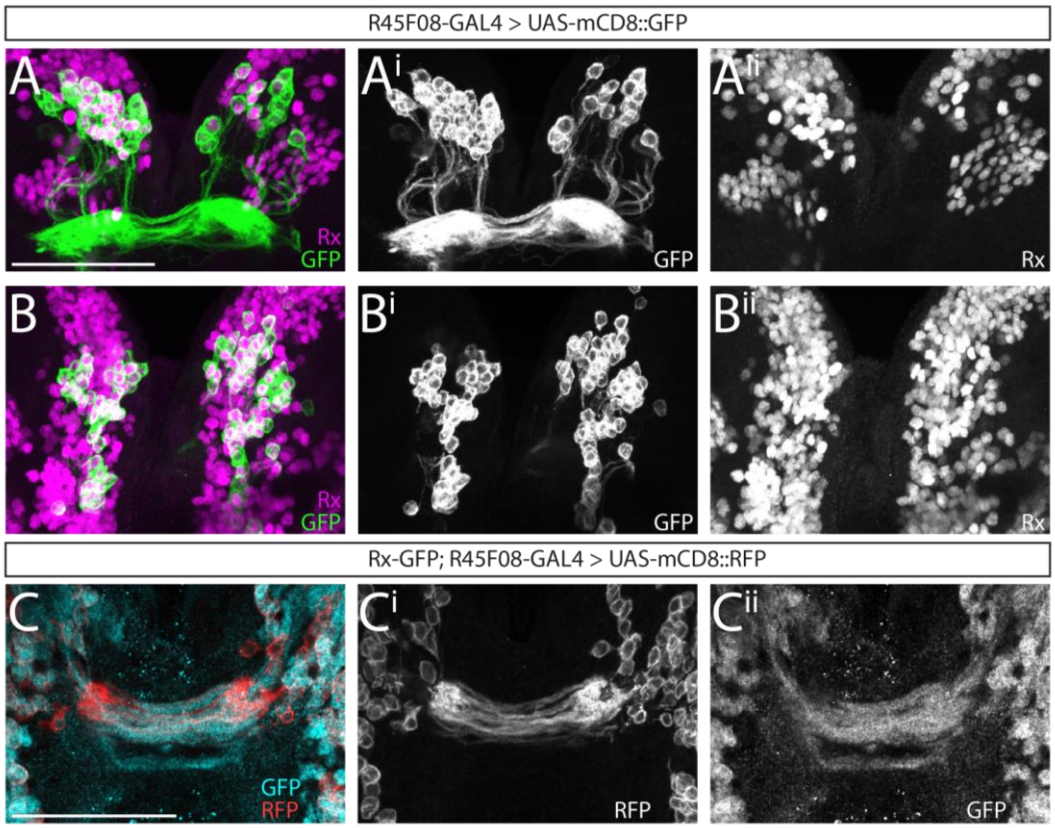

Supplementary Figure 3.1–6: Previously described *pointed*-positive cells of the central complex are a subset of Dm-Rx-positive cells. Displayed is co-localisation of Dm-Rx-positive neural cells and cells under the control of R45F08-GAL4 (Jenett et al., 2012; Riebli et al., 2013) shown in brains of *Drosophila* wandering third instar larvae. **A-A^{ii} and B-B^{ii}:** Antibody staining in a cross of the R45F08-GAL4 line and UAS-mCD8::GFP was performed against Dm-Rx (depicted in magenta) and GFP (green) to reveal the coexpression of cell bodies of lineages DM1-3/6, marked through the R45F08-GAL4 line, and Dm-Rx. Approximately 90% of the R45F08-GAL4 GFP positive cells were Dm-Rx-positive as well (A-A^{ii} first half, B-B^{ii} second half of the stack). **C-C^{ii}:** Antibody staining in animals (N=2) of the respective cross from subcrosses of the Rx-GFP line each with R45F08-GAL4 line and the UAS-mCD8::RFP (SMEs, see Shihavuddin et al. 2017). This resulted in a coexpression of GFP in a Dm-Rx expression pattern and RFP under control of R45F08-GAL4. Antibody staining against GFP (cyan) and RFP (red) revealed coexpression of both fluorescent proteins in midline crossing projections. Although RFP is membrane-bound and GFP cytoplasmic, there were several fascicles showing coexpression of RFP and GFP. This corroborated the high degree of overlap of Dm-Rx and DM1-3/6 lineage offspring shown in panels A and B. Scale bars represent 50 µm.

3.1.9.2. Supplementary Tables

Supplementary Table 3.1–1: Proposed lineages expressing Rx in the adult *Drosophila* (Dm) and *Tribolium* (Tc) brain. Listed are eleven lineages with identifier, name and description relative to the neuroaxis, as well as the position in Figure 3.1–1 and Supplementary Figure 3.1–5 and the degree how unequivocally the assignment of their stereotypical projections was. Identification of lineages is based on Lovick et al. (2013), Wong et al. (2013), https://www.mcdb.ucla.edu/Research/Hartenstein/dbla/index.html, and references therein. Abbreviations: PED peduncle, LAL lateral accessory lobes, AVLP anterior ventrolateral protocerebrum, SLP superior lateral protocerebrum, SMP superior medial protocerebrum, PB protocerebral bridge, MEF medial equatorial fascicle, CA calyx.

Lineage identifier (alternative)	Lineage name	Description (relative to neuraxis)	Fraction	*Dm:* projections identifiable?	*Tc:* projections identifiable?
DALcl1/2	dorso-anterior lateral, centro-lateral 1/2	n-ventro-lateral to PED, n-anterior to LAL	n-ventral	yes	no
DALl1/2	dorso-anterior lateral, lateral 1/2	n-anterior to AVLP, n-ventral and lateral to PED	n-ventral	yes, DALl1	no
DALv1/3	dorso-anterior lateral, ventral	n-ventral to AVLP, lateral to LAL	n-ventral	no	no
DPLal1-3	dorso-posterior lateral, antero-lateral 1-3	lateral to anterior SLP	n-ventral	partially, DPLal2/3	no
DPLc	dorso-posterior lateral, central	n-anterior to posterior SLP	n-ventral	yes	no
DAMv1/2	dorso-anterior medial ventral 1/2	n-anterior to SMP	n-ventral	yes	no
DM1 (DPMm1)	**dorso-medial 1 (dorso-posterior medial, medial 1)**	n-anterio-dorsal (Tc)/n-anterio-ventral (Dm) and medial to PB	**n-dorsal**	**yes**	**yes**
DM2/3 (DPMpm1/2)	**dorso-medial 2/3 (dorso-posterior medial, postero-medial 1/2)**	n-dorso-medial to PB	**n-dorsal**	**yes**	**yes**
DM4 (CM4)	**dorso-medial 4 (centromedial 4)**	n-posterio-lateral to PB, n-dorsal to MEF	**n-dorsal**	**yes**	**yes**
DM5/6 (CM1/3)	dorso-medial 5/6 (centromedial 1/3)	n-posterio-lateral to PB, n-posterio-dorsal to MEF	n-dorsal	no	no
CP2/3 (DL1/2)	centroposterior 2/3 (dorsolateral 1/2)	n-posterio-lateral to CA and n-dorsal to posterior PED	n-dorsal	yes	yes

Supplementary Table 3.1–2: Primer used in this study. For P1 to P12: black writing – annealing part, red – overlapping part, green – PAM modification

Name	Sequence	Purpose
Tc-rx-N_fw	ATGGAATCGGACCGTTGTGAAG	protein expression
Tc-rx-N_rev	CTTGCATCCGTCTCCCTC	protein expression
Golden Gate linker sequence fw	CCAGGTCTCATGGT	protein expression
Golden Gate linker sequence rev	GGGGGTCTCCTCGAGTCA	protein expression
GG_ccdB_F	ACATGATTGCGGCGTTGCC	KNE001 vector
GG_ccdB_R	TGTCTCTCGAGGAGACCGTCGACCTGCAGACT	KNE001 vector
GEKU-Rx-GFP_wt_fw	AGTTGCGAGATGTGCGAGT	homozygous stock generation
GEKU-Rx-GFP_wt_rev	CGTCCAGACTTGCCACTTTG	homozygous stock generation
GEKU-Rx-GFP_trans_rev	CTCTAAAATAAGGCGAAAGGC	homozygous stock generation
Tc-rx-probe-fw	ATGGAATCGGACCGTTGTGAAGA	full length rx probe
Tc-rx-probe-rev	GCAGTCCTTTGGTGATGTTCTCC	full length rx probe
I_P1_Back-F1	CCGGATGGCTCGAGTTTTTCAGCAAGATCACATCG CCTGGGATGCG	rx bicistronic construct
I_P2_Rev_F1	GACAATGGATACCATTCCCTTGTTCAGG	rx bicistronic construct
I_P3_F1-F2	CCTGAACAAGGGAATGGTATCCATTGTCGGGTCCG GCGCCACCAAC	rx bicistronic construct
I_P4_Rev_F2-F3	GTGAACAGCTCCTCGCCCTTGCTCACCATGGGGCC GGGGTTCTCCTCC	rx bicistronic construct
I_P5_F2-F3	GACGTGGAGGAGAACCCCGGCCCCATGGTGAGCAA GGGCGAGGAG	rx bicistronic construct
I_P6_Rev_Back-F3	AGAATATTGTAGGAGATCTTCTAGAAAGATCTACT TGTACAGCTCGTCCATGCCGAG	rx bicistronic construct
II_P7_Back-F4	CCGGATGGCTCGAGTTTTTCAGCAAGATCGTTAGT CGGTTCCTAGCTAAGTG	rx bicistronic construct, PAM of guide A modified
II_P8_Rev_F4-F5	CTCTAATTGAATTAGATCACATACGATTAGTATAA CAGATAAGCATTCC	rx bicistronic construct, PAM of guides B1-3 modified
II_P9_F4-F5	GCTTATCTGTTATACTAATCGTATGTGATCTAATT CAATTAGAGACTAATTCAATTAGAGC	rx bicistronic construct, PAM of guides B1-3 modified
II_P10_Rev_F5-F6	CATTAAGTAGCCTTGGATACATTGATGAGTTTGGA CAAAC	rx bicistronic construct
II_P11_F5-F6	GTCCAAACTCATCAATGTATCCAAGGCTACTTAAT GAGTTGATTAATAAG	rx bicistronic construct
II_P12_Rev_Ba-F6	GAATATTGTAGGAGATCTTCTAGAAAGATGTTCTT TCAATTTGTAAGACATAGGTTTTTAG	rx bicistronic construct
III_P13_Rev_F3	CTACTTGTACAGCTCGTCCATGCCGAG	rx bicistronic construct
III_P14_F3-F4	CTCGGCATGGACGAGCTGTACAAGTAGCGTTAGTC GGTTCCTAGCTAAGTG	rx bicistronic construct
DmRx_CDS_3'UTR_fw	CGTCTCTGCCACTAATTAGACAGC	rx SNP sequencing
DmRx_CDS_3'UTR_rev	GAATAGACTTCTTCGTCAGCCG	rx SNP sequencing
DmRx_3'UTR_int-region_fw	CGTGTTGTAAGTACATATTTCTGAGGCAG	rx SNP sequencing
DmRx_3'UTR_int-region_rev	CTTGAGGAGCGAGGCACAC	rx SNP sequencing
DmRx_trans-ver_fw	GTCGCCGCAGAACCTGAG	rx molecular screening
DmRx_trans-ver_rev	CATGGAGCCAGTAGTTCATGC	rx molecular screening
DmRx_trans-ver_nested_fw	CATAGAACTGCTCGATGTGG	rx molecular screening
DmRx_trans-ver_nested_rev	GATTCAACTGCGGCTACTGC	rx molecular screening
DmRx_trans_seq_Ct_fw	GACTGGCAAGGGTTCGAG	rx molecular screening
DmRx_trans_seq_iRe_rev	CATGTGAGTCCTTTGTTTGC	rx molecular screening

Supplementary Table 3.1–3: List of primary and secondary antibodies as well as dyes used in this study.

Antibody name	Antigen / Immunogen	Origin species	Source	Dilution
anti-Dm-Rx	*Drosophila* Rx N-terminal fragment	rabbit	gift from Dr. Uwe Walldorf (Saarbrücken, Germany), Davis et al. 2003	1:1000
anti-Tc-Rx	*Tribolium* Rx N-terminal fragment	guinea pig	this paper	1:750
anti-Engrailed 4D9	Engrailed/invected (Immunogen: Invected (C-terminal two-thirds of the invected protein); recombinant)	mouse	gift from Dr. Marita Buescher (Göttingen, Germany), DSHB	1:10
chk-anti-GFP	GFP (*Aequorea victoria*)	chicken	ab13970, Abcam (Cambridge, UK), used in Supplementary Figure 3 and 6	1:1500
rab-anti-GFP	GFP (*Aequorea victoria*)	rabbit	A11122, ThermoFisher Scientific/Invitrogen (MA, USA)	1:1000
anti-RFP	RFP (full length)	rabbit	ab62341, Abcam (Cambridge, UK)	1:1000
anti-Synapsin	Synapsin (Immunogen: GST-Synapsin-GST fusion protein expressed in E. coli and purified by glutathione affinity)	mouse	gift from Dr. Christian Wegener (Würzburg, Germany), DSHB	1:15-1:40
anti-α-acetylated Tubulin	α-acetylated Tubulin (Immunogen: acetylated tubulin from the outer arm of Strongylocentrotus purpuratus (sea urchin)	mouse	T7451, MERCK/Sigma-Aldrich (Darmstadt, Germany)	1:40
anti-rab-Alexafluor 488	rabbit (Gamma Immunoglobins Heavy and Light chains)	goat	A11070, ThermoFisher Scientific/Invitrogen (MA, USA)	1:1000 embryos, 1:500 other stages
anti-chk-Alexafluor 488	chicken (Gamma Immunoglobins Heavy and Light chains)	goat	A11039, ThermoFisher Scientific/Invitrogen (MA, USA)	1:1000 embryos, 1:500 other stages
anti-mou-Alexafluor 555	mouse (Gamma Immunoglobins Heavy and Light chains)	goat	A21425, ThermoFisher Scientific/Invitrogen (MA, USA)	1:1000 embryos, 1:500 other stages
anti-rab-Alexafluor 555	rabbit (Gamma Immunoglobins Heavy and Light chains)	goat	A21430, ThermoFisher Scientific/Invitrogen (MA, USA)	1:1000 embryos, 1:500 other stages
anti-rab-Alexafluor 647	rabbit (Gamma Immunoglobins Heavy and Light chains)	goat	A21245, ThermoFisher Scientific/Invitrogen (MA, USA)	1:1000 embryos, 1:500 other stages
anti-gp-Alexafluor 647	guinea pig (Gamma Immunoglobins Heavy and Light chains)	goat	A21450, ThermoFisher Scientific/Invitrogen (MA, USA)	1:1000 embryos, 1:500 other stages

Dye name	Source	Dilution
DAPI	D1306, ThermoFisher Scientific (MA, USA)	1:1000

Supplementary Table 3.1–4: *Drosophila* and *Tribolium* stocks used in this study.

Species	Stock name	Stock Number	Source	Description
Drosophila	**Rx-GFP**	**-**	**this paper**	**Genotype: w^{1118}, 3XP3-dsRED, rx^{GFP}; founder 374.2; primary line**
	w^{1118}	e.g. 3605	e.g. Bloomington Drosophila Stock Center	used for control experiments (Supplementary Figure 3)
	Act5C-Cas9, Lig4[169]	58492	Bloomington Drosophila Stock Center	Zhang et al. 2014, Cas9 line used for generation of Rx-GFP bicistronic line (Supplementary Figure 3)
	w^{1118}; wg^{Gla-1}/CyO	-	Wimmer Department, Göttingen (gift)	used to generate homozygous stocks of the Rx-GFP bicistronic line (Supplementary Figure 3)
	R45F08-Gal4	49565	Bloomington Drosophila Stock Center	Jenett et al. 2012, Riebli et al. 2013; used to determine overlap of lineages Dm1-3/6 to Rx expressing cells (Supplementary Figure 6)
	20xUAS-mCD8::GFP	32194	Bloomington Drosophila Stock Center	Chromosome 3, used to determine overlap of lineages Dm1-3/6 to Rx expressing cells (Supplementary Figure 6)
	UAS-mCD8::ChRFP	27392	Bloomington Drosophila Stock Center	Chromosome 3, used to determine overlap of lineages Dm1-3/6 to Rx expressing cells (Supplementary Figure 6)
Tribolium	**Rx-GFP**	**E01101**	**GEKU-base**	**Trauner et al. 2009, primary line**
	v^{w}	-	Lorenzen et al. 2002	$vermilion^{white}$, Lorenzen et al. 2002, used for control experiments (Supplementary Figure 2)

3.1.9.3. Supplementary Results

3.1.9.3.1. Mapping of Rx-positive cell groups to known lineages of the insect adult brain

We aimed at determining to which previously described lineages the Rx-positive cells belonged. The lineages in *Drosophila* had been described in Lovick et al. (2013), Wong et al. (2013) and the accompanying atlas. We reassigned them in the *Drosophila* brain and transferred the *Drosophila* knowledge to the *Tribolium* brain. Assignments of conserved Rx expressing cell groups in the cell body rind in both species' brains were based on two aspects. First, synapsin staining revealed common synapse-rich neuropils as well as synapse-absent tracts and fascicles that can be homologized between the two species. With this, domains of the *Tribolium* brain could be linked to domains and known lineages in *Drosophila*. Second, since Rx-positive lineages were defined by stereotypical projections, an additional antibody staining against GFP in the characterized Rx transgenic lines (Supplementary Figures 3.1–2 and 3.1–3) revealed some lineage-typical projections. Therefore, projections helped in some cases to verify lineage identity beyond cell body position (original stacks are deposited in the Supplementary data). However, for most lineages, projections were not distinguishable. We identified eleven lineages in both species that cover most of the Rx expressing cell groups in the adult brain (DALcl1/2, DALl1/2, DALv1/3, DPLal1-3, DPLc, DAMv1/2, DM1 (DPMm1), DM2/3 (DPMpm1/2), DM4 (CM4), DM5/6 (CM1/3), CP2/3 (DL1/2, Supplementary Figure 3.1–5, Supplementary Table 3.1–1): In the *Tribolium* brain, all n-ventral lineages were not marked by projections through our transgenic line. They have been identified due to the basic anatomical position of the cell bodies that was very similar to Rx expressing lineages in the *Drosophila* brain. In the *Drosophila* Rx-GFP line all n-ventral lineages were – if at all – only faintly marked by projections. Visible were projections (see Supplementary Table 3.1–1) of the lineage group DALc1/2 that projected n-posterior to the peduncle into the central complex, the likely dorsal tract of the DPLal2/3 lineage that projected into the superior lateral protocerebrum, the short projection of the DPLc1 sublineage and the dorso-medial projection of the DAMv1/2 lineage into the superior medial protocerebrum (see original data stacks). In the n-dorsal fraction, both projections of hemilineages of the CP2/3 lineage were visible in both species, one reaching n-anterior over the peduncle and projecting into the superior medial protocerebrum, one starting n-posterior of the peduncle and projecting n-ventro-anterior to it. With the available tools, we could not determine homology of lineages further. To verify this tentative lineage identification, based mostly on cell body location, specific transgenic lines need to be generated and subsequent antibody stainings need to be performed, particularly in *Tribolium*, to further reveal the characteristic projection patterns of each lineage.

3.1.9.3.2. Description of Rx-positive subgroups of DM1-4 lineages in *Tribolium* and *Drosophila*

In addition to the general descriptions of cell body location and projections on a lineage level (Figure 3.1–1, 2), DM1-4 lineages were previously divided into sub-groups and single tracts (Wong et al., 2013).We wanted to describe which of those sub-groups and tracts are visible in the *Drosophila* adult brain and describe analogous sub-groups and tracts in *Tribolium*. These groups were differently marked in the imaging lines in both species due to the different design of the transgenic lines (see Supplementary Figures 3.1–2 and 3.1–3). Note that the projections of individual tracts or neurons in the respective neuropils were hard to distinguish because a high number of cells were marked.

In *Drosophila*, the DM4 Rx expressing cell group consisted of three subgroups, one localized n-anterior, and two n-posterior to the lateral tip of the PB. They projected axons to form a common projection as part of the MEF which bifurcated near the midline, where parts went into a n-ventral midline crossing projection n-ventral to the whole CX. This projection might be partially shared by the upper intermediate tract of CM3 or the dorsal tract of CM1 (Wong et al., 2013). The other part projected mainly into the CBU ('intermediate tract; Wong et al., 2013). The DM3 Rx expressing group consisted of two groups, one more n-anterior, one n-posterior to the lateral side of the PB. The group's axons formed parts of the dlrCBU together with DM2 in the 'anterior-ventral tract' (Wong et al., 2013). Parts of these cells' axons projected into the n-dorsal plexus (also CBUppl, or FBppl, see e.g. Riebli et al., 2013), while substantial parts went in a more n-ventro-posterior part together with DM4. DM2 consisted of three groups, two n-anterior (one of which is more n-dorsal), one n-posterior to the PB. They projected together into the n-dorsal plexus of CBU ('anterior-ventral tract'; Wong et al., 2013), slightly more n-dorsal than DM3. The projection bifurcated, one more n-anterior, one more n-posterior. The DM1 group consisted of three subgroups, all n-anterior to the protocerebral bridge. One more n-ventral and slightly more lateral, two were more n-dorsal, of which one was n-anterior to the other. The n-ventral group formed a separate more lateral projection (potentially the 'anterior descending tract'; Wong et al., 2013) in comparison to the common projection of the other group ('anterior-ventral tract'; Wong et al., 2013).

In *Tribolium*, DM4 consisted of two groups localized n-anterior to the PB tip and one n-posterior to the PB tip. The bifurcation of the tract from both groups was similar to *Drosophila*, and they thus could also share a projection with a CM3 tract. A division into an n-anterior and n-posterior part was similar to *Drosophila*. A third group present in *Drosophila* was not marked or was not present in *Tribolium*. DM3 consisted of two main groups, one more n-anterior to the PB,

one n-posterior to the PB, an arrangement similar to *Drosophila*. They projected together with DM2 and 1 into the n-dorsal fraction of the CBU, while sharing the dlrCBU tunnel with DM3, with projections very similar to *Drosophila*. Cell bodies of DM2 were difficult to visualize but were slightly more medial to the DM3 belonging group. Hence approximate position was similar, but a subdivision in groups was hardly possible. Cell bodies of DM1 were sparse, with some n-anterior and some n-posterior to the protocerebral bridge, like *Drosophila* without a subdivision into groups possible. The projection into the CBU was very similar. Note that, in general, cell groups of DM1-3 were n-dorsal, and not like in *Drosophila* n-anterior to the PB.

3.1.9.4. Supplementary Material and Methods

3.1.9.4.1. KNE001 cloning and map (Eckermann, in preparation)

The vector KNE001 (pET SUMO-GoldenGate) was based on pET SUMOadapt (Bosse-Doenecke et al., 2008; modified from the pET SUMO expression vector; Hanington et al., 2006; Mossessova and Lima, 2000; material transfer agreement with Cornell University, U.S.A., ThermoFisher Scientific, MA, USA). The vector was extended by MSC-adapter sequences, containing most importantly BsaI type IIS recognition sites, allowing residue-free cloning of the CDS of interest in-frame with the ATG::6xHis::SUMO open reading frame, Chloramphenicol resistance and a ccdB death cassette (Bernard et al., 1994; Engler et al., 2008). By adding GoldenGate-linker sequences that contain BsaI cleavage sites (which do not equal the enzyme's recognition site) to the gene-specific forward and reverse primer, pET SUMO-GoldenGate and the CDS of in our case the N-terminal part of Tc-Rx can be cut and ligated into a product lacking the original restriction sites. The ccdB cassette in the original KNE001 vector ensured growth in successfully transformed colonies only.

For these modifications, a fragment containing lac promoter, CAT gene and ccdB death cassette was amplified with primers *GG_ccdB_F* and *GG_ccdB_R* (containing a XhoI-site) from pTALEN(NI)v2 (gift from Feng Zhang, Addgene Plasmid # 32189, Sanjana et al., 2012). Second, a NotI/XhoI digestion resulted in a 1.5 kb NotI_lacP-CAT_ccdB_XhoI fragment, which was ligated in the NotI/XhoI linearized pET SUMOadapt. Third, the new pET SUMO-GoldenGate was transformed in ccdB Survival™ 2 T1R Competent Cells (ThermoFisher Scientific, MA, USA).

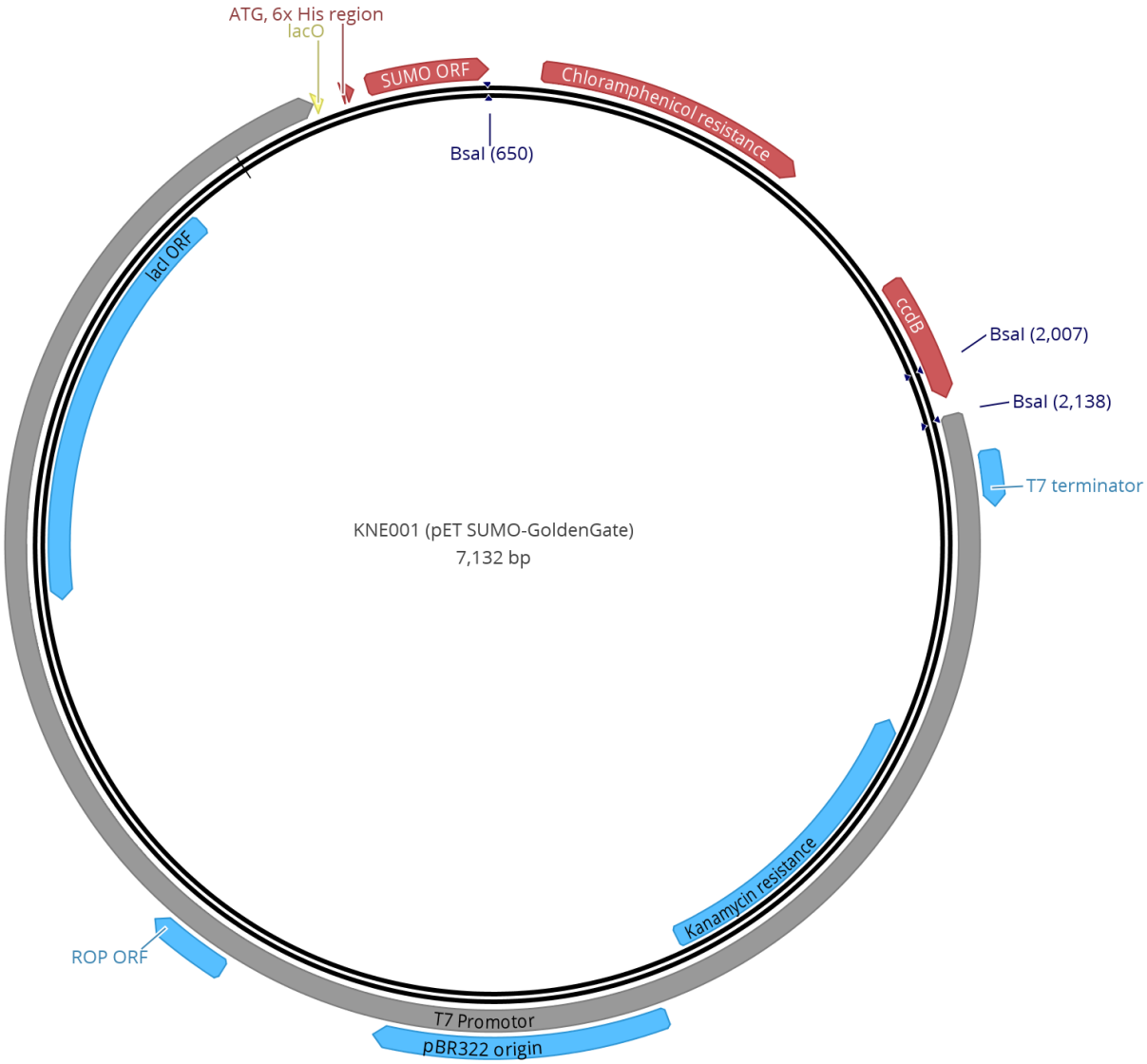

Vector map 1: KNE001 vector map (displayed with Geneious 11.1.5, https://www.geneious.com).

3.1.9.4.2. MF01 cloning and map

In the construct, we included an insect codon-optimized version of the P2A peptide (Kim et al., 2011), with following sequence:

GGGTCCGGCGCCACCAACTTCTCCCTGCTGAAGCAGGCCGGCGACGTGGAGGAGAACCCCG
GCCCC

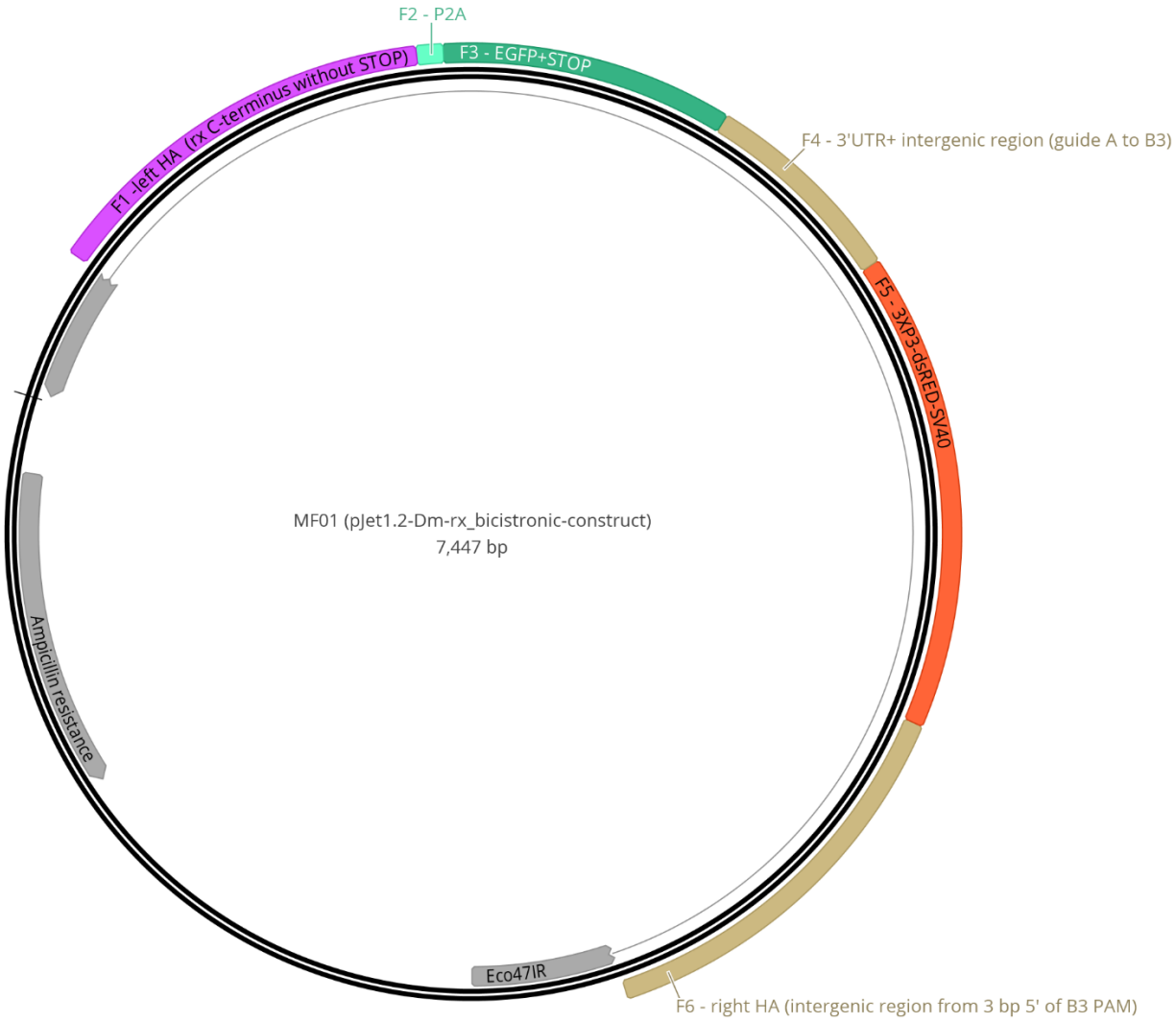

Vector map 2: MF01 vector map (displayed with Geneious 11.1.5, https://www.geneious.com).

3.2. Manuscript 2: The red flour beetle as model for comparative neural development: Genome editing to mark neural cells in *Tribolium* brain development

This manuscript is the methodological link between the main topic brain evolution and development and the new direction we propose. Through the generation of transgenic lines via genome editing we can mark genetic neural lineages, and subsequently, compare the development of marked cells. Thus far, Gilles et al. (2015) have shown that CRISPR in *Tribolium castaneum* is functional in several publications with specific applications. We complement this work by providing a manual on how to generate suitable CRISPR transgenic lines in *Tribolium* in a detailed fashion. With this work, we hope to provide a protocol that facilitates generation of CRISPR lines in *Tribolium* and possibly also non-model organisms that subsequently can be used to generate new insights into brain evolution.

Authors

Max S. Farnworth[*], Kolja N. Eckermann, Hassan M. M. Ahmed, Dominik S. Mühlen, Bicheng He, Gregor Bucher[*]

[*] = corresponding authors

Status

in press in Brain Development: Methods and Protocols, Second Edition (Springer Nature)

My contributions

- Conceptualisation of the method[1]
- Writing of the manuscript[2]
- Generation of data on which the method and protocol is based[3]
- Generation of figures[4]

[1] = together with KNE, HMMA, GB

[2] = together with KNE, HMMA, DSM, GB

[3] = together with DSM, BH

[4] = together with KNE

Title:

The red flour beetle as model for comparative neural development: Genome editing to mark neural cells in *Tribolium* brain development

Authors:

Max S. Farnworth[1,3,*], Kolja N. Eckermann[2,3], Hassan M. M. Ahmed[2], Dominik S. Mühlen[3,4], Bicheng He[1], Gregor Bucher[1,*]

[1] Department of Evolutionary Developmental Genetics, Johann-Friedrich-Blumenbach Institute, GZMB, University of Göttingen, Göttingen, Germany, [2] Department of Developmental Biology, Johann-Friedrich-Blumenbach Institute, GZMB, University of Göttingen, Göttingen, Germany, [3] Göttingen Graduate School for Neurosciences, Biophysics, and Molecular Biosciences (GGNB), Göttingen, Germany, [4] Department of Molecular Developmental Biology, Max-Planck-Institute for Biophysical Chemistry

[*] **Corresponding authors:** Max S. Farnworth m.farnworth@posteo.de, Gregor Bucher gbucher1@uni-goettingen.de

Running head: Genome editing approaches in *Tribolium*

Key words: CRISPR/Cas9, HDR, NHEJ, *Tribolium*, neural lineage, brain development, 2A peptide

3.2.1 ABSTRACT

With CRISPR/Cas (Clustered Regularly Interspaced Short Palindromic Repeats/CRISPR-associated) scientists working with *Tribolium castaneum* can now generate transgenic lines with site-specific insertions at their region of interest. We present two methods to generate in vivo imaging lines suitable for marking subsets of neurons with fluorescent proteins. The first method relies on homologous recombination and uses the self-cleaving 2A peptide to create a bicistronic mRNA. In such lines the target and the marker proteins are not fused but produced at equal amounts. This work-intensive method is compared with creating gene-specific enhancer traps that do not rely on homologous recombination. These are faster to generate but reflect the expression of the target gene less precisely. Which method to choose strongly depends on the aims of each research project and in turn impacts of how neural cells and their development are marked. We describe the necessary steps from designing constructs and guide RNAs to embryonic injection and making homozygous stocks.

3.2.2 INTRODUCTION

3.2.2.1 The red flour beetle as model for brain development and evolution

The brain is among the most complex structures of an organism and understanding its development has been a major challenge in developmental biology. highly advanced model systems with their plethora of tools and resources are spearheading this research and these ongoing efforts have been revealing basic principles of neural development of both deuterostomes and protostomes with the dipteran *Drosophila melanogaster* being the model for arthropods (Doe, 2017; Perry et al., 2017; Urbach and Technau, 2004). Another major enigma in the field is the developmental basis of the evolution of brain diversity (Arendt et al., 2016; Hartenstein and Stollewerk, 2015). In insects, for instance, the basic neuropil structure is highly conserved, but there is great variety of absolute brain size, relative size and shape of homologous neuropils (el Jundi and Heinze, 2016), in addition to heterochronic development (Koniszewski et al., 2016). In order to study evolutionary differences on a genetic and developmental level within insects a comparison of *Drosophila* to another insect species is required. Such a species should provide the tools for functional genetic work and transgenic approaches and as many resources as possible. While no insect species is in sight that will match the resources and the tool kit of *Drosophila melanogaster*, the red flour beetle *Tribolium castaneum* fulfils all necessary requirements. RNAi is strong and systemic such that all cells are targeted and the effect is transmitted to the offspring (Brown et al., 1999; Bucher et al., 2002; Tomoyasu and Denell, 2004). A genome-wide RNAi screen is being performed (Schmitt-Engel et al., 2015), transgenesis is well established (Berghammer et al., 1999) and enhancer trap screens have been performed (Lorenzen et al., 2007; Trauner et al., 2009). Recently, genome editing via CRISPR/Cas9 has been established in this species (Gilles et al., 2015).

Given this availability of robust tools for functional genetics in *Tribolium*, we think that this beetle has the potential to become the main comparative organism for studying the mechanisms of brain diversification in insects. One approach is to mark homologous cells in both species and compare similarities and differences throughout development (Koniszewski et al., 2016). We want to elaborate here on the possibilities of CRISPR/Cas to extend the *Tribolium* toolkit for brain development and evolution research.

For protocols about immunostaining and *in situ* hybridisation of embryonic, larval and adult brains in *Tribolium* please consult respective chapters in this book.

3.2.2.2 Using transgenic lines to study *Tribolium castaneum* brain development

In order to study the development of the *Tribolium* brain, subsets of neural cells need to be visualized. Of particular use is the visualization of whole neural cells including soma, projections and fine arborizations. In *Drosophila,* extensive enhancer trap screens (Hayashi et al., 2002; Mollereau et al., 2000; O'Kane and Gehring, 1987) have created collections of transgenic lines where the expression of genes and the respective anatomical structures are marked with expression of fluorescent proteins. In addition, large collections of lines have been generated where markers are under the control of specific enhancers and promotors (Pfeiffer et al., 2008). Subsequent immunostaining (e.g. Wu and Luo, 2006) or live-imaging (e.g. Jin et al., 2018) can generate fascinating insights into neural morphology and development.

An enhancer trap screen has been performed in *Tribolium castaneum* and some transgenic brain imaging lines have become available (Koniszewski et al., 2016; Trauner et al., 2009). However, the collection is comparably small such that transgenic lines suited for individual research projects will in many cases have to be generated.

Before the advent of CRISPR/Cas *Tribolium* transgenic lines were generated by enhancer trapping (Trauner et al., 2009) or by insertion of constructs containing a gene's regulatory regions (Koniszewski et al., 2016). In both cases the genetic construct is randomly integrated into the genome by transposon-mediated mutagenesis (Berghammer et al., 1999). In case of enhancer trap experiments, a construct devoid of enhancers, but comprising a basal promoter and reporter gene jumps randomly into a gene locus. Because of the proximity, the enhancers that control the expression of that gene start to regulate the reporter gene as well. In case of genes involved in brain development neural expression patterns are observed (Trauner et al., 2009). An alternative approach is to identify a gene of interest (GOI) and include parts of the regulatory region of this GOI in front of a reporter gene and let it integrate randomly (Eckert et al., 2004; Koniszewski et al., 2016). If functional enhancers are included in the construct, expression is at least partially similar to the one of the GOI. In both approaches, position effects are a major issue (John et al., 2016; Wilson et al., 1990). Depending on where the construct is inserted, reporter gene expression can be influenced by additional enhancer elements and/or loose regulation by others. In case of reporter constructs, only parts of the regulatory region are usually included leading to loss of important enhancers besides position effects. As consequence, the marker gene expression usually does not precisely reflect the GOI's expression.

CRISPR/Cas mediated genome editing can be used to in two ways to mark neural cells in *Tribolium*: First, enhancer trap constructs can specifically be targeted to loci of genes with

interesting neural expression obviating the need of time-consuming random screens. Second, homologous recombination allows engineering transgenic lines where the reporter is encoded by the same mRNA as the GOI. It therefore exactly mirrors GOI expression.

3.2.2.3 CRISPR/Cas

CRISPR (Clustered Regularly Interspaced Short Palindromic Repeats/CRISPR-associated) loci are repetitive elements that are part of the bacterial and archaeal adaptive immunity system (Jinek et al., 2012). They contain CRISPR-associated (Cas) genes that encode for endonucleases. One of those genes encodes for Cas9 which is part of the type II adaptive immunity response. This system is most widely exploited in genome editing, because it only requires one Cas protein, making the system more easy to use than type I and III (Hsu et al., 2014). The second major part of CRISPR loci are CRISPR arrays. They consist of repeat sequences and spacers which vary in sequence and correspond to foreign genetic elements (protospacers) of e.g. phages (Jinek et al., 2012). These arrays are transcribed as single RNA and further processed to CRISPR RNAs (crRNAs) (Hsu et al., 2014). Associated trans-activating CRISPR RNAs (tracrRNAs) hybridize with the repeat sequences, are cleaved to include only one spacer sequence per duplex which subsequently form a complex with the Cas9 protein (Hsu et al., 2014). This active complex is also referred to as chimeric RNA or guide RNA and uses the spacer sequence to bind to complementary DNA and the Cas9 protein cuts the foreign DNA three base pairs upstream of the PAM (protospacer adjacent motif) which is a nucleotide triplet specific for each Cas protein. The resulting double strand breaks (DSBs) can be repaired by two cellular repair mechanisms. The first mechanism is the error-prone non-homologous end joining (NHEJ). here, free DNA ends are fused often resulting in indels (insertion-deletions) that frequently cause frameshift mutations and gene disruption. Importantly, besides indels, available linear DNA fragments can be inserted during NHEJ repair as well. The second mechanism is homology-directed repair (HDR) where the DSB is repaired using homologous sequences as template such that indels are avoided.

The CRISPR/Cas9 system has been modified to edit genomes of diverse species at specific locations (Doudna and Charpentier, 2014; Gratz et al., 2013; Jinek et al., 2012) including *Tribolium* (Gilles et al., 2015). Genome editing can on one hand be used to generate mutations of a specific gene or to remove whole genes or other DNA elements. On the other hand, directed insertion of linear DNA fragments at specific loci by NHEJ is feasible. In addition, HDR allows tailoring genetic modifications with single base precision. hence, gene loci can be modified in multiple

ways including imaging lines suitable for neurodevelopmental research and other purposes (Gilles et al., 2015; Gratz et al., 2013; Hsu et al., 2014; Jinek et al., 2012).

3.2.2.4 Two major strategies to generate imaging lines using CRISPR/Cas9

In this chapter we highlight two strategies to make transgenic lines suitable for neurodevelopmental research in *Tribolium*. The first approach is the generation of enhancer traps in selected loci by NHEJ. Technically, this is the simpler approach, but the resulting reporter expression may lack precision. The second approach consists of the generation of bicistronic reporter lines using HDR. While the design is more demanding the reporter will reflect the expression of the targeted gene with high precision. The transformation efficiencies appear to be in a similar range in both approaches (Johannes Schinko, TriGenes, personal communication). Specifically for HDR observed rates (i.e. number of positive G_0 founders of fertile injected animals) are 0.5 % (Johannes Schinko, TriGenes, personal communication) and 0.65 % (Rylee et al., 2018). Hence, we strongly advise to inject high numbers of embryos to counteract the relatively low rates of integration.

3.2.2.5 Prerequisite: Selection of the gene of interest

Depending on the cells that one would like to mark, the GOI could for instance be a neural differentiation gene that marks certain cell types, e.g. an enzyme involved in the production of certain neurotransmitters. When using such differentiation markers, the expression of the respective reporter is expected to emerge rather late in development, i.e. during cell differentiation. Alternative GOIs are neural patterning genes that mark certain neuroblasts and/or neuroectodermal regions and later subsets of neural cells (Koniszewski et al., 2016). Here, reporter expression is expected both early in embryogenesis and later in the differentiated brain reflecting both early and late functions of such transcription factors. Due to the dynamics of patterning gene expression, the loss of expression in subsets of cells at certain stages might be observed as well.

3.2.2.6 Gene-specific enhancer traps via NHEJ:

3.2.2.6.1 Selecting the insertion sites within the GOI locus

The first strategy exploits NHEJ to generate enhancer traps in the regulatory region of a gene of interest (Trauner et al., 2009). Sites of insertion can greatly influence reporter gene expression. Therefore, mindful choice of target sites is crucial. The exact location of the insertion within the

locus of the GOI is defined by the DSBs which depends on appropriate guide RNAs. A mutation of the GOI might interfere with proper brain development or morphology, so that the insertion should not interrupt exons. Likewise, disruption of regulatory elements should be avoided, because these may lead to a mutant phenotype as well. As regulatory elements are difficult to predict based on DNA sequence, data on putative enhancers based on Faire or ATACseq experiments might be used to further exclude insertion sites (Dönitz et al., 2018, 2015; Lai et al., 2018). Unfortunately, it is unpredictable what location of an insertion will produce a good enhancer trap. In previous screens a large portion of enhancer traps identified was located upstream of the transcription start site (TSS) or in the first intron (Trauner et al., 2009; Häcker et al., 2003) reflecting the predominant location of enhancers around the TSS (Kvon et al., 2014). However, insertions downstream of the polyA signal are producing enhancer trap patterns as well. Given these uncertainties, it is recommended to design guide RNAs for at least two to three different insertion sites per GOI and produce independent lines for each. Note that gene annotations found on genome browsers (e.g. J-Browse at iBeetle-Base http://ibeetle-base.uni-goettingen.de/jbrowse/) were generated automatically and may contain errors. Hence, the annotation needs to be checked manually and in case of doubt, the TSS needs to be identified e.g. by RACE reactions.

3.2.2.6.2 Generation of the enhancer trap construct

Depending on needs, enhancer trap constructs to be inserted may have different designs. For imaging, the construct must contain a reporter gene, e.g. encoding EGFP (or a transactivator like GAL4; Schinko et al., 2010) under the control of a basal promotor. A basal promoter is a 300-400 bp region around the TSS which enables the binding of the polymerase but does not initiate transcription on its own (Figure 3.2–1A). Upon insertion into the genome, close-by enhancers will activate transcription from that promoter. In *Drosophila*, the basal heat shock promoter (bhsp) has been widely used in constructs and enhancer trap screens and a respective *Tribolium* bhsp has been successfully tested for that purpose (Schinko et al., 2012). Sequences of core promoters influence the interaction with enhancer elements modulating the expression of the reporter (Pfeiffer et al., 2008; Smale and Kadonaga, 2003). hence, using respective core promoters from neural genes might be an option. However, each new core promoter under consideration has to be functionally tested first. Next, the construct needs a transformation marker (Figure 3.2–1A) allowing for the identification of the few transformants between hundreds or thousands of non-transformed animals. The currently best option for brain imaging is the use of the 3XP3-*Tc-vermilion* marker which rescues the white eyes of the *Tribolium vermilion white* mutation to black eyes

(Lorenzen et al., 2002). This marker is easy to screen without epifluorescence and does not interfere with fluorescent brain imaging. Note that the artificial 3XP3-EGFP marker often used as transformation marker in beetles does not only drive expression in the eyes, but also in glia cells (Koniszewski et al., 2016). hence, if a fluorescent eye marker is used one has to choose a fluorophore such that overlap with the reporter protein is minimized.

Importantly, the construct needs to be linearized in order to be inserted into a double strand break (Figure 3.2–1A). This can be facilitated by flanking the construct with sequences that are targeted by additional guide RNAs that do not match the genome of *Tribolium*. Previously tested guide RNA sequences from other species are a good option. A guide RNA targeting the ebony locus from *Drosophila* was successfully tested (Klingler, personal communication and own experience), although an alternative target site to *Dm-yellow* was also used previously and is an alternative (Klingler, personal communication).

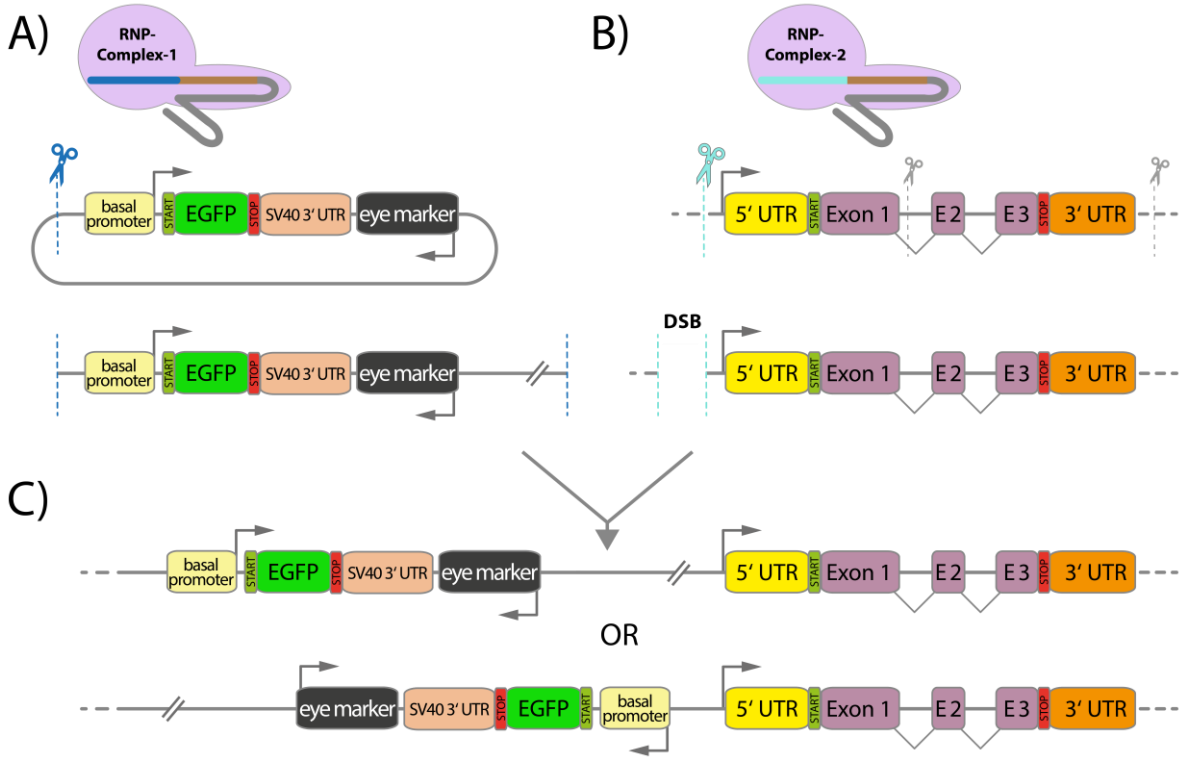

Figure 3.2–1: Strategy to generate gene-specific enhancer traps via CRISPR-based NHEJ. A. The repair template contains an enhancer trap cassette consisting of a basal promotor (bhsp68), a sequence encoding for EGFP and a SV40 3'UTR as termination sequence. The construct also contains an eye marker consisting of a 3XP3 promotor and the Tc-v gene and is oriented in the opposite direction so that the SV40 3'UTR can terminate transcription for both genes. A *Dm-ebony* sequence facilitates linearization of the construct upon Cas9 activity, when a Ribonucleoprotein (RNP) complex is formed in vivo. **B.** For insertion at a specific site of the gene locus an RNP is formed in vivo which contains a guide RNA sequence that mediates an exemplary cut upstream of the transcription start site of the targeted locus (blue scissor). In parallel experiments, insertions in the first intron and downstream of the GOI should be used (depicted as grey scissors). **C.** During the repair of the DSB in the genome the entire linear

enhancer trap construct including the backbone is integrated into the genomic locus at the DSB site. It can be integrated in both directions.

Such a construct has been cloned and used successfully for generating a number of enhancer traps of neural cells in *Tribolium* and is available from the authors and in the future via Addgene. It contains the abovementioned components, but in addition to EGFP drives the Cre recombinase in the same pattern. Judging from our still limited experience we tend to believe that simply linearizing the plasmid close to the basal promotor of the construct may be more efficient than cutting out the construct at both sides. The disadvantage of simple linearization is that the plasmid-backbone is still in the genome and might generate an artificial situation at the locus. Comparing different insertion sites in one GOI locus we found that the reporter patterns were in most cases related to the GOI, but also showed quite some differences probably depending on insertion site and orientation.

3.2.2.6.3 When to use this strategy

The enhancer trap approach has the advantage that the same construct can be used for all loci and does not need to be adopted specifically for each gene, substantially reducing the effort for cloning. A disadvantage can be that not the entire expression is captured by reporter expression and/or ectopic expression may occur. Hence, the resulting EGFP pattern may not be an exact copy of the GOI's expression. This can actually turn into an advantage when only a small subset of cells is marked such that following neural projections can be easier.

3.2.2.7 Bicistronic lines via HDR:

3.2.2.7.1 Principle of bicistronic expression by using 2A peptides

If a precise copy of the GOI expression is required, the more laborious generation of bicistronic lines is the option to choose. Essentially, the genome is edited such that an mRNA encoding both GOI and reporter gene is transcribed. The consequence of the fused mRNA is that both GOI and reporter are regulated from the same promoter in identical patterns and dynamics. This can be realized on one hand by constructing fusion proteins (Sarov et al., 2016). here, a reporter gene is inserted in frame with the GOI extending its ORF. however, the resulting fusion protein may have a strongly modified 3D structure and thus, may not function properly. Further, the signal of the reporter will only be present at the target protein's cellular location. In case of transcription factors, the nucleus would be marked, but not the projections. To avoid these restrictions, 2A peptides can be used to generate two separate proteins from one mRNA.

2A peptides are short, approximately 20 amino acid long peptides that cause 'ribosomal skipping' (Donnelly et al., 2001). An mRNA where the sequence of the GOI is separated from the reporter by a 2A sequence will lead to the translation of the GOI, interruption of the polypeptide chain within the 2A sequence and to subsequent translation of the reporter by the same ribosome (Kim et al., 2011; Szymczak-Workman et al., 2012). Hence, a reporter gene such as EGFP is expressed alongside the GOI in the same cells, in the same amount and without affecting GOI function. Importantly, it is expected that EGFP will be located in the cytoplasm resulting in marking of the whole neural cells including projections.

3.2.2.7.2 Design of the repair template

In the construct for the repair template, parts of the GOI, the 2A peptide and a reporter gene, e.g. EGFP, need to be cloned in-frame before a STOP codon (Figure 3.2–2). The original STOP codon of the GOI needs to be removed. The new STOP is followed by the 3'UTR containing the polyA signal of the endogenous gene. Upon integration, such a construct leads to the production of one mRNA which apart from its extension by the reporter is identical to the endogenous GOI mRNA. Downstream of the 3'UTR, a transformation marker needs to be included (see above for criteria for selection). The purpose of putting the artificial eye promotor 3XP3 (Berghammer et al., 1999) downstream of the bicistronic gene locus (Figure 3.2–2) is to reduce the chance of interference of these two transcription units.

In order to allow for homology dependent integration, sequences homologous to the DNA up- and downstream of the sequence to be edited need to be included. One sequence contains parts of the GOI sequence upstream of the STOP codon (5' homology arm) and the other is identical to sequences downstream of the 3'UTR (3' homology arm) (Figure 3.2–2B). hence, these homology arms flank the construct and serve for alignment of the construct to the chromosome during HDR. The construct does not need to be linearized for integration.

3.2.2.7.3 Selection of the guide RNAs

Homology dependent repair only occurs efficiently after DSBs initiate the repair process. For efficient insertion of the construct, the sequence to be replaced is cut out by two guide RNAs via CRISPR/Cas9: guide RNA 1 induces a DSB as close to the STOP codon of the GOI as possible (Figure 3.2–2A). The second guide RNA 2 introduces a DSB in the intergenic region downstream of but close to the 3'UTR. Using both guide RNAs at the same time will delete the entire 3'UTR (Figure 3.2–2A) and substitute it with the cassette including the 2A peptide, the reporter, the endogenous 3'UTR and the transformation marker (Figure 3.2–2C). It is important to make sure

that the guide RNAs do not target the homology arms or any other part of the repair template, because this would lead to fragmentation of the repair template prohibiting proper integration. hence, it is necessary to modify the PAM sequence in the repair template plasmid for both guide RNAs.

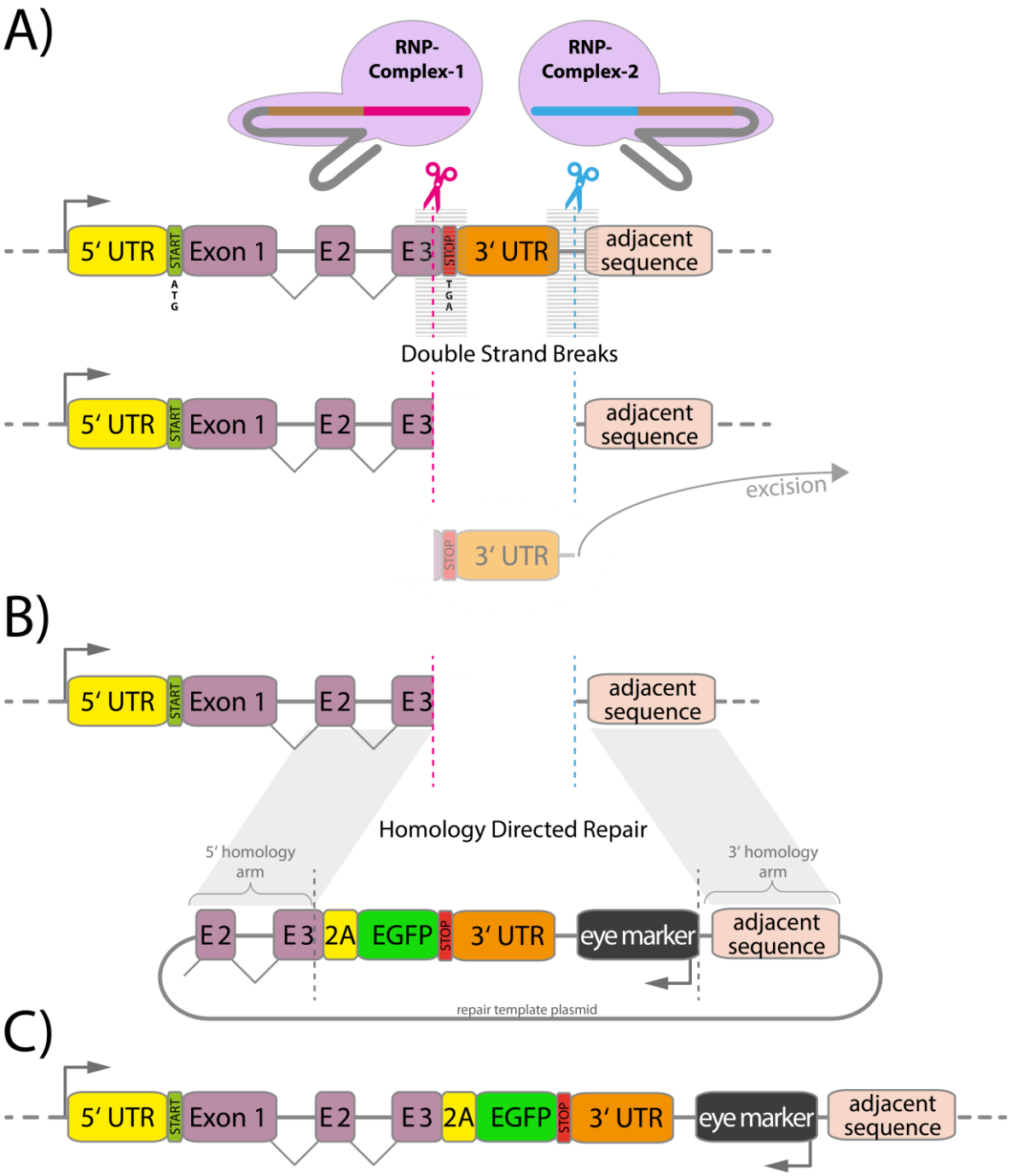

Figure 3.2–2: Strategy to generate bicistronic lines via CRISPR-based HDR. A. Two Ribonucleoprotein (RNP) complexes with guide RNA sequences 1 and 2 mediate double strand breaks (DSBs) in the genomic locus of the GOI. Guide RNA 1 mediates a cut near the STOP codon, guide RNA 2 right after the 3'UTR in the adjacent intergenic sequence. When both DSBs are induced the 3'UTR including the STOP codon gets excised. **B.** A repair template plasmid is provided containing homologous sequences 5' (5' homology arm) and 3' (3' homology arm) of

the DSBs, as well as sequences encoding a 2A peptide and EGFP cloned in frame to the GOI's last exon. Further, it contains the endogenous sequence that was excised containing the 3'UTR and an eye marker (3XP3-Tc-v-SV40). The repair template flanked by the homology arms gets integrated into the genomic locus via HDR. **C.** The modified transgenic locus contains two cistrons encoding for two distinct proteins, the endogenous 3'UTR and a subsequent eye marker.

3.2.2.7.4 When to use this strategy

The strategy of a bicistronic line should be chosen when the expression dynamics of the GOI have to be copied as exactly and comprehensively as possible. It also is a method with a very small chance of disrupting a gene's function. Disadvantages are that the strategy is much more work-intensive, because repair templates need to be cloned individually for each gene. Also, the size of the gene's 3'UTR might be a limiting factor, since larger constructs are more difficult to be inserted via HDR. To generate transgenic lines, the following steps need to be performed:

1. Sequencing of insertion locus
2. guide RNA design
3. guide RNA cloning
4. guide RNA efficiency test
5. Repair template and enhancer trap construct cloning
6. Embryonic injection
7. (Back-) Crossings of G_0 to wildtype
8. Screening for transgenics in F1
9. Characterization of the integration event
10. Generating homozygous stocks

3.2.3 MATERIALS

3.2.3.1 *Tribolium* husbandry

Standard equipment and supplies for molecular work as well as knowledge of *Tribolium castaneum* husbandry (Brown et al., 2009) are implied and not listed. For experiments beetles of *vermilion*^{white} (*v*^{w}) strain should be used (Lorenzen et al., 2002). Double-deionized water should be used at all steps, as well as analysis-grade Ethanol.

3.2.3.2 Genomic DNA extraction (see Note 1):

1. DNA extraction buffer (80 mM EDTA pH=8, 100 mM Tris pH=8, 0.5 % SDS, 100 µg/ml Proteinase K, added freshly)
2. Micro-Pestle suited for 1.5 ml tubes
3. Squishing buffer (10 mM Tris pH=8.2, 1 mM EDTA, 25 mM NaCl, 200 µg/ml Proteinase K, added freshly)
4. 10 mg/ml BSA
5. Wing buffer (10 mM Tris pH=8.2, 1 mM EDTA, 25 mM NaCl, 500 µg/ml Proteinase K, added freshly)
6. 24-well plates or similar
7. Dumont No. 5 forceps

3.2.3.3. DNA plasmid vectors and cloning

1. p(U6b-BsaI-gRNA), Addgene plasmid #65956
2. p(bhsp68-Cas9), Addgene plasmid # 65959
3. pBac[3xP3 g Tc' v], Addgene plasmid #86446
4. pCR™II vector or pJET1.2/blunt (Thermo Fisher Scientific, Waltham, U.S.A.)
5. *Bsa*I restriction enzyme
6. T4 DNA ligase and buffer
7. Transfection-grade plasmid-prep kits for purification
8. T7 Endonuclease I
9. DNA Assembly kit (e.g., Gibson Assembly® Cloning Kit (New England Biolabs, Ipswich, U.S.A.) or In-Fusion Cloning kit (Takara Bio Inc., Kusatsu, Japan))
10. *Dpn*I restriction enzyme

3.2.3.4. Embryonic injections

1. Borosilicate capillaries (e.g. from Ligenberg GmbH, Malsfeld, Germany) 10 mm x 1 mm
2. P-2000 micropipette puller (Sutter Instrument, Novato, U.S.A.) or similar
3. Optional: Microelectrode beveler (e.g. from Bachofer GmbH, Reutlingen, Germany)
4. FemtoJet® Microinjector (Eppendorf, Hamburg, Germany)
5. 0.45 µm (for 0.5 ml tubes) and 0.22 µm filters
6. 10x injection buffer (14 mM NaCl, 0.7 mM Na_2HPO_4 x $2H_2O$, 0.3 mM KH_2PO_4, 40 mM KCl, filter-sterilize with 0.22 µm filter, aliquot and store at -20°C)
7. Phenol red
8. Apple agar plates
9. bleach (DanKlorix, CP GABA GmbH, Hamburg, Germany)
10. Voltalef 10 S oil (Lehmann & Voss & Co., Hamburg, Germany)

3.2.4. METHODS

3.2.4.1. Sequencing of insertion locus

Even though the genome of *Tribolium* is available Richards et al., 2008) it is still necessary to sequence the regions to be targeted by Cas9, since beetle strains and laboratory stocks differ in sequence. Single nucleotide polymorphisms (SNPs) can occur in a potential target sequence and a different nucleotide in the PAM usually abolishes Cas9 function. In addition, differences in the rest of the target sequence can drastically reduce Cas9 efficiency (Hsu et al., 2014). For gene-specific enhancer traps the regions to be sequenced should comprise the potential insertion sites, thus mainly the region upstream of the transcription start site and first intron (Figure 3.2–1). In the case of bicistronic lines, we advise to sequence around 1 kB upstream of the STOP codon reaching 250 bp into the 3'UTR after the STOP for guide RNA 1, and 250 bp of the 3'UTR end as well as 1 kB of the downstream intergenic region for guide RNA 2 (Figure 3.2–2).

First, extract genomic DNA of adult v^{w} beetles (i.e. the strain in which you later want to integrate your CRISPR construct):

1. Put ~10 cold-anaesthetised adult beetles in a 1.5 ml tube, add 200 µl DNA extraction buffer.
2. Homogenize using a pestle suited for 1.5 ml tubes.
3. Put the homogenate in a heat block at 50°C for 1 h, mix by pipetting every 20 min.
4. Add 200 µl 5 M NaCl, mix, add 300 µl Chloroform and mix by inverting.
5. Spin down at 16,000 g for 15 min at RT.
6. Transfer 300 µl of the upper (aqueous) phase to a 1.5 ml tube.
7. Add 30 µl 7.8 M ammonium acetate, mix by pipetting and add ice-cold 600 µl 100 % Ethanol, invert 5-10x.
8. Keep at -20°C for at least 1 h.
9. Spin down at 16,000 g for 20 min at 4°C.
10. Discard supernatant.
11. Wash pellet with 300 µl 70 % Ethanol.
12. Spin pellet down at 16,000 g for 5 min at 4°C.
13. Repeat steps 10-12.
14. Remove as much of the supernatant as possible and air dry the pellet for ~10 min.
15. Resuspend DNA in 20 µl double-deionized H_2O.

Design suitable sets of primers to cover the areas to be sequenced (see Note 2). These should include primers to amplify the regions of interest (see Note 3) and sequencing primers that bind

within this amplicon. Sequencing results should be compared with the *Tribolium* reference genome (currently, GCF_000002335.3 Tcas5.2; please check http://ibeetle-base.uni-goettingen.de) (see Note 4).

3.2.4.2. guide RNA design

guide RNA sequences can be determined with the CRISPR Optimal Target Finder (see Note 5) at http://tools.flycrispr.molbio.wisc.edu/targetFinder/ (Gratz et al., 2014). The aim is to find target sites at the location where DSBs should be induced and that occur only at this location in order to avoid off-target effects (see Notes 6 to 9). For the generation of bicistronic lines two guide RNAs are used to excise the 3'UTR and substitute it with the construct. Hence, guide RNA 1 should cut as close to the gene's STOP codon as possible and guide RNA 2 downstream of but as near as possible to the end of the 3'UTR (Figure 3.2–2). These guide RNAs will likely bind to both the genome and the repair template. In order to avoid destruction of the latter, the respective sequence in the repair template should be modified (see section 3.2.4.5), but without affecting the encoded amino acid sequence. Unfortunately, this can further restrict suitable guide RNAs. In case of gene-specific enhancer traps, any target sites outside the exons and apart from putative regulatory elements can be chosen, but we recommend targets not too far from the transcription start site (Figure 3.2–1).

We recommend following settings for the target finder tool:

1. Set to finding all CRISPR targets. The U6 promotors needs a 5' Guanine for proper transcription (Mali et al., 2013) and a respective G is contained in the plasmid vector the guide RNA will be cloned in (see purple G in Figure 3.2–3). It is advisable to search for guide sequences that have a G at the 5' end in order to match the U6 promoter requirement. However, one mismatch at the 5' end of the guide has been shown to not much reduce efficiency. Hence, this is not an absolute requirement, especially because a G is available in the plasmid vector.
2. Guide RNA length of 20 bp is suitable in our experience.
3. Check for and use the latest released *Tribolium* genome release (check http://ibeetle-base.uni-goettingen.de).
4. It is advisable to restrict the search to target sites with only 'NGG' PAMs as 'NAG' PAMs have reduced efficiency (Hsu et al., 2013).
5. We use high stringency settings since maximum stringency criteria are based on cleavage effects in cell lines only.

The 'Design Experiment' button is helpful to extract the actual oligonucleotide sequences to be ordered. It automatically adds Gs if necessary. However, the overhangs generated will not be the correct ones for the plasmid containing the *Tribolium* U6 promotor (p(U6b-BsaI-gRNA, see Figure 3.2–3). To generate the correct overhangs, we recommend using the TriGenes guide RNA oligo design tool at https://trigenes.com/crispr/grna-oligo-design-tool/.

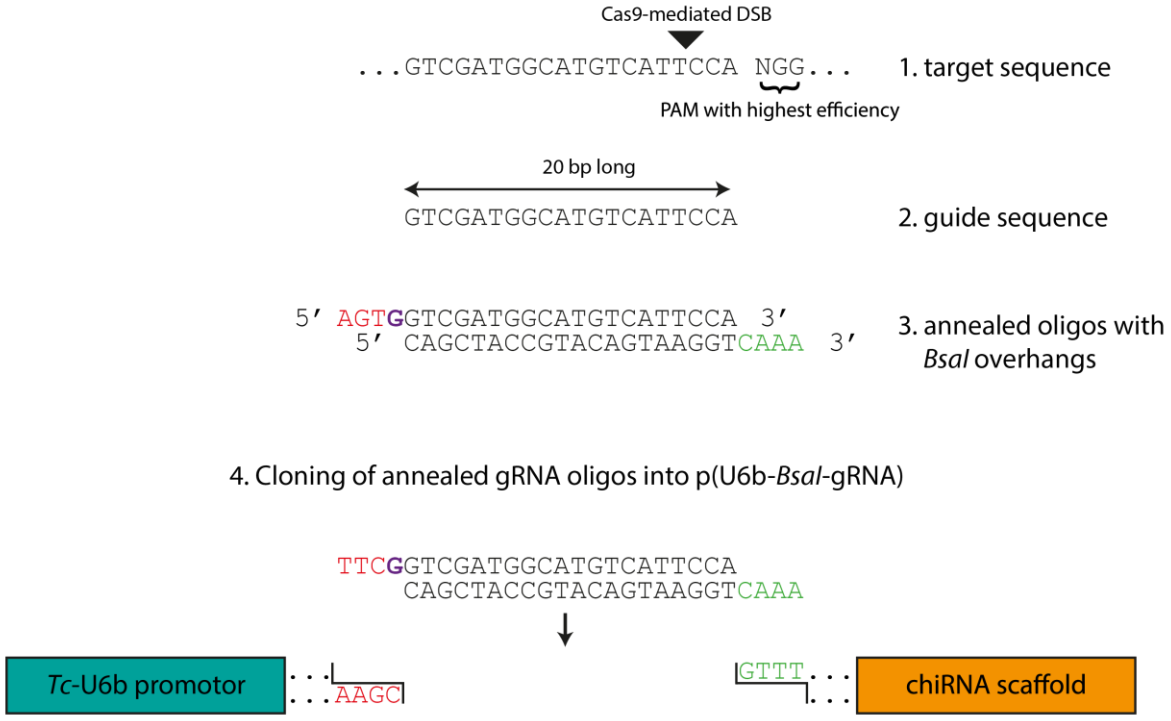

Figure 3.2–3: guide RNA design and cloning (figure partially modified from Gilles et al., 2015a): First a suitable target sequence is selected containing a 'NGG' PAM and with a seed sequence that does not occur elsewhere in the genome and, hence, cannot mediate off-target DSBs. The guide RNA sequence should be 20 bp long and does not contain the PAM which is already present in the construct. This guide RNA sequence will be synthesized by annealing two oligonucleotides that include suitable overhangs for the restriction enzyme *BsaI*. Annealed oligonucleotides (oligos) will be cloned into the plasmid p(U6b-BsaI-gRNA) containing a Tc-U6b promotor sequence and a downstream chiRNA scaffold (crRNA and tracrRNA) by Golden Gate cloning or regular ligation. The U6 promoter needs a G as the first base for transcription. As the backbone already contains a G 5' of the target sequence (purple G), a G does not need to be part of the original target sequence in order to facilitate proper transcription by the U6 promotor.

3.2.4.3. guide RNA cloning

We recommend using Golden Gate reactions to clone guide RNAs (Figure 3.2–3). An alternative protocol can be found under https://trigenes.com/crispr/grna-oligo-design-tool/.

1. Anneal oligonucleotides by mixing 10 µL of the forward and reverse oligonucleotide (100 µM) each with 80 µL double-deionized h_2O. heat to 98°C for 5 min on a heat block and let cool down slowly to approximately 40°C by switching off the heat block

and leaving the tubes in the block for 45-60 min (see Note 10). Monitor the temperature.

2. Set up following Golden Gate reaction for one guide RNA (scale up as master mix for all guide RNAs):
    a. 50 ng p(U6b-BsaI-gRNA) vector (see Note 11)
    b. 1 µL annealed oligonucleotides (10 µM)
    c. 1 µL ATP (10 mM)
    d. 1x Enzyme buffer
    e. 0.3 µL *BsaI*
    f. 0.3 µL T4 DNA Ligase
    g. X µL double-deionized H_2O up to 10 µL total volume
3. Perform Golden Gate reaction in thermocycler:
    a. heat lid to 40°C
    b. 37°C for 5 min
    c. 20°C for 10 min
    d. repeat ii. and iii. 10 to 15 times
4. Transform 5 µL of the reaction in chemically competent bacterial cells.
5. Sequence guide RNA sequence of each guide RNA plasmid including the U6 promotor and the whole chiRNA scaffold (guide RNA and tracrRNA) (Figure 3.2–3).
6. Prepare transfection-grade mini-preps of all guide RNA plasmids (midi-preps are not necessary for the testing stage) (see Note 12).

3.2.4.4. guide RNA efficiency test

Efficiency to guide the Cas9 nuclease can differ for each guide RNA. hence, before moving on to the next steps, especially for the HDR approach, efficiency needs to be tested (see Note 13). There are different methods to test guide RNA efficiency. However, in this chapter we focus on the T7 Endonuclease I (T7 Endo I) assay, since it only requires standard lab equipment (see Note 14).

The assay involves embryonic injection of guide RNAs individually along with Cas9 which will lead to different indels in variety of cells of the developing embryo. A PCR reaction is used to amplify the sequence encompassing the target site(s). Upon denaturing the PCR product and reannealing the single strands heteroduplexes are formed. At the site of an indel, the base pairing is disturbed such that a T7 Endo I digest will cut both strands at those non-annealed regions.

This can be visualised by gel-electrophoresis: If two fragments smaller than the amplicon are visible, the guide RNA has successfully mediated Cas9 targeting.

The protocol is very similar to the one at www.crisprflydesign.org.

Perform following steps:

1. Co-inject the combination of guide RNA (400 ng/µl) and Cas9 plasmid (500 ng/µl) into 100 embryos (needs to be done for each potential guide RNA) (see section 3.2.4.8 for injection procedure).
2. Incubate them for three days at 32°C (see section 3.2.4.8). Alongside the injected embryos, uninjected embryos of the same strain should be incubated and DNA isolated identically to the injected condition as control for potential differences in the sequence of individuals that will also result in heteroduplexes without a Cas9 cut.
3. Extract genomic DNA from injected embryos
    a. Collect 15-20 L1 larvae that survived and transfer to a 1.5 ml tube.
    b. Add 100 µl squishing buffer and homogenize with a yellow tip at the sides of the tube. Make sure to not use the same tip for a different guide RNA batch.
    c. Incubate the homogenate for 1 h at 55°C.
    d. Inactivate the Proteinase K at 95°C for 6-8 min.
    e. Spin the homogenate down for 15 min at 16,000 g at 4°C.
    f. Use 5 µl supernatant as template for a 50 µl PCR reaction. It is recommended to add 2.5 µl of a 10 mg/ml BSA solution.
4. PCR amplify sequence encompassing target site and perform T7 endo I assay (see Note 15)
    a. Design primers to amplify ~700 bp, flanking target sites asymmetrically, resulting in two distinguishable bands after T7 endo I treatment.
    b. Run two 50 µl PCR reactions to generate enough material and gel-purify the kit of choice.
    c. Denature and reanneal 400 ng of the PCR product in 1x T7 endo I buffer (total volume 19 µl) as described under 3.2.4.3 with a heat block.
    d. Add 0.7 µl (7 U) T7 Endo I.
    e. Incubate at 37°C for 20 min.
    f. Stop the reaction immediately by adding 2 µl of 0.25 M EDTA.
    g. Run the assay on a 1.5 % agarose gel alongside the same amount of DNA of uncut DNA as control.

If the guide RNA is highly efficient, bands corresponding to the sequence upstream and downstream of the target will be seen. An uncut fraction will be visible as well. Successful genome editing has been performed with guide RNAs where the cut bands were much weaker than the main band at the size of the PCR product. The intensity of uncut and cut bands can thus vary, but do not directly relate to whether the guide RNA works in effect.

3.2.4.5. Repair template and enhancer trap construct cloning

The construct will be provided in form of a plasmid. Construct cloning greatly differs between the two strategies, and in themselves strategies can be adapted to personal needs and situations (see Notes 16-22).

We recommend assembling the repair template not with classic restriction digest/ ligation cloning, but using DNA assembly cloning kits (e.g., Gibson Assembly® Cloning Kit (New England Biolabs, Ipswich, U.S.A.) or In-Fusion Cloning kit (Takara Bio Inc., Kusatsu, Japan)). This is especially beneficial when cloning repair templates for bicistronic lines.

3.2.4.6. Generation of enhancer trap construct:

To generate a universally usable enhancer trap construct following parts should be assembled:

1. **3XP3-*Tc'v*-SV40**: The recommended eye marker consists of the eye-specific promotor 3XP3 (Berghammer et al., 1999), the rescue genomic *Tc-vermillion* gene and the termination sequence SV40 (Horn et al., 2002). This can be retrieved from plasmid #86446 from Addgene. SV40 will work bidirectionally and thus does not need to be included in the enhancer trap cassette.
2. **bhsp68-EGFP**: The enhancer trap cassette consists of EGFP and the basal promoter of the heat-shock protein 68 (bhsp68) which acts as basal promotor. This cassette should be oriented in the opposite direction to the eye marker, so that SV40 can act as terminal sequence for both parts. Sequences can be retrieved from plasmids at Addgene.
3. **Exogenous guide RNA target site** (Figure 3.2–1): Using megapriming cloning (Ulrich et al., 2012), a guide RNA target site should be included that is not found in the *Tribolium* genome. We used a guide RNA sequence from the *Drosophila ebony* gene, specifically (GAACCGGGCAGCCCGCCTCC TGG). This sequence should be located near the ends of the construct to be inserted and will lead to linearization of the plasmid thereby facilitating the integration of the repair template by NHEJ (Martin Klingler, personal communication).

Such a construct has been assembled and successfully tested by the authors. In addition to the abovementioned components, it contains a bicistronic mRNA encoding for EGFP and the Cre recombinase. The plasmid can be obtained from the authors.

Prepare transfection-grade midi-preps of all constructs. Check for integrity of these preparations by sequencing at least the coding regions of the repair template or enhancer trap construct.

3.2.4.7. Generation of bicistronic repair template:

The generation of a bicistronic repair template depends on the guide RNAs of choice and its design needs to await the successful testing and selection of the guide RNAs to be used. See above and Figure 3.2.–2 for basic design.

Following parts need to be assembled:

1. **Backbone**: We recommend using pCR™II vector or pJET1.2/blunt (Thermo Fisher Scientific, Waltham, U.S.A.) as these are small vectors. The size of the complete repair template can be quite large.
2. **5' homology arm**: The ~1 kB 5' homology arm (see Beumer et al., 2013 for a detailed analysis on the efficiency of differently long homology arms) should always end right before the gene's STOP codon irrespective of which guide RNA is used (see Note 23), so that in the repair template sequence you will have 1 kB of ORF sequence fused to the 2A sequence (instead of the STOP) followed by the reporter sequence – all in frame (Figure 3.2–2).
3. **2A peptide**: We recommend using the P2A peptide sequence as this was shown to be most efficient (Kim et al., 2011). You can introduce this ~70 bp sequence either similar to the others by amplifying it from a donor plasmid or by having the sequence as part of the primer/oligonucleotide for the assembly reaction. Both have proven to work (see Note 24).
4. **EGFP**: This sequence can be retrieved from numerous sources. Make sure that the STOP codon is included or that you include it as part of the assembly primer.
5. **3'UTR**: This part also includes parts of the intergenic region. It starts after the gene's STOP and ends at the cut position of guide RNA 2. Cut positions are always 3 bp upstream of the PAM (Tycko et al., 2016).
6. **3XP3-*Tc'v*-SV40**: The recommended eye marker consists of the eye-specific promotor 3XP3 (Berghammer et al., 1999), the rescue genomic *Tc-vermillion* gene and the termination

sequence SV40 (Horn et al., 2002). This can be retrieved from plasmid #86446 from Addgene.

7. **3' homology arm**: The ~1 kB 3' homology arm will start at the guide RNA 2 cut site (Figure 3.2–2).

To avoid that the repair template itself will be targeted by Cas9, PAMs must be mutated in the repair template, removing the PAM sequence 'NAG' or 'NGG'. If the PAM is located in a coding sequence, mutations must be chosen such that the amino acid sequence is not changed. This mutation can be introduced during the amplification processes for the homology arms and 3' UTR by simply including these modified sequences in the primer sequence. This can be also achieved with a separate PCR mutagenesis or megapriming (see e.g. Ulrich et al., 2012 for details). Both processes involve amplification of the whole plasmid and a subsequent *DpnI* digestion to remove the original methylated plasmid which does not contain the intended modification.

3.2.4.8. Embryonic injection

The procedure for embryonic injections is based on standard protocols (Berghammer et al., 1999; Eckermann et al., 2018; Posnien et al., 2009).

1. Prepare injection needles (Use Borosiliate capillaries for injections). Use a P-2000 micropipette puller to form the needle applying the following settings: heat=350, Fil=4, Vel=50, Del=225, PUL=150 or other pullers with respective settings. The capillaries should be similar to those used for *Drosophila* injection. Open and sharpen the needle either manually using a tweezer or a scissor or by using a microelectrode beveler and check after each sharpening step (see Note 25).
2. Prepare injection mix: Mix all purified plasmids to following concentrations and a volume of 10-20 µl: Repair template and p(bhsp68-Cas9) 500 ng/µl; Inject individual guide RNAs with 400 ng/ µl and guide RNA 1 and 2 simultaneously with a concentration of 250 ng/µl each. Mix 8 µl plasmid mix with 1 µl 10X injection buffer and 1 µl Phenol red. Filter-sterilize with a 0.45 µm filter for 0.5 ml tubes by putting mixtures on the filter inside a tube and centrifuge for 5 min at 11,000 g.
3. Place v^{w} beetles on white flour and let them lay eggs for 1 h at 28°C.
4. Remove embryos and let them develop further for 1 h at 28°C.
5. This can be repeated to get fresh embryos as often as necessary.
6. Wash embryos in 1 % bleach (equivalent to 0.05% sodium hypochlorite) for up to 3 min in a 150 µm gaze sieve. Extended bleaching can lead to mortality.
7. Wash embryos thoroughly in room temperature water.

8. Make sure that all flour is removed.
9. Moisten an object slide with water.
10. Transfer embryos on the object slide with a fine brush, arrange them in a line near the long edge of the slide (90 embryos can fit on one side). The more pointed posterior side of the egg should point towards the outside (see Note 26).
11. Place slide on an apple agar plate.
12. Load needle with 4 µl of injection mix.
13. Place needle in the microinjector.
14. Test the needle position and opening by placing it into a drop of Voltalef® oil (VWR) on a slide.
15. The droplet size should be roughly a 5th of the embryo size.
16. Constant pressure should be adjusted so that no liquid is leaking.
17. Inject into first posterior third so that you see either movement in the embryo or red stain.
18. Do not move the needle inside the embryo and do not inject too deeply and not too much, there should be no leakage.
19. Put the slide back on an apple agar plate and collect in an airtight box and keep them at 32°C for 72 h. high humidity is required for the injected embryos to survive. However, drops of water are deleterious for hatched larvae. Hence, it is important to keep the embryos as long as possible under high humidity, but upon hatching of the first animal they should be dried.
20. Transfer larvae to whole grain flour.

3.2.4.9. (Back-) Crossings of G_0 to wildtype

1. Rear injected animals at 32°C until they pupate, sex them and keep them separately.
2. Set up single crosses by crossing each injected adult to three *v*^{w} wildtype animals of the opposite sex.
3. Rear single crosses at 32°C and remove the parental generation when the next generation starts to pupate.

3.2.4.10. Screening for transgenics in G_1

1. Using a suitable stereomicroscope, screen G_1 animals for black eyes. The pupal stage is best as these do not move. When screening adults, they have to be anesthetised either by CO_2 or by placing them on ice.

2. For both strategies, keep all positive animals and subsequent offspring as founder lines, as they can differ in quality and strength of the signal. This is especially true for gene-specific enhancer traps.
3. Cross each positive G_1 separately to v^w to generate offspring that can be screened for the expression in the (developing) brain.
4. Depending on your GOI, its expression amount and timing, choose a time point where individuals can be easily prepared in a larger scale.
5. Prepare embryos for anti-GFP immunostaining (see Buescher et al. in this book), larvae or adults accordingly to detect native GFP expression (after preparation, directly put in mounting medium and imaged), or anti-GFP immunostaining (see Hunnekuhl et al. in this book).
6. Overlap to the GOI can be tested with an antibody against the protein of interest, if available, or alternatively with *in situ* hybridisation (see Hunnekuhl et al. in this book).

Select 3-5 founder lines which have the strongest expression, with the highest degree of overlap to the GOI.

3.2.4.11. Characterization of the integration event

1. Check for proper integration at the expected location by designing primers for amplicons spanning at least the regions surrounding the DSBs or the whole inserted construct.
2. Extract genomic DNA similar to 3.2.4.1.
3. Perform standard PCR.
4. Make homozygous stocks of all of the selected.

3.2.4.12. Generating homozygous stocks

Having homozygous stocks makes subsequent experiments much easier, be it live-imaging or subsequent genetics. The following protocol is based on genotyping individuals using DNA extracted from wing tissue (Strobl et al., 2017):

1. Sex individuals as pupae and rear sexes separately until adult stage.
2. On the experiment day, prepare ice, wing buffer, glass slides, forceps, as well as a 24-well plate with small amounts of flour in the wells.
3. Put 0.5 ml tubes on ice, put beetles in a vial on ice for cold anaesthetisation.
4. Prepare glass side for preparation by wrapping it in parafilm.
5. Put a beetle with one forceps on its right side, head to the left, left elytron up.
6. Hold at the thorax and try to enter under elytra with other forceps carefully.

7. If the elytron lifts, take out hindwing, and rip and cut first at thicker more distal dark part of the wing and then rip carefully at more proximal parts.
8. Be careful to not remove the whole hindwing as this might leave a wound in the thorax.
9. Put the wing in the tube keeping it cool at all times, put the beetle in a well, both well and tube marked with a unique identifier for each beetle.
10. Repeat preparation for all.
11. Put wings on -80°C for 15 min.
12. Add 10 µl of buffer to the wing, and crushing it on the tube wall, rolling it and pushing tissue up and down with a thin pipette tip (this can take 2 min per wing).
13. Spin down shortly.
14. Put tubes on 37°C for 1 h.
15. Put wings on 75°C for 20 min.
16. Spin down the evaporated water.
17. Perform PCR.

- The wildtype (wt) amplicon (hence the insertion area without inserted construct) should be always smaller so that you always see the wt band at least if its heterozygous (since smaller amplicons will outcompete bigger ones in PCR); this makes the PCR less error prone.
- Amplicon size difference should be at least 200 bp and amplicon size between 300-800 bp. We recommend ~40 cycles to promote the amplification of the smaller wt band.

18. Put beetles that are homozygous for marker all together and raise homozygous stocks.

3.2.5. NOTES

1. Any method for genomic DNA isolation will suffice (e.g. kits). These are the protocols we used.
2. Primers should be designed carefully so that unique sites are amplified, the melting temperature is high, and no secondary structures are likely to form. For sequencing primers and the sequencing reactions themselves, please consult the company you are using. If recommendations are followed, mistakes or suboptimal sequencing results may be avoided.
3. The areas to be sequenced can also be subcloned into a blunt cloning vector, such as pJET1.2, if sequencing from an amplicon does not yield good results.
4. It is highly recommended to use a suitable software that allows in silico cloning, analysis of sequencing data, etc. Use of such will greatly aid the cloning work.
5. There are other design tools available. We have used the one mentioned above nearly exclusively, but we recommend considering other tool websites as well.
6. If a region is particulary low in GC-content, an alternative to Cas9 is CPf1 where the PAM is needs to be T-rich ('TTN') (Zetsche et al., 2015).
7. If there is an otherwise suitable guide RNA sequence which would mediate cuts in one off target, a T7 Endo I assay can be performed with two regions to be amplified for this guide RNA, one for the aimed target region, one for the off-target region. If the guide RNA mediates DSBs also in the off-target, this will be seen in the T7 endo I assay and the guide RNA can be discarded.
8. Guide RNAs can also be chosen by investigating whether the sequence can form hairpins, including the tracrRNA as this can greatly influence efficiency of the guide RNA. This can be done by the tool http://chopchop.cbu.uib.no/ (Labun et al., 2016; Montague et al., 2014). So far, the *Tribolium* genome cannot be used as reference, but you can ask the website administrators to include the genome of choice.
9. It might be advantageous to restrictively target the template strand with a guide RNA of choice, see (Clarke et al., 2018).
10. Oligo annealing can be alternatively achieved by programming a thermocycler to ramp down to 25°C with a rate of -0.1°C/s. This follows the advice found at http://flycrispr.molbio.wisc.edu/protocols/gRNA.
11. It would be worthwhile to test which of the three U6 promotors in the *Tribolium* genome is the most effective in driving Cas9 transcription, similar to (Port et al., 2014). Two were

cloned and no pronounced difference was observed (Gilles et al., 2015). We have only used p(U6b-BsaI-gRNA).

12. In case transfection-grade kits are not available, use normal kits, but add a precipitation step to increase DNA purity and remove salts:
    - Mix ~50 µg DNA with 10 µl 3 M Sodium acetate pH=5.2 (NaOAc) and fill up with H_2O to a total volume of 100 µl.
    - Add 800 µl 100 % Ethanol (analysis grade).
    - Keep at -80°C for 2 h or o/n.
    - Centrifuge at 4°C at maximum speed for 30 min.
    - Remove supernatant.
    - Wash with 500 µl pre-cooled 70 % Ethanol.
    - Centrifuge at 4°C at maximum speed for 15 min.
    - Repeat steps e) to g) once.
    - Remove as much of the supernatant as possible and air dry the pellet for ~10 min.
    - Resuspend in 15-30 µl h_2O.
13. If you design gene-specific enhancer traps, you could also skip this part and inject mixes with all available guide RNAs. You would need to inject more embryos but save time potentially by avoiding this assay. The same is true for when guide RNAs of choice are really close to each other or even overlapping, this is even true for building a bicistronic line. For example, if three guide RNAs for cut-site A and two for cut-site B are strongly overlapping to each other, it might be a good alternative to prepare six different injection mixes instead of testing them beforehand. This is an issue of personal preference and should not be considered as a rule, as it is also dependent on each individual experiment.
14. An alternative to T7 Endonuclease I assays is high resolution melting analysis (Bassett et al., 2013) which requires a qPCR machine, but is more sensitive to detect guide RNA functionality. Both methods can be used.
15. The T7 Endonuclease I assay is very sensitive to the amount of enzyme added, the temperature, as well as the length of incubation. So, make sure that the amounts as well as the timing are exact.
16. It could be advantageous to design a way to remove the eye marker after stocks are made homozygous. In *Drosophila* this is usually achieved by introducing loxP sites (Gratz et al., 2013). In *Tribolium* the option is to introduce exogenous sequences from *Drosophila* such as guide RNAs of ebony on both sides of the eye marker via PCR mutagenesis. Then after the *Tribolium* stock was made homozygous using the eye marker, it can be removed by

injecting the line with the suitable guide RNAs for the introduced target sequences. A fraction of injected embryos will lose the eye marker and those can be used for further experiments. This strategy reduces the potential influence of the 3XP3 promotor on the gene's and marker gene's expression. We note, however, that we have so far not observed strong influence of the eye marker.

17. An alternative bicistronic repair template could be using only guide RNA 1 and putting the eye marker directly after a SV40 sequence following the fluorescent protein. This is especially useful if the 3'UTR of your gene of interest is too big to be considered as part of the construct. The eye marker influence can then be reduced by cutting the eye marker out (as in Note 16).
18. The repair templates can be modified in multiple fashions. One could substitute EGFP with other fluorescent proteins of other colours or brightness, or with GAL4 to cross with suitable UAS lines. Also, tricistronic lines with the gene, a fluorescent protein and GAL4 are possible. However, the size can be a constraint for cloning and HDR and can be a potential disadvantage. Ideas for multiple variations can be potentially gathered in (Gratz et al., 2013).
19. Repair template size can be a constraint, as rates of integration might decrease. We have successfully integrated 2.5 kB, but the homologous recombination mechanism itself was employed integrating constructs as big as 13 kB (Keeler et al., 1996).
20. You can also provide Cas9 as protein which is more efficient than providing Cas9 via a plasmid (Zuris et al., 2015).
21. Cas9 expression is driven by bhsp68. It would be better to have Cas9 under control of a germ-line specific promoter. This is actually under construction in our lab.
22. Providing guide RNA and a repair template as single stranded DNA can increase CRISPR efficiency drastically (Gratz et al., 2013). In most cases, single stranded repair template had strong size restrictions, so that our strategies could not have worked. However, using a production system especially for long single stranded DNAs can circumvent these limitations (e.g. https://www.takarabio.com/products/gene-function/gene-editing/crispr-cas9/long-ssdna-for-knockins).
23. For bicistronic construct cloning, you can already start amplifying the 5' homology arm as this always ends with the last codon before the STOP and is, hence, independent of guide RNA choice. The design of 3' UTR and 3' homology arm depends on the chosen guide RNA, so this needs to be postponed to after guide RNA tests (but see Note 13).

24. The sequence for the P2A peptide is <70 bp in size, so using a Megapriming protocol, you could also introduce this sequence not as part of the assembly mix, but afterwards, with very long primers.
25. Sharpening needles carefully takes longer but increases survival rate substantially.
26. To easily transfer embryos from sieve to object slide, they should be kept wet and should be moved on the shortest distances as possible.

3.2.6. ACKNOWLEDGEMENTS

We express our gratitude to Prof. Martin Klingler for discussions on the gene-specific enhancer trap strategy and Dr. Stefan Dippel for discussions on the bicistronic line strategy. In addition, we want to thank Patricio Ferrer Murguia for useful additional information.

3.3. Manuscript 3: Immunohistochemistry and fluorescent whole mount RNA *in situ* hybridization in larval and adult brains of *Tribolium*

This manuscript offers a detailed description of basic methods of immunohistochemistry and in situ hybridisation but in larval and adult brain, so far undescribed in *Tribolium*. This work complements the CRISPR-related manuscript 2 and builds and describes the methods that were partially employed in manuscript 1. Proper immunohistochemistry in different stages is adamant for a proper generation of images, which in turn are the basis for all analyses. Hence, this manuscript offers further methodological support establishing *Tribolium* as a model system suitable for multi-faceted neurobiological work. We hope that methods described help and support the neurobiological research in *Tribolium* and neuroevolutionary research in general.

Authors

Vera S. Hunnekuhl[*], Janna Siemanowski, **Max S. Farnworth**, Bicheng He, Gregor Bucher[*]

[*] = corresponding authors

Status

in press in Brain Development: Methods and Protocols, Second Edition (Springer Nature)

My contributions

- Conceptualisation of the immunohistochemistry methodology[1]
- Writing of the manuscript[2]
- Generation of data for figures[3]

[1] = together with VSH, JS, BH

[2] = together with VSH, GB

[3] = together with VSH

Title:

Immunohistochemistry and fluorescent whole mount RNA *in situ* hybridization in larval and adult brains of *Tribolium*

Authors:

Vera S. Hunnekuhl[1,*], Janna Siemanowski[1], Max S. Farnworth[1,2], Bicheng He[1], Gregor Bucher[1,*]

[1] Department of Evolutionary Developmental Genetics, Johann-Friedrich-Blumenbach Institute, GZMB, University of Göttingen, Göttingen, Germany, [2] Göttingen Graduate School for Neurosciences, Biophysics, and Molecular Biosciences (GGNB), Göttingen, Germany

[*] **Corresponding authors:** Vera S. Hunnekuhl vera.terblanche@uni-goettingen.de, Gregor Bucher gbucher1@uni-goettingen.de

Running head: Brain *in situ* hybridization and immunohistochemistry

Key words: *in situ* hybridization, Gene expression, Antibody staining, Fluorescence labelling, Insect brain, *Tribolium castaneum*, Red Flour Beetle

3.3.1. ABSTRACT

Arthropod brains are fascinating structures that exhibit great complexity but also contain conserved elements that can be recognized between species. There is a long tradition of research in insect neuroanatomy, cell biology and in studying the genetics of insect brain development. Recently, the beetle *Tribolium castaneum* has gained attention as a model for insect head and brain development and many anterior patterning genes have so far been characterized in beetle embryos. The outcome of embryonic anterior development is the larval, and subsequently, the adult brain. A basic requirement to understand genetic cell type diversity within these structures is the ability to localize mRNA and protein of neural genes. here we detail our protocols for RNA *in situ* hybridization in combination with immunohistochemistry, optimized for dissected brains of larval and adult beetles.

3.3.2. INTRODUCTION

Traditionally most research in insect brain development has focused on the fly *Drosophila melanogaster* as a genetically tractable organism (Hirth, 2003; Lichtneckert and Reichert, 2005; Younossi-Hartenstein et al., 1997). In addition, research on the orthopteran species *Schistocerca gregaria h*as offered insights into the cellular composition of the developing brain of a hemimetabolous insect, and on the origin of specific brain structures, such as the central complex, from identified cell lineages (Boyan and Williams, 2011; Boyan and Reichert, 2011; Ludwig et al., 1999). More recently, the beetle *Tribolium castaneum* has been introduced as a third model for studying arthropod brain development (Koniszewski et al., 2016; Posnien et al., 2011). The species has a sequenced genome (Richards et al., 2008) and is amenable to RNA interference, CRISPR genome editing and other functional genetic techniques (Gilles et al., 2015; Schinko et al., 2012, 2010; Schmitt-Engel et al., 2015) (for a detailed protocol for performing CRISPR in *Tribolium* please see Farnworth et al., in press in this issue). Therefore, *Tribolium* can be regarded as an insect genetic model second only to *Drosophila*. Moreover, some aspects of head and brain development seem to be more conservative in this beetle, as it does not undergo the process of head involution known from *Drosophila* (Posnien et al., 2010). In addition, large parts of the *Tribolium* brain are already developed at the beginning of the first larval stage, whereas in *Drosophila* the development of some brain structures, such as the central complex, is shifted to late larval and pupal stages (Koniszewski et al., 2016).

In particular the central complex (CX), an intriguing anterior brain structure that is conserved among insects and beyond (Loesel et al., 2002; Strausfeld, 2012), has become subject of studies on *Tribolium* brain development. Parts of the CX derive from the *six3*-positive anterior median region, and a number of additional transcription factors have been implicated in the patterning of neuropils deriving from this region (Koniszewski et al., 2016; Posnien et al., 2011). Current research aims to connect specific structures of the brain (such as the CX and its substructures, but also others as for example mushroom bodies or antennal lobes) to their embryonic progenitors (see Buescher et al., in press of this issue for embryonic *in situ* hybridization). Characterizing the transcriptional profile of neural cells in the larval and adult brain allows identifying continuity with embryonic cells, which in turn can imply a common developmental origin of these cells. Furthermore, characterization of the neurotransmitter and neuropeptide content of neural cells will lead to a better understanding of the cellular composition of brain structures and will open new avenues for cross species comparisons of neural organization, and will hence contribute to a better understanding of brain evolution in general (Koniszewski et al., 2016). In addition, transgenic beetles that carry fluorescent reporters (mostly GFP) linked to a

gene locus are becoming available. Antibodies binding the GFP reporter help to enhance visibility of this reporter in fixed material, and they can be combined with a second antibody that stains the axonal scaffold as a reference.

To follow up these leads of research, our lab has established protocols for the dissection of larval and adult brains, for fluorescent RNA *in situ* staining and for antibody labelling.

3.3.3. MATERIALS

3.3.3.1. Beetle stock keeping and generation of larvae

We keep adult beetles of the wild type San Bernadino (SB) strain and of transgenic reporter lines on whole grain flour (including 50 g yeast per kg flour) at 23°C. For experiments on adult brains individuals are directly taken from the stock and are dissected.

To raise larvae to a defined age, timed egg collections are set up. For that the beetles are separated from the flour using an 800 µm pore width sieve and are then put on white flour, the time pointed noted, and kept at 32°, e.g. over night. The eggs are collected by first separating the beetles from the flour (using the 800 µm sieve) and then separating the eggs from the white flour using a 300 µm sieve. Eggs are transferred into a fresh container and kept at 32°C until they reach the desired age. If enough flour is present in the container, they do not need any further care. It is however important to make sure that larvae are not too dense as overcrowding will limit food supply and lead to non-synchronized and delayed growth.

3.3.3.2. Dissections and fixations

We use autoclaved bottles or sterile tubes for all buffers and solutions. All aqueous buffers are made with double deionized water (ddH_2O) and are either autoclaved or filter-sterilized before use. The formaldehyde containing fixation, methanol for dehydration and hybridization buffers are harmful and must be used under a fume hood.

1. PBS (phosphate buffered saline): Prepare a stock solution of 10x PBS by dissolving 80 g NaCl, 2 g KCl, 2 g KH_2PO_4 and 11.5 g Na_3HPO_4 in 1 l double distilled water (ddH_2O). The pH is adjusted to 7.4 using NaOH. To make 1x PBS, 100 ml of 10x PBS are added to 900 ml of ddH_2O.
2. PBT (phosphate buffer saline plus 0.1 % Triton): We use PBT made with Triton rather than Tween-20 for all our washing and incubation steps as we think this harsher detergent may improve permeability, without having adverse effects on tissue integrity. Prepare a stock of 10 % Triton in 1x PBS. For the final working solution combine 100 ml 1x PBS, 10 ml 10 % Triton and 890 ml ddH_2O.
3. Fixation: To make a solution of 4 % formaldehyde in PBT provide 1 ml PBT in a small 1.5 ml centrifuge tube and add 140 µl of a 37 % commercially available formaldehyde solution (Merck). The dissected brains can be directly transferred into this tube for fixation. Brains that are supposed to be stained with Phalloidin require a fixative free of methanol.

Prepare a 4 % formaldehyde/PBT solution using 16 % methanol-free formaldehyde (Thermo Scientific) and dissolve 1:4 in PBT.

3.3.3.3. Antibody labelling

4. Blocking solution: For blocking prior and during antibody incubation use 3 % albumin fraction of bovine origin (AppliChem) in PBT. We avoid using any preservatives such as sodium azide since they can damage some enzyme-conjugated antibodies. Instead we always prepare the blocking solution freshly on the day of use. Also see **NOTE 1** for blocking of secondary antibodies.
5. DAPI stock solution: Add 5 mg of DAPI powder (Merck) to 1 ml of ddH_2O and dissolve (vortexing or sonication may be required). Aliquots can be stored in the freezer for several months. Use at a working concentration of 1:1000 v/v.

3.3.3.4. *in situ* hybridization

6. Saline Sodium Citrate buffer (SSC): To make a stock of 20x SSC buffer dissolve 175 g NaCl and 88.2 g trisodium citrate ($Na_3C_6H_5O_7$) in 800 ml ddH_2O. Adjust to pH 5.5 by using HCl and fill to 1 l. This buffer is used in the hybridization buffers at a 5x concentration (see below), the stock can be stored at room temperature.
7. Hybridization buffer BT (Hybe-BT): Our basic hybridization buffer for dissected brains contains 500 ml formamide, 250 ml SSC (pH 5.5), 250 ml ddH2O and 0.15 % Triton (1.5 ml of the 100 % stock per 1 l of Hybe-BT buffer). Hybe-AT can be stored at room temperature.
8. Hybridization buffer AT (Hybe-AT): To make Hybe-AT buffer first combine 2 ml yeast RNA, 400 µl heparin (50 mg/ml) and 8 ml salmon sperm DNA (10 mg/ml) in a falcon tube and boil the mixture at a minimum of 95°C in a water bath for 10 minutes. Then, the falcon tube is put on ice for 3 minutes and then the solution is combined with 400 ml Hybe-AT in a bottle and is thoroughly mixed. For long term storage Hybe-AT is aliquoted into 15 ml falcon tubes and kept in the freezer at -20°C.
9. Maleic acid buffer with Triton (MAB-T): Dissolve 11.6 g maleic acid, 8.76 g NaCl and 8.6 g NaOH (to pH 7.5) in 1 l ddH2O.
10. MAB-T and 2 % Roche blocking reagent: Add 2 mg Roche blocking reagent powder in 10 ml MAB-T. heat up the tube to about 60°C and invert for approximately 1 h on a rotating wheel for the reagent to dissolve. Make fresh solution for every day of use.

3.3.3.5. Mounting medium

11. For microscopic inspection of fluorescently labelled specimens we preferentially mount the brains in Vectashield (Vector Laboratories), which is a marketed medium with fluorescence preserving properties. It is very important to choose a mounting medium corresponding to immersion media used later during microscopy. The refraction indices of mounting and immersion medium need to be as similar as possible. Clearing media like RapiClear (SunJin, Taiwan) enhance the penetration of tissues and resolution by confocal microscopy but do not preserve the fluorescence as well (see **NOTE 2**).

3.3.4. METHODS

3.3.4.1. Planning experiments

3.3.4.1.1. Choosing suitable antibodies

We normally design our experiments in the way that we use a general axonal marker such as antibodies against acetylated Tubulin (mouse, Sigma) (figure 3.3–1A) or synapsin (mouse, DHSB Hybridoma Bank) (figure 3.3–1B) in combination with a more specific antigen of interest, which may only stain a small subset of neurons (figure 3.3–1C). To stain against endogenous GFP expression present in transgenic lines, we use a GFP antibody (rabbit, Invitrogen or chicken, Abcam) (figure 3.3–1E). We use synapsin and anti-acetylated Tubulin produced in mice, so that the other primary antibody used on the same specimen must come from a different host species. If that is not the case, alternative cross-reactive neural markers are commercially available. Another possibility to stain the nervous system is to use primary conjugated Phalloidin (binding to F-actin) (see figure 3.3–1D and see below for notes on Phalloidin stainings). Secondary antibodies must be chosen based on the host species of the primary antibodies and on the available imaging setup.

3.3.4.1.2. Probes for RNA *in situ* hybridization

In our experience probes of a length of about 800 bp to 1.2 kb work well in *in situ* hybridizations on brains. We follow standard protocols for probe synthesis using the Roche RNA labelling kit. For one-colour *in situs*, we normally work with probes that are DIG labelled, but Fluorescein labelled probes also work well.

3.3.4.1.3. Considerations on material preparation before starting

Dissecting brains from adults and larvae of *Tribolium* is not difficult but may require a bit of practice and is time consuming if large numbers of brains are required. After fixation, brains that are destined for RNA *in situ* hybridization need to be dehydrated and stored in methanol for at least one night (or long term) before proceeding with the staining protocol. We recommend to also dehydrate the brains that are used for immunohistochemistry. We noticed that for example the antibody against synapsin that we use as a default neural marker works better after methanol storage and rehydration.

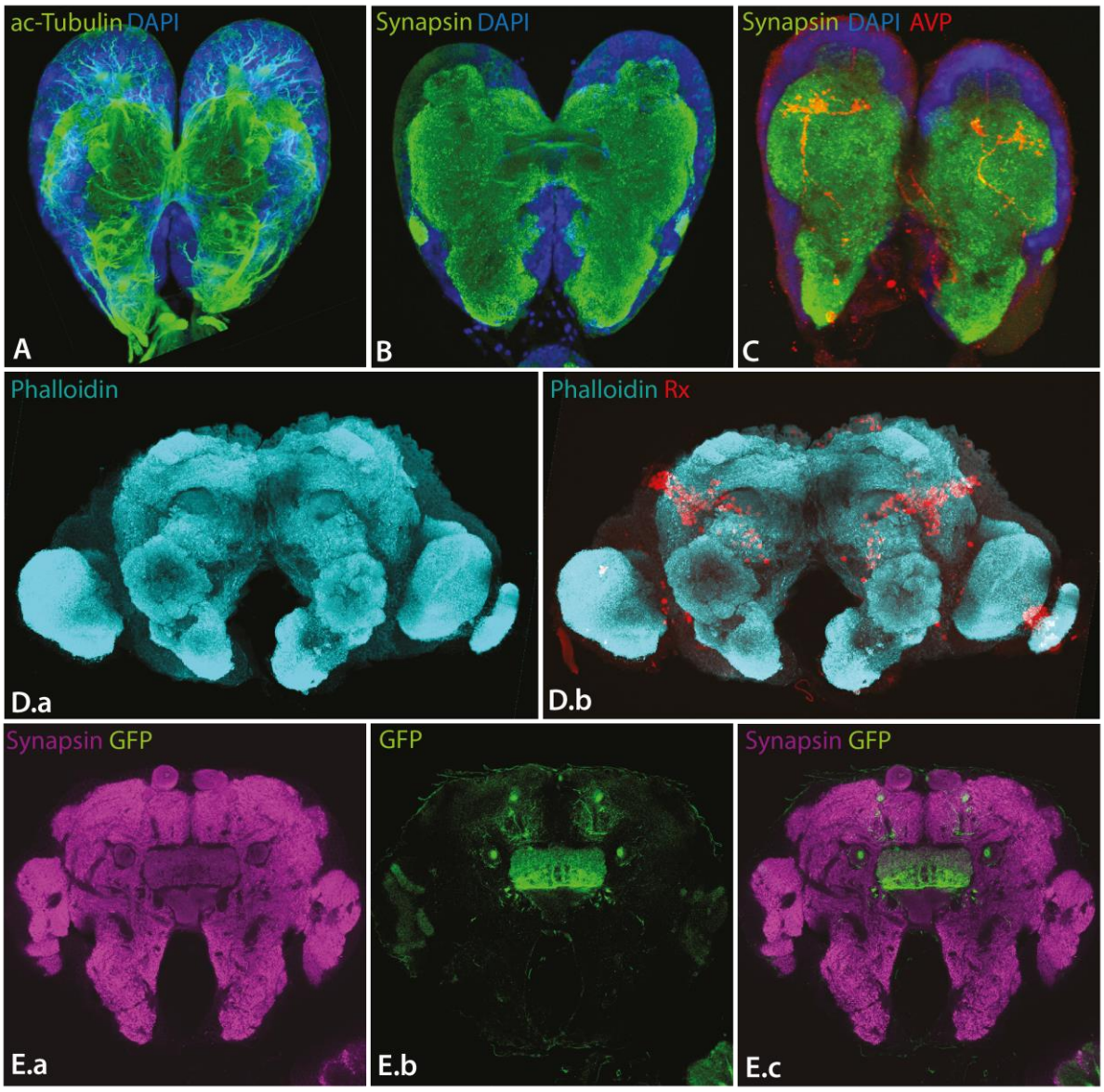

Figure 3.3–1: Immunohistochemistry in larval and adult brains. Z-projections of confocal microscopy image stacks. **A)** A larval brain is labelled with an anti-acetylated-Tubulin antibody. This type of staining often suffers from poor depth penetration, but nervous connections and cell borders in the periphery are well stained. **B)** Larval brain labelled with anti-synapsin. The neuropil of the brain is labelled. Staining with this marker works very robustly and with good depth penetration. No single neuron can be distinguished. **C)** An antibody against AVP (a neuropeptide) stains single branching neurons in each brain half. **D)** Adult brain stained with Phalloidin (an F-actin label) and an antibody raised against Rx-protein. Phalloidin can be used as neural marker on specimens that were not dehydrated in methanol. **E)** Adult brain from a transgenic line carrying a GFP reporter upstream of the *rx* gene coding sequence, labelled with a combination of anti-synapsin for brain morphology and an antibody against GFP.

3.3.4.2. Dissections and fixation (1 day)

3.3.4.2.1. Larval brains dissection

If larvae are kept on white flour, they are best separated from the flour with a 300 µm sieve. Larvae kept on full grain flour have to be picked one by one using forceps or a fine wet paintbrush.

1. Place a 10 ml falcon with PBT on ice and wait for it to cool down. Also put a 1.5 ml centrifuge tube with the fixation solution and three black glass dishes on ice (see figure 3.3–2A). Fill dishes with ice-cold PBT.
2. Now place a tube with larvae on ice (figure 3.3–2A). After a few minutes the larvae become immobile and can be picked up with forceps or a fine wet paintbrush.
3. Take the whole larvae through 1-3 rinsing steps in ice cold PBT to get rid of flour and dirt.
4. Now place one of the cold dishes with PBT under a dissection microscope and transfer the larvae into it one at a time.
5. Using a black dish (figure 3.3–2A) is recommended to best see the white brains (figure 3.3–2C). If that is not available, place a transparent dish on a black background.
6. To dissect brains, use two extra-fine and sharp Dumont No. 5 tweezers for the dissections.
7. Place one pair of tweezers at the level of the last pair of walking legs, vertical to the longitudinal axis (figure 3.3–2B). Now apply firm pressure and cut along the edge with the second pair of tweezers to separate the anterior part of the larvae from the remaining body with a clean cut.
8. Remove the trunk from the dish to keep the buffer clean.
9. Now hold the head of the larva between one pair of tweezers without squashing it and gently knock against the anterior head capsule with the second pair. This will make the contents of the anterior body come out (mainly anterior gut, some glandular tissue and the nervous system).
10. Once you have identified the brain among these tissues (see figure 3.3–2C), gently remove any additional tissues that may be attached to it.
11. Now push the freed brain to a location with clean buffer and suck it up with a pipette fitted with a 1 ml blue tip.
12. Directly transfer the brain into the fixation solution with the pipette. Try to transfer as little dissection buffer as possible into the tube for fixation.

13. We allow maximal 45 minutes for a batch of brains to be dissected and fixed together in one tube to not extend the time of fixation for too long.

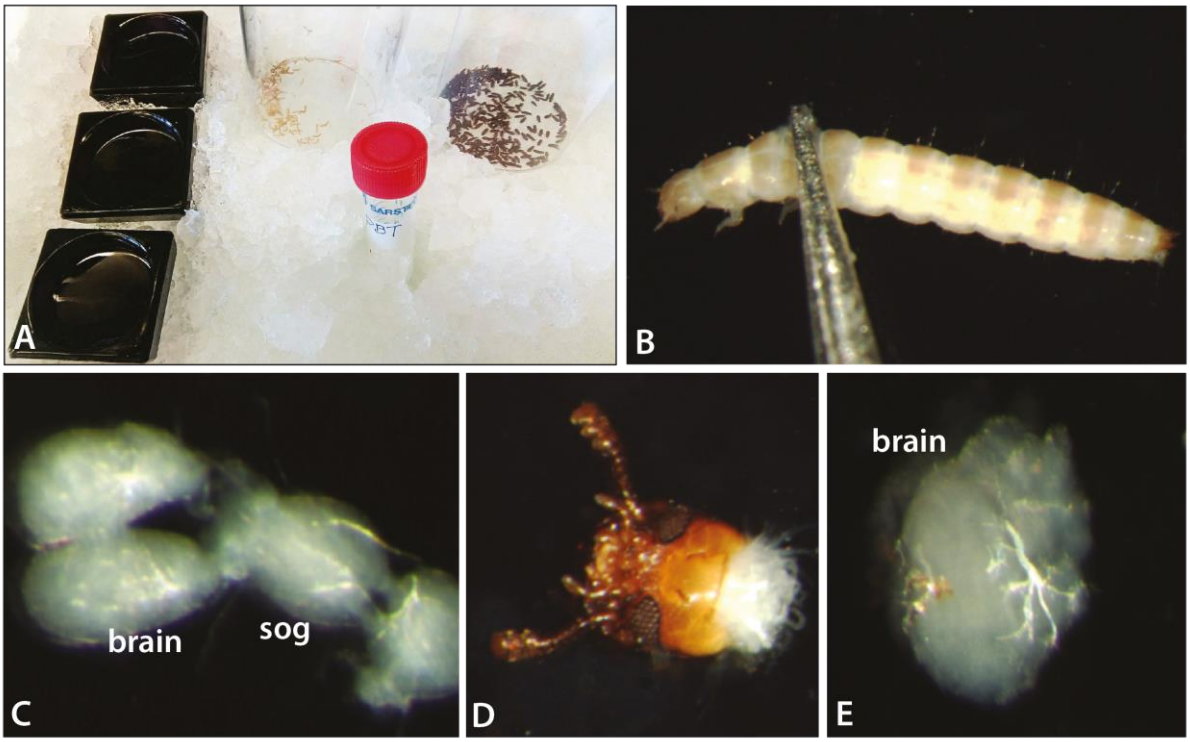

Figure 3.3–2: Dissection of larval and adult brains. A) Black dissection dishes are placed on ice to cool down, together with larvae (left vial) and adult beetles (right vial). After few minutes on ice the beetles become immobile and can be transferred into a dissection dish with ice cold PBT and placed under a dissection microscope. **B)** Larvae are held with one pair of sharp forceps at the level of the third legs. Use a second pair of tweezers (not shown) to cut along the edge of the first pair to remove the trunk of the larvae. Now the nervous system can be pushed out by holding the head and knocking against it with tweezers. **C)** The anterior nervous system (brain and suboesophageal ganglion (sog)) as seen on a black background through a dissection microscope. **D)** An adult beetle head is cut off from the thorax with forceps and placed on the dorsal side. Place tips of tweezers on the eyes and dissect off the head capsule with a second pair. **E)** An adult brain on black background as seen through a dissection microscope.

3.3.4.2.2. Larval brains fixation and dehydration

1. After the brains are transferred into the 4 % formaldehyde solution, keep them on ice for one hour (the brains dissected first will hence be fixed up to 1 h 45 min, which in our experience is tolerable).
2. Remove the formaldehyde solution from the tube and replace by 1 ml PBT.
3. Proceed with six washing steps in PBT on ice (without agitation), including 5 minutes incubation each. Also see **NOTE 3**.
4. Take the brains through a series of increasing methanol concentrations: first take off 250 µl and add the same volume of methanol. Invert and let the brains sink. Proceed by

taking off and replacing 500 µl, 750 µl and 1000 µl. In the higher concentrations the brains will sink more slowly, allow a few minutes between the steps. Wash one additional time in 100 % methanol. Also see **NOTE 3**.

5. Place tube with brains in 100 % methanol to -20°C for short or long-time storage.

3.3.4.2.3. Adult brains dissection

1. A 1.5 ml centrifuge tube filled with 4 % formaldehyde solution (in PBT) is placed on ice and is cooled down.
2. The adult beetles are put on a plastic dish and placed on ice until the animals become immobile (figure 3.3–2A).
3. Then single specimens are picked up with forceps and transferred into a black dissection dish filled with ice cold PBT. The dish is placed under the stereomicroscope for dissection.
4. To dissect brains from the adult beetles first separated the head is from the body with a sharp cut using tweezers.
5. Place the head with the ventral site up (figure 3.3–2D). Then one pair of forceps (Dumont No. 5) is used to hold the head down by inserting it into the eyes, while another pair of forceps is used to remove the ventral cuticle of the head capsule beginning from the side close to the thorax and thus exposes the brain.
6. Then the remaining head capsule and tissues around the brain are carefully removed.
7. Once the brain is freed from all surrounding cuticle and tissues (figure 3.3–2E), it is transferred into a tube with 4 % formaldehyde solution on ice.
8. Aim to process beetle brains to be fixed in one batch within 45 min to avoid adding too much extra time to the fixation.

3.3.4.2.4. Adult brains fixation and dehydration

1. The duration of the fixation for adult brains to be used in RNA *in situ* hybridization is 2 h (plus maximal 45 min duration of the dissections, see above).
2. Washing and dehydration is carried out in the same way as with the larval brains (see 3.3.4.2.2). Also see **NOTE 3**.

3.3.4.3. Immunostaining of brains using a cell specific antigen in combination with a ubiquitous neural marker

For immunostaining of larval brains use the following protocol. Adult brains are processed in the same way as larval brains, the only difference is that many antibodies need significantly longer incubation times. For example, staining an adult brain with the synaptic marker anti-synapsin worked best when incubated for 72 h, with an addition of 0.3 % Triton to the medium. Incubation of the secondary (anti-mouse-A555, anti-rabbit-A488, etc.) works well at 4-8°C overnight, or up to 48 h. Also see **NOTE 4, 5, 6, 7** and **8**.

Day 1

1. Fixed brains stored in methanol are rehydrated in a series of ascending methanol concentration.
2. First make sure that the volume of methanol in the tube with the brains is 1 ml. Remove 250 µl of the methanol and add 250 µl PBT. Invert the tube a few times and wait for the brains to sink to the bottom.
3. Remove 500 µl solution from the tube and replace by 500 µl PBT. Invert tube and let the brains sink.
4. Remove 750 µl solution and replace by 750 µl PBT. Invert and let brains sink.
5. Remove 900 µl (or as much volume as possible without sucking up any brains) and replace by the same volume of PBT. Invert and let brains sink.
6. Carry out 6 x 5 min washes in PBT.
7. Block brains for at least 1 h in PBT + 3 % BSA.
8. Dissolve the first primary antibody (normally the one against the cell specific antigen) at an appropriate concentration in PBT + 3 % BSA (see **NOTE 8**). A small volume of app. 100 µl is enough to stain a large number of brains dissected brains in a 1.5 ml tube. We stain app. 30 brains in one incubation, but this can be upscaled if required. The time required for dissection is the limiting factor to the number of brains used.
9. Remove the blocking solution and add the antibody solution.
10. Incubate in the antibody for 3-4 h at room temperature or overnight at 4-8°C.

Day 2

11. Remove solution with the primary antibody and replace by one 1 ml PBT.
12. Proceed with 4 x 20 min washes in PBT.
13. Block for 1 h in PBT + 3 % BSA.

14. Dissolve second primary antibody (normally a neural marker, e.g. anti-synapsin from mouse) in PBT + 3 % BSA at an appropriate solution (1:40 v/v for anti-synapsin serum).
15. Incubate the antibody at 4-8°C overnight.

Also see **NOTE 8** and **9**.

Day 3

16. Remove primary antibody solution and replace by 1 ml PBT.
17. Perform 4 x 20 min washes in PBT.
18. Block for 1 h in PBT + 3 % BSA.
19. Dissolve appropriate secondary antibodies against your primary markers in one solution (in PBT); use a concentration of 1:500 v/v of each. Use alternatively labelled secondary antibodies, e.g. anti-rabbit-A488 in combination with anti-mouse-A555, depending on the primary antibodies used and on your imaging setup.
20. Remove blocking solution and replace by antibody solution. Incubate at 4-8°C overnight.

Day 4

21. Final washing steps and DAPI staining.
22. Remove secondary antibody solution and replace by 1 ml PBT.
23. Include DAPI 1:1000 v/v of stock solution in PBT in your first washing step (20 min).
24. Perform 4 x 20 min washes in PBT.
25. Now the staining is complete. Proceed to mounting (see 3.3.4.6) on the same day. Stained specimens can be stored in PBT at 4°C for few days, but are ideally mounted soon after completion of the staining protocol.

3.3.4.4. Phalloidin staining of larvae and adult brains

1. Brains fixed for 1 h (larvae) or 2 h (adults) are washed in PBT (6x) after fixation. They are not dehydrated but directly taken through the staining process.
2. If Phalloidin staining is combined with a specific antibody, the brains should first be taken through the antibody staining protocol (steps described under 3.3.4.3, day 1 and 3) using only one primary and one suitable secondary secondary).
3. A Phalloidin staining solution with a concentration of 1:40 - 1:100 v/v is prepared in PBT (use 0.3 % Triton for adult brains, and see **NOTE 10**).

4. Following the washing steps after fixation (or after incubation of the secondary antibody) as much PBT as possible is removed and the Phalloidin staining solution is added to the tube with the brains.
5. Incubate at 4-8°C overnight. Alternatively, combine the Phalloidin incubation with the over-night incubation of the secondary antibody.
6. Wash 4 x 20 min, include DAPI 1:1000 v/v in one of the first washing steps if desired.

3.3.4.5. Fluorescent RNA *in situ* hybridization (ISH) followed by antibody labelling of the axonal scaffold

The protocol for fluorescent ISH followed by antibody labelling (see figure 3.3–3) is the same for larval and adult brains, with exception of different fixation times. Also, as outlined above, staining of the axonal scaffold with anti-synapsin (figure 3.3–3C) requires a longer incubation time of app. 72 h (see **NOTES 5 and 7**).

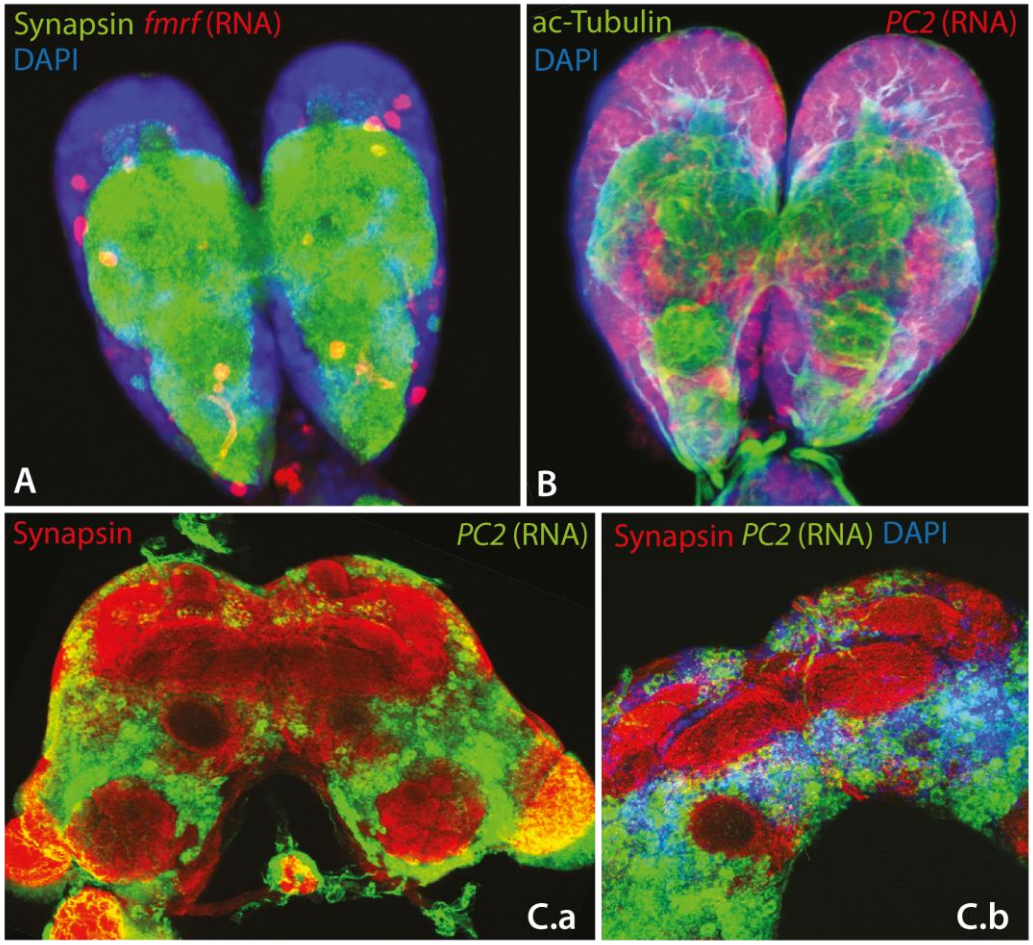

Figure 3.3–3: Fluorescent RNA *in situ* hybridization on larval and adult beetle brains. Z-projections of confocal microscopy image stacks. **A)** Larval brain stained against synapsin and *in situ* labelled against *fmfr*, a gene encoding neuropeptides that is expressed in few individual cells of the brain. **B)** Larval brain stained with the neural

marker anti-ac.-Tubulin and against RNA of *PC2*, a neural protein convertase. **C)** Adult brain stained against synapsin and *PC2*-RNA that is expressed in many of the brain neurons. C.b shows an enlarged substack of C.a, focusing on the central brain. The combination with DAPI staining of nuclei shows that many but not all brain neurons are *in situ* stained, reflecting differential expression of the gene.

Day 1

1. Rehydrate brains stored in methanol through a series of increasing PBT concentration as described above (3.3.4.3, steps 1-5).
2. Wash 4 x 5 min in PBT.
3. Prepare a 4 % formaldehyde solution in PBT.
4. Postfix the brains for 15 minutes in 4 % formaldehyde.
5. Remove fixation solution and perform 6 x 5 min washes in PBT.
6. For prehybridization take off the larger part of the PBT in the tube with the sample, only leaving 250 µl. Add 250 µl Hybe-BT buffer (so that the ratio of Hybe-BT: PBT is 1:1).
7. Mix gently and let brains sink.
8. Take off the solution and replace by 500 µl Hybe-BT.
9. Incubate for 10 min, mix gently after 5 min and let the brains sink.
10. Remove Hybe-BT and replace by 500 µl Hybe-AT.
11. Incubate for 1 h at 65°C.
12. While specimens are taken through the pre-hybridization step, dilute probes in 30 µl of Hybe-AT (typically 1 µl probe/ 30 µl Hybe-AT but see NOTE 11).
13. Heat probes to 95°C for 2 min on a heat block or in a water bath to remove potential secondary structures.
14. Put on ice for 1 min, then pre-warm to 65°C in the incubator.
15. After the 1 h pre-hybridization step, aspirate as much of the Hybe-AT from the tube as possible.
16. Add probe dilution to the brains and incubate overnight at 65°C.

Day 2

17. Pre-warm PBT and Hybe-BT for the washing steps to 65°C.
18. Add 500 µl Hybe-BT to the samples, keep at 65°C until specimens settle down.
19. Take off solution and replace by 500 µl Hybe-BT, let specimens sink.
20. Take off solution and replace by 500 µl fresh Hybe-BT, incubate for 15 min.
21. Add 500 µl PBT to the sample (so that PBT: Hybe-BT ratio is 1:1). Keep at 65°C until brains settle down.

22. Perform one more wash in PBT at 65°C (15 min).
23. Now proceed at room temperature. Perform 3 x 15 min washes in PBT.
24. Replace PBT by MAB-T and incubate for 15 min.
25. Prepare blocking solution by dissolving Roche blocking reagent in MAB-T (2 % w/v).
26. Replace MAB-T buffer in the tube with the specimens by the blocking solution and incubate for 1 h.
27. Prepare antibody solution by dissolving an anti-DIG-peroxidase (POD) antibody (see note below) 1:2000 v/v in the MAB-T-blocking solution. Also see NOTE 12 for antibodies used for *in situ*.
28. Remove blocking solution from the brains and replace by the antibody solution.
29. Incubate overnight at 4-8°C.

Day 3

Fluorescent labelling reaction: An enzymatic labelling reaction is used to fluorescently visualize gene expression (figure 3.3–3). We normally conduct a peroxidase dependent tyramide signal amplification (TSA) reaction (see figure 3.3–3). The preparation of the reagents is described in the accompanying protocol for embryonic *in situs* of this issue (Buescher et al., in press). Alternatively, a commercial TSA-kit can be used (e.g. Perkin Elmer). Instructions below are based on the use of self-made reagents, if you are using a kit, follow instructions given in the manual. See **NOTE 13** for alternatively performing a Fast Red reaction and see **NOTE 14** on performing two-colour *in situ* hybridization (figure 3.3–4C).

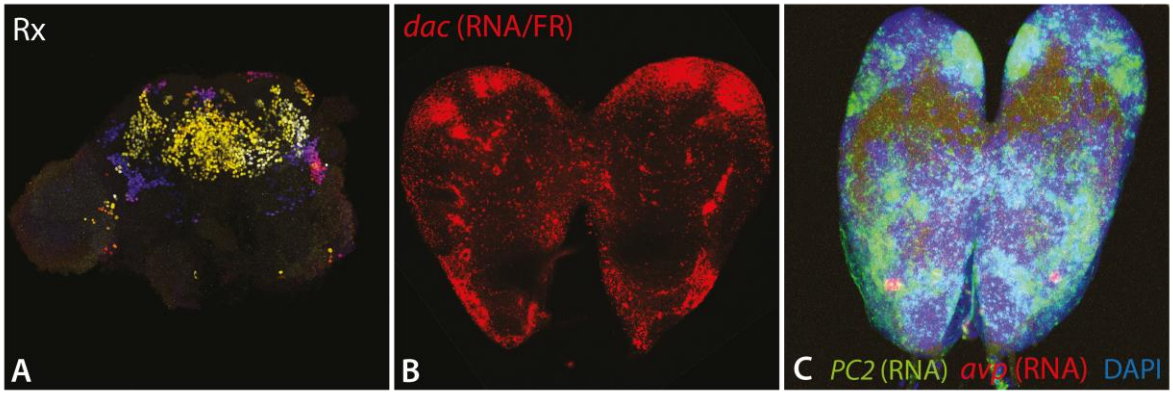

Figure 3.3–4: Potential modifications to our recommended standard protocol. Z-projections of confocal microscopy image stacks. **A)** Adult brain treated with clearing medium prior to imaging. Shown is a color-coded projection of a Z-stack created with FIJI (Schindelin et al., 2012). **B)** Larval brain hybridized with a *dachshund* (*dac*) RNA probe and stained with Fast Red. Expression is predominantly seen in the cells associated with the mushroom bodies. **C)** Larval brain taken through double *in situ* hybridization against *PC2* and *avp* (which is only expressed in one single cell in each brain half) using TSA reactions with different colour reactions (A488 and A555). The staining

that is carried out first (here: PC2) often suffers from reduced intensity, likely caused by the acidic treatment for enzyme inactivation.

30. Remove antibody solution from the specimens and replace by 1 ml MAB-T. Let brains sink and exchange solution against fresh MAB-T.
31. Perform 3 x 1 h washes in MAB-T.
32. During the last washing step, prepare the TSA staining solution. Combine 250 µl MAB-T with 2.5 µl 4-iodophenol (of the 100x stock), 2.5 µl of a 0.3 % H_2O_2 solution (final concentration of H_2O_2 in the staining solution is 0,003 %) and 1 µl of the tyramide conjugate -555 (red) or -488 (green). Keep in the dark.
33. Remove MAB-T and add the staining solution to the brains, keep in the dark for 30 min.
34. Remove staining solution and add 1 ml MAB-T. Let brains sink and exchange solution one more time.
35. Exchange MAB-T by 1 ml PBT. Perform 2 x 20 min washes in PBT. If no further antibody labelling is conducted, a nuclear staining using DAPI (1:1000 v/v) can be included in the first wash and the specimens can be mounted subsequently (see 3.3.4.6).
36. If the brain neurons are to be immunolabelled, proceed with the blocking step and with subsequent primary antibody incubation (anti-synapsin: figure 3.3–3A, 3.3–3C; anti-ac.-Tubulin: figure 3.3–3B) of the IHC protocol 3.3.4.3.

3.3.4.6. Mounting for fluorescence- or confocal microscopy.

To mount stained larval and adult brains place a microscope slide under a dissection microscope and add a drop of mounting medium (see materials and also see **NOTE 2**) on the slide. Now, with a pipette, transfer a single brain into the drop with as little solution as possible. Use fine tweezers or similar tools to layout the brain flat and to remove all dirt or attached tissues. Now prepare a cover slip (18 x 18 mm or 22 x 22 mm) with small plasticine feet on the edges and gently lower it on the medium. Apply as much pressure on the slide as required for the brain to lie flat but be careful not to squeeze it. Alternatively, transparent, ring-shaped stickers can be used to create a more standardized distance between slide and cover slip. Add transparent nail polish over the corners of the cover slip to fix it to the slide. Proceed to microscopic inspection.

3.3.5. NOTES

1: Blocking for antibody stainings

As a default blocking agent, we use 3 % BSA/PBT (see Materials) prior to and during antibody incubations. It is possible to improve the blocking effect (and hence reduce background) by using serum derived from the animal that the secondary antibody was raised in if available. E.g. use goat serum as a blocking reagent for goat-anti mouse antibodies (use at 5 % for pre-incubation blocking and at 2 % during antibody incubation).

2: Use of a clearing medium

We have used RapiClear 1.47 (SunJin Lab) as a clearing medium with a refraction index suited for the immersion media we use and for the size of *Tribolium* brains. Warm the RapiClear medium to 37°C and apply to brains after removing the washing buffer beforehand. It will completely clear the brains at room temperature in 1-5 minutes with only remaining trachea visible. Diffraction of light through the white tissue is strongly reduced, increasing the signal to noise ratio. There is no need for linear Z compensation, even in thick adult brains (see figure 3.3–4A). You will notice an increase in the visibility of cell projections. however, we find that repeated imaging of the same specimen quickly decreases signal intensity, hinting that the anti-fade properties of RapiClear are not as strong as of Vectashield and other fluorescence preserving media.

3: Check discarded buffer

During all washing steps, make sure that the brains sink to the bottom of the tube before you change the solution. Pipette every solution that you take off from the tube into a black dish and check under a dissection microscope that no brain has been sucked up. If a brain is seen in the dish, transfer it back into the tube. The brains sink relatively well in aqueous solution, but tend to float more in the methanol containing solutions used for dehydration and in the hybridization, buffers used during the RNA *in situ* protocol.

4: Avoid intense agitation during washing steps

Dissected brains, especially from larvae, are small and fragile. Therefore, we avoid too much agitation of the sample and do not use rotating wheel shakers, which can cause the brain to get stuck to the lid of the tubes. If available, use a horizontal shaker at a low speed, but we regularly perform the washing steps without agitation and just slightly shake the tubes by hand from time to time.

5: Antibody incubation

Antibody penetration into adult brains may sometimes be difficult and some antibodies work better with a milder fixation (40 minutes in 4 % formaldehyde). Another mean to improve permeability in adult brains is to increase the proportion of Triton in the PTB used for all steps from 0.1 % to up to 0.3 %.

6: Brains used for Phalloidin staining

These brains are fixed for 1 h in a 4 % methanol-free formaldehyde solution. Use PBT with 0.3 % Triton for subsequent washing steps. Do not dehydrate the brains but directly proceed to the staining reaction.

7: Timing of the antibody staining

We have lined out the protocol here in a way that primary and secondary antibodies are incubated overnight in cold conditions. This is however flexible and has to be optimized for each antibody combination. Some primary antibodies work well when incubated only for a few hours at room temperature, while others may need significantly longer. hence, the protocol given here spans several days, but the workload on each day is relatively low.

8: Concentrations of primary antibodies

The concentration depends on the specific antibody and is either defined by prior experience or trial and error. Monoclonals are normally efficient at lower concentrations than polyclonals. The antibodies that we often use and that are commercially available are used at the following concentrations (v/v): mouse anti-ac.-Tubulin (Sigma) 1:50, mouse anti-synapsin (DHSB Hybridoma Bank) 1:40, rabbit anti-AVP (Calbiochem) 1:200 and chicken anti-GFP (Abcam) 1:1000.

9: Combining primary antibodies in one incubation

When using a specific combination of antibody labelling for the first time we normally incubate both primary antibodies sequentially as described. After this many antibody solutions can also be re-used multiple times. With many combinations it is possible to incubate both primaries in one solution, but this has to be tried out for each individual reaction.

10: Phalloidin

Phalloidin is available from different suppliers with different primary fluorescent labels. We successfully used green Phalloidin (A488 conjugated, life technologies) and the red Phalloidin (A568, from Thermofisher Scientific). The stock solution is prepared according to the supplier's instructions. We are getting good results by using a concentration of 1:40 v/v (Phalloidin stock/PBT) for adult brains and 1:100 v/v for larval brains.

11: RNA probe concentration

We adjust our probes to a concentration of 100 ng/µl and start using 1 µl in 30 µl hybridization buffer. After the first reaction this concentration can be adjusted for each individual probe depending on signal strength and signal to background ratio. We use concentrations ranging from 0.1 µl to 2 µl in 30 µl reactions.

12: Antibodies used in *in situ* hybridization

The choice of antibody used in the *in situ* hybridization depends on the label of the RNA probe (DIG; Fluorescein; etc.) and on the type of colour-producing reaction that is used for visualization. We use anti-DIG-POD (Roche) for TSA reactions and anti-DIG-AP (Roche) antibodies for Fast Red reactions (see **NOTE 13** below).

13: Using Fast Red as an alternative dye for RNA visualization

An alkaline phosphatase dependent Fast Red reaction, producing a red fluorescent signal can be used as an alternative to TSA (see figure 3.3–4B). The Fast Red staining can also be seen under a stereomicroscope without fluorescence light setup. It has been reported that Fast Red labelling works in species where a TSA reaction does not produce any result, suggesting it may be more robust or more sensitive. however, because it takes significantly longer than TSA and is prone to produce unspecific staining in surface tissues and general background, it is not our preferred staining reaction and we have so far not established protocols to combine it with antibody labelling. Data from other species does however suggest, that a combinatorial stain is well possible (Hunnekuhl and Akam, 2014).

To perform a Fast Red reaction on your specimens under point 3.3.4.5 you have to use an alkaline phosphatase coupled antibody against your probe label (e.g.: anti-DIG-AP, Roche). Following antibody incubation proceed with the following steps:

37. Remove antibody solution from the specimens and replace by 1 ml PBT. Let brains sink and exchange solution against fresh PBT.

38. Perform 3x 1 h washes in PBT.
39. Remove PBT and replace by 1 ml 0.1 M Tris-HCl (incl. 0.1 % Triton, pH 8.2).
40. Exchange Tris-HCl solution three more times.
41. While the embryos are washing, prepare the Fast Red staining solution by dissolving 1 Fast Red tablet (Roche) in 2 ml 0.1 M Tris-HCl (incl. 0.1 % Triton, pH 8.2). Spin down the solution at 15.000 rpm for 2 min, transfer supernatant into a fresh tube and discard pellet. Note that the Fast Red chemicals age over time such that stock solutions cannot be kept for long time. Prepare staining solutions freshly on the day of use.
42. To start the staining reaction remove Tris-HCl buffer from the brains and add sufficient amount of the staining solution.
43. Keep in the dark, but periodically monitor the reaction under a dissection microscope. It may take several hours for the staining to develop. If necessary, it can be put to 4°C overnight and development can be continued the following day. Exchange staining solution if very long reaction times are required.
44. When the staining is developed, stop reaction by 3 x 5 minutes in PBT.
45. Use DAPI for 20 min (1:1000 v/v in PBT), wash 3 x 5 min and proceed to mounting for microscopic inspection.

14: Two-colour *in situ* hybridization

It is possible to perform two-colour *in situ* hybridization using two RNA probes with different labels (e.g. DIG and Fluorescein). Incubate both probes together (under 3.3.4.5) and then first use an anti-DIG-POD antibody. Perform a first TSA staining reaction using a green substrate (A488). After this the POD conjugate of the antibody needs to be deactivated by acidic treatment (e.g. 3 x 5 min washes in 0.1 M glycine, pH 2.2). After washing in PBT, incubate a second anti-Fluorescein-POD antibody overnight. Carry out a second TSA reaction using a red dye (A555).

However, when performing two-colour *in situ* labelling on brains we experience problems with the intensity and quality of the stains (see figure 3.3–4C) and the protocols to perform this in *Tribolium* brains still requires improvement.

15: Poor signal in antibody staining

A poor signal in antibody staining can often be improved by adjusting time and concentration of the primary antibodies used. This is mostly done by trial and error. Some of the antibodies we use are incubated up to three days at 4°C, and with an increased concentration of Triton (0.3 %) in the incubation buffer.

Another mean to increase antibody penetration is by digesting specimens with proteinase K, trypsin, or mercaptoethanol containing reductive buffers. We do not normally perform such digestions on dissected brains as they are likely to have an impact on the tissues and cells, but protocols are widely available in the literature if required (Bodies et al., 2014; Hunnekuhl and Akam, 2014; Schinko et al., 2009; Yoshida-Noro et al., 2000).

16: Poor signal in RNA *in situ* hybridization

A weak signal in *in situ* staining can be due to low expression levels of the gene or to poor probe penetration. If you suspect that the gene of interest is only weakly expressed, design a probe that covers as much of the open reading frame and untranslated regions as possible. It is also possible to design two or more non-overlapping probes against the same gene and mix them prior to hybridization. Long probes can be digested to smaller fragments in carbonate buffer (80 mM $NaHCO_3$, 120 mM Na_2CO_3) at 65°C for improved penetration (Dearden and Akam, 2001). Add required volume of probe to 30 µl carbonate buffer and incubate at 65°C for 5-10 min. To stop the reaction, remove carbonate buffer and add 30 µl Hybe-AT. Proceed with probe incubation (step 13, 3.3.4.5, day 1).

4. Discussion

4.1. Implications of presented work

4.1.1. Implications for central complex development and evolution

Manuscript 1 provides the first detailed account of heterochrony in central complex development between *Tribolium* and *Drosophila*. As such, the analysis is starting point for a multitude of questions (see below). The most unexpected finding was the precocious gain of functionality of the larval central body that results in an immature developmental form of the central body. This form does not equal an adult form and hence, calls the current view into question that a fully formed adult-like upper division of the central body is present in larvae of some species. Further, this finding raises questions about the behavioural links and anatomy of said structure, to be answered in future studies. Moreover, central complex heterochrony not only consists of several shifts, but also a change in sequence of an otherwise conserved order.

4.1.2. Implications for studies in brain evolution and development

With this work I introduce genetic neural lineages as tools to generate insights into brain development and evolution (manuscript 1). Constructing transgenic lines that mark such lineages in *Tribolium* has been described in manuscript 2. Manuscript 3 has provided additional methods to perform staining techniques at several stages of development in *Tribolium* and allows data on brain development to be generated in the future. With these contributions, we first provide a method of lineage marking that is relatively easy to transfer to additional species, in contrast to other methods used (see Introduction). Therefore, multi-species comparisons on the level of cell development can be performed in the future. Second, we provide tools that further establish *Tribolium castaneum* as a neurobiological model organism (see Koniszewski et al., 2016 for additional tools) providing an alternative model system beside *Drosophila* that allows to study central complex development in a less derived species (Koniszewski et al., 2016).

In the following, I will illustrate further points that can be answered, with emphasis on the question of central complex heterochrony. Further questions that warrant answering from manuscripts 2 and 3 can be found in this segment as well.

4.2. Open questions on the *Drosophila – Tribolium* comparison

4.2.1. Is the definition of homologous cells by similar morphology and single gene expression sufficient?

We have based our homology statement in manuscript 1 on the morphological similarity of central complex neurons of DM1-4 lineages and their shared expression of *rx*. We concluded that, in the framework of the overall homologous central complex, observed similarities of these cell groups strongly indicate homology. Moreover, the conserved nature of DM1-4 neural lineages in insect brains corroborated homology (e.g. Boyan et al. 2017).

Previous comparisons between highly divergent animal clades used morphological similarity of cells as basis for subsequent testing of homology by shared gene expression. For example, Wolff and Strausfeld (2016; 2015) have identified shared morphological commonalities between arthropod mushroom bodies, invertebrate brain centres and vertebrate hippocampus by a shared set of morphological characters and shared expression of a set of proteins. Similarly, Strausfeld and Hirth (2013a) identified a correspondence of vertebrate basal ganglia and the insect central complex by using morphological criteria, shared gene expression and neuromodulator content. Neuromodulators (i.e. neurotransmitters and – peptides) are highly conserved in some cases (Katz and Lillvis, 2014) and have been used to identify corresponding morphological domains (Homberg et al., 2018). Moreover, they often maintain their cellular localisation through development, as is the case for several neuromodulators in the developing *Schistocerca* central complex (Herbert et al., 2010). In some cases, however, they can also deviate strongly between species as is the case for nitric oxide (Rabinovich et al., 2016).

Although we approach homology in a similar way to previous accounts, we deviate in two aspects from these descriptions (Arendt, 2005; Strausfeld and Hirth, 2013a; Thoen et al., 2017; Wolff and Strausfeld, 2016; 2015). First, we use only one gene to determine genetically based homology. However, the use of one gene to identify homology can be problematic (Arendt, 2005; Janssen, 2017; Scholtz, 2001). Genes such as *engrailed* are not only part of a conserved gene network but also expressed in other regions that might not be homologous. This is, however, a specific issue of identifying homologous structures in early development, as their regions of distinct adult anatomical structures might still overlap. We determine shared *rx* expression in the brain, however. Moreover, adding a second gene to our strategy would result in considerable additional efforts to be made, as our strategy is based on gene-specific transgenic lines. Hence, a possibility to further verify homology would be to construct an additional transgenic line marking expression of a second gene, with a different fluorescent protein as marker. These transgenic lines

would first need to be generated, then crossed, potentially leading to fitness effects, and hence, additional effort would need to be considered for such steps.

Second, we refrained from using neuromodulator expression as an identifier of homologous cells. Pfeiffer and Homberg (2014) have reviewed the use of neuromodulators for certain cell groups of the central complex in various species. Their summarizing table highlights that some neuromodulators are expressed in highly different structures in some animals. Hence, while some neuromodulators (such as GABA, Homberg et al., 2018; or Serotonin, Katz and Harris-Warrick, 1999) are conserved, others are not, e.g. Octopamine (Pfeiffer and Homberg, 2014). Moreover, our observation was that most neuromodulators do not mark the cell body of expressing neurons sufficiently (Koniszewski et al., 2016). Hence, they are useful to determine anatomical correspondences (e.g. Strausfeld and Hirth, 2013a), but not cell body groups. In that sense, in manuscript 1 we proposed to use GABA staining to confirm that the larval central body of *Tribolium* does not contain characteristics of a lower division of the central body on the gross level (Homberg et al., 2018).

To conclude, we used several criteria to determine homologous cell groups, but determining homology remains a critical issue for these kinds of studies.

4.2.2. Is a comparison of two distant species useful in evolutionary research?

In manuscript 1 we compared the development of the central complex between two distant holometabolous species which shared a common ancestor approximately 300 million years ago (Misof et al., 2014). Important insights into brain morphology have been made by comparison of species even within the same genus (Keesey et al., 2019) or order (Kollmann et al., 2016). We have opted for a comparison between orders of insects, i.e. Coleoptera and Diptera, because the divergence of central complex timing was thought to be pronounced between the two species (Koniszewski et al., 2016). This difference was the desired model to investigate how heterochrony in general is achieved on a cellular level.

It is possible that differences in central complex heterochrony are also present in more closely related species, as Panov (1959) has indicated, for example, that some Coleopteran species have a larval central body while others have not. A comparison of these species within one order can be used to further study the variation in central complex development. However, the level of detail that is achievable is the important criterion for such experiments. Only a few species are genetically amenable (Chen et al., 2016). While we claim that CRISPR/Cas9 makes genetic amenability relatively easy to achieve (through its adaptability, e.g. loss-of-function, gain-of-function, knock-ins; Gratz et al., 2013; manuscript 1 and 2), it would still require several preceding

experiments of transgenic line construction that require a lot of time. Moreover, micro-injection of eggs and multi-generational rearing are prerequisites for every species to construct transgenic lines analogously usable for genetic neural lineage marking (manuscript 1 and 2). For example, multi-generational rearing is hardly possible in *Heliconius* butterflies, limiting CRISPR/Cas use to mosaically modified animals (S.H. Montgomery, personal communication). Therefore, drawbacks for some species are whether CRISPR-mediated transgenesis is possible, while for all species time required for transgenic lines and possibly establishing CRISPR techniques can be a significant drawback. This means that an *ad hoc* comparison of central complex development and evolution in e.g. several Coleopteran species is only possible on the level of basic immunohistochemical staining, but less so on the level of genetic neural lineages marked through specific transgenic lines. I propose to perform such experiments as well, because such data can identify the degree of variability regarding central complex development and brain evolution between more closely related species, and more orders of insects. Hence, a more descriptive comparison in many species compared with deeper genetic and cellular analysis in few genetically tractable model organisms appears to be a fruitful mix of approaches.

Nevertheless, one hemimetabolous insect as outgroup for comparative functional studies is badly missing. One of the best choices, *Gryllus bimaculatus* where CRIPSR has been used before (Watanabe et al., 2017), would help to answer questions on the previously illustrated third mode of central complex developmental timing, i.e. complete embryonic development (Koniszewski et al., 2016). We discuss the possibility that *Tribolium* shows a derived mode of sequence heterochrony in central complex development that causes precocious presence of a functional central body, while *Schistocerca* and *Drosophila* might show a more ancestral state of central complex development (manuscript 1). *Schistocerca* data (Boyan et al., 2017; Boyan and Liu, 2016) indicate this interpretation, but so far, the literature lacks synapsin staining and comparable time steps, which would be necessary to make firm conclusions. In *Schistocerca* some functional genetic approaches like RNAi have been used successfully (Wynant et al., 2012) and the immense amount of data on brain development would be an advantage (see e.g. Boyan and Liu, 2016). However, so far, a genome, CRISPR and thus, transgenesis are missing. Therefore, the genetically amenable *Gryllus* would be used as proxy for a hemimetabolous insect to construct a *rx* transgenic line and mark genetic neural lineages.

To deepen the level of central complex heterochrony characterisation, and thus equal efforts on other heterochronies (Fritsch et al., 2013), more species can be added, with transgenic lines for *rx* constructed. With this, the use of phylogenetic approaches with event assignment along a

phylogenetic tree or quantitative approaches can be used (both reviewed in Smith, 2001; Fritsch et al., 2013).

To summarize, the number of species included in manuscript 1 is justified by technical limitations but is also not yet enough to convincingly support all hypotheses stated. Adding one hemimetabolous functional model organism and a number of more species for descriptive purposes would be a reasonable approach to complement the picture.

4.3. Modifications of transgenic lines to expand the toolbox

We used a *rx* enhancer trap of *Tribolium* to compare to a *rx* bicistronic line in *Drosophila*. Through the more restricted marking of *rx* expression in this enhancer trap, a limited number of cells and projections could be studied. A construction of a bicistronic line in *Tribolium* – analogous to the *Drosophila rx* line – would allow to mark all *rx* expressing cells. Insights from manuscript 1 may then be expanded from a subset of lineages to the entire genetic neural lineage. Such a bicistronic line is currently generated in our lab using the methods described in manuscript 2. With it, more global analyses – particularly regarding the role of *rx*-positive cells – can be answered (see below).

Moreover, modifications of the strategy used in manuscript 1 and in detail described in manuscript 2 could be first, to remove the eye transformation marker. With this, any influence of the 3XP3 promotor can be excluded. This would also alleviate the need to use two guides. It would, however, require either loxP sites flanking the marker and Cre recombinase to excise it (e.g. see Figure 3 in Gratz et al., 2013; or analogous techniques) or exogenous guide RNAs flanking the eye transformation marker (see manuscript 2, will be attempted for the Tc-*rx* bicistronic line). Moreover, GFP could be substituted with membrane bound EGFP, potentially making identification of coexpression easier and increasing fluorescent signal through more specific localisation. Recently, membrane-bound fluorescent proteins were used in *Tribolium* (G. Bucher personal communication) – these would have to be tested for marking axons before they could be used.

4.4. Questions regarding central complex development and evolution

4.4.1. What is the functional role of *rx* in central complex development?

In manuscript 1, we have used the transcription factor *rx* only as marker of homologous cell groups. However, previous work illustrates important roles of this gene in insect brain development and other developmental processes. Rx is expressed in all bilaterians nearly exclusively in the anterior-median region of the embryo head and was therefore suitable to mark

homologous genetic neural lineages in manuscript 1 (e.g. Tosches and Arendt, 2013). In vertebrates, *rx* orthologs are mostly involved in eye development (Furukawa et al., 1997; London et al., 2009; Martinez-De Luna et al., 2011; Nelson et al., 2009; Pan et al., 2010; Strickler et al., 2002; Zilinski et al., 2004) and partially required for brain development as well (Lu et al., 2013; Mathers et al., 1997; Medina-Martinez et al., 2009). Functions in the developing eye are shared only with some invertebrates, particularly *Platynereis dumerilii* (Arendt et al., 2004; Tessmar-Raible et al., 2007), while *Drosophila* deviates to vertebrates regarding *rx* function: Davis et al. (2003) have shown that *Drosophila rx* is not required for eye but for brain development, specifically for the central complex (note, however, expression of *rx* in the developing medulla and optic lobe; Erclik et al., 2017; Suzuki and Sato, 2017, respectively). Moreover, Kraft et al. (2016) illustrate that *rx* is involved in mushroom body lineages, including roles in proliferation, further confirmed in part by a transgenic RNAi screen (Neumüller et al., 2011). Expression in the clypeo-labral domain of the insect head has been reported as well, including phenotypes of such (Davis et al., 2003; Eggert et al., 1998; Posnien et al., 2011). In contrast to such labral expression stands a lack of it in onychophorans (Janssen et al., 2017). Therefore, the wealth of data about *rx* indicates that some functions and expression regions may be conserved across bilaterians, while others might not.

Rx is involved in central complex development (de Velasco et al., 2007), confirmed through phenotypic modification of central complex structures (Davis et al., 2003; Koniszewski, 2011). Most notably, the time point of lethality of *rx* loss-of-function phenotypes corresponds with the appearance of a functional central complex neuropil. Both phenotypes, however, are not well understood. In *Tribolium*, a RNAi-mediated knockdown causes modification and midline-splitting of brain structures, marked with a transgenic line labelling neuropil-ensheathing glia. Hence, the phenotype was described by an indirect marker for *rx* and central complex modification, which lacks the resolution to really understand the origin of the phenotype (Koniszewski, 2011). In *Drosophila*, modification of the ellipsoid body has been observed in a null mutant with basic histology and a GAL4 transgenic line (not specific for *rx*) marking a small set of neurons projecting into the ellipsoid body (Davis et al., 2003). Again, phenotypic description appears not be complete, even more so, since manuscript 1 illustrates that *rx* expressing cells mark all neuropils of the central complex at least partially, with the ellipsoid body marked weaker than the other neuropils. Moreover, Erclik et al. (2017), Suzuki and Sato (2017) indicate a role of *rx* in the developing eye, possibly contradicting the main finding of Davis et al. (2003) of *rx* function in the *Drosophila* eye. Hence, more detailed analyses of the *rx* phenotype should help clarify possible contradictions and investigate the specific role for central complex development.

For *Tribolium*, a more detailed analysis might require the generation of CRISPR-mediated *rx* knockout (as described in Gilles et al., 2015; Gratz et al., 2013). For *Drosophila*, the available null mutant might be used to verify, and add, roles of *rx* in development. A useful alternative would be a T2A-GAL4 knockdown line which leads to GAL4 expression in the pattern of the endogenous gene while at the same time generating strong mutants, achieved by stalling expression of the endogenous gene through the insertion of a polyadenylation signal in the gene's intron (Lee et al., 2018; BDSC # 79247, FBti0199573). Expression of *rx* cells could thus be monitored in a *rx* mutant background.

Hence, while basic knowledge of *rx* function in insects is available, detailed descriptions of loss-of-function phenotypes would be necessary to understand the function of this gene, and to shed light on the possible differences of its function between *Drosophila* and *Tribolium*, and deviations between insects and other animal clades.

4.4.2. Why is there central complex heterochrony?

In manuscript 1 we have described the pattern of central complex heterochrony between *Drosophila* and *Tribolium* in detail. Why such heterochrony occurs can only be speculated, as causality is hard to prove in brain evolution (Northcutt, 2002), since it must involve multidisciplinary approaches including behavioural analysis. Following projects could be performed to at least contribute to answering why heterochrony arises.

Strausfeld (1999, 2012) has noted a correlation between the presence of walking legs and presence of the central body, thus indicating that the ability to move by using legs (in contrast to crawling through wave-like contractions of *Drosophila* larvae) requires a central complex neuropil. In addition, Strausfeld (2012, see figure 11.12) also correlates differences in central complex anatomy with motor repertoire. Several questions arise from these correlations and the work in manuscript 1, of which answers can help understand why heterochrony appears:

What is the motor repertoire of *Tribolium* larvae? How does it differ to *Drosophila* larvae, i.e. is it more complex, reflecting the early presence of a larval central complex and walking legs? Can *Tribolium* larvae make specific turns, i.e. shortening the stride of one side of the leg while lengthening the other? Are they able to orient their movement in a more sophisticated way than *Drosophila* larvae? Also, what can they perform in loss of function phenotypes of genes that modify the larval central body, and what does the identical mutation lead to in *Drosophila* larvae, lacking larval central complex structures? The motor (and behavioural) repertoire of an animal form with a larva-specific central complex with a low degree of decussated fibres has not been described so far, but might be compared to Diplopods (Millipedes) and Chilopods (Centipedes),

as these only contract longitudinal muscles of their body wall to move their appendages, but still have decussated midline brain structures, or even other basal arthropod groups (Boyan et al., 2015; Loesel et al., 2002; Strausfeld, 2012). Investigating the behaviour of *Tribolium* larvae in connection with the knowledge presented in manuscript 1 might modify longstanding assumptions of the role of central complex for insect behaviour and evolution. Behavioural tests of *Drosophila* (e.g. Strauss and Heisenberg, 1993) can be adapted to *Tribolium* to detect movement patterns including turns. Such tests can also be used in a loss-of-function background where the larval central body is modified or missing. *rx* knockdown might not be suitable as there are *rx*-positive cells in many neuropils of the brain and L1 larvae die early after hatching (Koniszewski, 2011). Genes with a more specific expression and phenotype in the central complex might be more suited for such experiments through which the function of the larval central body can be studied simultaneously (M. Buescher, personal communication).

In addition, larvae of holometabolous insects have walking legs in differing degree of elaboration (compare for example walking legs of the lady bird *Coccinella magnifica* with those of *Tribolium castaneum* or Lepidopterans such as *Manduca sexta*). Is this divergence also reflected in differences in larval central body anatomy? If so, this would deepen the tentative correlations described earlier. For this, brains of freshly hatched larvae of several species (e.g. ten) would be dissected and stained, possibly with a common set of antibodies, e.g. synapsin (to indicate functionality), acetylated α-Tubulin (to indicate tracts) and several neuromodulators such as GABA (Homberg et al., 2018), Serotonin (5-HT) and Tachykinin-related peptide (see Koniszewski et al., 2016). These should highlight, in the tradition of previous anatomical descriptions (Strausfeld, 2012), details of elaboration and anatomy of the central body and their correlation with complexity of leg morphology and walking behaviour.

4.5. Which genetic and cellular processes cause heterochrony?

4.5.1. Species differences in DM1-4 proliferation and quiescence during embryogenesis and larval phase

Columnar neurons, like the described Rx-positive neurons of this work, are thought to arise from type II neuroblasts of the DM1-4 lineages. Hence, these neuroblasts need to be examined regarding the question of neuroblast proliferation patterns and quiescence in the central complex. The most obvious mechanism behind central complex heterochrony would be that the lineages of DM1-4 that build this structure proliferate at different times or with different rates in *Drosophila* and *Tribolium*. DM1-4 neuroblasts (Álvarez and Díaz-Benjumea, 2018; Andrade et al., 2019; Riebli et al., 2013; Sullivan et al., 2019; Walsh and Doe, 2017) are type II neuroblasts that undergo an

amplificative proliferation pattern (Boyan and Reichert, 2011; Homem and Knoblich, 2012). They generate a series of intermediate neural progenitors producing 4-6 ganglion mother cells (GMCs) which produce 8-12 neurons (Boone and Doe, 2008; Walsh and Doe, 2017). Type I neuroblasts do not have this intermediate form, and produce a series of ganglion mother cells, that then produce postmitotic neurons (Boyan and Reichert, 2011; Homem and Knoblich, 2012). The resulting number of cells is approximately three times smaller (110 vs 450 cells, (Bello et al., 2008; Boone and Doe, 2008; Boyan and Reichert, 2011). Hence, DM1-4 undergo specific modes of proliferation. Moreover, while neuroblasts such as mushroom body neuroblasts can proliferate continuously (Ito and Hotta, 1992; Kraft et al., 2016; Kunz et al., 2012; Prokop and Technau, 1994), neuroblasts such as DM1-4 undergo a phase of quiescence in *Drosophila* that starts at the end of embryogenesis and ceases at the end of the first larval instar developmental period (Homem and Knoblich, 2012; Ito and Hotta, 1992).

While manuscript 1 shows the position of cell bodies and projection patterns, it can reveal patterns of proliferation and quiescence only indirectly, and not at all patterns of apoptosis. Do DM1-4 neuroblasts proliferate at different rates? Do they undergo quiescence in *Tribolium* like in *Drosophila* and at similar stages of development? Do they have differing apoptosis patterns? A proliferation assay and screening for apoptotic cells would answer these questions and shed light on evolutionary modifications in proliferative modes and quiescence.

A proliferation assay can be performed with tools available in both species (through cross-reacting antibodies; Koniszewski et al., 2016). Proliferation is best investigated using EdU (5-ethynyl-2'-deoxyuridine) incorporation assays (Cappella et al., 2008; similar to Poon et al., 2016; Siemanowski et al., 2015). Alternatives are antibodies against Phospho-Histone-H3 and Cyclin A or E. Phospho-Histone-H3 is known to cross react in *Tribolium* (Koniszewski et al., 2016) but it marks only a fraction of dividing cells. EdU, in contrast, can be used such that a long phase of incorporation precedes staining, thus marking all cells that divided in a set time window (e.g. Poon et al., 2016). Such an assay is currently performed in our lab for embryos and early larvae. For this, embryos of both species are micro-injected with EdU, allowed to develop further for the same amount of relative developmental time, fixed and stained for EdU and suitable genes, for instance Rx (but, see below). Subsequent imaging and quantification of EdU double-positive cells in the area of DM1-4 neuroblasts promises to reveal whether there are different patterns of proliferation in embryonic development for the entire lineages or restricted to the *rx*-positive cells. For later stages, we will perform either feeding assays or injection of larvae for both species (Poon et al., 2016). Alternatively, larval brains can be dissected and incubated for a short amount of time (Poon et al., 2016).

Apoptosis in insect brains can involve either the neuroblast, marking the end of proliferation, or offspring cells, leading to a reshaping of neuronal circuits (Pinto-Teixeira et al., 2017). Both can be detected using a cross-reacting Death Caspase-1 antibody (Kitzmann et al., 2017).

In summary, cross-reacting antibodies and EdU incorporation assays can answer questions about how heterochrony is facilitated on a cellular level.

One drawback of our *rx* imaging lines is, however, that they appear not to mark the DM1-4 neuroblasts neither in *Drosophila* nor in *Tribolium*. Hence, to determine quiescence, other markers need to be established. Even in *Drosophila*, DM1-4 neuroblasts have not been unequivocally linked to the embryonic neuroblast map by Urbach and Technau (2003b) (V. Hartenstein, personal communication), although pointed and two transgenic lines seem to be a promising start (Riebli et al., 2013). Here, DM1-4 neuroblasts have possibly been identified (line GAL4$^{14\text{-}94}$), but not linked to an embryonic expression yet. These transgenic lines might not be specific enough for clear identification in the embryo, however. Hence, how to identify DM1-4 neuroblasts, intermediate progenitors and ganglion mother cells, i.e. proliferating cell types (Homem and Knoblich, 2012), is a challenge across species. Current efforts in our lab are likely to reveal such factors, which could then be used to compare division patterns in both species. A possibility would be to combine a candidate gene with *rx* to identify DM1-4 neuroblasts. Using *rx*, DM1-4 lineages can be identified in the middle to late embryo (see manuscript 1). A staining against *rx* and an alternative gene going back from middle to late embryo into earlier stages consecutively, should then allow to see an overlap in marked cells and lineage offspring at some stage. Overlapping cells can then be followed back without Rx staining, to the start of DM1-4 neuroblast delamination.

Alternative markers that characterise type II neuroblasts generally such as *pointed*, *deadpan* and absence of staining of *asense* (He et al., 2019, Walsh and Doe, 2017) would be suitable to identify DM1-4 and answer the separate question whether type II neuroblasts exist in *Tribolium* (a question that might also be answered using mostly morphological means, see Boyan et al., 2010). However, for DM1-4 neuroblast identification, they might not be specific enough, making interpretations more difficult.

In summary, methods involving EdU proliferation assays promise to answer questions regarding the cellular cause of heterochrony between the *Drosophila* and *Tribolium* central complex neuropils. The identification of neuroblasts belonging to DM1-4 that develop the central complex, however, still requires the establishment of respective tools and markers.

4.5.2. Which genes and hormones cause heterochrony?

If the cellular mechanisms underlying heterochrony involve proliferation and apoptosis, genes that regulate these processes should be involved in the genetic mechanism of central complex heterochrony. Such genes are partially reviewed in Homem and Knoblich (2012), and include genes of the *hippo* pathway (Ding et al., 2016; Poon et al., 2016), *grainy head* (Almeida and Bray, 2005), *prospero* (Bayraktar et al., 2010; Lai and Doe, 2014), neuroblast temporal identity factors (Kang and Reichert, 2015; Maurange et al., 2008; Tsuji et al., 2008), *eyeless* (Sipe and Siegrist, 2017), the *brain tumor* gene (Bello et al., 2006), *RhoA* (Lee et al., 2000b), *DE-Cadherin* (Dumstrei et al., 2003) and genes involved in axon pruning (Schuldiner and Yaron, 2015), spindle orientation (Cabernard and Doe, 2009; Lee et al., 2006) and nitric oxide processing (Rabinovich et al., 2016). Additional genes of interest might be included in screen data (Moda et al., 2013; Reuter et al., 2003).

Besides genes, hormones are also involved in neural development, particularly insulin, juvenile hormone and ecdysone (Cayre et al., 2000, p. 200, 2005; Chell and Brand, 2010; Lee et al., 2000a; Malaterre et al., 2003; Malun et al., 2003; Sousa-Nunes et al., 2011). Juvenile hormone and ecdysone are involved in several processes of insect development, including the regulation of metamorphosis (Jindra et al., 2013; Truman and Riddiford, 2002, 1999). Since a hemimetabolous insect like *Schistocerca gregaria* develops its central complex neuropils during embryogenesis, while the holometabolous *Drosophila* and *Tribolium* develop only parts of the central complex during embryogenesis, hormones involved in metamorphosis might influence central complex heterochrony as well. Importantly, these hormones are indeed involved in neural development. For example, ecdysone receptors are required for neural remodelling (Lee et al., 2000a; Schubiger et al., 1998). Juvenile hormone is involved in development of the optic lobe (Riddiford et al., 2018, 2010), while Insulin is involved in quiescence (Sousa-Nunes et al., 2011).

All these candidates can be confirmed by loss of function approaches. For hormones, their respective receptors can be targeted by RNAi. In *Tribolium*, large scale RNAi screens have been performed (Schmitt-Engel et al., 2015). In a similar fashion, but on a smaller scale, a selection of genes and hormone receptors can be targeted at specific points during development. RNAi can be performed in the *rx* transgenic line background used in manuscript 1 to visualize the potentially shifted development. In *Drosophila*, several available libraries of transgenic tools can be used, i.e. mutant transgenic lines (Lee et al., 2018), transgenic RNAi lines (Dietzl et al., 2007) and temperature-inducible transgenic lines to knock down genes at specific time points (McGuire et al., 2004).

Upon RNAi, brains of first instar larvae and later stages can be dissected, and stained for the transgenic lines and/or structural markers such as synapsin and acetylated α-Tubulin to reveal any effects on central complex development. For example, it is possible that knockdown of genes involved in quiescence might cause premature proliferation in *Drosophila* (Ding et al., 2016), but a differing result in *Tribolium*. If quiescence occurs only in some parts of the central complex neuroblasts or not at all, a knockdown of a quiescence gene might either reveal that such genes have acquired a different function if the phenotype is not at all relatable to *Drosophila*. Alternatively, the phenotype might be comparable to *Drosophila*, but less severe. Another exemplary scenario might be that modifying the Ecdysone pathway through knockdown of its receptors results in shifted development of the central complex.

4.6. Future studies

4.6.1. What is the cell type composition of the larval central body of *Tribolium*?

Manuscript 1 revealed that *Tribolium* central complex development involves a precocious presence of a functional central body and protocerebral bridge neuropil. Both neuropils are distinct in anatomy from their adult counterpart. Various cell types have been characterized in adults but not in larval central complex neuropils. Investigating the larval central body can reveal new or larva-specific cell types or projection patterns.

While our analyses revealed unique anatomical characters of the larval central body, they did not include anatomical descriptions on a single-cell or high-resolution level that could reveal what kind of cell types occur in this structure. For example, single cell resolution can help to answer the question whether the larval central body of *Tribolium* also consists of pontine neurons (i.e. such columnar neurons that connect several columns in the upper division of the central body with each other), with specific anatomical characteristics of small undifferentiated neurons, as found in *Drosophila* (Andrade et al., 2019; manuscript 1).

There are several techniques in *Drosophila* that result in labelling of a few cells including their detailed projections. Most suited is the 'flybow' technique (Hadjieconomou et al., 2011) as it can be used in combination with the existing transgenic lines, e.g. for *rx*, that mark genetic neural lineages, to generate single cell marked clones in permanent, but *rx*-specific, fashion. The combination of less cells marked, but still retaining *rx* specificity should answer questions about cell types and decussation patterns in the larval central complex.

'Flybow' comprises previously characterised GAL4 lines that can be modified by removal of a set of up to four fluorescent proteins with Cre/LoxP recombination (Hadjieconomou et al., 2011). One of four fluorescent proteins is activated, and a subset of cells marked. Cre

recombination is efficient in *Tribolium* and an alternative CRISPR-mediated excision of loxP sites has been successfully employed (Gilles et al., 2019). For 'flybow' to work, the *rx* transgenic lines or other lines such as in He et al. (2019) need to contain the Cre recombinase and loxP sites. Such modifications can be conducted with techniques described in manuscript 1 and 2.

The application of clonal labelling might be aided by expansion microscopy. Here, tissue can be enlarged in a hydrogel and imaged with higher resolution without requiring additional microscopes beyond standard confocal microscopes (Cahoon et al., 2017; Jiang et al., 2018). This might be used for the thick and stacked fascicles in the late *Tribolium* embryo, containing the DM1-4 tracts, as these are hardly distinguishable through standard imaging (manuscript 1). Expansion microscopy might resolve this stack of fibres in combination with clonal analysis and thus reveal whether fascicle switching has occurred. Similarly, ramifications in two different columns typical for pontine neurons might be revealed through this technique.

Alternatively, FIB-SEM (focused ion-beam scanning electron microscopy) can be used in combination with an HRP-coupled GFP antibody in the transgenic line background. The brown precipitate of the HRP-based reaction will label where GFP is expressed and thus where the larval central body is. This structure can then be scanned, and specific cells reconstructed.

Hence, techniques are available to characterize the larval central body on a higher resolution level. Moreover, the use of these techniques can be expanded to other stages of *Tribolium* brain development.

4.6.2. Atlas of *Tribolium* brain development contrasted to *Drosophila*

An insect brain can be divided into synapse-rich compartments, tunnels that are devoid of synapses and the cell body rind consisting of cell bodies (Ito et al., 2014; Pereanu et al., 2010). The *Drosophila* brain has been globally characterised not only in the adult stage (Lovick et al., 2013; Pereanu et al., 2010; Wong et al., 2013), but also larval stages (Andrade et al., 2019; Hartenstein et al., 2015). Such descriptions of compartments and fascicle tunnels can be the basis of mechanistic and functional approaches (Omoto et al., 2017).

Similar descriptions can be performed in the *Tribolium* brain, building on the present basic anatomical descriptions (Dreyer et al., 2010; Koniszewski et al., 2016). Moreover, such comparative descriptions can be extended to developmental periods. It would be interesting to detect any deviations between *Tribolium* and the already published compartments and tunnels and their developmental periods of the *Drosophila* brain. Such comparative descriptions in high anatomical detail throughout the developing brain are rare, if at all available in insects (see

accounts on an adult ant brain; Bressan et al., 2015), but also in all animals, to the best of my knowledge.

Description of compartments can be based on synapsin stains (as in manuscript 1, potentially reusing the same data). Description of tunnels can be based on acetylated α-Tubulin and transgenic lines such as the *rx* transgenic line (He et al., 2019; M. Buescher, unpublished, manuscript 1) that also mark fractions of tunnels. However, tracts have usually been detected and described with two different antibodies, against neurotactin and neuroglian (e.g. Wong et al., 2013). Neuroglian labels secondary lineages, hence cells produced by neuroblasts after quiescence (Homem and Knoblich, 2012), while neurotactin labels primary lineages. A distinction of primary and secondary tracts in *Tribolium* could illustrate a quiescence phase (or the absence of it). Moreover, both antibodies are more specific for neuronal tracts than acetylated α-Tubulin (V. Hartenstein, personal communication). Unfortunately, the *Drosophila* antibodies do not cross-react with the *Tribolium* antigens and thus, analogous antibodies would need to be generated, if the antigen is present and annotated in *Tribolium*.

Nevertheless, available antibodies and the transgenic lines already allow a detailed account of *Tribolium* brain development. This can then be contrasted to *Drosophila* brain development and give a global analysis of any deviations, including deviations on timing of functional appearance of neuropils besides the central complex.

4.6.3. Volumetric data of insect brains can be used in phylogenetic comparative analyses

Data on mammalian brains including brain area sizes of several hundred species have been analysed using phylogenetic comparative methods (e.g. DeCasien et al., 2017; Isler and van Schaik, 2012; Powell et al., 2017). Inclusion of social, ecological and life history data have been used to test specific hypotheses of brain evolution. Phylogenetic comparative analysis is regularly included in analyses of brain sizes of several species to account for phylogenetic history (Nunn and Barton, 2001). Nunn and Barton (2001) illustrate the necessity including phylogenetic data into comparisons of data points such as brain sizes.

Analogous analyses in insects are mostly missing thus far (but see Dreyer et al., 2010; Montgomery and Merrill, 2016; for analyses on a limited number of species without inclusion of any ecological, social or life history information) although volumetric data on brain areas is available for several species (e.g. www.insectbraindb.org; el Jundi and Heinze, 2016). Without the necessity of generating new data, phylogenetic comparative analyses could be performed in a short time frame. An important drawback is whether these brains have been fixed and imaged

identically, as this can modify the absolute volume of the brains. Montgomery and Merrill (2016) have used corrective values for differences in imaging. Possibly, similar corrections can be included for fixation differences. Such differences need to be considered as potential error sources.

Nevertheless, the opportunity is there to correlate phylogenetically corrected brain and neuropil volumes with social, ecological and life history traits, if available (such as for *Heliconius* butterflies, Jiggins, 2017). With this, specific hypotheses can be tested. For example, what are the influences of home range size on brain and mushroom body size in all available insects?

4.7. Future directions for brain development and evolution

I have illustrated the advantages of using insect brains for evolutionary research (2.2 Introduction). Nevertheless, studies on brain evolution in insects are relatively rare. This is particularly true for evolutionary developmental research, although such analyses can reveal mechanisms underlying brain evolution, such as the precocious development of the central body in *Tribolium*. This doctoral thesis contributes an aspect to the understanding of insect brain development and evolution, particularly for the central complex. I think that the use of genetic neural lineages and their further elaboration for single cell marking opens a field of research on this topic. Alternative approaches to the ones presented in manuscripts 1-3 are single-cell sequencing (Konstantinides et al., 2018) which hopefully complement approaches proposed here. In any case, the inclusion of more species with functional genetic tools, such as *Tribolium* and others that represent the diversity in the phylogeny, can contribute to reveal the cellular and genetic mechanisms of brain evolution.

5. References

Alberch, P., 1991. From genes to phenotype: dynamical systems and evolvability. Genetica 84, 5–11. https://doi.org/10.1007/BF00123979

Alberch, P., Gould, S.J., Oster, G.F., Wake, D.B., 1979. Size and shape in ontogeny and phylogeny. Paleobiology 5, 296–317. https://doi.org/10.1017/S0094837300006588

Almeida, M.S., Bray, S.J., 2005. Regulation of post-embryonic neuroblasts by *Drosophila* Grainyhead. Mechanisms of Development 122, 1282–1293. https://doi.org/10.1016/j.mod.2005.08.004

Álvarez, J.-A., Díaz-Benjumea, F.J., 2018. Origin and specification of type II neuroblasts in the *Drosophila* embryo. Development 145, dev158394. https://doi.org/10.1242/dev.158394

Andrade, I.V., Riebli, N., Nguyen, B.-C.M., Omoto, J.J., Cardona, A., Hartenstein, V., 2019. Developmentally Arrested Precursors of Pontine Neurons Establish an Embryonic Blueprint of the *Drosophila* Central Complex. Current Biology 29/3, 412-425e3. https://doi.org/10.1016/j.cub.2018.12.012

Arendt, D., 2008. The evolution of cell types in animals: emerging principles from molecular studies. Nature Reviews Genetics 9, 868–882. https://doi.org/10.1038/nrg2416

Arendt, D., 2005. Genes and homology in nervous system evolution: Comparing gene functions, expression patterns, and cell type molecular fingerprints. Theory in Biosciences 124, 185–197. https://doi.org/10.1007/BF02814483

Arendt, D., Bertucci, P.Y., Achim, K., Musser, J.M., 2019. Evolution of neuronal types and families. Current Opinion in Neurobiology, Neuronal Identity 56, 144–152. https://doi.org/10.1016/j.conb.2019.01.022

Arendt, D., Tessmar-Raible, K., Snyman, H., Dorresteijn, A.W., Wittbrodt, J., 2004. Ciliary Photoreceptors with a Vertebrate-Type Opsin in an Invertebrate Brain. Science 306, 869–871. https://doi.org/10.1126/science.1099955

Arendt, D., Tosches, M.A., Marlow, H., 2016. From nerve net to nerve ring, nerve cord and brain--evolution of the nervous system. Nat. Rev. Neurosci. 17, 61–72. https://doi.org/10.1038/nrn.2015.15

Arendt, D., Benito-Gutierrez E., Brunet T., Marlow H., 2015. Gastric pouches and the mucociliary sole: setting the stage for nervous system evolution. Philosophical Transactions of the Royal Society B: Biological Sciences 370, 20150286. https://doi.org/10.1098/rstb.2015.0286

Bainbridge, S.P., Bownes, M., 1981. Staging the metamorphosis of *Drosophila melanogaster*. J Embryol Exp Morphol 66, 57–80.

Barton, R.A., 2004. From The Cover: Binocularity and brain evolution in primates. Proceedings of the National Academy of Sciences 101, 10113–10115. https://doi.org/10.1073/pnas.0401955101

Barton, R.A., 1998. Visual specialization and brain evolution in primates. Proceedings of the Royal Society B: Biological Sciences 265, 1933–1937. https://doi.org/10.1098/rspb.1998.0523

Barton, R.A., Harvey, P.H., 2000. Mosaic evolution of brain structure in mammals. Nature 405, 1055. https://doi.org/10.1038/35016580

Bassett, A.R., Tibbit, C., Ponting, C.P., Liu, J.-L., 2013. Highly Efficient Targeted Mutagenesis of *Drosophila* with the CRISPR/Cas9 System. Cell Reports 4, 220–228. https://doi.org/10.1016/j.celrep.2013.06.020

Bayraktar, O.A., Boone, J.Q., Drummond, M.L., Doe, C.Q., 2010. *Drosophila* type II neuroblast lineages keep Prospero levels low to generate large clones that contribute to the adult brain central complex. Neural Development 5, 26. https://doi.org/10.1186/1749-8104-5-26

Bayraktar, O.A., Doe, C.Q., 2013. Combinatorial temporal patterning in progenitors expands neural diversity. Nature 498, 449–455. https://doi.org/10.1038/nature12266

Bello, B., Reichert, H., Hirth, F., 2006. The brain tumor gene negatively regulates neural progenitor cell proliferation in the larval central brain of *Drosophila*. Development 133, 2639–2648. https://doi.org/10.1242/dev.02429

Bello, B.C., Izergina, N., Caussinus, E., Reichert, H., 2008. Amplification of neural stem cell proliferation by intermediate progenitor cells in *Drosophila* brain development. Neural Dev 3, 5. https://doi.org/10.1186/1749-8104-3-5

Berghammer, A., Bucher, G., Maderspacher, F., Klingler, M., 1999. A system to efficiently maintain embryonic lethal mutations in the flour beetle *Tribolium castaneum*. Development Genes and Evolution 209, 382–389. https://doi.org/10.1007/s004270050268

Berghammer, A.J., Klingler, M., Wimmer, E.A., 1999. A universal marker for transgenic insects. Nature 402, 370. https://doi.org/10.1038/46463

Bernard, P., Gabarit, P., Bahassi, E.M., Couturier, M., 1994. Positive-selection vectors using the F plasmid ccdB killer gene. Gene 148, 71–74. https://doi.org/10.1016/0378-1119(94)90235-6

Beumer, K.J., Trautman, J.K., Mukherjee, K., Carroll, D., 2013. Donor DNA Utilization During Gene Targeting with Zinc-Finger Nucleases. G3 3, 657–664. https://doi.org/10.1534/g3.112.005439

Biffar, L., Stollewerk, A., 2014. Conservation and evolutionary modifications of neuroblast expression patterns in insects. Developmental Biology 388, 103–116. https://doi.org/10.1016/j.ydbio.2014.01.028

Bodies, E., Dakou, E., Vanbekbergen, N., Corradi, S., Kemp, C.R., Willems, E., Leyns, L., 2014. Whole-Mount *In situ* Hybridization (WISH) Optimized for Gene Expression Analysis in Mouse Embryos and Embryoid Bodies, in: *In situ* Hybridization Protocols. https://doi.org/10.1007/978-1-4939-1459-3

Böhm, A., Szucsich, N.U., Pass, G., 2012. Brain anatomy in Diplura (Hexapoda). Frontiers in Zoology 9, 26. https://doi.org/10.1186/1742-9994-9-26

Bolker, J.A., 2014. Model species in evo-devo: a philosophical perspective. Evolution & Development 16, 49–56. https://doi.org/10.1111/ede.12056

Boone, J.Q., Doe, C.Q., 2008. Identification of *Drosophila* type II neuroblast lineages containing transit amplifying ganglion mother cells. Developmental Neurobiology 68, 1185–1195. https://doi.org/10.1002/dneu.20648

Bosse-Doenecke, E., Weininger, U., Gopalswamy, M., Balbach, J., Knudsen, S.M., Rudolph, R., 2008. High yield production of recombinant native and modified peptides exemplified by ligands for G-protein coupled receptors. Protein Expression and Purification 58, 114–121. https://doi.org/10.1016/j.pep.2007.10.012

Bossing, T., Technau, G.M., 1994. The fate of the CNS midline progenitors in *Drosophila* as revealed by a new method for single cell labelling. Development 120, 1895–1906.

Boyan, G., Liu, Y., Khalsa, S.K., Hartenstein, V., 2017. A conserved plan for wiring up the fan-shaped body in the grasshopper and *Drosophila*. Dev Genes Evol 227, 253–269. https://doi.org/10.1007/s00427-017-0587-2

Boyan, G., Williams, L., 2011. Embryonic development of the insect central complex: Insights from lineages in the grasshopper and *Drosophila*. Arthropod Structure & Development, Evolution of the Arthropod Nervous System: Part 2 40, 334–348. https://doi.org/10.1016/j.asd.2011.02.005

Boyan, G., Williams, L., Legl, A., Herbert, Z., 2010. Proliferative cell types in embryonic lineages of the central complex of the grasshopper *Schistocerca gregaria*. Cell Tissue Research. 341, 259–277. https://doi.org/10.1007/s00441-010-0992-6

Boyan, G., Williams, L., Liu, Y., 2015. Conserved patterns of axogenesis in the panarthropod brain. Arthropod Structure & Development 44, 101–112. https://doi.org/10.1016/j.asd.2014.11.003

Boyan, G.S., Liu, Y., 2016. Development of the Neurochemical Architecture of the Central Complex. Frontiers in Behavioral Neuroscience 167. https://doi.org/10.3389/fnbeh.2016.00167

Boyan, G.S., Reichert, H., 2011. Mechanisms for complexity in the brain: Generating the insect central complex. Trends in Neurosciences. https://doi.org/10.1016/j.tins.2011.02.002

Boyan, G.S., Williams, J.L.D., 1997. Embryonic development of the pars intercerebralis/central complex of the grasshopper. Dev Gene Evol 207, 317–329. https://doi.org/10.1007/s004270050119

Boyan, G.S., Williams, J.L.D., Herbert, Z., 2008. Fascicle switching generates a chiasmal neuroarchitecture in the embryonic central body of the grasshopper *Schistocerca gregaria*. Arthropod Structure & Development 37, 539–544. https://doi.org/10.1016/j.asd.2008.07.005

Bressan, J.M.A., Benz, M., Oettler, J., Heinze, J., Hartenstein, V., Sprecher, S.G., 2015. A map of brain neuropils and fiber systems in the ant *Cardiocondyla obscurior*. Front. Neuroanat. 8. https://doi.org/10.3389/fnana.2014.00166

Brown, S.J., Mahaffey, J.P., Lorenzen, M.D., Denell, R.E., Mahaffey, J.W., 1999. Using RNAi to investigate orthologous homeotic gene function during development of distantly related insects. Evolution and Development 1, 11–15. https://doi.org/10.1046/j.1525-142x.1999.99013.x

Brown, S.J., Shippy, T.D., Miller, S., Bolognesi, R., Beeman, R.W., Lorenzen, M.D., Bucher, G., Wimmer, E.A., Klingler, M., 2009. The red flour beetle, *Tribolium castaneum* (Coleoptera): a model for studies of development and pest biology. Cold Spring Harb Protoc 2009, pdb.emo126. https://doi.org/10.1101/pdb.emo126

Bucher, G., Scholten, J., Klingler, M., 2002. Parental RNAi in *Tribolium* (Coleoptera). Current Biology 12, R85–R86. https://doi.org/10.1016/S0960-9822(02)00666-8

Buescher, M., Oberhofer, G., Garcia-Perez, N.C., Bucher, G. in press. A protocol for double *in situ* hybridization and immunohistochemistry for the study of embryonic brain development in *Tribolium castaneum*, in: Brain Development: Methods and Protocols, 2nd edition.

Buffry, A.D., Mendes, C.C., McGregor, A.P., 2016. Chapter Four - The Functionality and Evolution of Eukaryotic Transcriptional Enhancers, in: Friedmann, T., Dunlap, J.C., Goodwin, S.F. (Eds.), Advances in Genetics. Academic Press, pp. 143–206. https://doi.org/10.1016/bs.adgen.2016.08.004

Cabernard, C., Doe, C.Q., 2009. Apical/Basal Spindle Orientation Is Required for Neuroblast Homeostasis and Neuronal Differentiation in *Drosophila*. Developmental Cell 17, 134–141. https://doi.org/10.1016/j.devcel.2009.06.009

Cahoon, C.K., Yu, Z., Wang, Y., Guo, F., Unruh, J.R., Slaughter, B.D., Hawley, R.S., 2017. Superresolution expansion microscopy reveals the three-dimensional organization of the *Drosophila* synaptonemal complex. Proceedings of the National Academy of Sciences 114, E6857–E6866. https://doi.org/10.1073/pnas.1705623114

Campos-Ortega, J.A., Hartenstein, V., 1985. The Embryonic Development of *Drosophila melanogaster*. Springer-Verlag, New York.

Cappella, P., Gasparri, F., Pulici, M., Moll, J., 2008. A novel method based on click chemistry, which overcomes limitations of cell cycle analysis by classical determination of BrdU incorporation, allowing multiplex antibody staining. Cytometry Part A 73A, 626–636. https://doi.org/10.1002/cyto.a.20582

Cayre, M., Malaterre, J., Scotto-Lomassese, S., Aouane, A., Strambi, C., Strambi, A., 2005. Hormonal and sensory inputs regulate distinct neuroblast cell cycle properties in adult cricket brain. Journal of Neuroscience Research 82, 659–664. https://doi.org/10.1002/jnr.20672

Cayre, M., Strambi, C., Strambi, A., Charpin, P., Ternaux, J.-P., 2000. Dual effect of ecdysone on adult cricket mushroom bodies. European Journal of Neuroscience 12, 633–642. https://doi.org/10.1046/j.1460-9568.2000.00947.x

Çelik, A., Wernet, M.F., 2017. Decoding Neural Circuit Structure and Function: Cellular Dissection Using Genetic Model Organisms. Springer.

Chell, J.M., Brand, A.H., 2010. Nutrition-Responsive Glia Control Exit of Neural Stem Cells from Quiescence. Cell 143, 1161–1173. https://doi.org/10.1016/j.cell.2010.12.007

Chen, L., Wang, G., Zhu, Y.-N., Xiang, H., Wang, W., 2016. Advances and perspectives in the application of CRISPR/Cas9 in insects. Dongwuxue Yanjiu 37, 136–143. https://doi.org/10.13918/j.issn.2095-8137.2016.4.220

Chittka, L., Niven, J., 2009. Are Bigger Brains Better? Current Biology 19, R995–R1008. https://doi.org/10.1016/j.cub.2009.08.023

Clarke, R., Heler, R., MacDougall, M.S., Yeo, N.C., Chavez, A., Regan, M., Hanakahi, L., Church, G.M., Marraffini, L.A., Merrill, B.J., 2018. Enhanced Bacterial Immunity and Mammalian Genome Editing via RNA-Polymerase-Mediated Dislodging of Cas9 from Double-Strand DNA Breaks. Molecular Cell 71, 42-55.e8. https://doi.org/10.1016/j.molcel.2018.06.005

Conway Morris Simon, Hoyal Cuthill Jennifer F., Gerber Sylvain, 2015. Hunting Darwin's Snark: which maps shall we use? Interface Focus 5, 20150078. https://doi.org/10.1098/rsfs.2015.0078

Davis, R.J., Tavsanli, B.C., Dittrich, C., Walldorf, U., Mardon, G., 2003. *Drosophila* retinal homeobox (drx) is not required for establishment of the visual system, but is required for brain and clypeus development. Developmental Biology 259, 272–287. https://doi.org/10.1016/S0012-1606(03)00201-X

De Beer, G., Sir, 1899-1972, 1951. Embryos and ancestors.

de Velasco, B., Erclik, T., Shy, D., Sclafani, J., Lipshitz, H., McInnes, R., Hartenstein, V., 2007. Specification and development of the pars intercerebralis and pars lateralis, neuroendocrine command centers in the *Drosophila* brain. Developmental Biology 302, 309–323. https://doi.org/10.1016/j.ydbio.2006.09.035

Dearden, P.K., Akam, M., 2001. Early embryo patterning in the grasshopper, *Schistocerca gregaria*: wingless, decapentaplegic and caudal expression. Development (Cambridge, England) 128, 3435–3444.

DeCasien, A.R., Williams, S.A., Higham, J.P., 2017. Primate brain size is predicted by diet but not sociality. Nature Ecology & Evolution 1, 0112. https://doi.org/10.1038/s41559-017-0112

Denes, A.S., Jekely, G., Steinmetz, P.R., Raible, F., Snyman, H., Prud'homme, B., Ferrier, D.E., Balavoine, G., Arendt, D., 2007. Molecular architecture of annelid nerve cord supports common origin of nervous system centralization in bilateria. Cell 129, 277–88.

Dietzl, G., Chen, D., Schnorrer, F., Su, K.-C., Barinova, Y., Fellner, M., Gasser, B., Kinsey, K., Oppel, S., Scheiblauer, S., Couto, A., Marra, V., Keleman, K., Dickson, B.J., 2007. A genome-wide transgenic RNAi library for conditional gene inactivation in *Drosophila*. Nature 448, 151–156. https://doi.org/10.1038/nature05954

Ding, R., Weynans, K., Bossing, T., Barros, C.S., Berger, C., 2016. The Hippo signalling pathway maintains quiescence in *Drosophila* neural stem cells. Nature Communications 7, 10510. https://doi.org/10.1038/ncomms10510

Dippel, S., Kollmann, M., Oberhofer, G., Montino, A., Knoll, C., Krala, M., Rexer, K.-H., Frank, S., Kumpf, R., Schachtner, J., Wimmer, E.A., 2016. Morphological and Transcriptomic Analysis of a Beetle Chemosensory System Reveals a Gnathal Olfactory Center. BMC Biology 14. https://doi.org/10.1186/s12915-016-0304-z

Doe, C.Q., 2017. Temporal Patterning in the *Drosophila* CNS. Annu. Rev. Cell Dev. Biol. 33, 219–240. https://doi.org/10.1146/annurev-cellbio-111315-125210

Dönitz, J., Gerischer, L., Hahnke, S., Pfeiffer, S., Bucher, G., 2018. Expanded and updated data and a query pipeline for iBeetle-Base. Nucleic Acids Research 46, D831–D835. https://doi.org/10.1093/nar/gkx984

Dönitz, J., Schmitt-Engel, C., Grossmann, D., Gerischer, L., Tech, M., Schoppmeier, M., Klingler, M., Bucher, G., 2015. iBeetle-Base: a database for RNAi phenotypes in the red flour beetle *Tribolium castaneum*. Nucl. Acids Res. 43, D720–D725. https://doi.org/10.1093/nar/gku1054

Donnelly, M.L.L., Luke, G., Mehrotra, A., Li, X., Hughes, L.E., Gani, D., Ryan, M.D., 2001. Analysis of the aphthovirus 2A/2B polyprotein 'cleavage' mechanism indicates not a proteolytic reaction, but a novel translational effect: a putative ribosomal 'skip.' Journal of General Virology 82, 1013–1025. https://doi.org/10.1099/0022-1317-82-5-1013

Doudna, J.A., Charpentier, E., 2014. Genome editing. The new frontier of genome engineering with CRISPR-Cas9. Science 346, 1258096. https://doi.org/10.1126/science.1258096

Dreyer, D., Vitt, H., Dippel, S., Goetz, B., El Jundi, B., Kollmann, M., Huetteroth, W., Schachtner, J., Dreyer, D., Vitt, H., Dippel, S., Goetz, B., Jundi, B. el, Kollmann, M., Huetteroth, W., Schachtner, J., 2010. 3D standard brain of the red flour beetle *Tribolium castaneum*: a tool to study metamorphic development and adult plasticity. Front. Syst. Neurosci. 4, 3. https://doi.org/10.3389/neuro.06.003.2010

Dumstrei, K., Wang, F., Hartenstein, V., 2003. Role of DE-Cadherin in Neuroblast Proliferation, Neural Morphogenesis, and Axon Tract Formation in *Drosophila* Larval Brain Development. J. Neurosci. 23, 3325–3335. https://doi.org/10.1523/JNEUROSCI.23-08-03325.2003

Dunbar, R.I.M., 1998. The social brain hypothesis. Evolutionary Anthropology: Issues, News, and Reviews 6, 178–190. https://doi.org/10.1002/(SICI)1520-6505(1998)6:5<178::AID-EVAN5>3.0.CO;2-8

Dunbar, R.I.M., Shultz, S., 2017. Why are there so many explanations for primate brain evolution? Phil. Trans. R. Soc. B 372, 20160244. https://doi.org/10.1098/rstb.2016.0244

Dunbar, R.I.M., Shultz, S., 2007. Evolution in the Social Brain. Science 317, 1344–1347. https://doi.org/10.1126/science.1145463

Eckermann, K.N., Ahmed, H.M.M., KaramiNejadRanjbar, M., Dippel, S., Ogaugwu, C.E., Kitzmann, P., Isah, M.D., Wimmer, E.A., 2018. Hyperactive piggyBac transposase improves transformation efficiency in diverse insect species. Insect Biochem. Mol. Biol. 98, 16–24. https://doi.org/10.1016/j.ibmb.2018.04.001

Eckert, C., Aranda, M., Wolff, C., Tautz, D., 2004. Separable stripe enhancer elements for the pair-rule gene hairy in the beetle *Tribolium*. EMBO Rep 5, 638–42.

Edgecombe G.D., Ma X., Strausfeld N.J., 2015. Unlocking the early fossil record of the arthropod central nervous system. Philosophical Transactions of the Royal Society B: Biological Sciences 370, 20150038. https://doi.org/10.1098/rstb.2015.0038

Eggert, T., Hauck, B., Hildebrandt, N., Gehring, W.J., Walldorf, U., 1998. Isolation of a *Drosophila* homolog of the vertebrate homeobox gene Rx and its possible role in brain and eye development. Proceedings of the National Academy of Sciences 95, 2343–2348.

Eifert, C., Farnworth, M., Schulz-Mirbach, T., Riesch, R., Bierbach, D., Klaus, S., Wurster, A., Tobler, M., Streit, B., Indy, J.R., Arias-Rodriguez, L., Plath, M., 2015. Brain size variation in extremophile fish: local adaptation versus phenotypic plasticity. J Zool 295, 143–153. https://doi.org/10.1111/jzo.12190

El Jundi, B., Heinze, S., 2016. Three-dimensional atlases of insect brains., in: Neurohistology and Imaging: Basic Techniques. Springer (Humana Press, New York).

el Jundi, B., Warrant, E.J., Pfeiffer, K., Dacke, M., 2018. Neuroarchitecture of the dung beetle central complex. Journal of Comparative Neurology 526/16, 2612-2630. https://doi.org/10.1002/cne.24520

Enard, W., 2016. The Molecular Basis of Human Brain Evolution. Current Biology 26, R1109–R1117. https://doi.org/10.1016/j.cub.2016.09.030

Engler, C., Kandzia, R., Marillonnet, S., 2008. A One Pot, One Step, Precision Cloning Method with High Throughput Capability. PLOS ONE 3, e3647. https://doi.org/10.1371/journal.pone.0003647

Erclik, T., Li, X., Courgeon, M., Bertet, C., Chen, Z., Baumert, R., Ng, J., Koo, C., Arain, U., Behnia, R., Del Valle Rodriguez, A., Senderowicz, L., Negre, N., White, K.P., Desplan, C., 2017. Integration of temporal and spatial patterning generates neural diversity. Nature 541, 365–370. https://doi.org/10.1038/nature20794

Farnworth, M.S., Eckermann, K.N., Ahmed, H.M., Mühlen, D.S., He, B., Bucher, G. in press. The red flour beetle as model for comparative neural development: Genome editing to mark neural cells in *Tribolium* brain development. Brain Development: Methods and Protocols, 2nd edition.

Farries, M.A., 2013. How 'Basal" Are the Basal Ganglia?' BBE 82, 211–214. https://doi.org/10.1159/000356101

Farris, S.M., 2013. Evolution of Complex Higher Brain Centers and Behaviors: Behavioral Correlates of Mushroom Body Elaboration in Insects. BBE 82, 9–18. https://doi.org/10.1159/000352057

Farris, S.M., 2008. Structural, Functional and Developmental Convergence of the Insect Mushroom Bodies with Higher Brain Centers of Vertebrates. BBE 72, 1–15. https://doi.org/10.1159/000139457

Farris, S.M., Sinakevitch, I., 2003. Development and evolution of the insect mushroom bodies: towards the understanding of conserved developmental mechanisms in a higher brain center. Arthropod Structure & Development, Development of the Arthropod Nervous System: a Comparative and Evolutionary Approach 32, 79–101. https://doi.org/10.1016/S1467-8039(03)00009-4

Finlay, B.L., Darlington, R.B., 1995. Linked regularities in the development and evolution of mammalian brains. Science 268, 1578–1584. https://doi.org/10.1126/science.7777856

Florio, M., Albert, M., Taverna, E., Namba, T., Brandl, H., Lewitus, E., Haffner, C., Sykes, A., Wong, F.K., Peters, J., Guhr, E., Klemroth, S., Prufer, K., Kelso, J., Naumann, R., Nusslein, I., Dahl, A., Lachmann, R., Paabo, S., Huttner, W.B., 2015. Human-specific gene ARHGAP11B promotes basal progenitor amplification and neocortex expansion. Science 347, 1465–1470. https://doi.org/10.1126/science.aaa1975

Franconville, R., Beron, C., Jayaraman, V., 2018. Building a functional connectome of the *Drosophila* central complex. eLife 7, e37017. https://doi.org/10.7554/eLife.37017

Fritsch, M., Bininda-Emonds, O.R., Richter, S., 2013. Unraveling the origin of Cladocera by identifying heterochrony in the developmental sequences of Branchiopoda. Frontiers in Zoology 10, 35. https://doi.org/10.1186/1742-9994-10-35

Fritsch, M., Richter, S., 2010. The formation of the nervous system during larval development in *Triops cancriformis* (Bosc) (crustacea, Branchiopoda): An immunohistochemical survey. Journal of Morphology 271, 1457–1481. https://doi.org/10.1002/jmor.10892

Furukawa, T., Kozak, C.A., Cepko, C.L., 1997. rax, a novel paired-type homeobox gene, shows expression in the anterior neural fold and developing retina. Proceedings of the National Academy of Sciences 94, 3088–3093. https://doi.org/10.1073/pnas.94.7.3088

Giandomenico, S.L., Lancaster, M.A., 2017. Probing human brain evolution and development in organoids. Current Opinion in Cell Biology, Cell Architecture 44, 36–43. https://doi.org/10.1016/j.ceb.2017.01.001

Gilles, A.F., Averof, M., 2014. Functional genetics for all: engineered nucleases, CRISPR and the gene editing revolution. EvoDevo 5, 43. https://doi.org/10.1186/2041-9139-5-43

Gilles, A.F., Schinko, J.B., Averof, M., 2015. Efficient CRISPR-mediated gene targeting and transgene replacement in the beetle *Tribolium castaneum*. Development 142, 2832–2839. https://doi.org/10.1242/dev.125054

Gilles, A.F., Schinko, J.B., Schacht, M.I., Enjolras, C., Averof, M., 2019. Clonal analysis by tunable CRISPR-mediated excision. Development 146, dev170969. https://doi.org/10.1242/dev.170969

Godfrey, R.K., Gronenberg, W., 2019. Brain evolution in social insects: advocating for the comparative approach. J Comp Physiol A 205, 13–32. https://doi.org/10.1007/s00359-019-01315-7

Gold, K.S., Brand, A.H., 2014. Optix defines a neuroepithelial compartment in the optic lobe of the *Drosophila* brain. Neural Development 9, 18. https://doi.org/10.1186/1749-8104-9-18

Gomez, C., Özbudak, E.M., Wunderlich, J., Baumann, D., Lewis, J., Pourquié, O., 2008. Control of segment number in vertebrate embryos. Nature 454, 335–339. https://doi.org/10.1038/nature07020

Gonzalez-Voyer, A., Winberg, S., Kolm, N., 2009. Brain structure evolution in a basal vertebrate clade: evidence from phylogenetic comparative analysis of cichlid fishes. BMC Evolutionary Biology 9, 238. https://doi.org/10.1186/1471-2148-9-238

Gordon, D.G., Zelaya, A., Arganda-Carreras, I., Arganda, S., Traniello, J.F.A., 2019. Division of labor and brain evolution in insect societies: Neurobiology of extreme specialization in the turtle ant *Cephalotes varians*. PLOS ONE 14, e0213618. https://doi.org/10.1371/journal.pone.0213618

Gould, S.J., 2000. Of coiled oysters and big brains: how to rescue the terminology of heterochrony, now gone astray. Evolution & Development 2, 241–248. https://doi.org/10.1046/j.1525-142x.2000.00067.x

Gould, S.J., 1977. Ontogeny and Phylogeny. Harvard University Press, Harvard.

Gratz, S.J., Ukken, F.P., Rubinstein, C.D., Thiede, G., Donohue, L.K., Cummings, A.M., O'Connor-Giles, K.M., 2014. Highly Specific and Efficient CRISPR/Cas9-Catalyzed Homology-Directed Repair in *Drosophila*. Genetics 196, 961–971. https://doi.org/10.1534/genetics.113.160713

Gratz, S.J., Wildonger, J., Harrison, M.M., O'Connor-Giles, K.M., 2013. CRISPR/Cas9-mediated genome engineering and the promise of designer flies on demand. Fly 7, 249–255. https://doi.org/10.4161/fly.26566

Häcker, U., Nystedt, S., Barmchi, M.P., Horn, C., Wimmer, E.A., 2003. piggyBac-based insertional mutagenesis in the presence of stably integrated P elements in *Drosophila*. Proceedings of the National Academy of Sciences 100, 7720–7725. https://doi.org/10.1073/pnas.1230526100

Hadjieconomou, D., Rotkopf, S., Alexandre, C., Bell, D.M., Dickson, B.J., Salecker, I., 2011. Flybow: genetic multicolor cell labeling for neural circuit analysis in *Drosophila melanogaster*. Nature Methods 8, 260–266. https://doi.org/10.1038/nmeth.1567

Hähnlein, I., Bicker, G., 1997. Glial patterning during postembryonic development of central neuropiles in the brain of the honeybee. Dev Gene Evol 207, 29–41. https://doi.org/10.1007/s004270050089

Hales, K.G., Korey, C.A., Larracuente, A.M., Roberts, D.M., 2015. Genetics on the Fly: A Primer on the *Drosophila* Model System. Genetics 201, 815–842. https://doi.org/10.1534/genetics.115.183392

Hanington, P.C., Barreda, D.R., Belosevic, M., 2006. A Novel Hematopoietic Granulin Induces Proliferation of Goldfish (*Carassius auratus* L.) Macrophages. J. Biol. Chem. 281, 9963–9970. https://doi.org/10.1074/jbc.M600631200

Harrison, P.W., Montgomery, S.H., 2017. Genetics of Cerebellar and Neocortical Expansion in Anthropoid Primates: A Comparative Approach. BBE. https://doi.org/10.1159/000477432

Hartenstein, V., 2019. Development of the Nervous System of Invertebrates, in: Byrne, J.H. (Ed.), The Oxford Handbook of Invertebrate Neurobiology. Oxford University Press, pp. 70–122. https://doi.org/10.1093/oxfordhb/9780190456757.013.3

Hartenstein, V., Spindler, S., Pereanu, W., Fung, S., 2008. The Development of the *Drosophila* Larval Brain, in: Technau, G.M. (Ed.), Brain Development in *Drosophila* Melanogaster, Advances in Experimental Medicine and Biology. Springer New York, New York, NY, pp. 1–31. https://doi.org/10.1007/978-0-387-78261-4_1

Hartenstein, V., Stollewerk, A., 2015. The Evolution of Early Neurogenesis. Developmental Cell 32, 390–407. https://doi.org/10.1016/j.devcel.2015.02.004

Hartenstein, V., Younossi-Hartenstein, A., Lovick, J.K., Kong, A., Omoto, J.J., Ngo, K.T., Viktorin, G., 2015. Lineage-associated tracts defining the anatomy of the *Drosophila* first instar larval brain. Developmental Biology 406, 14–39. https://doi.org/10.1016/j.ydbio.2015.06.021

Hayashi, S., Ito, K., Sado, Y., Taniguchi, M., Akimoto, A., Takeuchi, H., Aigaki, T., Matsuzaki, F., Nakagoshi, H., Tanimura, T., Ueda, R., Uemura, T., Yoshihara, M., Goto, S., 2002. GETDB, a database compiling expression patterns and molecular locations of a collection of gal4 enhancer traps. genesis 34, 58–61. https://doi.org/10.1002/gene.10137

He, B., Buescher, M., Farnworth, M.S., Strobl, F., Stelzer, E., Koniszewski, N.D.B., Mühlen, D., Bucher, G., 2019. An ancestral apical brain region contributes to the central complex under the control of foxQ2 in the beetle *Tribolium castaneum*. bioRxiv 661199. https://doi.org/10.1101/661199

Heinze, S., 2017. Unraveling the neural basis of insect navigation. Current Opinion in Insect Science, Neuroscience * Pheromones 24, 58–67. https://doi.org/10.1016/j.cois.2017.09.001

Heinze, S., Homberg, U., 2008. Neuroarchitecture of the central complex of the desert locust: Intrinsic and columnar neurons. Journal of Comparative Neurology 511, 454–478. https://doi.org/10.1002/cne.21842

Heinze, S., Homberg, U., 2007. Maplike representation of celestial E-vector orientations in the brain of an insect. Science 315, 995–997. https://doi.org/10.1126/science.1135531

Herbert, Z., Rauser, S., Williams, L., Kapan, N., Güntner, M., Walch, A., Boyan, G., 2010. Developmental expression of neuromodulators in the central complex of the grasshopper *Schistocerca gregaria*. Journal of Morphology 271, 1509–1526. https://doi.org/10.1002/jmor.10895

Herculano-Houzel, S., 2017. Numbers of neurons as biological correlates of cognitive capability. Current Opinion in Behavioral Sciences, Comparative cognition 16, 1–7. https://doi.org/10.1016/j.cobeha.2017.02.004

Herculano-Houzel, S., 2012. The remarkable, yet not extraordinary, human brain as a scaled-up primate brain and its associated cost. Proceedings of the National Academy of Sciences 109, 10661–10668. https://doi.org/10.1073/pnas.1201895109

Herczeg, G., Urszán, T.J., Orf, S., Nagy, G., Kotrschal, A., Kolm, N., 2019. Brain size predicts behavioural plasticity in guppies (*Poecilia reticulata*): An experiment. Journal of Evolutionary Biology 32, 218–226. https://doi.org/10.1111/jeb.13405

Hirth, F., 2003. An urbilaterian origin of the tripartite brain: developmental genetic insights from *Drosophila*. Development 130, 2365–2373. https://doi.org/10.1242/dev.00438

Ho, F.K., 1961. Optic Organs of *Tribolium* confusum and T. castaneum and Their Usefulness in Age Determination (Coleoptera: Tenebrionidae). Ann Entomol Soc Am 54, 921–925. https://doi.org/10.1093/aesa/54.6.921

Homberg, U., 2008. Evolution of the central complex in the arthropod brain with respect to the visual system. Arthropod Structure & Development 37, 347–362. https://doi.org/10.1016/j.asd.2008.01.008

Homberg, U., 1994. Flight-correlated activity changes in neurons of the lateral accessory lobes in the brain of the locust *Schistocerca gregaria*. J Comp Physiol A 175, 597–610. https://doi.org/10.1007/BF00199481

Homberg, U., Humberg, T.-H., Seyfarth, J., Bode, K., Pérez, M.Q., 2018. GABA immunostaining in the central complex of dicondylian insects. Journal of Comparative Neurology 526, 2301–2318. https://doi.org/10.1002/cne.24497

Homem, C.C.F., Knoblich, J.A., 2012. *Drosophila* neuroblasts: a model for stem cell biology. Development 139, 4297–4310. https://doi.org/10.1242/dev.080515

Honkanen, A., Adden, A., Freitas, J. da S., Heinze, S., 2019. The insect central complex and the neural basis of navigational strategies. Journal of Experimental Biology 222, jeb188854. https://doi.org/10.1242/jeb.188854

Horn, C., Schmid, B.G.M., Pogoda, F.S., Wimmer, E.A., 2002. Fluorescent transformation markers for insect transgenesis. Insect Biochem. Mol. Biol. 32, 1221–1235.

Hsu, P.D., Lander, E.S., Zhang, F., 2014. Development and Applications of CRISPR-Cas9 for Genome Engineering. Cell 157, 1262–1278. https://doi.org/10.1016/j.cell.2014.05.010

Hsu, P.D., Scott, D.A., Weinstein, J.A., Ran, F.A., Konermann, S., Agarwala, V., Li, Y., Fine, E.J., Wu, X., Shalem, O., Cradick, T.J., Marraffini, L.A., Bao, G., Zhang, F., 2013. DNA targeting specificity of RNA-guided Cas9 nucleases. Nat. Biotechnol. 31, 827–832. https://doi.org/10.1038/nbt.2647

Huetteroth, W., El Jundi, B., El Jundi, S., Schachtner, J., 2010. 3D-reconstructions and virtual 4D-visualization to study metamorphic brain development in the sphinx moth *Manduca sexta*. Front. Syst. Neurosci. 4. https://doi.org/10.3389/fnsys.2010.00007

Hunnekuhl, V.S., Akam, M., 2014. An anterior medial cell population with an apical-organ-like transcriptional profile that pioneers the central nervous system in the centipede *Strigamia maritima*. Developmental Biology 396, 136–149. https://doi.org/10.1016/j.ydbio.2014.09.020

Isler, K., van Schaik, C.P., 2012. Allomaternal care, life history and brain size evolution in mammals. Journal of Human Evolution 63, 52–63. https://doi.org/10.1016/j.jhevol.2012.03.009

Isler, K., van Schaik, C.P., 2006. Metabolic costs of brain size evolution. Biology Letters 2, 557–560. https://doi.org/10.1098/rsbl.2006.0538

Ito, K., Awasaki, T., 2008. Clonal Unit Architecture of the Adult Fly Brain, in: Technau, G.M. (Ed.), Brain Development in *Drosophila melanogaster*, Advances in Experimental Medicine and Biology. Springer New York, New York, NY, pp. 137–158. https://doi.org/10.1007/978-0-387-78261-4_9

Ito, K., Hotta, Y., 1992. Proliferation pattern of postembryonic neuroblasts in the brain of *Drosophila melanogaster*. Developmental Biology 149, 134–148. https://doi.org/10.1016/0012-1606(92)90270-Q

Ito, K., Shinomiya, K., Ito, M., Armstrong, J.D., Boyan, G., Hartenstein, V., Harzsch, S., Heisenberg, M., Homberg, U., Jenett, A., Keshishian, H., Restifo, L.L., Rössler, W., Simpson, J.H., Strausfeld, N.J., Strauss, R., Vosshall, L.B., 2014. A Systematic Nomenclature for the Insect Brain. Neuron 81, 755–765. https://doi.org/10.1016/j.neuron.2013.12.017

Ito, M., Masuda, N., Shinomiya, K., Endo, K., Ito, K., 2013. Systematic Analysis of Neural Projections Reveals Clonal Composition of the *Drosophila* Brain. Current Biology 23, 644–655. https://doi.org/10.1016/j.cub.2013.03.015

Iwai, Y., Usui, T., Hirano, S., Steward, R., Takeichi, M., Uemura, T., 1997. Axon Patterning Requires D N-cadherin, a Novel Neuronal Adhesion Receptor, in the *Drosophila* Embryonic CNS. Neuron 19, 77–89. https://doi.org/10.1016/S0896-6273(00)80349-9

Izergina, N., Balmer, J., Bello, B., Reichert, H., 2009. Postembryonic development of transit amplifying neuroblast lineages in the *Drosophila* brain. Neural Development 4, 44. https://doi.org/10.1186/1749-8104-4-44

Janssen, R., 2017. Comparative analysis of gene expression patterns in the arthropod labrum and the onychophoran frontal appendages, and its implications for the arthropod head problem. EvoDevo 8, 1. https://doi.org/10.1186/s13227-016-0064-4

Jeffery, J.E., Bininda-Emonds, O.R.P., Coates, M.I., Richardson, M.K., 2002a. Analyzing evolutionary patterns in amniote embryonic development. Evol. Dev. 4, 292–302.

Jeffery, J.E., Richardson, M.K., Coates, M.I., Bininda-Emonds, O.R.P., 2002b. Analyzing Developmental Sequences Within a Phylogenetic Framework. Syst Biol 51, 478–491. https://doi.org/10.1080/10635150290069904

Jenett, A., Rubin, G.M., Ngo, T.-T.B., Shepherd, D., Murphy, C., Dionne, H., Pfeiffer, B.D., Cavallaro, A., Hall, D., Jeter, J., Iyer, N., Fetter, D., Hausenfluck, J.H., Peng, H., Trautman, E.T., Svirskas, R.R., Myers, E.W., Iwinski, Z.R., Aso, Y., DePasquale, G.M., Enos, A., Hulamm, P., Lam, S.C.B., Li, H.-H., Laverty, T.R., Long, F., Qu, L., Murphy, S.D., Rokicki, K., Safford, T., Shaw, K., Simpson, J.H., Sowell, A., Tae, S., Yu, Y., Zugates, C.T., 2012. A GAL4-Driver Line Resource for *Drosophila* Neurobiology. Cell Reports 2, 991–1001. https://doi.org/10.1016/j.celrep.2012.09.011

Jenner, R.A., Wills, M.A., 2007. The choice of model organisms in evo–devo. Nature Reviews Genetics 8, 311–314. https://doi.org/10.1038/nrg2062

Jiang, N., Kim, H.-J., Chozinski, T.J., Azpurua, J.E., Eaton, B.A., Vaughan, J.C., Parrish, J.Z., 2018. Superresolution imaging of *Drosophila* tissues using expansion microscopy. MBoC 29, 1413–1421. https://doi.org/10.1091/mbc.E17-10-0583

Jiggins, C.D., 2017. The Ecology and Evolution of *Heliconius* Butterflies. Oxford University Press.

Jin, E.J., Kiral, F.R., Ozel, M.N., Burchardt, L.S., Osterland, M., Epstein, D., Wolfenberg, H., Prohaska, S., Hiesinger, P.R., 2018. Live Observation of Two Parallel Membrane Degradation Pathways at Axon Terminals. Current Biology 28, 1027-1038.e4. https://doi.org/10.1016/j.cub.2018.02.032

Jindra, M., Palli, S.R., Riddiford, L.M., 2013. The Juvenile Hormone Signaling Pathway in Insect Development. Annual Review of Entomology 58, 181–204. https://doi.org/10.1146/annurev-ento-120811-153700

Jinek, M., Chylinski, K., Fonfara, I., Hauer, M., Doudna, J.A., Charpentier, E., 2012. A Programmable Dual-RNA–Guided DNA Endonuclease in Adaptive Bacterial Immunity. Science 337, 816–821. https://doi.org/10.1126/science.1225829

John, A.V., Sramkoski, L.L., Walker, E.A., Cooley, A.M., Wittkopp, P.J., 2016. Sensitivity of Allelic Divergence to Genomic Position: Lessons from the *Drosophila* tan Gene. G3: Genes, Genomes, Genetics 6, 2955–2962. https://doi.org/10.1534/g3.116.032029

Johnston, D.S., 2002. The art and design of genetic screens: *Drosophila melanogaster*. Nature Reviews Genetics 3, 176. https://doi.org/10.1038/nrg751

Kang, K.H., Reichert, H., 2015. Control of neural stem cell self-renewal and differentiation in *Drosophila*. Cell Tissue Res 359, 33–45. https://doi.org/10.1007/s00441-014-1914-9

Katz, P.S., 2007. Evolution and development of neural circuits in invertebrates. Current Opinion in Neurobiology 17, 59–64. https://doi.org/10.1016/j.conb.2006.12.003

Katz, P.S., Harris-Warrick, R.M., 1999. The evolution of neuronal circuits underlying species-specific behavior. Current Opinion in Neurobiology 9, 628–633. https://doi.org/10.1016/S0959-4388(99)00012-4

Katz, P.S., Lillvis, J.L., 2014. Reconciling the deep homology of neuromodulation with the evolution of behavior. Current Opinion in Neurobiology, SI: Neuromodulation 29, 39–47. https://doi.org/10.1016/j.conb.2014.05.002

Keeler, K.J., Dray, T., Penney, J.E., Gloor, G.B., 1996. Gene targeting of a plasmid-borne sequence to a double-strand DNA break in *Drosophila melanogaster*. Mol. Cell. Biol. 16, 522–528.

Keesey, I.W., Grabe, V., Gruber, L., Koerte, S., Obiero, G.F., Bolton, G., Khallaf, M.A., Kunert, G., Lavista-Llanos, S., Valenzano, D.R., Rybak, J., Barrett, B.A., Knaden, M., Hansson, B.S., 2019. Inverse resource allocation between vision and olfaction across the genus *Drosophila*. Nat Commun 10, 1162. https://doi.org/10.1038/s41467-019-09087-z

Keyte, A.L., Smith, K.K., 2014. Heterochrony and developmental timing mechanisms: Changing ontogenies in evolution. Seminars in Cell & Developmental Biology, mRNA stability and degradation & Timing of mammalian embryogenesis & Positioning of the Mitotic Spindle 34, 99–107. https://doi.org/10.1016/j.semcdb.2014.06.015

Khaitovich, P., Hellmann, I., Enard, W., Nowick, K., Leinweber, M., Franz, H., Weiss, G., Lachmann, M., Pääbo, S., 2005. Parallel Patterns of Evolution in the Genomes and Transcriptomes of Humans and Chimpanzees. Science 309, 1850–1854. https://doi.org/10.1126/science.1108296

Khoueiry, P., Girardot, C., Ciglar, L., Peng, P.-C., Gustafson, E.H., Sinha, S., Furlong, E.E., 2017. Uncoupling evolutionary changes in DNA sequence, transcription factor occupancy and enhancer activity. eLife 6, e28440. https://doi.org/10.7554/eLife.28440

Kim, C.-W., 1959. The Differentiation Centre Inducing the Development from Larval to Adult Leg in *Pieris brassicae* (Lepidoptera). Development 7, 572–582.

Kim, J.H., Lee, S.-R., Li, L.-H., Park, H.-J., Park, J.-H., Lee, K.Y., Kim, M.-K., Shin, B.A., Choi, S.-Y., 2011. High Cleavage Efficiency of a 2A Peptide Derived from Porcine Teschovirus-1 in Human Cell Lines, Zebrafish and Mice. PLOS ONE 6, e18556. https://doi.org/10.1371/journal.pone.0018556

Kitzmann, P., Weißkopf, M., Schacht, M.I., Bucher, G., 2017. A key role for foxQ2 in anterior head and central brain patterning in insects. Development 144, 2969–2981. https://doi.org/10.1242/dev.147637

Kollmann, M., Schmidt, R., Heuer, C.M., Schachtner, J., 2016. Variations on a Theme: Antennal Lobe Architecture across Coleoptera. PLOS ONE 11, e0166253. https://doi.org/10.1371/journal.pone.0166253

Koniszewski, N., 2011. Functional analysis of embryonic brain development in *Tribolium castaneum*. http://hdl.handle.net/11858/00-1735-0000-0006-AE25-0

Koniszewski, N.D.B., Kollmann, M., Bigham, M., Farnworth, M., He, B., Büscher, M., Hütteroth, W., Binzer, M., Schachtner, J., Bucher, G., 2016. The insect central complex as model for heterochronic brain development—background, concepts, and tools. Dev Genes Evol 226, 209–219. https://doi.org/10.1007/s00427-016-0542-7

Konstantinides, N., Degabriel, S., Desplan, C., 2018. Neuro-evo-devo in the single cell sequencing era. Current Opinion in Systems Biology, • Big data acquisition and analysis • Development and differentiation 11, 32–40. https://doi.org/10.1016/j.coisb.2018.08.001

Kotrschal, K., Van Staaden, M.J., Huber, R., 1998. Fish Brains: Evolution and Anvironmental Relationships. Reviews in Fish Biology and Fisheries 8, 373–408. https://doi.org/10.1023/A:1008839605380

Kraft, K.F., Massey, E.M., Kolb, D., Walldorf, U., Urbach, R., 2016. Retinal homeobox promotes cell growth, proliferation and survival of mushroom body neuroblasts in the *Drosophila* brain. Mechanisms of Development 142, 50–61. https://doi.org/10.1016/j.mod.2016.07.003

Kraft, K.F., Urbach, R., 2014. Analysis of Complete Neuroblast Cell Lineages in the *Drosophila* Embryonic Brain via DiI Labeling, in: Sprecher, S.G. (Ed.), Brain Development: Methods and Protocols, Methods in Molecular Biology. Humana Press, Totowa, NJ, pp. 37–56. https://doi.org/10.1007/978-1-62703-655-9_3

Kumar, A., Fung, S., Lichtneckert, R., Reichert, H., Hartenstein, V., 2009. Arborization pattern of *Engrailed* - positive neural lineages reveal neuromere boundaries in the *Drosophila* brain neuropil. The Journal of Comparative Neurology 517, 87–104. https://doi.org/10.1002/cne.22112

Kunz, T., Kraft, K.F., Technau, G.M., Urbach, R., 2012. Origin of *Drosophila* mushroom body neuroblasts and generation of divergent embryonic lineages. Development 139, 2510–2522. https://doi.org/10.1242/dev.077883

Kvon, E.Z., Kazmar, T., Stampfel, G., Yáñez-Cuna, J.O., Pagani, M., Schernhuber, K., Dickson, B.J., Stark, A., 2014. Genome-scale functional characterization of *Drosophila* developmental enhancers in vivo. Nature 512, 91–95. https://doi.org/10.1038/nature13395

Labun, K., Montague, T.G., Gagnon, J.A., Thyme, S.B., Valen, E., 2016. CHOPCHOP v2: a web tool for the next generation of CRISPR genome engineering. Nucleic Acids Res 44, W272–W276. https://doi.org/10.1093/nar/gkw398

Lai, S.-L., Doe, C.Q., 2014. Transient nuclear Prospero induces neural progenitor quiescence. eLife 3, e03363. https://doi.org/10.7554/eLife.03363

Lai, Y.-T., Deem, K.D., Borràs-Castells, F., Sambrani, N., Rudolf, H., Suryamohan, K., El-Sherif, E., Halfon, M.S., McKay, D.J., Tomoyasu, Y., 2018. Enhancer identification and activity evaluation in the red flour beetle, *Tribolium castaneum*. Development 145. https://doi.org/10.1242/dev.160663

Larsen, C., Shy, D., Spindler, S.R., Fung, S., Pereanu, W., Younossi-Hartenstein, A., Hartenstein, V., 2009. Patterns of growth, axonal extension and axonal arborization of neuronal lineages in the developing *Drosophila* brain. Developmental Biology 335, 289–304. https://doi.org/10.1016/j.ydbio.2009.06.015

Lee, C.-Y., Andersen, R.O., Cabernard, C., Manning, L., Tran, K.D., Lanskey, M.J., Bashirullah, A., Doe, C.Q., 2006. *Drosophila* Aurora-A kinase inhibits neuroblast self-renewal by regulating aPKC/Numb cortical polarity and spindle orientation. Genes Dev. 20, 3464–3474. https://doi.org/10.1101/gad.1489406

Lee, P.-T., Zirin, J., Kanca, O., Lin, W.-W., Schulze, K.L., Li-Kroeger, D., Tao, R., Devereaux, C., Hu, Y., Chung, V., Fang, Y., He, Y., Pan, H., Ge, M., Zuo, Z., Housden, B.E., Mohr, S.E., Yamamoto, S., Levis, R.W.,

Spradling, A.C., Perrimon, N., Bellen, H.J., 2018. A gene-specific T2A-GAL4 library for *Drosophila*. eLife 7, e35574. https://doi.org/10.7554/eLife.35574

Lee, T., Luo, L., 2001. Mosaic analysis with a repressible cell marker (MARCM) for *Drosophila* neural development. Trends in Neurosciences 24, 251–254. https://doi.org/10.1016/S0166-2236(00)01791-4

Lee, T., Marticke, S., Sung, C., Robinow, S., Luo, L., 2000a. Cell-Autonomous Requirement of the USP/EcR-B Ecdysone Receptor for Mushroom Body Neuronal Remodeling in *Drosophila*. Neuron 28, 807–818. https://doi.org/10.1016/S0896-6273(00)00155-0

Lee, T., Winter, C., Marticke, S.S., Lee, A., Luo, L., 2000b. Essential Roles of *Drosophila* RhoA in the Regulation of Neuroblast Proliferation and Dendritic but Not Axonal Morphogenesis. Neuron 25, 307–316. https://doi.org/10.1016/S0896-6273(00)80896-X

Lichtneckert, R., Reichert, H., 2008. Anteroposterior Regionalization of the Brain: Genetic and Comparative Aspects, in: Technau, G.M. (Ed.), Brain Development in *Drosophila* Melanogaster, Advances in Experimental Medicine and Biology. Springer New York, New York, NY, pp. 32–41. https://doi.org/10.1007/978-0-387-78261-4_2

Lichtneckert, R., Reichert, H., 2005. Insights into the urbilaterian brain: Conserved genetic patterning mechanisms in insect and vertebrate brain development. Heredity 94, 465–477. https://doi.org/10.1038/sj.hdy.6800664

Lihoreau, M., Latty, T., Chittka, L., 2012. An Exploration of the Social Brain Hypothesis in Insects. Front. Physiol. 3. https://doi.org/10.3389/fphys.2012.00442

Loesel, R., Nässel, D.R., Strausfeld, N.J., 2002. Common design in a unique midline neuropil in the brains of arthropods. Arthropod Structure and Development 31, 77–91. https://doi.org/10.1016/S1467-8039(02)00017-8

Logan, C.J., Avin, S., Boogert, N., Buskell, A., Cross, F.R., Currie, A., Jelbert, S., Lukas, D., Mares, R., Navarrete, A.F., Shigeno, S., Montgomery, S.H., 2018. Beyond brain size: Uncovering the neural correlates of behavioral and cognitive specialization. https://doi.org/10.3819/CCBR.2018.130008

London, N.J.S., Kessler, P., Williams, B., Pauer, G.J., Hagstrom, S.A., Traboulsi, E.I., 2009. Sequence alterations in RX in patients with microphthalmia, anophthalmia, and coloboma. Mol Vis 15, 162–167.

Lorenzen, M.D., Brown, S.J., Denell, R.E., Beeman, R.W., 2002. Cloning and characterization of the *Tribolium castaneum* eye-color genes encoding tryptophan oxygenase and kynurenine 3-monooxygenase. Genetics 160, 225–234.

Lorenzen, M.D., Kimzey, T., Shippy, T.D., Brown, S.J., Denell, R.E., Beeman, R.W., 2007. piggyBac-based insertional mutagenesis in *Tribolium castaneum* using donor/helper hybrids. Insect Mol Biol 16, 265–275.

Losos, J.B., 2014. The Princeton guide to evolution.

Lovick, J.K., Ngo, K.T., Omoto, J.J., Wong, D.C., Nguyen, J.D., Hartenstein, V., 2013. Postembryonic lineages of the *Drosophila* brain: I. Development of the lineage-associated fiber tracts. Developmental Biology 384, 228–257. https://doi.org/10.1016/j.ydbio.2013.07.008

Lovick, J.K., Omoto, J.J., Ngo, K.T., Hartenstein, V., 2017. Development of the anterior visual input pathway to the *Drosophila* central complex. J Comp Neurol 525, 3458–3475. https://doi.org/10.1002/cne.24277

Lowe, C.J., Wu, M., Salic, A., Evans, L., Lander, E., Stange-Thomann, N., Gruber, C.E., Gerhart, J., Kirschner, M., 2003. Anteroposterior Patterning in Hemichordates and the Origins of the Chordate Nervous System. Cell 113, 853–865. https://doi.org/10.1016/S0092-8674(03)00469-0

Lu, F., Kar, D., Gruenig, N., Zhang, Z.W., Cousins, N., Rodgers, H.M., Swindell, E.C., Jamrich, M., Schuurmans, C., Mathers, P.H., Kurrasch, D.M., 2013. Rax Is a Selector Gene for Mediobasal Hypothalamic Cell Types. J. Neurosci. 33, 259–272. https://doi.org/10.1523/JNEUROSCI.0913-12.2013

Ludwig, P., Williams, J.L.D., Lodde, E., Reichert, H., Boyan, G.S., 1999. Neurogenesis in the median domain of the embryonic brain of the grasshopper *Schistocerca gregaria*. Journal of Comparative Neurology 414, 379–390. https://doi.org/10.1002/(SICI)1096-9861(19991122)414:3<379::AID-CNE7>3.0.CO;2-5

Luque, J., Feldmann, R.M., Vernygora, O., Schweitzer, C.E., Cameron, C.B., Kerr, K.A., Vega, F.J., Duque, A., Strange, M., Palmer, A.R., Jaramillo, C., 2019. Exceptional preservation of mid-Cretaceous marine arthropods and the evolution of novel forms via heterochrony. Science Advances 5, eaav3875. https://doi.org/10.1126/sciadv.aav3875

Maddrell, S.H.P., 2018. How the simple shape and soft body of the larvae might explain the success of endopterygote insects. Journal of Experimental Biology 221, jeb177535. https://doi.org/10.1242/jeb.177535

Maeso Ignacio, Irimia Manuel, Tena Juan J., Casares Fernando, Gómez-Skarmeta José Luis, 2013. Deep conservation of cis-regulatory elements in metazoans. Philosophical Transactions of the Royal Society B: Biological Sciences 368, 20130020. https://doi.org/10.1098/rstb.2013.0020

Malaterre, J., Strambi, C., Aouane, A., Strambi, A., Rougon, G., Cayre, M., 2003. Effect of hormones and growth factors on the proliferation of adult cricket neural progenitor cells in vitro. Journal of Neurobiology 56, 387–397. https://doi.org/10.1002/neu.10244

Mali, P., Yang, L., Esvelt, K.M., Aach, J., Guell, M., DiCarlo, J.E., Norville, J.E., Church, G.M., 2013. RNA-Guided Human Genome Engineering via Cas9. Science 339, 823–826. https://doi.org/10.1126/science.1232033

Malun, D., Moseleit, A.D., Grünewald, B., 2003. 20-hydroxyecdysone inhibits the mitotic activity of neuronal precursors in the developing mushroom bodies of the honeybee, *Apis mellifera*. Journal of Neurobiology 57, 1–14. https://doi.org/10.1002/neu.10251

Manseau, L., Baradaran, A., Brower, D., Budhu, A., Elefant, F., Phan, H., Philp, A.V., Yang, M., Glover, D., Kaiser, K., Palter, K., Selleck, S., 1997. GAL4 enhancer traps expressed in the embryo, larval brain, imaginal discs, and ovary of *Drosophila*. Developmental Dynamics 209, 310–322. https://doi.org/10.1002/(SICI)1097-0177(199707)209:3<310::AID-AJA6>3.0.CO;2-L

Martín-Durán, J.M., Pang, K., Børve, A., Lê, H.S., Furu, A., Cannon, J.T., Jondelius, U., Hejnol, A., 2017. Convergent evolution of bilaterian nerve cords. Nature. https://doi.org/10.1038/nature25030

Martinez-De Luna, R.I., Kelly, L.E., El-Hodiri, H.M., 2011. The Retinal Homeobox (Rx) gene is necessary for retinal regeneration. Developmental Biology 353, 10–18. https://doi.org/10.1016/j.ydbio.2011.02.008

Mathers, P.H., Grinberg, A., Mahon, K.A., Jamrich, M., 1997. The Rx homeobox gene is essential for vertebrate eye development. Nature 387, 603–607. https://doi.org/10.1038/42475

Maurange, C., Cheng, L., Gould, A.P., 2008. Temporal Transcription Factors and Their Targets Schedule the End of Neural Proliferation in *Drosophila*. Cell 133, 891–902. https://doi.org/10.1016/j.cell.2008.03.034

Mazza, M.E., Pang, K., Reitzel, A.M., Martindale, M.Q., Finnerty, J.R., 2010. A conserved cluster of three PRD-class homeobox genes (*homeobrain, rx* and *orthopedia*) in the Cnidaria and Protostomia. EvoDevo 1, 3. https://doi.org/10.1186/2041-9139-1-3

McGuire, S.E., Mao, Z., Davis, R.L., 2004. Spatiotemporal Gene Expression Targeting with the TARGET and Gene-Switch Systems in *Drosophila*. Sci. STKE 2004, pl6–pl6. https://doi.org/10.1126/stke.2202004pl6

Medina-Martinez, O., Amaya-Manzanares, F., Liu, C., Mendoza, M., Shah, R., Zhang, L., Behringer, R.R., Mahon, K.A., Jamrich, M., 2009. Cell-Autonomous Requirement for Rx Function in the Mammalian Retina and Posterior Pituitary. PLOS ONE 4, e4513. https://doi.org/10.1371/journal.pone.0004513

Miller, I.F., Barton, R.A., Nunn, C.L., n.d. Quantitative uniqueness of human brain evolution revealed through phylogenetic comparative analysis. eLife 8. https://doi.org/10.7554/eLife.41250

Misof, B., *et al.* 2014. Phylogenomics resolves the timing and pattern of insect evolution. Science 346, 763–767. https://doi.org/10.1126/science.1257570

Moda, L.M., Vieira, J., Freire, A.C.G., Bonatti, V., Bomtorin, A.D., Barchuk, A.R., Simões, Z.L.P., 2013. Nutritionally Driven Differential Gene Expression Leads to Heterochronic Brain Development in Honeybee Castes. PLOS ONE 8, e64815. https://doi.org/10.1371/journal.pone.0064815

Mollereau, B., Wernet, M.F., Beaufils, P., Killian, D., Pichaud, F., Kühnlein, R., Desplan, C., 2000. A green fluorescent protein enhancer trap screen in *Drosophila* photoreceptor cells. Mechanisms of Development 93, 151–160. https://doi.org/10.1016/S0925-4773(00)00287-2

Monecke, T., Buschmann, J., Neumann, P., Wahle, E., Ficner, R., 2014. Crystal Structures of the Novel Cytosolic 5'-Nucleotidase IIIB Explain Its Preference for m7GMP. PLOS ONE 9, e90915. https://doi.org/10.1371/journal.pone.0090915

Montague, T.G., Cruz, J.M., Gagnon, J.A., Church, G.M., Valen, E., 2014. CHOPCHOP: a CRISPR/Cas9 and TALEN web tool for genome editing. Nucleic Acids Res 42, W401–W407. https://doi.org/10.1093/nar/gku410

Montgomery, S.H., Merrill, R.M., 2016. Divergence in brain composition during the early stages of ecological specialisation in *Heliconius* butterflies. Journal of Evolutionary Biology. https://doi.org/10.1111/jeb.13027

Montgomery, S.H., Mundy, N.I., Barton, R.A., 2016. Brain evolution and development: adaptation, allometry and constraint. Proc. R. Soc. B 283, 20160433. https://doi.org/10.1098/rspb.2016.0433

Moroz, L.L., *et al.* 2014. The ctenophore genome and the evolutionary origins of neural systems. Nature 510, 109–114. https://doi.org/10.1038/nature13400

Mossessova, E., Lima, C.D., 2000. Ulp1-SUMO Crystal Structure and Genetic Analysis Reveal Conserved Interactions and a Regulatory Element Essential for Cell Growth in Yeast. Molecular Cell 5, 865–876. https://doi.org/10.1016/S1097-2765(00)80326-3

Muscedere Mario L., Gronenberg Wulfila, Moreau Corrie S., Traniello James F. A., 2014. Investment in higher order central processing regions is not constrained by brain size in social insects. Proceedings of the Royal Society B: Biological Sciences 281, 20140217. https://doi.org/10.1098/rspb.2014.0217

Mysore, K., Subramanian, K.A., Sarasij, R.C., Suresh, A., Shyamala, B.V., VijayRaghavan, K., Rodrigues, V., 2009. Caste and sex specific olfactory glomerular organization and brain architecture in two sympatric ant species *Camponotus sericeus* and *Camponotus compressus* (Fabricius, 1798). Arthropod Structure & Development 38, 485–497. https://doi.org/10.1016/j.asd.2009.06.001

Namba, T., Huttner, W.B., 2017. Neural progenitor cells and their role in the development and evolutionary expansion of the neocortex. Wiley Interdisciplinary Reviews: Developmental Biology 6, e256. https://doi.org/10.1002/wdev.256

Nelson, S.M., Park, L., Stenkamp, D.L., 2009. Retinal homeobox 1 is required for retinal neurogenesis and photoreceptor differentiation in embryonic zebrafish. Developmental Biology 328, 24–39. https://doi.org/10.1016/j.ydbio.2008.12.040

Neubauer, S., Hublin, J.-J., Gunz, P., 2018. The evolution of modern human brain shape. Science Advances 4, eaao5961. https://doi.org/10.1126/sciadv.aao5961

Neumüller, R.A., Richter, C., Fischer, A., Novatchkova, M., Neumüller, K.G., Knoblich, J.A., 2011. Genome-Wide Analysis of Self-Renewal in *Drosophila* Neural Stem Cells by Transgenic RNAi. Cell Stem Cell 8, 580–593. https://doi.org/10.1016/j.stem.2011.02.022

Neuser, K., Triphan, T., Mronz, M., Poeck, B., Strauss, R., 2008. Analysis of a spatial orientation memory in *Drosophila*. Nature 453, 1244–1247. https://doi.org/10.1038/nature07003

Nielsen, C., Martinez, P., 2003. Patterns of gene expression: homology or homocracy? Dev Genes Evol 213, 149–154. https://doi.org/10.1007/s00427-003-0301-4

Nii, R., Oguchi, K., Shinji, J., Koshikawa, S., Miura, T., 2019. Reduction of a nymphal instar in a dampwood termite: heterochronic shift in the caste differentiation pathways. EvoDevo 10, 10. https://doi.org/10.1186/s13227-019-0123-8

Nijhout, H.F., Emlen, D.J., 1998. Competition among body parts in the development and evolution of insect morphology. Proc Natl Acad Sci U S A 95, 3685–3689.

Northcutt, R.G., 2002. Understanding Vertebrate Brain Evolution. Integr Comp Biol 42, 743–756. https://doi.org/10.1093/icb/42.4.743

Nunn, C.L., Barton, R.A., 2001. Comparative methods for studying primate adaptation and allometry. Evolutionary Anthropology: Issues, News, and Reviews 10, 81–98.

Nunn, C.L., Smith, K.K., 1998. Statistical Analyses of Developmental Sequences: The Craniofacial Region in Marsupial and Placental Mammals. The American Naturalist 152, 82–101. https://doi.org/10.1086/286151

O'Kane, C.J., Gehring, W.J., 1987. Detection *in situ* of genomic regulatory elements in *Drosophila*. Proceedings of the National Academy of Sciences 84, 9123–9127. https://doi.org/10.1073/pnas.84.24.9123

Omoto, J.J., Keleş, M.F., Nguyen, B.-C.M., Bolanos, C., Lovick, J.K., Frye, M.A., Hartenstein, V., 2017. Visual Input to the *Drosophila* Central Complex by Developmentally and Functionally Distinct Neuronal Populations. Current Biology 27, 1098–1110. https://doi.org/10.1016/j.cub.2017.02.063

Ostrovsky, A., Cachero, S., Jefferis, G., 2013. Clonal Analysis of Olfaction in *Drosophila*: Immunochemistry and Imaging of Fly Brains. Cold Spring Harb Protoc 2013, pdb.prot071720. https://doi.org/10.1101/pdb.prot071720

Pai, A., 2019. *Tribolium*☆, in: Choe, J.C. (Ed.), Encyclopedia of Animal Behavior (Second Edition). Academic Press, Oxford, pp. 231–241. https://doi.org/10.1016/B978-0-12-809633-8.01216-4

Pan, Y., Martinez-De Luna, R.I., Lou, C.-H., Nekkalapudi, S., Kelly, L.E., Sater, A.K., El-Hodiri, H.M., 2010. Regulation of photoreceptor gene expression by the retinal homeobox (Rx) gene product. Developmental Biology, Special Section: Gene Expression and Development 339, 494–506. https://doi.org/10.1016/j.ydbio.2009.12.032

Panov, A.A., 1959. Structure of the insect brain at successive stages of postembryonic development. II. the central body. Entomological Review 38, 276–283.

Payne, J.L., Wagner, A., 2019. The causes of evolvability and their evolution. Nature Reviews Genetics 20, 24. https://doi.org/10.1038/s41576-018-0069-z

Pereanu, W., Hartenstein, V., 2006. Neural lineages of the *Drosophila* brain: a three-dimensional digital atlas of the pattern of lineage location and projection at the late larval stage. J. Neurosci. 26, 5534–5553. https://doi.org/10.1523/JNEUROSCI.4708-05.2006

Pereanu, W., Kumar, A., Jennett, A., Reichert, H., Hartenstein, V., 2010. Development-based compartmentalization of the *Drosophila* central brain. Journal of Comparative Neurology 518, 2996–3023. https://doi.org/10.1002/cne.22376

Perry, M., Konstantinides, N., Pinto-Teixeira, F., Desplan, C., 2017. Generation and Evolution of Neural Cell Types and Circuits: Insights from the *Drosophila* Visual System. Annu. Rev. Genet. 51, 501–527. https://doi.org/10.1146/annurev-genet-120215-035312

Peters, R.S., Meusemann, K., Petersen, M., Mayer, C., Wilbrandt, J., Ziesmann, T., Donath, A., Kjer, K.M., Aspöck, U., Aspöck, H., Aberer, A., Stamatakis, A., Friedrich, F., Hünefeld, F., Niehuis, O., Beutel, R.G., Misof, B., 2014. The evolutionary history of holometabolous insects inferred from transcriptome-based phylogeny and comprehensive morphological data. BMC Evolutionary Biology 14, 52. https://doi.org/10.1186/1471-2148-14-52

Pfeiffer, B.D., Jenett, A., Hammonds, A.S., Ngo, T.-T.B., Misra, S., Murphy, C., Scully, A., Carlson, J.W., Wan, K.H., Laverty, T.R., Mungall, C., Svirskas, R., Kadonaga, J.T., Doe, C.Q., Eisen, M.B., Celniker, S.E., Rubin, G.M., 2008. Tools for neuroanatomy and neurogenetics in *Drosophila*. Proc. Natl. Acad. Sci. U.S.A. 105, 9715–9720. https://doi.org/10.1073/pnas.0803697105

Pfeiffer, B.D., Ngo, T.-T.B., Hibbard, K.L., Murphy, C., Jenett, A., Truman, J.W., Rubin, G.M., 2010. Refinement of tools for targeted gene expression in *Drosophila*. Genetics 186, 735–755. https://doi.org/10.1534/genetics.110.119917

Pfeiffer, K., Homberg, U., 2014. Organization and Functional Roles of the Central Complex in the Insect Brain. Annual Review of Entomology 59, 165–184. https://doi.org/10.1146/annurev-ento-011613-162031

Pigliucci, M., 2008. Is evolvability evolvable? Nature Reviews Genetics 9, 75–82. https://doi.org/10.1038/nrg2278

Pinto-Teixeira, F., Konstantinides, N., Desplan, C., 2017. Programmed cell death acts at different stages of *Drosophila* neurodevelopment to shape the central nervous system. FEBS Letters 2435–2453. https://doi.org/10.1002/1873-3468.12298@10.1002/(ISSN)1873-3468(CAT)FreeReviewContent(VI)SIReviews

Pollen, A.A., Bhaduri, A., Andrews, M.G., Nowakowski, T.J., Meyerson, O.S., Mostajo-Radji, M.A., Di Lullo, E., Alvarado, B., Bedolli, M., Dougherty, M.L., Fiddes, I.T., Kronenberg, Z.N., Shuga, J., Leyrat, A.A., West, J.A., Bershteyn, M., Lowe, C.B., Pavlovic, B.J., Salama, S.R., Haussler, D., Eichler, E.E., Kriegstein, A.R., 2019. Establishing Cerebral Organoids as Models of Human-Specific Brain Evolution. Cell 176, 743-756.e17. https://doi.org/10.1016/j.cell.2019.01.017

Poon, C.L.C., Mitchell, K.A., Kondo, S., Cheng, L.Y., Harvey, K.F., 2016. The Hippo Pathway Regulates Neuroblasts and Brain Size in *Drosophila melanogaster*. Current Biology 26, 1034–1042. https://doi.org/10.1016/j.cub.2016.02.009

Port, F., Chen, H.-M., Lee, T., Bullock, S.L., 2014. Optimized CRISPR/Cas tools for efficient germline and somatic genome engineering in *Drosophila*. Proceedings of the National Academy of Sciences 111, E2967–E2976. https://doi.org/10.1073/pnas.1405500111

Posnien, N., Koniszewski, N.D.B., Hein, H.J., Bucher, G., 2011. Candidate Gene Screen in the Red Flour Beetle *Tribolium* Reveals Six3 as Ancient Regulator of Anterior Median Head and Central Complex Development. PLoS Genetics 7, e1002416. https://doi.org/10.1371/journal.pgen.1002416

Posnien, N., Schinko, J., Grossmann, D., Shippy, T.D., Konopova, B., Bucher, G., 2009. RNAi in the Red Flour Beetle (*Tribolium*). Cold Spring Harb Protoc 2009, pdb.prot5256. https://doi.org/10.1101/pdb.prot5256

Posnien, N., Schinko, J.B., Kittelmann, S., Bucher, G., 2010. Genetics, development and composition of the insect head - A beetle's view. Arthropod Structure and Development 39, 399–410. https://doi.org/10.1016/j.asd.2010.08.002

Powell, L.E., Isler, K., Barton, R.A., 2017. Re-evaluating the link between brain size and behavioural ecology in primates. Proc. R. Soc. B 284, 20171765. https://doi.org/10.1098/rspb.2017.1765

Prieto-Godino, L.L., Rytz, R., Cruchet, S., Bargeton, B., Abuin, L., Silbering, A.F., Ruta, V., Dal Peraro, M., Benton, R., 2017. Evolution of Acid-Sensing Olfactory Circuits in Drosophilids. Neuron 93, 661-676.e6. https://doi.org/10.1016/j.neuron.2016.12.024

Prokop, A., Technau, G.M., 1994. Normal Function of the mushroom body defect Gene of *Drosophila* Is Required for the Regulation of the Number and Proliferation of Neuroblasts. Developmental Biology 161, 321–337. https://doi.org/10.1006/dbio.1994.1034

Rabinovich, D., Yaniv, S.P., Alyagor, I., Schuldiner, O., 2016. Nitric Oxide as a Switching Mechanism between Axon Degeneration and Regrowth during Developmental Remodeling. Cell 164, 170–182. https://doi.org/10.1016/j.cell.2015.11.047

Raff, E.C., Raff, R.A., 2000. Dissociability, modularity, evolvability. Evolution & Development 2, 235–237. https://doi.org/10.1046/j.1525-142x.2000.00069.x

Raff, R.A., 2000. Evo-devo: the evolution of a new discipline. Nature Reviews Genetics 1, 74. https://doi.org/10.1038/35049594

Raff, R.A., 1996. The shape of life: Genes, Development and the Evolution of Animal Form. Univ. Chicago Press, Chicago.

Raff, R.A., Wray, G.A., 1989. Heterochrony: Developmental mechanisms and evolutionary results. Journal of Evolutionary Biology 2, 409–434. https://doi.org/10.1046/j.1420-9101.1989.2060409.x

Reichert, H., 2009. Evolutionary conservation of mechanisms for neural regionalization, proliferation and interconnection in brain development. Biology Letters 5, 112–116. https://doi.org/10.1098/rsbl.2008.0337

Reichert, H., Boyan, G., 1997. Building a brain: developmental insights in insects. Trends in Neurosciences 20, 258–264. https://doi.org/10.1016/S0166-2236(96)01034-X

Reuter, J.E., Nardine, T.M., Penton, A., Billuart, P., Scott, E.K., Usui, T., Uemura, T., Luo, L., 2003. A mosaic genetic screen for genes necessary for *Drosophila* mushroom body neuronal morphogenesis. Development 130, 1203–1213. https://doi.org/10.1242/dev.00319

Riddiford, L.M., Truman, J.W., Mirth, C.K., Shen, Y., 2010. A role for juvenile hormone in the prepupal development of *Drosophila melanogaster*. Development 137, 1117–1126. https://doi.org/10.1242/dev.037218

Riddiford, L.M., Truman, J.W., Nern, A., 2018. Juvenile hormone reveals mosaic developmental programs in the metamorphosing optic lobe of *Drosophila melanogaster*. Biology Open 7, bio034025. https://doi.org/10.1242/bio.034025

Riebli, N., Viktorin, G., Reichert, H., 2013. Early-born neurons in type II neuroblast lineages establish a larval primordium and integrate into adult circuitry during central complex development in *Drosophila*. Neural Dev 8, 6. https://doi.org/10.1186/1749-8104-8-6

Riemensperger, T., Isabel, G., Coulom, H., Neuser, K., Seugnet, L., Kume, K., Iché-Torres, M., Cassar, M., Strauss, R., Preat, T., Hirsh, J., Birman, S., 2011. Behavioral consequences of dopamine deficiency in the *Drosophila* central nervous system. Proceedings of the National Academy of Sciences 108, 834–839. https://doi.org/10.1073/pnas.1010930108

Roberts, D.B. (Ed.), 1998. *Drosophila*: a practical approach, 2nd ed. ed, Practical approach series. IRL Press at Oxford University Press, Oxford, [Eng.] ; New York.

Rothwell, W.F., Sullivan, W., 2007. Fixation of *Drosophila* Embryos. Cold Spring Harb Protoc 2007, pdb.prot4827. https://doi.org/10.1101/pdb.prot4827

Rylee, J.C., Siniard, D.J., Doucette, K., Zentner, G.E., Zelhof, A.C., 2018. Expanding the genetic toolkit of *Tribolium castaneum*. PLOS ONE 13, e0195977. https://doi.org/10.1371/journal.pone.0195977

Sanjana, N.E., Cong, L., Zhou, Y., Cunniff, M.M., Feng, G., Zhang, F., 2012. A transcription activator-like effector toolbox for genome engineering. Nature Protocols 7, 171–192. https://doi.org/10.1038/nprot.2011.431

Sarov, M., Barz, C., Jambor, H., Hein, M.Y., Schmied, C., Suchold, D., Stender, B., Janosch, S., Kj, V.V., Krishnan, R.T., Krishnamoorthy, A., Ferreira, I.R., Ejsmont, R.K., Finkl, K., Hasse, S., Kämpfer, P., Plewka, N., Vinis, E., Schloissnig, S., Knust, E., Hartenstein, V., Mann, M., Ramaswami, M., VijayRaghavan, K., Tomancak, P., Schnorrer, F., 2016. A genome-wide resource for the analysis of protein localisation in *Drosophila*. eLife 5, e12068. https://doi.org/10.7554/eLife.12068

Sarrazin, A.F., Peel, A.D., Averof, M., 2012. A Segmentation Clock with Two-Segment Periodicity in Insects. Science 336, 338–341. https://doi.org/10.1126/science.1218256

Schindelin, J., Arganda-Carreras, I., Frise, E., Kaynig, V., Longair, M., Pietzsch, T., Preibisch, S., Rueden, C., Saalfeld, S., Schmid, B., Tinevez, J.-Y., White, D.J., Hartenstein, V., Eliceiri, K., Tomancak, P., Cardona, A., 2012. Fiji: an open-source platform for biological-image analysis. Nat Methods 9, 676–682. https://doi.org/10.1038/nmeth.2019

Schinko, J., Posnien, N., Kittelmann, S., Koniszewski, N., Bucher, G., 2009. Single and Double Whole-Mount *In situ* Hybridization in Red Flour Beetle (*Tribolium*) Embryos. Cold Spring Harb Protoc 2009, pdb.prot5258. https://doi.org/10.1101/pdb.prot5258

Schinko, J.B., Hillebrand, K., Bucher, G., 2012. Heat shock-mediated misexpression of genes in the beetle *Tribolium castaneum*. Development Genes and Evolution 222, 287–298. https://doi.org/10.1007/s00427-012-0412-x

Schinko, J.B., Weber, M., Viktorinova, I., Kiupakis, A., Averof, M., Klingler, M., Wimmer, E.A., Bucher, G., 2010. Functionality of the GAL4/UAS system in *Tribolium* requires the use of endogenous core promoters. BMC Developmental Biology 10, 53. https://doi.org/10.1186/1471-213X-10-53

Schmitt-Engel, C., Schultheis, D., Schwirz, J., Ströhlein, N., Troelenberg, N., Majumdar, U., Dao, V.A., Grossmann, D., Richter, T., Tech, M., Dönitz, J., Gerischer, L., Theis, M., Schild, I., Trauner, J., Koniszewski, N.D.B., Küster, E., Kittelmann, S., Hu, Y., Lehmann, S., Siemanowski, J., Ulrich, J., Panfilio, K.A., Schröder, R., Morgenstern, B., Stanke, M., Buchhholz, F., Frasch, M., Roth, S., Wimmer, E.A., Schoppmeier, M., Klingler, M., Bucher, G., 2015. The iBeetle large-scale RNAi screen reveals gene functions for insect development and physiology. Nature Communications 6, 7822. https://doi.org/10.1038/ncomms8822

Scholtz, G., 2001. Evolution of developmental patterns in arthropods: the analysis of gene expression and its bearing on morphology and phylogenetics. Zoology 103, 99–111.

Scholtz, G., Gerberding, M., 2002. Cell Lineage of Crustacean Neuroblasts, in: Wiese, K. (Ed.), The Crustacean Nervous System. Springer Berlin Heidelberg, pp. 406–416.

Schubiger, M., Wade, A.A., Carney, G.E., Truman, J.W., Bender, M., 1998. *Drosophila* EcR-B ecdysone receptor isoforms are required for larval molting and for neuron remodeling during metamorphosis. Development 125, 2053–2062.

Schuldiner, O., Yaron, A., 2015. Mechanisms of developmental neurite pruning. Cell. Mol. Life Sci. 72, 101–119. https://doi.org/10.1007/s00018-014-1729-6

Schulz-Mirbach, T., Eifert, C., Riesch, R., Farnworth, M.S., Zimmer, C., Bierbach, D., Klaus, S., Tobler, M., Streit, B., Indy, J.R., Arias-Rodriguez, L., Plath, M., 2016. Toxic hydrogen sulphide shapes brain anatomy: a comparative study of sulphide-adapted ecotypes in the *Poecilia mexicana* complex. Journal of Zoology. https://doi.org/10.1111/jzo.12366

Sherwood, C.C., Gómez-Robles, A., 2017. Brain Plasticity and Human Evolution. Annual Review of Anthropology 46, 399–419. https://doi.org/10.1146/annurev-anthro-102215-100009

Shihavuddin, A., Basu, S., Rexhepaj, E., Delestro, F., Menezes, N., Sigoillot, S.M., Del Nery, E., Selimi, F., Spassky, N., Genovesio, A., 2017. Smooth 2D manifold extraction from 3D image stack. Nature Communications 8, 15554. https://doi.org/10.1038/ncomms15554

Siemanowski, J., Richter, T., Dao, V.A., Bucher, G., 2015. Notch signaling induces cell proliferation in the labrum in a regulatory network different from the thoracic legs. Dev. Biol. 408, 164–177. https://doi.org/10.1016/j.ydbio.2015.09.018

Simões, A.R., Rhiner, C., 2017. A Cold-Blooded View on Adult Neurogenesis. Front. Neurosci. 11. https://doi.org/10.3389/fnins.2017.00327

Sipe, C.W., Siegrist, S.E., 2017. Eyeless uncouples mushroom body neuroblast proliferation from dietary amino acids in *Drosophila*. eLife 6, e26343. https://doi.org/10.7554/eLife.26343

Smale, S.T., Kadonaga, J.T., 2003. The RNA Polymerase II Core Promoter. Annual Review of Biochemistry 72, 449–479. https://doi.org/10.1146/annurev.biochem.72.121801.161520

Smith, K.K., 2003. Time's arrow: heterochrony and the evolution of development. Int. J. Dev. Biol. 47, 613–621.

Smith, K.K., 2002. Sequence Heterochrony and the Evolution of Development. Journal of Morphology 252, 82–97. https://doi.org/10.1002/jmor.10014

Smith, K.K., 2001. Heterochrony revisited: the evolution of developmental sequences. Biol J Linn Soc 73, 169–186. https://doi.org/10.1111/j.1095-8312.2001.tb01355.x

Sokoloff, A., 1974. The Biology of *Tribolium*. Clarendon Press, Oxford.

Sokoloff, A., 1972. The biology of *Tribolium*: with special emphasis on genetic aspects. Clarendon Press, Oxford.

Sommer, R.J., 2009. The future of evo–devo: model systems and evolutionary theory. Nature Reviews Genetics 10, 416–422. https://doi.org/10.1038/nrg2567

Sousa-Nunes, R., Yee, L.L., Gould, A.P., 2011. Fat cells reactivate quiescent neuroblasts via TOR and glial insulin relays in *Drosophila*. Nature 471, 508–512. https://doi.org/10.1038/nature09867

Spindler, S.R., Hartenstein, V., 2010. The *Drosophila* neural lineages: a model system to study brain development and circuitry. Development Genes and Evolution 220, 1–10. https://doi.org/10.1007/s00427-010-0323-7

Steinmetz, P.R., Urbach, R., Posnien, N., Eriksson, J., Kostyuchenko, R.P., Brena, C., Guy, K., Akam, M., Bucher, G., Arendt, D., 2010. Six3 demarcates the anterior-most developing brain region in bilaterian animals. EvoDevo 1, 14. https://doi.org/10.1186/2041-9139-1-14

Stöckl, A., Heinze, S., Charalabidis, A., el Jundi, B., Warrant, E., Kelber, A., 2016. Differential investment in visual and olfactory brain areas reflects behavioural choices in hawk moths. Scientific Reports 6, 26041. https://doi.org/10.1038/srep26041

Stollewerk, A., 2016. A flexible genetic toolkit for arthropod neurogenesis. Philosophical Transactions of the Royal Society B: Biological Sciences 371, 20150044. https://doi.org/10.1098/rstb.2015.0044

Stork, N.E., 2018. How Many Species of Insects and Other Terrestrial Arthropods Are There on Earth? Annual Review of Entomology 63, 31–45. https://doi.org/10.1146/annurev-ento-020117-043348

Stork, N.E., McBroom, J., Gely, C., Hamilton, A.J., 2015. New approaches narrow global species estimates for beetles, insects, and terrestrial arthropods. Proceedings of the National Academy of Sciences 112, 7519–7523. https://doi.org/10.1073/pnas.1502408112

Strausfeld N.J., Hirth Frank, 2016. Introduction to 'Homology and convergence in nervous system evolution.' Philosophical Transactions of the Royal Society B: Biological Sciences 371, 20150034. https://doi.org/10.1098/rstb.2015.0034

Strausfeld, N.J., 2019. The Divergent Evolution of Arthropod Brains: Ground Pattern Organization and Stability Through Geological Time, in: Byrne, J.H. (Ed.), The Oxford Handbook of Invertebrate Neurobiology. Oxford University Press, pp. 30–70. https://doi.org/10.1093/oxfordhb/9780190456757.013.2

Strausfeld, N.J., 2012. Arthropod Brains: Evolution, functional elegance, and historical significance. The Belknap Press of Harvard University Press.

Strausfeld, N.J., 2009. Brain organization and the origin of insects: an assessment. Proceedings of the Royal Society of London B: Biological Sciences rspb.2008.1471. https://doi.org/10.1098/rspb.2008.1471

Strausfeld, N.J., 2005. The evolution of crustacean and insect optic lobes and the origins of chiasmata. Arthropod Structure & Development, Arthropod Brain Morphology and Evolution 34, 235–256. https://doi.org/10.1016/j.asd.2005.04.001

Strausfeld, N.J., 1999. Chapter 24 A Brain Region in Insects That Supervises Walking, in: Binder, M.D. (Ed.), Progress in Brain Research, Peripheral and Spinal Mechanisms in the Neural Control of Movement. Elsevier, pp. 273–284. https://doi.org/10.1016/S0079-6123(08)62863-0

Strausfeld, N.J., 1998. Crustacean – Insect Relationships: The Use of Brain Characters to Derive Phylogeny amongst Segmented Invertebrates. BBE 52, 186–206. https://doi.org/10.1159/000006563

Strausfeld, N. J., Hirth, F., 2013. Deep Homology of Arthropod Central Complex and Vertebrate Basal Ganglia. Science 340, 157–161. https://doi.org/10.1126/science.1231828

Strausfeld, Nicholas J., Hirth, F., 2013. Homology versus Convergence in Resolving Transphyletic Correspondences of Brain Organization. BBE 82, 215–219. https://doi.org/10.1159/000356102

Strausfeld, N.J., Ma, X., Edgecombe, G.D., 2016. Fossils and the Evolution of the Arthropod Brain. Current Biology 26, R989–R1000. https://doi.org/10.1016/j.cub.2016.09.012

Strausfeld, N.J., Sinakevitch, I., Brown, S.M., Farris, S.M., 2009. Ground plan of the insect mushroom body: Functional and evolutionary implications. Journal of Comparative Neurology 513, 265–291. https://doi.org/10.1002/cne.21948

Strauss, R., Heisenberg, M., 1993. A higher control center of locomotor behavior in the *Drosophila* brain. J. Neurosci. 13, 1852–1861. https://doi.org/10.1523/JNEUROSCI.13-05-01852.1993

Strickler, A.G., Famuditimi, K., Jeffery, W.R., 2002. Retinal homeobox genes and the role of cell proliferation in cavefish eye degeneration. Int. J. Dev. Biol. 46, 285–294. https://doi.org/10.1387/ijdb.12068949

Striedter, G.F., 2005. Principles of brain evolution. Sinauer Associates, Sunderland, Mass.

Striedter, G.F., 2002. Brain homology and function: an uneasy alliance. Brain research bulletin 57, 239–242.

Strobl, F., Ross, J.A., Stelzer, E.H.K., 2017. Non-lethal genotyping of *Tribolium castaneum* adults using genomic DNA extracted from wing tissue. PLOS ONE 12, e0182564. https://doi.org/10.1371/journal.pone.0182564

Strobl, F., Stelzer, E.H., 2016. Long-term fluorescence live imaging of *Tribolium castaneum* embryos: principles, resources, scientific challenges and the comparative approach. Current Opinion in Insect Science 18, 17–26. https://doi.org/10.1016/j.cois.2016.08.002

Strobl, F., Stelzer, E.H.K., 2014. Non-invasive long-term fluorescence live imaging of *Tribolium castaneum* embryos. Development 141, 2331–2338. https://doi.org/10.1242/dev.108795

Sullivan, L.F., Warren, T.L., Doe, C.Q., 2019. Temporal identity establishes columnar neuron morphology, connectivity, and function in a *Drosophila* navigation circuit. eLife 8, e43482. https://doi.org/10.7554/eLife.43482

Suzuki, T., Sato, M., 2017. Inter-progenitor pool wiring: An evolutionarily conserved strategy that expands neural circuit diversity. Developmental Biology 431, 101–110. https://doi.org/10.1016/j.ydbio.2017.09.029

Szymczak-Workman, A.L., Vignali, K.M., Vignali, D.A.A., 2012. Design and Construction of 2A Peptide-Linked Multicistronic Vectors. Cold Spring Harbor Protocols 2012, pdb.ip067876-pdb.ip067876. https://doi.org/10.1101/pdb.ip067876

Tessmar-Raible, K., Raible, F., Christodoulou, F., Guy, K., Rembold, M., Hausen, H., Arendt, D., 2007. Conserved Sensory-Neurosecretory Cell Types in Annelid and Fish Forebrain: Insights into Hypothalamus Evolution. Cell 129, 1389–1400. https://doi.org/10.1016/j.cell.2007.04.041

Thoen, H.H., Marshall, J., Wolff, G.H., Strausfeld, N.J., 2017. Insect-Like Organization of the Stomatopod Central Complex: Functional and Phylogenetic Implications. Front. Behav. Neurosci. 11. https://doi.org/10.3389/fnbeh.2017.00012

Tomoyasu, Y., Denell, R.E., 2004. Larval RNAi in *Tribolium* (Coleoptera) for analyzing adult development. Dev Genes Evol 214, 575–578. https://doi.org/10.1007/s00427-004-0434-0

Tosches, M.A., Arendt, D., 2013. The bilaterian forebrain: an evolutionary chimaera. Current Opinion in Neurobiology, Development of neurons and glia 23, 1080–1089. https://doi.org/10.1016/j.conb.2013.09.005

Trauner, J., Schinko, J., Lorenzen, M.D., Shippy, T.D., Wimmer, E.A., Beeman, R.W., Klingler, M., Bucher, G., Brown, S.J., 2009. Large-scale insertional mutagenesis of a coleopteran stored grain pest, the red flour beetle *Tribolium castaneum*, identifies embryonic lethal mutations and enhancer traps. BMC Biology 7, 73. https://doi.org/10.1186/1741-7007-7-73

Tribolium Genome Sequencing Consortium, Richards, S. *et al.* 2008. The genome of the model beetle and pest *Tribolium castaneum*. Nature 452, 949–955. https://doi.org/10.1038/nature06784

Truman, J.W., Riddiford, L.M., 2002. Endocrine Insights into the Evolution of Metamorphosis in Insects. Annu. Rev. Entomol. 47, 467–500. https://doi.org/10.1146/annurev.ento.47.091201.145230

Truman, J.W., Riddiford, L.M., 1999. The origins of insect metamorphosis. Nature 401, 447. https://doi.org/10.1038/46737

Tsuboi, M., Bijl, W. van der, Kopperud, B.T., Erritzøe, J., Voje, K.L., Kotrschal, A., Yopak, K.E., Collin, S.P., Iwaniuk, A.N., Kolm, N., 2018. Breakdown of brain–body allometry and the encephalization of birds and mammals. Nature Ecology & Evolution 2, 1492. https://doi.org/10.1038/s41559-018-0632-1

Tsuboi, M., Gonzalez-Voyer, A., Kolm, N., 2014. Phenotypic integration of brain size and head morphology in Lake Tanganyika Cichlids. BMC evolutionary biology 14, 1.

Tsuji, T., Hasegawa, E., Isshiki, T., 2008. Neuroblast entry into quiescence is regulated intrinsically by the combined action of spatial Hox proteins and temporal identity factors. Development 135, 3859–3869. https://doi.org/10.1242/dev.025189

Tycko, J., Myer, V.E., Hsu, P.D., 2016. Methods for Optimizing CRISPR-Cas9 Genome Editing Specificity. Molecular Cell 63, 355–370. https://doi.org/10.1016/j.molcel.2016.07.004

Uhlen, M., Bandrowski, A., Carr, S., Edwards, A., Ellenberg, J., Lundberg, E., Rimm, D.L., Rodriguez, H., Hiltke, T., Snyder, M., Yamamoto, T., 2016. A proposal for validation of antibodies. Nat. Methods 13, 823–827. https://doi.org/10.1038/nmeth.3995

Ulrich, A., Andersen, K.R., Schwartz, T.U., 2012. Exponential Megapriming PCR (EMP) Cloning—Seamless DNA Insertion into Any Target Plasmid without Sequence Constraints. PLOS ONE 7, e53360. https://doi.org/10.1371/journal.pone.0053360

Urbach, R., Technau, G.M., 2008. Dorsoventral patterning of the brain: a comparative approach. Advances in experimental medicine and biology 628, 42–56.

Urbach, R., Technau, G.M., 2004. Neuroblast formation and patterning during early brain development in *Drosophila*. Bioessays 26, 739–751. https://doi.org/10.1002/bies.20062

Urbach, R., Technau, G.M., 2003a. Early steps in building the insect brain: neuroblast formation and segmental patterning in the developing brain of different insect species. Arthropod Structure & Development 32, 103–123. https://doi.org/10.1016/S1467-8039(03)00042-2

Urbach, R., Technau, G.M., 2003b. Molecular markers for identified neuroblasts in the developing brain of *Drosophila*. Development 130, 3621–3637. https://doi.org/10.1242/dev.00533

van Schaik, C.P., Isler, K., Burkart, J.M., 2012. Explaining brain size variation: from social to cultural brain. Trends in Cognitive Sciences 16, 277–284. https://doi.org/10.1016/j.tics.2012.04.004

Viktorin, G., 2014. Using MARCM to Study *Drosophila* Brain Development, in: Sprecher, S.G. (Ed.), Brain Development: Methods and Protocols, Methods in Molecular Biology. Humana Press, Totowa, NJ, pp. 79–96. https://doi.org/10.1007/978-1-62703-655-9_6

Wagner Andreas, 2008. Robustness and evolvability: a paradox resolved. Proceedings of the Royal Society B: Biological Sciences 275, 91–100. https://doi.org/10.1098/rspb.2007.1137

Walsh, K.T., Doe, C.Q., 2017. *Drosophila* embryonic type II neuroblasts: origin, temporal patterning, and contribution to the adult central complex. Development 144, 4552–4562. https://doi.org/10.1242/dev.157826

Watanabe, T., Noji, S., Mito, T., 2017. Genome Editing in the Cricket, *Gryllus bimaculatus*, in: Hatada, I. (Ed.), Genome Editing in Animals: Methods and Protocols, Methods in Molecular Biology. Springer New York, New York, NY, pp. 219–233. https://doi.org/10.1007/978-1-4939-7128-2_18

Wegerhoff, R., 1999. GABA and serotonin immunoreactivity during postembryonic brain development in the beetle *Tenebrio molitor*. Microscopy Research and Technique 45, 154–164. https://doi.org/10.1002/(SICI)1097-0029(19990501)45:3<154::AID-JEMT3>3.0.CO;2-5

Wegerhoff, R., Breidbach, O., 1992. Structure and development of the larval central complex in a holometabolous insect, the beetle *Tenebrio molitor*. Cell & Tissue Research 268, 341–358. https://doi.org/10.1007/BF00318803

Wegerhoff, R., Breidbach, O., Lobemeier, M., 1996. Development of locustatachykinin immunopositive neurons in the central complex of the beetle *Tenebrio molitor*. Journal of Comparative Neurology 375, 157–166. https://doi.org/10.1002/(SICI)1096-9861(19961104)375:1<157::AID-CNE10>3.0.CO;2-S

Whitfield, J.B., Doyen, J.T., Purcell, A.H., Daly, H.V., 2013. Daly and Doyen's introduction to insect biology and diversity, 3rd ed. ed. Oxford University Press, New York.

Williams, J.L., Boyan, G.S., 2008. Building the central complex of the grasshopper *Schistocerca gregaria*: axons pioneering the w, x, y, z tracts project onto the primary commissural fascicle of the brain. Arthropod Struct Dev 37, 129–40.

Williams, J.L.D., 1975. Anatomical studies of the insect central nervous system: a ground plan of the midbrain and an introduction to the central complex in the locust *Schistocerca gregaria* (Orthoptera). Journal of Zoology 204, 1269–1280.

Wilson, C., Bellen, H., Gehring, W., 1990. Position Effects on Eukaryotic Gene-Expression. Annu. Rev. Cell Biol. 6, 679–714. https://doi.org/10.1146/annurev.cb.06.110190.003335

Wolff Gabriella H., Strausfeld Nicholas J., 2016. Genealogical correspondence of a forebrain centre implies an executive brain in the protostome–deuterostome bilaterian ancestor. Philosophical Transactions of the Royal Society B: Biological Sciences 371, 20150055. https://doi.org/10.1098/rstb.2015.0055

Wolff, G.H., Strausfeld, N.J., 2015. Genealogical Correspondence of Mushroom Bodies across Invertebrate Phyla. Current Biology 25, 38–44. https://doi.org/10.1016/j.cub.2014.10.049

Wolff, T., Iyer, N.A., Rubin, G.M., 2015. Neuroarchitecture and neuroanatomy of the *Drosophila* central complex: A GAL4-based dissection of protocerebral bridge neurons and circuits. Journal of Comparative Neurology 523, 997–1037. https://doi.org/10.1002/cne.23705

Wolff, T., Rubin, G.M., 2018. Neuroarchitecture of the *Drosophila* central complex: A catalog of nodulus and asymmetrical body neurons and a revision of the protocerebral bridge catalog. J Comp Neurol 526, 2585–2611. https://doi.org/10.1002/cne.24512

Wong, D.C., Lovick, J.K., Ngo, K.T., Borisuthirattana, W., Omoto, J.J., Hartenstein, V., 2013. Postembryonic lineages of the *Drosophila* brain: II. Identification of lineage projection patterns based on MARCM clones. Developmental Biology 384, 258–289. https://doi.org/10.1016/j.ydbio.2013.07.009

Wu, J.S., Luo, L., 2006. A protocol for dissecting *Drosophila melanogaster* brains for live imaging or immunostaining. Nature Protocols 1, 2110–2115. https://doi.org/10.1038/nprot.2006.336

Wynant, N., Verlinden, H., Breugelmans, B., Simonet, G., Vanden Broeck, J., 2012. Tissue-dependence and sensitivity of the systemic RNA interference response in the desert locust, *Schistocerca gregaria*. Insect Biochemistry and Molecular Biology 42, 911–917. https://doi.org/10.1016/j.ibmb.2012.09.004

Yang, J.S., Awasaki, T., Yu, H.-H., He, Y., Ding, P., Kao, J.-C., Lee, T., 2013. Diverse neuronal lineages make stereotyped contributions to the *Drosophila* locomotor control center, the central complex. Journal of Comparative Neurology 521, 2645–2662. https://doi.org/10.1002/cne.23339

Yoshida-Noro, C., Myohara, M., Kobari, F., Tochinai, S., 2000. Nervous system dynamics during fragmentation and regeneration in *Enchytraeus japonensis* (Oligochaeta, Annelida). Development Genes and Evolution 210, 311–319. https://doi.org/10.1007/s004270050318

Young, J.M., Armstrong, J.D., 2010. Building the central complex in *Drosophila*: The generation and development of distinct neural subsets. Journal of Comparative Neurology 518, 1525–1541. https://doi.org/10.1002/cne.22285

Younossi-Hartenstein, A., Green, P., Liaw, G.J., Rudolph, K., Lengyel, J., Hartenstein, V., 1997. Control of early neurogenesis of the *Drosophila* brain by the head gap genes tll, otd, ems, and btd. Developmental Biology 182, 270–283. https://doi.org/10.1006/dbio.1996.8475

Yu, H.-H., Awasaki, T., Schroeder, M.D., Long, F., Yang, J.S., He, Y., Ding, P., Kao, J.-C., Wu, G.Y.-Y., Peng, H., Myers, G., Lee, T., 2013. Clonal development and organization of the adult *Drosophila* central brain. Curr. Biol. 23, 633–643. https://doi.org/10.1016/j.cub.2013.02.057

Zetsche, B., Gootenberg, J.S., Abudayyeh, O.O., Slaymaker, I.M., Makarova, K.S., Essletzbichler, P., Volz, S.E., Joung, J., van der Oost, J., Regev, A., Koonin, E.V., Zhang, F., 2015. Cpf1 Is a Single RNA-Guided Endonuclease of a Class 2 CRISPR-Cas System. Cell 163, 759–771. https://doi.org/10.1016/j.cell.2015.09.038

Zhang, X., Koolhaas, W.H., Schnorrer, F., 2014. A Versatile Two-Step CRISPR- and RMCE-Based Strategy for Efficient Genome Engineering in *Drosophila*. G3: Genes, Genomes, Genetics 4, 2409–2418. https://doi.org/10.1534/g3.114.013979

Zilinski, C., Brownell, I., Hashimoto, R., Medina-Martinez, O., Swindell, E.C., Jamrich, M., 2004. Expression of FoxE4 and Rx Visualizes the Timing and Dynamics of Critical Processes Taking Place during Initial Stages of Vertebrate Eye Development. DNE 26, 294–307. https://doi.org/10.1159/000082271

Zube, C., Rössler, W., 2008. Caste- and sex-specific adaptations within the olfactory pathway in the brain of the ant Camponotus floridanus. Arthropod Structure & Development 37, 469–479. https://doi.org/10.1016/j.asd.2008.05.004

Zupanc, G.K.H., 2001. A Comparative Approach towards the Understanding of Adult Neurogenesis. BBE 58, 246–249. https://doi.org/10.1159/000057568

Zuris, J.A., Thompson, D.B., Shu, Y., Guilinger, J.P., Bessen, J.L., Hu, J.H., Maeder, M.L., Joung, J.K., Chen, Z.-Y., Liu, D.R., 2015. Cationic lipid-mediated delivery of proteins enables efficient protein-based genome editing *in vitro* and *in vivo*. Nature Biotechnology 33, 73–80. https://doi.org/10.1038/nbt.3081

Zwarts, L., Vanden Broeck, L., Cappuyns, E., Ayroles, J.F., Magwire, M.M., Vulsteke, V., Clements, J., Mackay, T.F.C., Callaerts, P., 2015. The genetic basis of natural variation in mushroom body size in *Drosophila melanogaster*. Nature Communications 6, 10115. https://doi.org/10.1038/ncomms10115